



This document was prepared for the ETI by third parties under contract to the ETI. The ETI is making these documents and data available to the public to inform the debate on low carbon energy innovation and deployment.

Programme Area: Marine

Project: PerAWAT

Title: Design and Testing Specification

Abstract:

This document describes how the results of discussions and numerical modelling have been combined to form a specification for the physical modelling of arrays of tidal energy converters (TECs) at coastal basin scale. The results of physical modelling at this scale will allow for comparison with the numerical models being developed, allowing an assessment of the impact of arrays of devices upon the coastal basin scale flow. Physical testing is to be undertaken by HR Wallingford at the Coastal Research Facility (CRF). Two idealised tidal site geometries have been selected following a review of tidal energy sites in the UK, they being a channel and a headland. These will be recreated within a 20m x 9m working section in the CRF. Numerical modelling has been undertaken to inform the site scale and geometry, layouts to be studied, the boundary conditions and to produce simulation results for comparison with the experimental data.

Context:

The Performance Assessment of Wave and Tidal Array Systems (PerAWaT) project, launched in October 2009 with £8m of ETI investment. The project delivered validated, commercial software tools capable of significantly reducing the levels of uncertainty associated with predicting the energy yield of major wave and tidal stream energy arrays. It also produced information that will help reduce commercial risk of future large scale wave and tidal array developments.

Disclaimer:

The Energy Technologies Institute is making this document available to use under the Energy Technologies Institute Open Licence for Materials. Please refer to the Energy Technologies Institute website for the terms and conditions of this licence. The Information is licensed 'as is' and the Energy Technologies Institute excludes all representations, warranties, obligations and liabilities in relation to the Information to the maximum extent permitted by law. The Energy Technologies Institute is not liable for any errors or omissions in the Information and shall not be liable for any loss, injury or damage of any kind caused by its use. This exclusion of liability includes, but is not limited to, any direct, indirect, special, incidental, consequential, punitive, or exemplary damages in each case such as loss of revenue, data, anticipated profits, and lost business. The Energy Technologies Institute does not guarantee the continued supply of the Information. Notwithstanding any statement to the contrary contained on the face of this document, the Energy Technologies Institute confirms that the authors of the document have consented to its publication by the Energy Technologies Institute.

**ETI Marine Programme Project
PerAWaT MA1003
WG4WP4 D1 DESIGN AND TESTING
SPECIFICATION**

Client	Energy Technologies Institute
Contact	Geraldine Newton-Cross
Document No	104333-UKBR-R-1-A
Issue	A
Status	Final
Classification	Not to be disclosed other than in line with the terms of the Technology Contract
Date	25 th Jan 2012

Author: S P Way

Checked by: M D Thomson

Approved by: R I Rawlinson-Smith

IMPORTANT NOTICE AND DISCLAIMER

1. This report (“Report”) is prepared and issued by Garrad Hassan & Partners Ltd (“GH” or “Garrad Hassan”) for the sole use of the client named on its title page (the “Client”) on whose instructions it has been prepared, and who has entered into a written agreement directly with Garrad Hassan. Garrad Hassan’s liability to the Client is set out in that agreement. Garrad Hassan shall have no liability to third parties (being persons other than the Client) in connection with this Report or for any use whatsoever by third parties of this Report unless the subject of a written agreement between Garrad Hassan and such third party. The Report may only be reproduced and circulated in accordance with the Document Classification and associated conditions stipulated or referred to in this Report and/or in Garrad Hassan’s written agreement with the Client. No part of this Report may be disclosed in any public offering memorandum, prospectus or stock exchange listing, circular or announcement without the express written consent of Garrad Hassan. A Document Classification permitting the Client to redistribute this Report shall not thereby imply that Garrad Hassan has any liability to any recipient other than the Client.
2. This report has been produced from information relating to dates and periods referred to in this report. The report does not imply that any information is not subject to change.

KEY TO DOCUMENT CLASSIFICATION

Strictly Confidential	:	For disclosure only to named individuals within the Client’s organisation.
Private and Confidential	:	For disclosure only to individuals directly concerned with the subject matter of the Report within the Client’s organisation.
Commercial in Confidence	:	Not to be disclosed outside the Client’s organisation
GH only	:	Not to be disclosed to non GH staff
Client’s Discretion	:	Distribution for information only at the discretion of the Client (subject to the above Important Notice and Disclaimer).
Published	:	Available for information only to the general public (subject to the above Important Notice and Disclaimer and Disclaimer).

REVISION HISTORY

Issue	Issue date	Summary
A	25/01/12	Original issue (electronic version only)

CONTENTS

EXECUTIVE SUMMARY

1	INTRODUCTION	2
1.1	Scope of this Document	2
1.2	Purpose of this document	2
1.3	Specific tasks associated with WG4 WP4 D1	2
1.4	WG4 WP4 D1 acceptance criteria	2
2	ADDRESSING THE ACCEPTANCE CRITERIA	4
2.1	Working group minutes	4
2.2	Numerical modelling, justification and design	4
2.3	Test specification and experimental programme	4

APPENDIX 1 - OUTCOME OF WORKGROUP MEETINGS FOR WG4WP1

APPENDIX 2 - SPECIFICATION FOR PHYSICAL SCALE MODELLING

EXECUTIVE SUMMARY

This document describes how the results of discussions and numerical modelling have been combined to form a specification for the physical modelling of arrays of tidal energy converters (TECs) at coastal basin scale. The results of physical modelling at this scale will allow for comparison with the numerical models being developed, allowing an assessment of the impact of arrays of devices upon the coastal basin scale flow.

Physical testing is to be undertaken by HR Wallingford at the Coastal Research Facility (CRF). Two idealised tidal site geometries have been selected following a review of tidal energy sites in the UK, they being a channel and a headland. These will be recreated within a 20m x 9m working section in the CRF.

Numerical modelling has been undertaken to inform the site scale and geometry, layouts to be studied, the boundary conditions and to produce simulation results for comparison with the experimental data.

Emulators representing arrays of TECs will be built from a number of porous discs. Multiple array layouts formed of up to three array emulators will be exposed to steady and oscillatory flow conditions. Measurements of thrust on the emulators will be collected using load cells. Flow measurements (the locations of which have been informed by numerical modelling) are recorded with current meters and acoustic Doppler velocimeters (ADV). Surface elevation will be recorded using wave probes.

1 INTRODUCTION

1.1 Scope of this Document

This document constitutes the first deliverable (D1) of working group four, work package four (WG4 WP4) of the PerAWAT (Performance Assessment of Wave and Tidal Arrays) project commissioned by the Energy Technologies Institute (ETI). This report has been prepared by GL Garrad Hassan (GH), Scott Draper (SD), University of Manchester (UoM), University of Oxford (UoO), Électricité de France (EDF) and HR Wallingford (HRW).

This document describes the design and test specification required for physical modelling of arrays of tidal energy converters (TECs) at a coastal basin scale, including numerical modelling and a justification for the chosen experimental setup.

1.2 Purpose of this document

The purpose of WG4WP4 is to investigate the impact of arrays of TECs on the global flow field through the use of physical modelling.

The specific objective of WG4WP4 D1 is to provide and justify a design and testing specification for the physical scale experiments and put in place a fixed price contract with the subcontractor (HRW) for the physical experiments.

1.3 Specific tasks associated with WG4 WP4 D1

WG4WP4 D1 comprises the following aspects

- Delivery of a design and testing specification report
- A fixed price contract in place with subcontractor to realise the testing programme, with all relevant Technology Contract conditions cascaded.

1.4 WG4 WP4 D1 acceptance criteria

The acceptance criteria as stated in the PerAWAT technology contract is as follows:

- Delivery of a design and testing specification report including:
 1. Working group meeting minutes (to inform tidal site designs)
 2. Justification for the selected sites for numerical modelling
 3. Definition of the physical testing facility to be numerically modelled
 4. Numerical modelling methodology
 5. Numerical modelling results including:
 - a. Investigation to find a suitable scale for the tidal site
 - b. Prediction of the impact of arrays on the global flow field (e.g. the change in flow speed and/or thrust on array)
 - c. Justification for the selection of sites to be modelled physically
 6. Specification for array emulators: details of the operating points (porosity, flow rates), experimental programme.

7. Specification for the for the physical scale geometric form (in a standard format to enable manufacture).
8. Inflow and exit boundary conditions
9. Specification for the measurement points, instrument type, sample frequencies, acceptable error
10. A detailed experimental programme for the coastal basin experiments (including proposed array layouts and varies environmental conditions).

2 ADDRESSING THE ACCEPTANCE CRITERIA

2.1 Working group minutes

The results of the working group meetings (acceptance criteria 1) are compiled into the document in Appendix 1 "Outcome of Workgroup Meetings for WG4WP4 D1". This document contains the results of discussions (via telephone calls, teleconferences and electronic mail) amongst the working group with regards to the technical scope required for an experimental programme considering arrays of tidal energy converters at coastal basin scale.

2.2 Numerical modelling, justification and design

The justification for modelling the selected sites (acceptance criteria 2) is presented in Appendix 2: "WG4 WP4, Milestone 1: Specification for Physical Scale Modelling". This document describes how tidal energy sites around the UK were reviewed with particular initial focus on the Pentland Firth. Due to the complexity of the bathymetry and the requirements for an undistorted 1/1000th scale model small deviations in the model would represent large changes at full-scale bathymetry with very low flow speeds in the CRF. After review of the other sites it was shown that many have a resemblance to either a channel or headland geometry, therefore these were chosen to be modelled.

The definition of the facility to be modelled (acceptance criteria 3) is contained in Appendix 1 and Appendix 2. The Coastal Research Facility (CRF), which is managed by HR Wallingford, is described in both documents. However, the layouts and geometry of the experimental bathymetry is described in Appendix 2. The numerical modelling methodology used (acceptance criteria 4) and the numerical modelling results (acceptance criteria 5) are also presented Appendix 2

The numerical modelling has been used to inform the selection of array layouts, boundary conditions, locations of instrumentation, locations of emulators, bed roughness and the size of headland.

2.3 Test specification and experimental programme

The array emulator specification and operating points (acceptance criteria 6) are defined in Appendix 1 following the discussions of the workgroup. The array emulators are to be constructed from a series of porous discs, 110mm in diameter with a coefficient of thrust (C_T) of 0.9. The discs are to be placed 1.2 diameters apart from centre to centre forming emulators approximately 1.8m across (resulting in a local blockage ratio of 36% (disc areas over cross-sectional area occupied by discs. Note the channel blockage ratio will vary between 7% to 26% depending on the channel geometry and number of rows of devices). The discs are suspended from M6 threaded rod from a square hollow section nominally 30mm wide.

The geometry of the channel and headland (acceptance criteria 7) are described in Appendix 2 with dimensioned drawings of the geometry for the physical experiments. The boundary conditions (acceptance criteria 8) for the numerical and physical experiments are also described in Appendix 2.

The measurement points and instrument setup (criteria 9) and are shown in Appendix 2. These are compiled with the geometry and boundary conditions to form a detailed experimental plan in Appendix 1.

APPENDIX 1
OUTCOME OF WORKGROUP MEETINGS FOR WG4WP1
DOCUMENT 104333-UKBR-T-01-A

APPENDIX 2
SPECIFICATION FOR PHYSICAL SCALE MODELLING
DOCUMENT 11600

TECHNICAL NOTE

Title	Outcome of workgroup meetings for WG4WP4 D1
Client	Energy Technologies Insitute
Contact	Gerry Newton-Cross
Document No.	104333-UKBR-T-01-A
Issue	A
Classification	Not to be disclosed outside of the terms of the Technology Contract
Author	S. P. Way
Checked	R. I. Rawlinson Smith
Approved	R. I. Rawlinson Smith

History

Issue:	Date:	Summary
A	22.12.11	Original document (electronic version only)

Important Notice and Disclaimer

1. This technical note (“Technical Note”) is prepared and issued by Garrad Hassan & Partners Ltd (“GH” or “Garrad Hassan”) for the sole use of the client named on its title page (the “Client”) on whose instructions it has been prepared, and who has entered into a written agreement directly with Garrad Hassan. Garrad Hassan’s liability to the Client is set out in that agreement. Garrad Hassan shall have no liability to third parties (being persons other than the Client) in connection with this Report or for any use whatsoever by third parties of this Report unless the subject of a written agreement between Garrad Hassan and such third party. The Technical Note may only be reproduced and circulated in accordance with the Document Classification and associated conditions stipulated or referred to in this Technical Note and/or in Garrad Hassan’s written agreement with the Client. No part of this Technical Note may be disclosed in any public offering memorandum, prospectus or stock exchange listing, circular or announcement without the express written consent of Garrad Hassan. A Document Classification permitting the Client to redistribute this Technical Note shall not thereby imply that Garrad Hassan has any liability to any recipient other than the Client.
2. This Technical Note has been produced from information relating to dates and periods referred to in this report. The Technical Note does not imply that any information is not subject to change.

Key to Document Classification

Strictly Confidential:	For disclosure only to named individuals within the Client’s organisation.
Private and Confidential:	For disclosure only to individuals directly concerned with the subject matter of the Technical Note within the Client’s organisation.
Commercial in Confidence:	Not to be disclosed outside the Client’s organisation
GH only:	Not to be disclosed to non GH staff
Client’s Discretion	Distribution for information only at the discretion of the Client (subject to the above Important Notice and Disclaimer).
Published:	Available for information only to the general public (subject to the above Important Notice and Disclaimer).

© 2010 Garrad Hassan & Partners Ltd

1 INTRODUCTION

This technical note forms part of Deliverable 1 for Work Package 4 of Work Group 4 as part of the Performance Assessment of Wave and Tidal Array Systems (PerAWaT).

This document contains the results of discussions (via telephone calls, teleconferences and electronic mail) amongst the working group with regards to the technical scope required for an experimental programme considering arrays of tidal energy converters at coastal basin scale. The scope also reflects a programme that is feasible when considered within the budget by the sub-contractor HR Wallingford. The working group for WG4WP4 includes:

- The University of Manchester
- Scott Draper (formerly University of Oxford)
- Electricite de France
- HR Wallingford

The scope is included within the sub-contract between Garrad Hassan and HR Wallingford.

2 TECHNICAL SCOPE

Background

Description of HR Wallingford's Coastal Research Facility (CRF)

The CRF is a unique wave and current basin that was designed for fundamental and applied coastal research. The CRF can generate waves, wave-driven currents and tidal currents for investigations into nearshore and coastal processes related to the behaviour and influence of: waves & currents, pollutants & contaminants, sediments & structures. Specification: Basin external dimensions: 54m by 27m, Basin internal dimensions: 36m by 20m, Basin test area: 20m by 15m. Shore-parallel currents are circulated through four independent reversible computer-controlled pumps, each with a capacity of 0.3m³/s. The pumps are controllable in either direction, continuously through zero, so tidal or uni-directional flows can be generated. The currents are introduced into either end of the basin through 40 0.5m wide inlet flumes each controlled by its own undershot weir. These allow the cross-shore distribution of the longshore current to be controlled. The maximum offshore near surface current speed in 0.5m water depth is 0.14m/s, unless the flow is constrained in a narrower flume within the basin.

Description of the available instrumentation for physical model studies at HR Wallingford

Equipment for measuring water surface elevation and flow velocities are available and are detailed in the measurement apparatus list given in the Table 1 of Appendix 1.

1. The general arrangement for the experiments

(A) Base Case Geometry

A previous experimental study concerning sand mounds in oscillatory flows has been undertaken in the wave and current basin at HR Wallingford (see Stansby et al. (2009)). It is proposed that for research continuity and to reduce the risks associated with this novel area of research, the same idealised channel geometry is used (see Figure A1 in Appendix 1 for the original configuration).

The dimensions of the test are approximately 20 metres long by 9 metres wide with tapering at both ends (as shown in the Figure 1 below).

Bed roughness on the channel bed and the sloping sides of the headland should ideally have a roughness length (z_0) of approximately 10 mm (corresponding to a Nikuradse roughness of 30 mm). Side wall roughness of the channel can be smooth, such as using well-pointed concrete blocks.

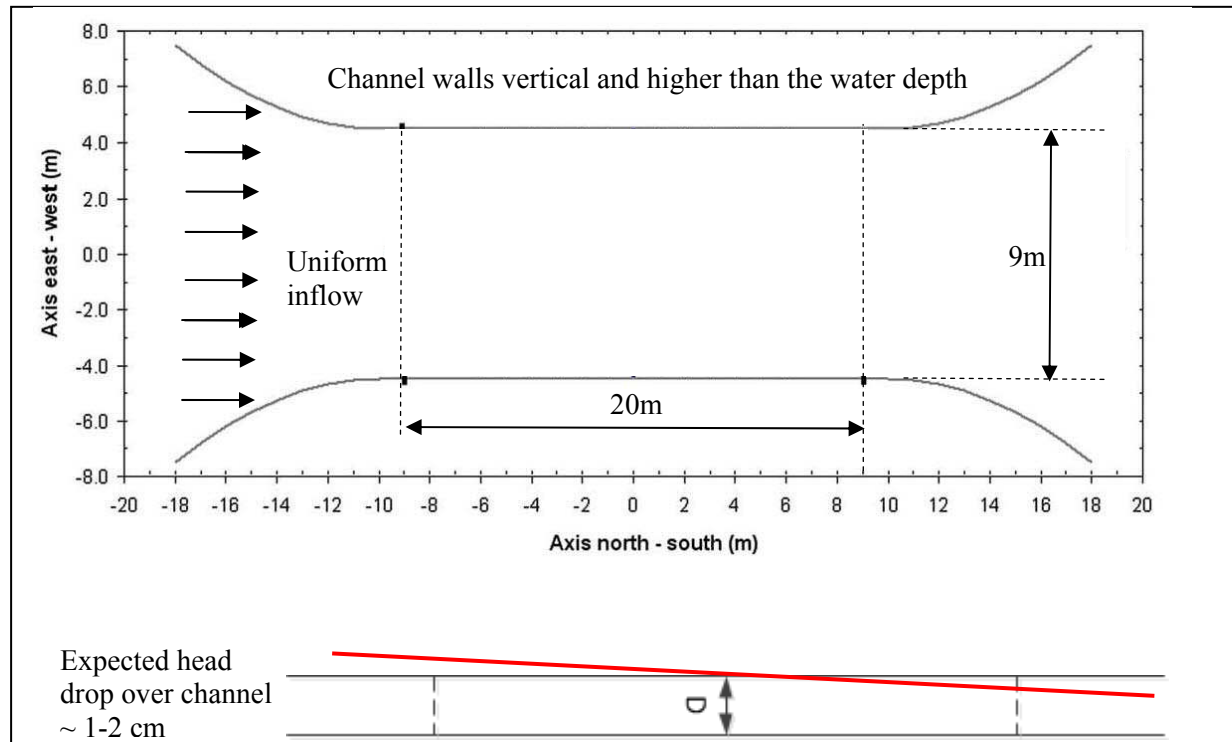


Figure 1 General geometry layout

(B) Headland Geometry

Two types of basin geometry are to be modelled. These consist of the base case geometry (the 'Channel') and a case including a Headland as shown in Figure 2. The exact geometry and location of the Headland is to be supplied by GH to HRW, the form of the Headland is given in Appendix 1.

To minimise cost it is expected that the first experiments will be conducted with the Channel followed by the Headland located within the channel (approximately half way down, as shown in Figure 2 below).

(C) Required Flow (Boundary) Conditions

For the base case geometry and the alternative geometries the required flow conditions are

- Steady flow: Uniform flowrate across the channel, providing depth-averaged velocities ranging between 0-0.5 m/s and a mean water depth of 20 cm averaged along the channel. The most likely value for depth-averaged steady flow is ~0.5m/s for the Channel cases and ~0.3m/s for Headland cases)
- Oscillatory flow: For the oscillatory flow conditions a peak flowrate across the channel, providing depth-averaged velocities ranging between 0-0.5 m/s. The flow rate should vary sinusoidally with time from this peak flowrate with a period of 1200sec.

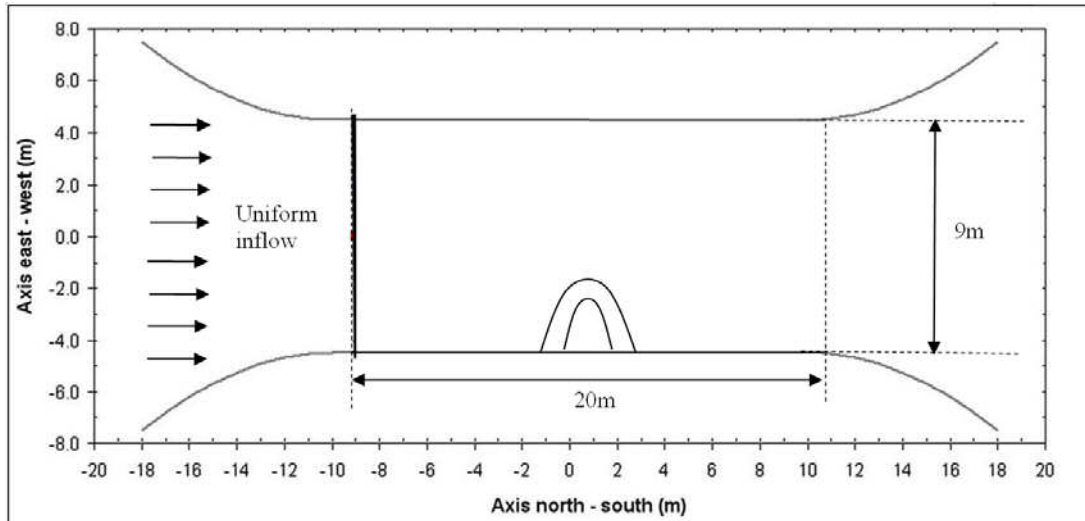


Figure 2 General geometry layout including headland

(D) Array Emulators

Emulators, representing arrays of tidal turbines are to be installed in the test section. The addition of tidal array emulators will require an overhead support system. It is thought that for these experiments such a system will consist of a number of beams spanning the width of the flume that can be moved along the channel length on rails or equivalent, thus reducing the effort required to move the beams. A single array emulator is expected to consist of 2 ~0.9m assemblies made from a number of porous discs, assembled as two units. These can be clamped together to form a single assembly if required.

(A working design of the measurement assembly is explained in the section entitled, 'Equipment and instrumentation requirements', later in this note). There will be multiple emulators (up to 3 per run), arranged in various layouts as shown in Appendix 2. An example is given below. The envelope of location of these array emulators will be constrained to the central third of the channel i.e. $\sim \pm 4\text{m}$.

The approximate layouts for these emulators and the approximate locations of the measurements are specified in Appendix 2. It is intended that the instruments and emulators will be suspended from beams

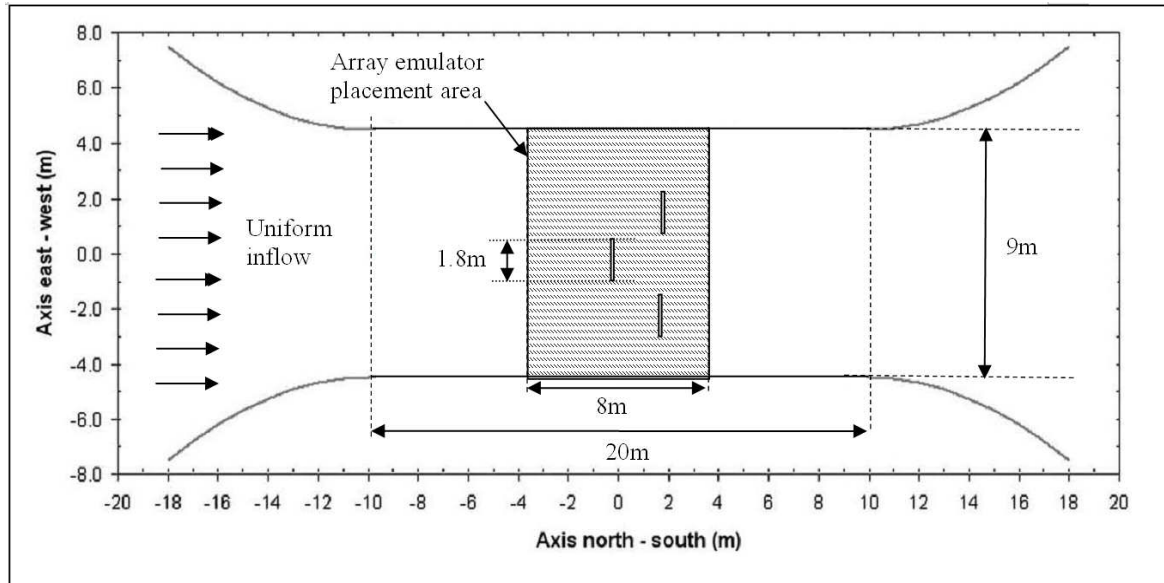


Figure 3 Location of array placement area

2. Measurement requirements

The primary measurements of interest are:

- The flow field (via point wise velocity measurements made using ADVs and propeller current meters) to gain an understanding of the spatial variability within the flow field.
- The free surface elevation (via wave probes) to help characterise the effect of seabed drag and any head loss due to the array emulators.
- The drag force on each array emulator via the use of S beams placed in the load path between the emulator strips and the strip support structure.
- The time that measurements are recorded, to allow the state of measurements relative to each other to be evaluated

Further measurement requirements are dependant on the type of experiment undertaken.

The baseline experiments are required to characterise the undisturbed flow, i.e. the flow without any emulators present. Measurements across the channel will check the lateral uniformity at both the inflow and outflow locations. The lateral uniformity will also need to be checked across the channel mid point. Depth flow profiles will need to be recorded at some of the locations specified in Appendix 2; however this is subject to change. For the geometries including the headland, more spatial variability in the flow measurement locations will be required. The approximate locations for instruments are shown in Appendix 2.

Both steady and time varying flows are to be considered. For the time varying conditions concurrent measurements are required.

(A) Baseline Calibration Tests

Specially, for the baseline/calibration tests (per basin geometry)

- Flow (ADV and current meter) measurements
 - Taken at the locations specified in Appendix 2, approximately mid water depth.

- At some of the locations highlighted in Appendix 2 (subject to change) velocity measurements through the water depth but within the operating limits of the ADVs will be required to characterise the mean velocity profile and turbulent fluctuations. (The ADV sampling volume must be more than 10 mm off the bed due to interference from reflections, and at least 60 mm below the water surface.) For the Headland cases the measurement points specified in Appendix 2 are required to characterise the flow around the headland and the resulting eddy behind it.
- All ADV measurements should be of sufficient duration (>10,000 data points) to characterise turbulent fluctuations and Reynolds Stresses.
- Surface elevation
 - Measurements of water depth are required at the same points as the ADV and current meter measurement points, or as close as is reasonably practical, to determine the time varying flow rate through the channel (see Appendix 2).

(B) Array tests (per basin geometry)

- Velocity measurements
 - The focus of the ADV and current meter measurements is to understand both the upstream and downstream flow changes due to the presence of the array emulators. The specific location of the flow measurement points is therefore specific to the each array layout
 - Measurements of the velocity profile through-depth are required at multiple locations as specified in Appendix 2. All ADV measurements should be of sufficient duration to characterise turbulent fluctuations and Reynolds Stresses (>10,000 data points).
 - The range of flow velocity is expected to be from 0 to 0.5 m/s.
- Surface elevation measurements
 - Measurements at the same point as the velocity measurements points.
 - Expected range in elevation change is expected to be less than 3 cm. A minimum resolution of approximately 1mm is required.
- Array emulator thrust measurement
 - For each array emulator the thrust is to be measured continuously during each test. Note: The thrust measurement system may need to be calibrated prior to each test.
 - The drag force on the emulators is expected to be of the order of 5 N/m up to approximately 10N/m. Thus a working range of thrust force on each emulator is 0-20N with a resolution and accuracy of the order of 0.1N (hence the need for a well balanced and calibrated system).

3. Equipment and instrumentation requirements

HR Wallingford will be required to provide the following equipment and instrumentation:

- It is noted that HR Wallingford have 3 ADVs and 25 current meters. Both are suitable for flow measurements at these scales, however current meters only allow for measurement of flow in one dimension. The ideal total number of measurement locations is large to cover as much of the experiment as possible at as high as resolution as is possible. It is anticipated that it will be more cost effective to rent extra ADVs than increase the experimental time that would be required to cover the multiple locations. The optimum number of ADVs will be dependant on the ability to efficiently move ADVs and current meters between locations within the experimental domain. It is thought that when the

array emulators are in position the ability to move the ADVs and current meters will be limited. Hence hiring additional ADVs is thought to be more cost effective, however, this is clearly dependant on the relative cost between the facility charge and the ADV hire charge. A target estimate of the number of ADVs is 10, with GH anticipating that HR Wallingford will have to hire 4 additional ADVs for the experiments dependant upon availability from suppliers, with a further 3 to be supplied by the University of Manchester.

- Surface elevation probes/wave probes are required at the same locations as instruments measuring the flow, or as close as is reasonably practical.
- Array emulator thrust measurement system. UoM will provide the emulator assemblies to be used, however, HR Wallingford will be required to provide the array emulator support structure and S beam sensors. A proposed set-up is shown below. This set-up is dependant on the HR Wallingford equipment and final emulator design so further consideration/design is likely. It is thought that the rigidity of the connections to the carriage are of key importance, as well as good alignment of gantry and minimising the vibration of the carriage.
- Data acquisition PC(s) to allow all concurrent measurements to be recorded at the instrument frequency rate with a timestamp.

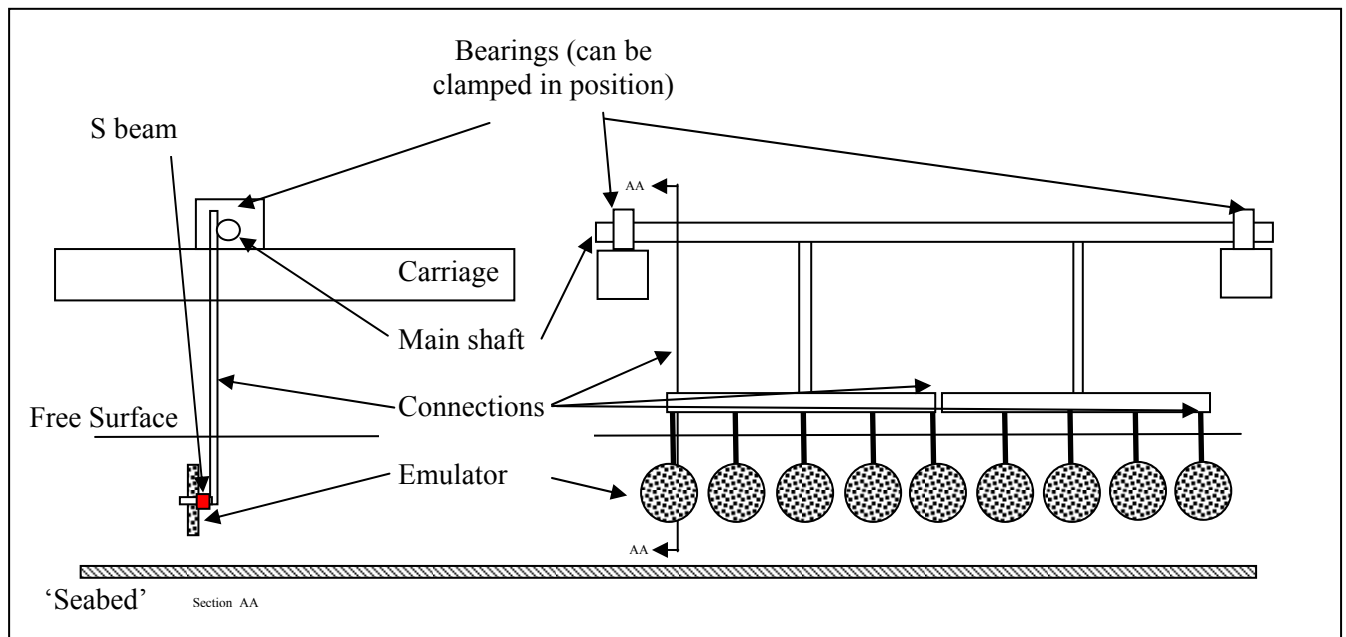


Figure 4 Initial emulator mounting design

4. Accuracy of bathymetry and array emulator placement

The approximate scale of the model will be $1/300^{\text{th}}$, implying that an error of 1 cm in the placement of the bathymetry and/or array emulators will equal a 3 metre misplacement in the prototype and could considerably alter, for example, the locations of maximum currents. To achieve good model accuracy will therefore require very careful construction and experiment set-up.

Due to the small magnitude of applied thrust, the accuracy of the measurements may be limited. To minimise the uncertainty around the measurement a rigid support structure will be required. Load cells will be individually calibrated in the electronics laboratory before the test series.

The measurement system can also be tested within the flume using a weight and pulley system to maintain confidence in these measurements.

5. Scope of Work

The main tasks to be undertaken by HR Wallingford include:

1. Equipment construction
 - a. Basin construction: build test bed and bathymetry geometries to the required accuracy
 - b. Set-up facility inlet and outlet system
 - c. Construct array emulator support structure
 - d. Acquire additional ADVs to bring total number to 10 depending on availability
 - e. Construct/set-up instrumentation system support structure
 - f. Install instrumentation and data-logging equipment
2. Initial tests
 - a. Flow instrumentation calibration/checks: wave gauges/elevation sensors, ADVs, current meters
 - b. Develop the required inflow and through channel conditions (water depth and mean flow speed). Check elevation drop along the channel per geometry configuration.
 - c. Characterise base flow for each geometry configuration.
 - d. Calibrate array emulators thrust measurement instrumentation (per array emulator and per test).
3. Conduct test schedule (see section 6)
 - a. Varying flow conditions (steady and unsteady)
 - b. Vary array configurations

6. Test list

Layouts are detailed in Appendix 2. Note that this gives an indication of the required tests, however particulars (such as length of time data is required for and number of repeats) are still subject to change.

The amount of data in one location should be enough to characterise Reynolds Stresses using ADVs (approximately 10,000 points). At 25Hz this would require 400s worth of data. Approximately 30 minutes of data is required for steady inflow conditions and this should be built up from runs at a number of depths.

In summary, there are 19 sets of tests detailed below, corresponding to the layouts described. Of these, the 11 specified as 'Required' form the minimum set of experiments that shall be completed within the experimental programme, with a further 8 experiments to be undertaken after if time and budget allows. There are 7 layouts using the Channel geometry and a further 12 using the Headland geometry.

CHANNEL GEOMETRY TESTS

Test set 1 layout: Baseline Tests: Required

Calibration and Characterisation tests - Without array emulators

- i. Steady inflow condition
Baseline flow and surface elevation characterisation. Multiple depths at depth profile locations. No repeat. Collect 30mins of suitable data.

- ii. Oscillatory inflow condition
Baseline flow and surface elevation characterisation. Repeat for 3 periods
times depending on progress.

Test 2 layout: Array Emulator Tests: Required

- i. Steady inflow condition
Flow, surface elevation and emulator thrust measurements. Collect 30
minutes of suitable data. Multiple depths at depth profile locations.
- ii. Oscillatory inflow condition
Flow, surface elevation and emulator thrust characterisation. Repeat for 3
periods depending on progress.

Test 3 layout: Baseline Tests: Required

- i. Steady inflow condition
Baseline flow and surface elevation characterisation. Multiple depths at depth
profile locations. No repeat. Collect 30mins of suitable data.
- ii. Oscillatory inflow condition
Baseline flow and surface elevation characterisation. Repeat for 3 periods
depending on progress.

Note: based on depth profile result the subsequent along-channel instrument locations may be shifted
away from the centre of the channel.

Test 4 layout: Array Emulator Tests: Required

- i. Steady inflow condition
Flow, surface elevation and emulator thrust measurements. Collect 30
minutes of suitable data
- ii. Oscillatory inflow condition
Flow, surface elevation and emulator thrust characterisation. Repeat for 3
periods depending on progress.

Test 5 layout: Array Emulator Tests: Optional further work

- i. Steady inflow condition
Flow, surface elevation and emulator thrust measurements. Collect 30
minutes of suitable data
- ii. Oscillatory inflow condition
Flow, surface elevation and emulator thrust characterisation. Repeat for 3
periods depending on progress.

Test 6 layout: Array Emulator Tests: Optional further work

- i. Steady inflow condition
Flow, surface elevation and emulator thrust measurements. Collect 30
minutes of suitable data
- ii. Oscillatory inflow condition
Flow, surface elevation and emulator thrust characterisation. Repeat for 3
periods depending on progress.

Test 7 layout: Array Emulator Tests: Optional further work

- i. Steady inflow condition
Flow, surface elevation and emulator thrust measurements. Collect 30 minutes of suitable data
- ii. Oscillatory inflow condition
Flow, surface elevation and emulator thrust characterisation. Repeat for 3 periods depending on progress.

HEADLAND GEOMETRY TESTS

Test set 8 layout: Baseline Tests: Required

Calibration and Characterisation tests - Without array emulators

- i. Steady inflow condition
Baseline flow and surface elevation characterisation. Multiple depths at depth profile locations. No repeat. Collect 30mins of suitable data.
- ii. Oscillatory inflow condition
Baseline flow and surface elevation characterisation. Repeat for 3 periods times depending on progress.

Test set 9 layout: Array Emulator Tests: Required

- i. Steady inflow condition
Flow, surface elevation and emulator thrust measurements. Collect 30 minutes of suitable data
- ii. Oscillatory inflow condition
Flow, surface elevation and emulator thrust characterisation. Repeat for 3 periods depending on progress.

Test set 10 layout: Array Emulator Tests: Required

- i. Steady inflow condition
Flow, surface elevation and emulator thrust measurements. Collect 30 minutes of suitable data
- ii. Oscillatory inflow condition
Flow, surface elevation and emulator thrust characterisation. Repeat for 3 periods depending on progress.

Test set 11 layout: Array Emulator Tests: Required

- i. Steady inflow condition
Flow, surface elevation and emulator thrust measurements. Collect 30 minutes of suitable data
- ii. Oscillatory inflow condition
Flow, surface elevation and emulator thrust characterisation. Repeat for 3 periods depending on progress.

Test set 12 layout: Array Emulator Tests: Required

- i. Steady inflow condition
Flow, surface elevation and emulator thrust measurements. Collect 30 minutes of suitable data
- ii. Oscillatory inflow condition
Flow, surface elevation and emulator thrust characterisation. Repeat for 3 periods depending on progress.

Test set 13 layout: Array Emulator Tests: Optional

- i. Steady inflow condition
Flow, surface elevation and emulator thrust measurements. Collect 30 minutes of suitable data
- ii. Oscillatory inflow condition
Flow, surface elevation and emulator thrust characterisation. Repeat for 3 periods depending on progress.

Test set 14 layout: Baseline Tests: Required

Calibration and Characterisation tests - Without array emulators

- iii. Steady inflow condition
Baseline flow and surface elevation characterisation. Multiple depths at depth profile locations. No repeat. Collect 30mins of suitable data.
- iv. Oscillatory inflow condition
Baseline flow and surface elevation characterisation. Repeat for 3 periods times depending on progress.

Test set 15 layout: Array Emulator Tests: Required

- i. Steady inflow condition
Flow, surface elevation and emulator thrust measurements. Collect 30 minutes of suitable data
- ii. Oscillatory inflow condition
Flow, surface elevation and emulator thrust characterisation. Repeat for 3 periods depending on progress.

Test set 16 layout: Array Emulator Tests: Optional

- i. Steady inflow condition
Flow, surface elevation and emulator thrust measurements. Collect 30 minutes of suitable data
- ii. Oscillatory inflow condition
Flow, surface elevation and emulator thrust characterisation. Repeat for 3 periods depending on progress.

Test set 17 layout: Array Emulator Tests: Optional

- i. Steady inflow condition

Flow, surface elevation and emulator thrust measurements. Collect 30 minutes of suitable data

- ii. Oscillatory inflow condition
Flow, surface elevation and emulator thrust characterisation. Repeat for 3 periods depending on progress.

Test set 18 layout: Array Emulator Tests: Optional

- i. Steady inflow condition
Flow, surface elevation and emulator thrust measurements. Collect 30 minutes of suitable data
- ii. Oscillatory inflow condition
Flow, surface elevation and emulator thrust characterisation. Repeat for 3 periods depending on progress.

Test set 19 layout: Array Emulator Tests: Optional

- i. Steady inflow condition
Flow, surface elevation and emulator thrust measurements. Collect 30 minutes of suitable data
- ii. Oscillatory inflow condition
Flow, surface elevation and emulator thrust characterisation. Repeat for 3 periods depending on progress.

Time scales

The programme outline within the current PerAWaT contract requires the tests to be reported by May 2012.

It is anticipated that a four week programme of work should be available for the experiments. Of this time, approximately 1 week is needed to set-up the coastal models and establish an experimental procedure.

HR Wallingford has advised that a 1 month lead time is sufficient to prepare for an 8 week program of work.

Deliverables from HR Wallingford

A log of each experiment containing all the required metadata, calibration results and test results.

Information to be provided to HR Wallingford:

A detailed description of the basin construction for each experiment

A detailed description of the inflow conditions for each experiment

A detailed description of the experimental set-up and instrumentation for each experiment.

APPENDIX 1

ADDITIONAL INFORMATION

Table 1 List of HR Wallingford instrumentation

Equipment and instrumentation	Quantity	Notes
<i>Instrumentation</i>		
Wave generation PC systems	10	
Data acquisition PC systems (64 channel or greater)	8	
Supplementary data acquisition systems	10	
Wave probes	150	
Water level followers	8	
Pitot tubes	10	
Miniature propeller current meters	34	(with 25 logging systems)
ADV current meters	3	
In line load cells	22	
6-axis force cells	4	
Pressure transducers	60	
Ship mooring line transducers	36	
Ship fender transducers	24	
Qualysis (non contact) motion measurement systems	4	With spare cameras
Bed profilers (2D)	2	
3D Laser scanners	2	
SLR cameras	6	With remote triggering
Camcorders	11	
<i>Additional pumps</i>		
Small capacity pumps	20	1 cusec or less
Large capacity pumps	20	1 to 20 cusecs

Previous experimental set-up at CRF at HR Wallingford.

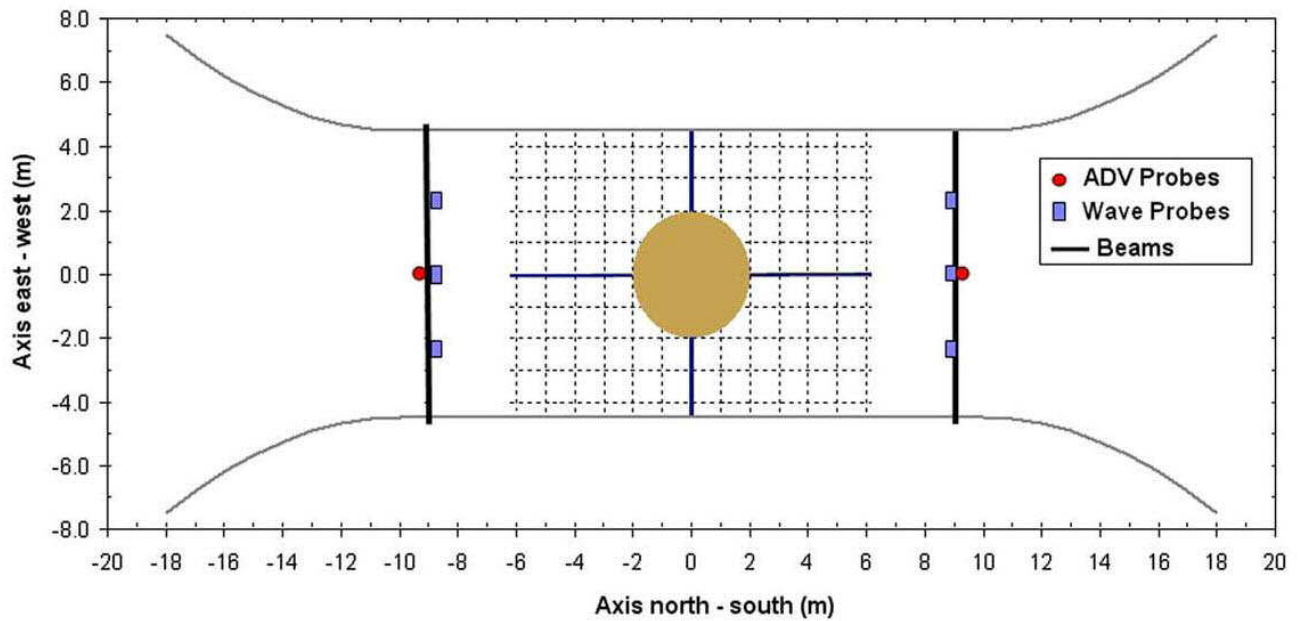


Figure A5 General geometry layout (Stansby et al)

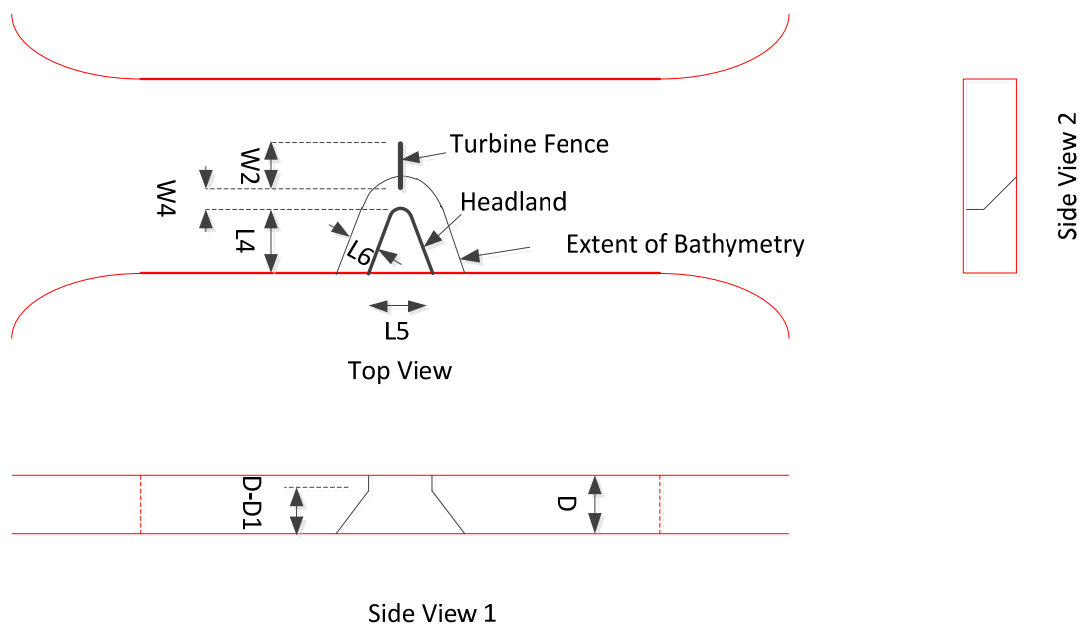


Figure A6 Representation of headland geometry

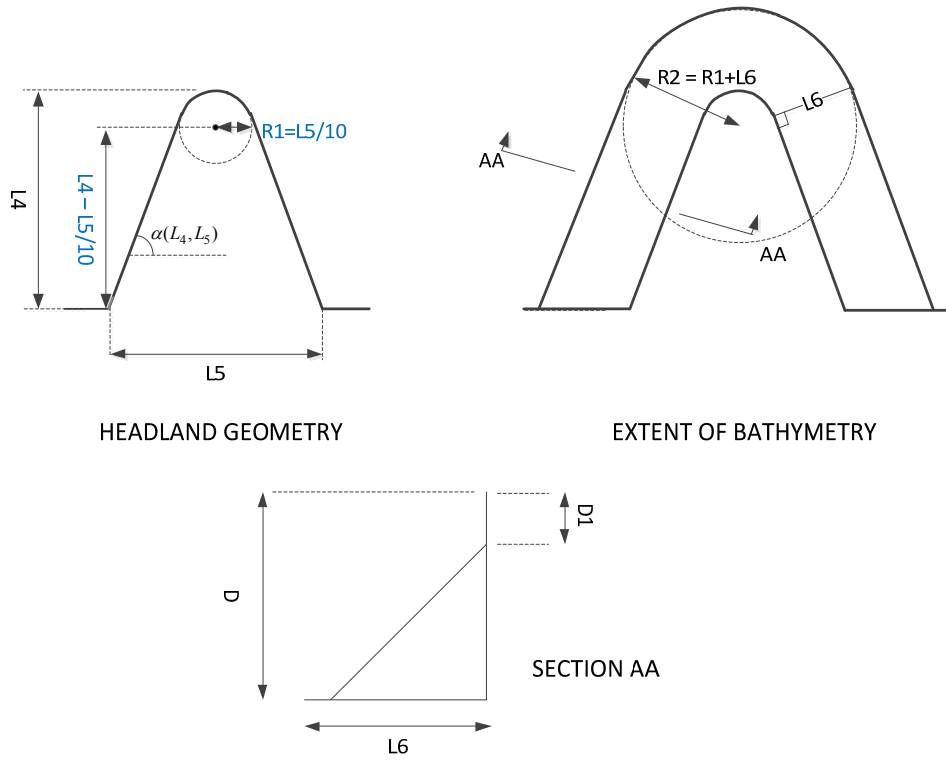
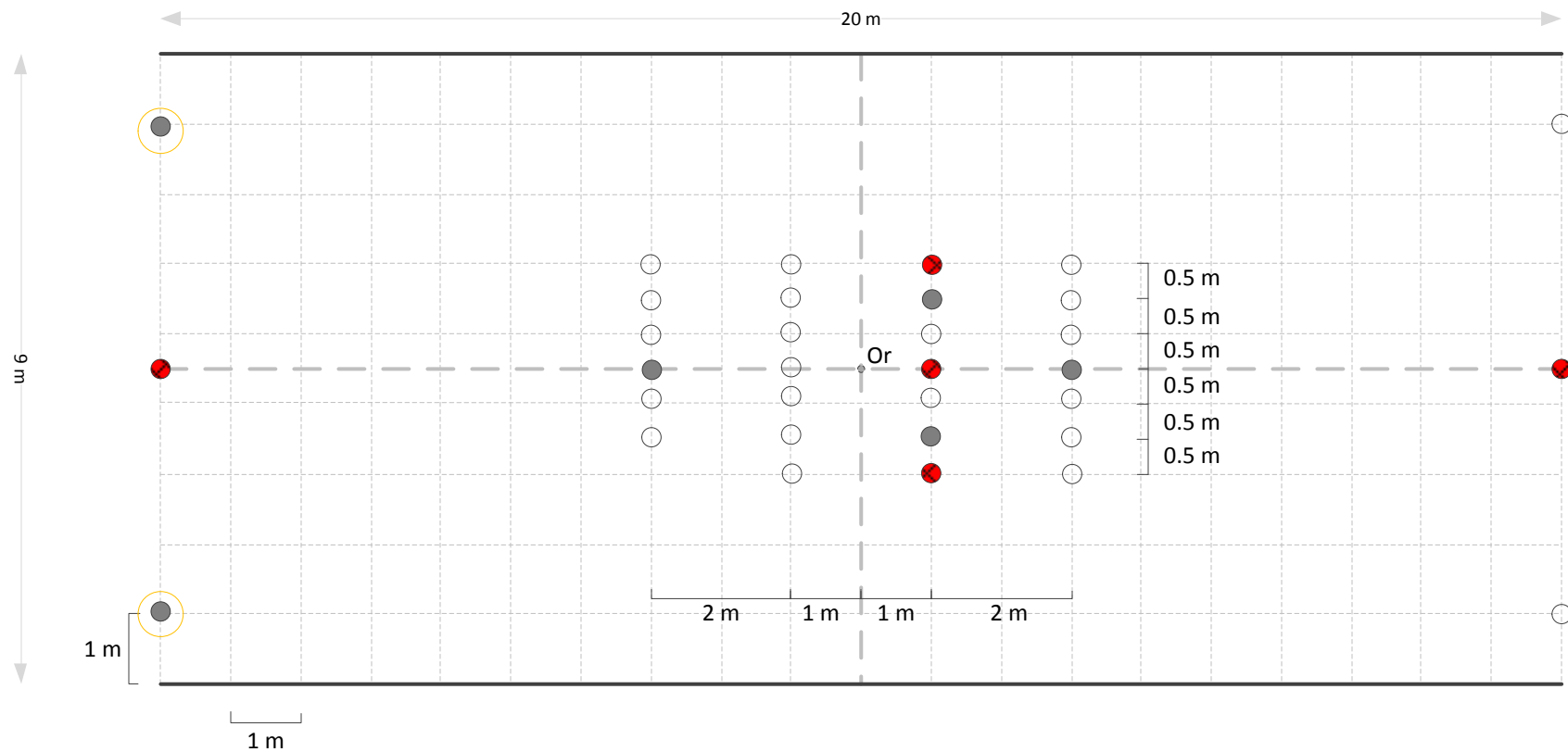







Figure A7: Relative headland geometry

APPENDIX 2
EXPERIMENTAL LAYOUTS



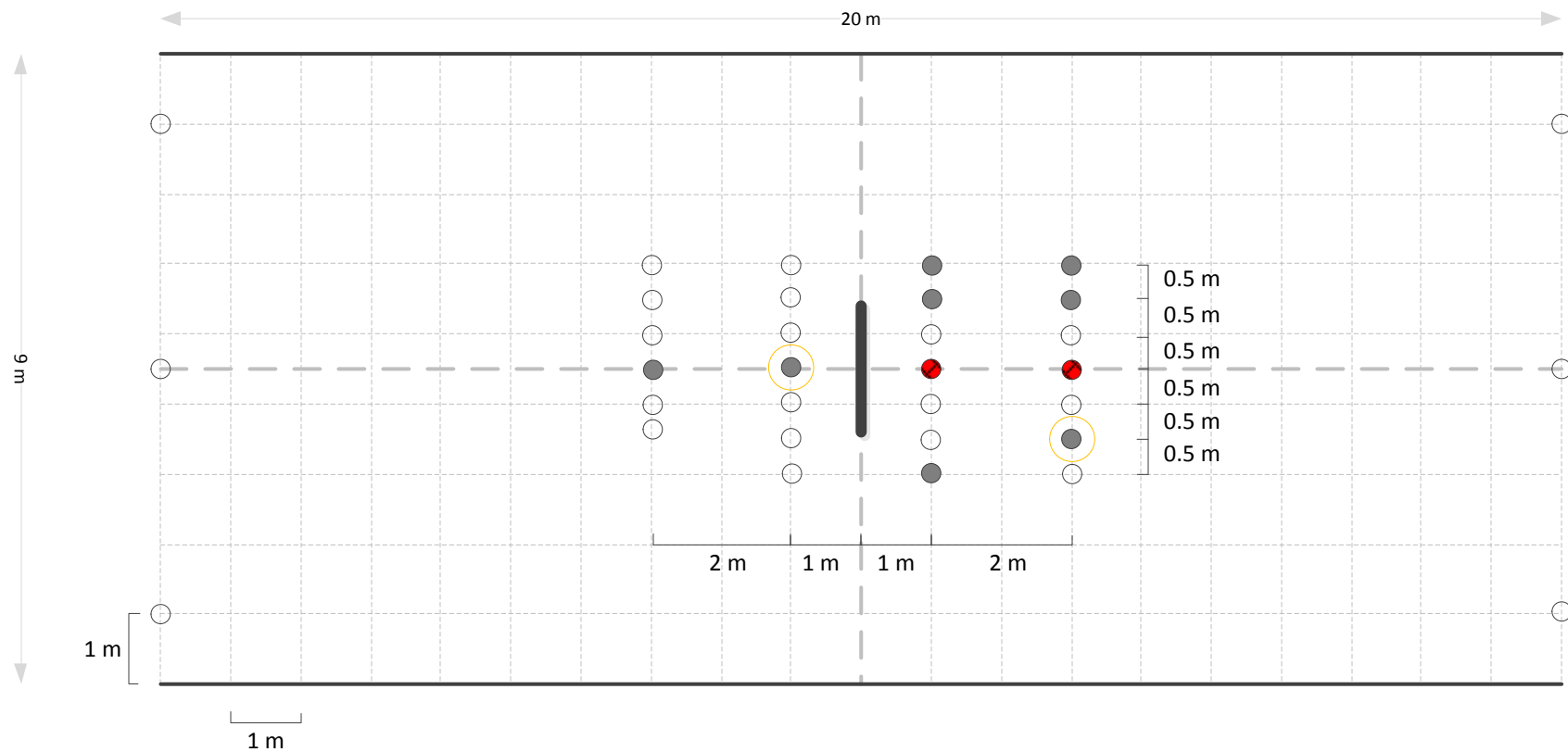
 This could be changed to propeller meter if not enough ADVs


Key

-  ADV point measurement
-  ADV depth profile (minimum 5 locations spaced evenly throughout depth)
-  Propeller meter measurement
-  Turbine Fence





NOTE: (1) Wave probes to be placed at all locations where velocity measurements are made
 (2) Or denotes the origin
 (3) All fences are 1.8 m long

Test 1: Close grid no turbine	
PerAWAT	Date: 15/12/2011



 This could be changed to propeller meter if not enough ADVs

Key

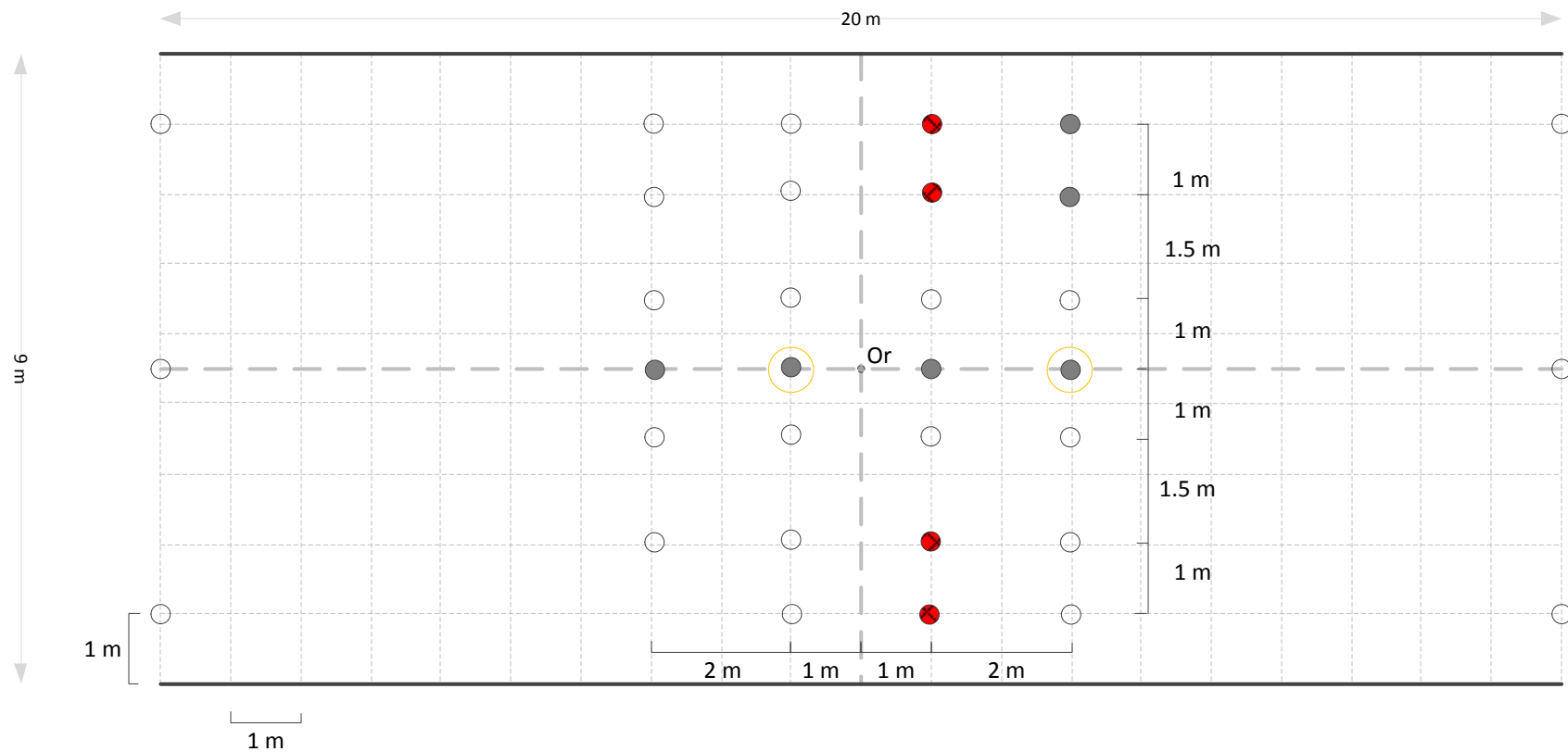
-  ADV point measurement
-  ADV depth profile (minimum 5 locations spaced evenly throughout depth)
-  Propeller meter measurement
-  Turbine fence


NOTE: (1) Wave probes to be placed at all locations where velocity measurements are made
 (2) Or denotes the origin
 (3) All fences are 1.8 m long: Fence centre at (0,0)

Test 2: Close grid with turbine





PerAWAT

Date: 15/12/2011



 This could be changed to propeller meter if not enough ADVs

Key

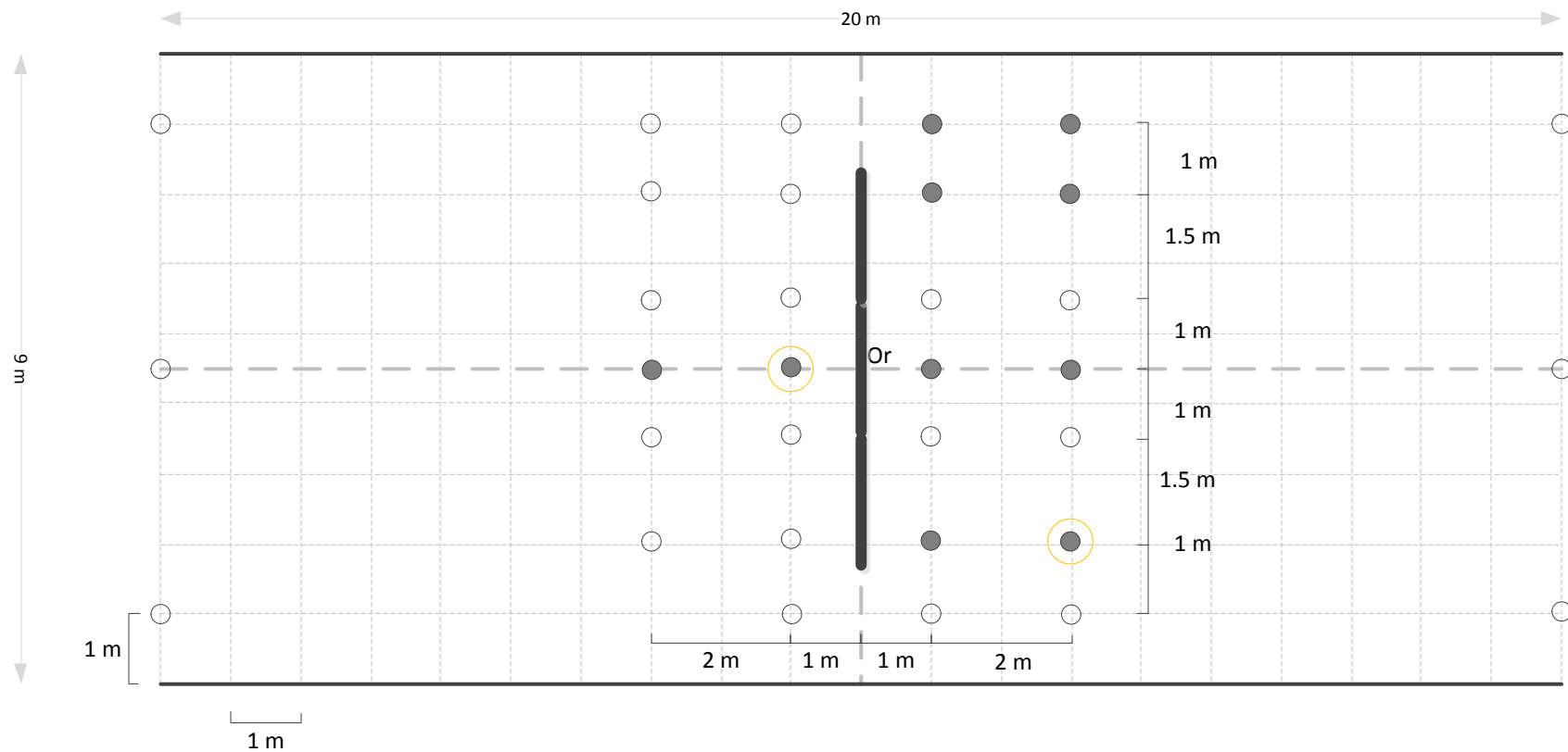
-  ADV point measurement
-  ADV depth profile (minimum 5 locations spaced evenly throughout depth)
-  Propeller meter measurement
-  Turbine Fence


NOTE: (1) Wave probes to be placed at all locations where velocity measurements are made
 (2) Or denotes the origin
 (3) All fences are 1.8 m long

Test 3: Wider grid no turbines





PerAWAT

Date: 15/12/2011



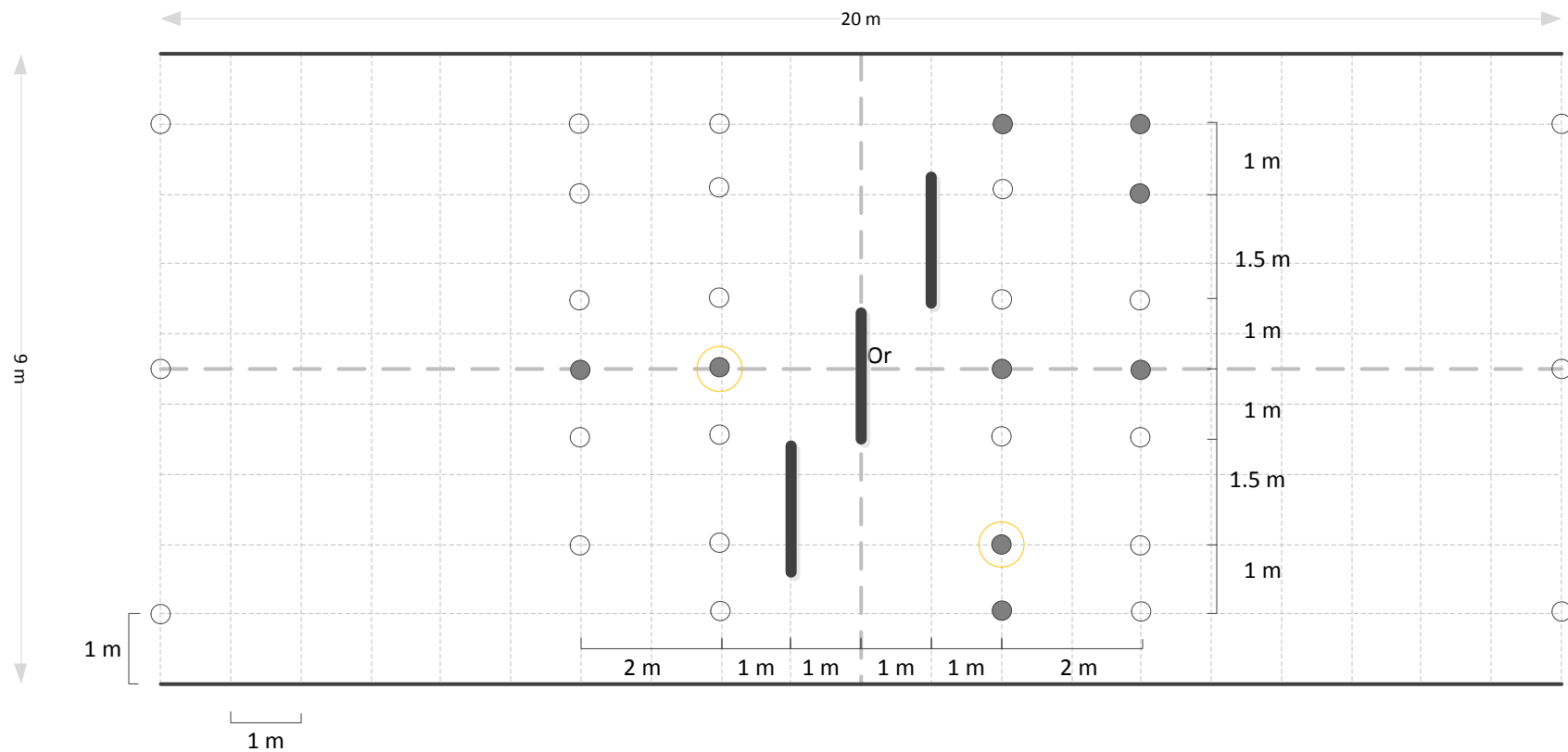
 This could be changed to propeller meter if not enough ADVs


Key

-  ADV point measurement
-  ADV depth profile (minimum 5 locations spaced evenly throughout depth)
-  Propeller meter measurement
-  Turbine Fence





NOTE: (1) Wave probes to be placed at all locations where velocity measurements are made
 (2) Or denotes the origin
 (3) All fences are 1.8 m long: Fence centres at (0,0), (0,1.8), (0,-1.8)

Test 4: Wider grid all together	
PerAWAT	Date: 15/12/2011



 This could be changed to propeller meter if not enough ADVs

Key

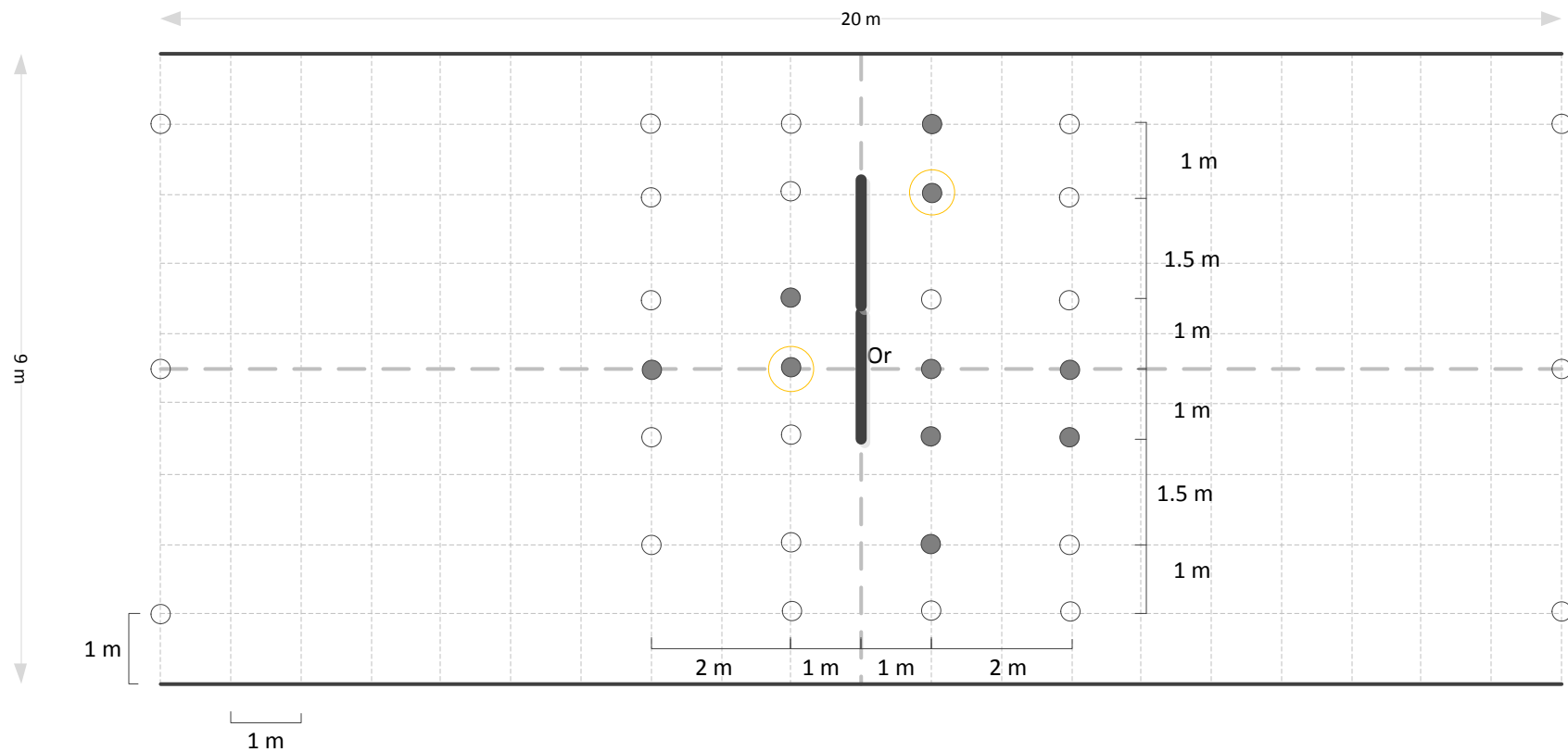
-  ADV point measurement
-  ADV depth profile (minimum 5 locations spaced evenly throughout depth)
-  Propeller meter measurement
-  Turbine Fence


NOTE: (1) Wave probes to be placed at all locations where velocity measurements are made
 (2) Or denotes the origin
 (3) All fences are 1.8 m long: Fence centres at (0,0), (-1,1.8),(1,-1.8)

Test 5: Staggard





PerAWAT

Date: 15/12/2011



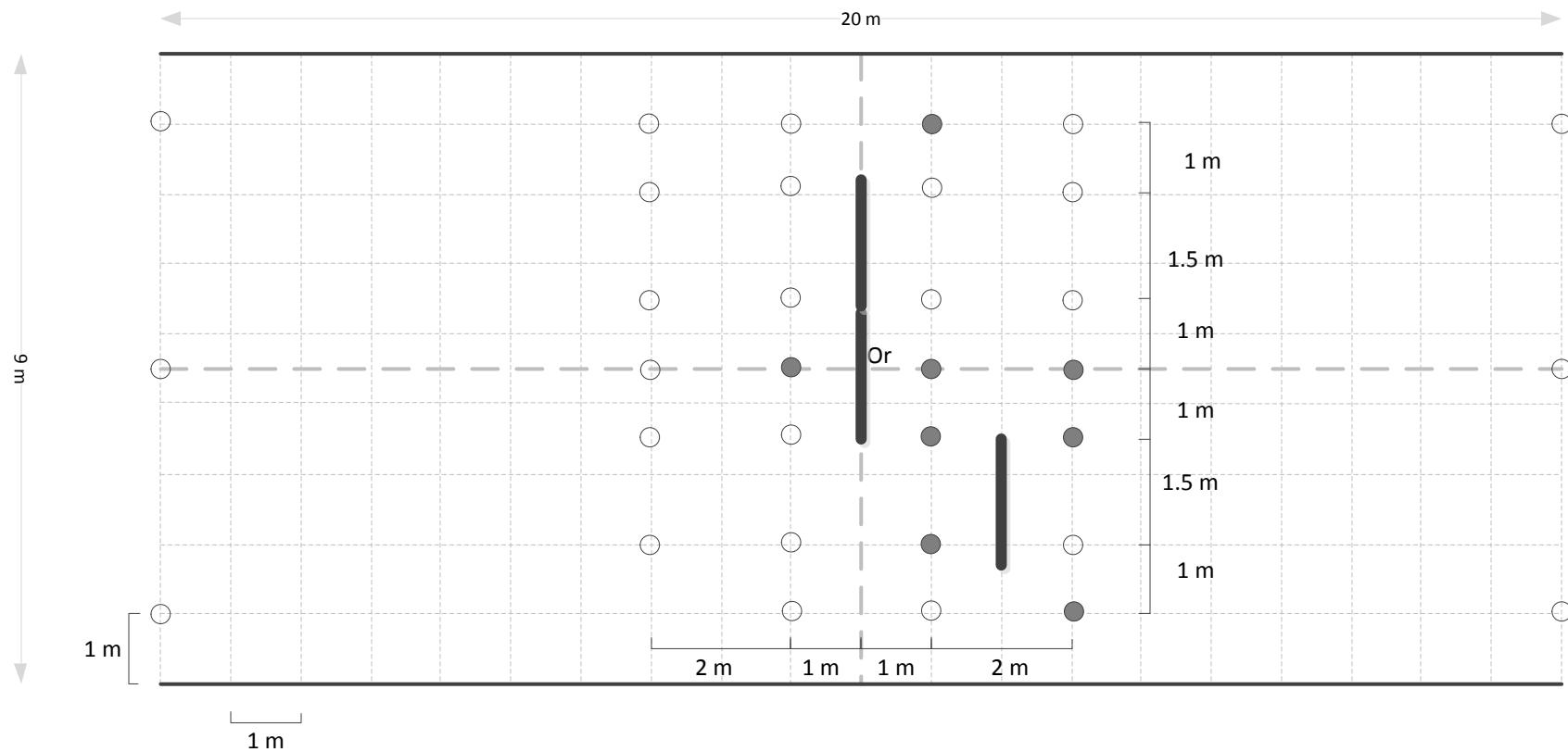
 This could be changed to propeller meter if not enough ADVs

Key

-  ADV point measurement
-  ADV depth profile (minimum 5 locations spaced evenly throughout depth)
-  Propeller meter measurement
-  Turbine Fence

NOTE: (1) Wave probes to be placed at all locations where velocity measurements are made
 (2) Or denotes the origin
 (3) All fences are 1.8 m long: Fence centres at (0,0), (0,1.8)

Test 6:Wide grid asymmetric	
PerAWAT	Date: 15/12/2011



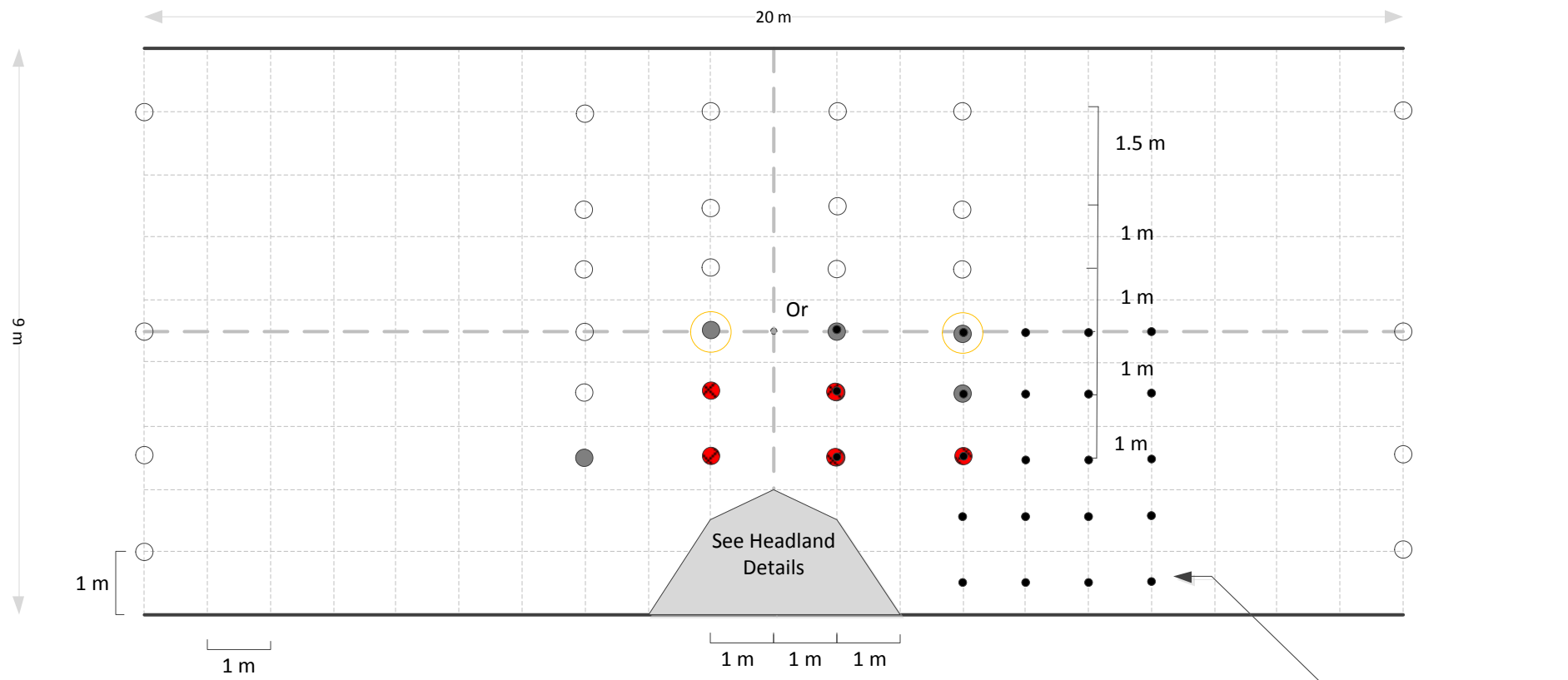
Key

- ADV point measurement
- ⊗ ADV depth profile (minimum 5 locations spaced evenly throughout depth)
- Propeller meter measurement
- ▬ Turbine Fence

○ This could be changed to propeller meter if not enough ADVs

NOTE: (1) Wave probes to be placed at all locations where velocity measurements are made
 (2) Or denotes the origin
 (3) All fences are 1.8 m long: Fence centres at (0,0), (0,1.8), (1,-1.8)

Test 7: Wider grid 2 asymmetric	
PerAWAT	Date: 15/12/2011



○ This could be changed to propeller meter if not enough ADVs

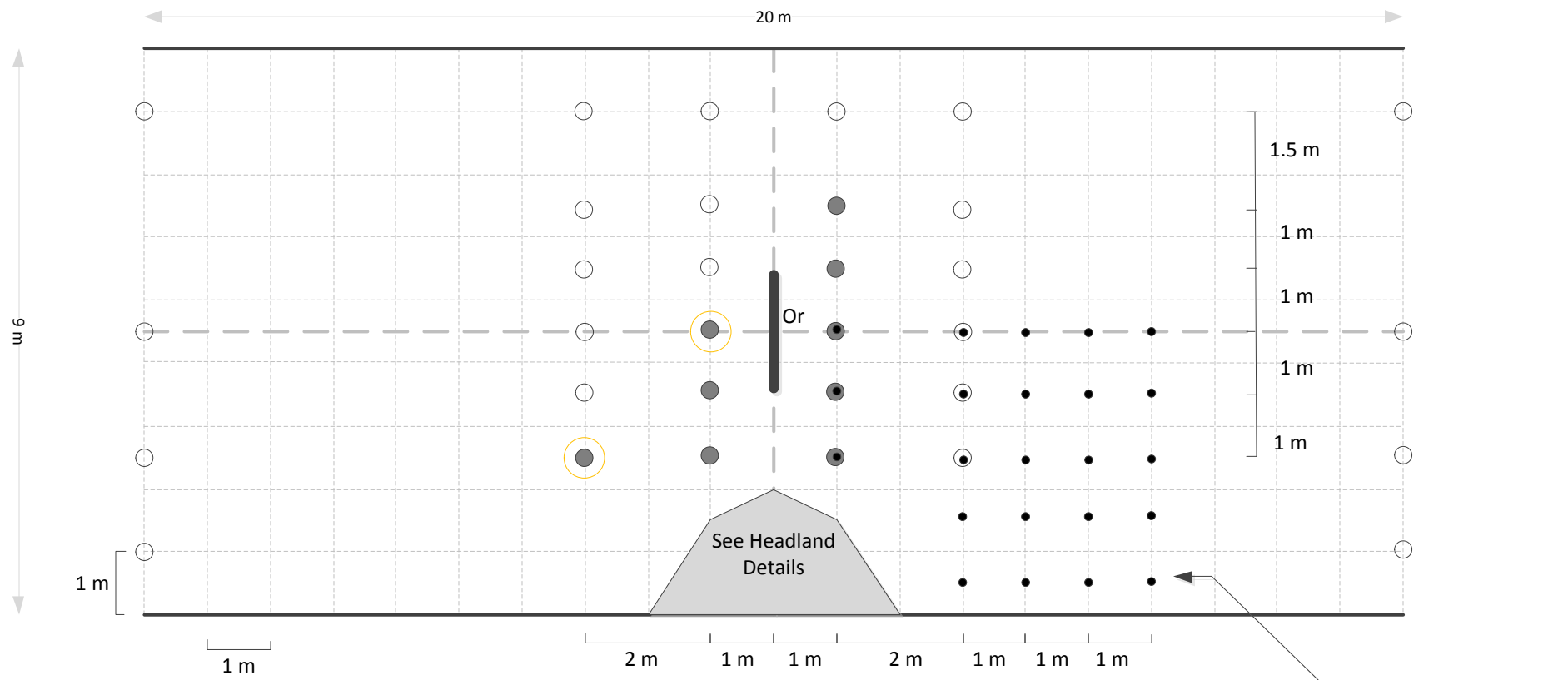
Points in Second Measurement

Key

- ADV point measurement
- ⊗ ADV depth profile (minimum 5 locations spaced evenly throughout depth)
- Propeller meter measurement
- ▬ Turbine Fence

NOTE: (1) Wave probes to be placed at all locations where velocity measurements are made
 (2) Or denotes the origin
 (3) All fences are 1.8 m long

Test 8: Base Case 1	
PerAWAT	Date: 15/12/2011

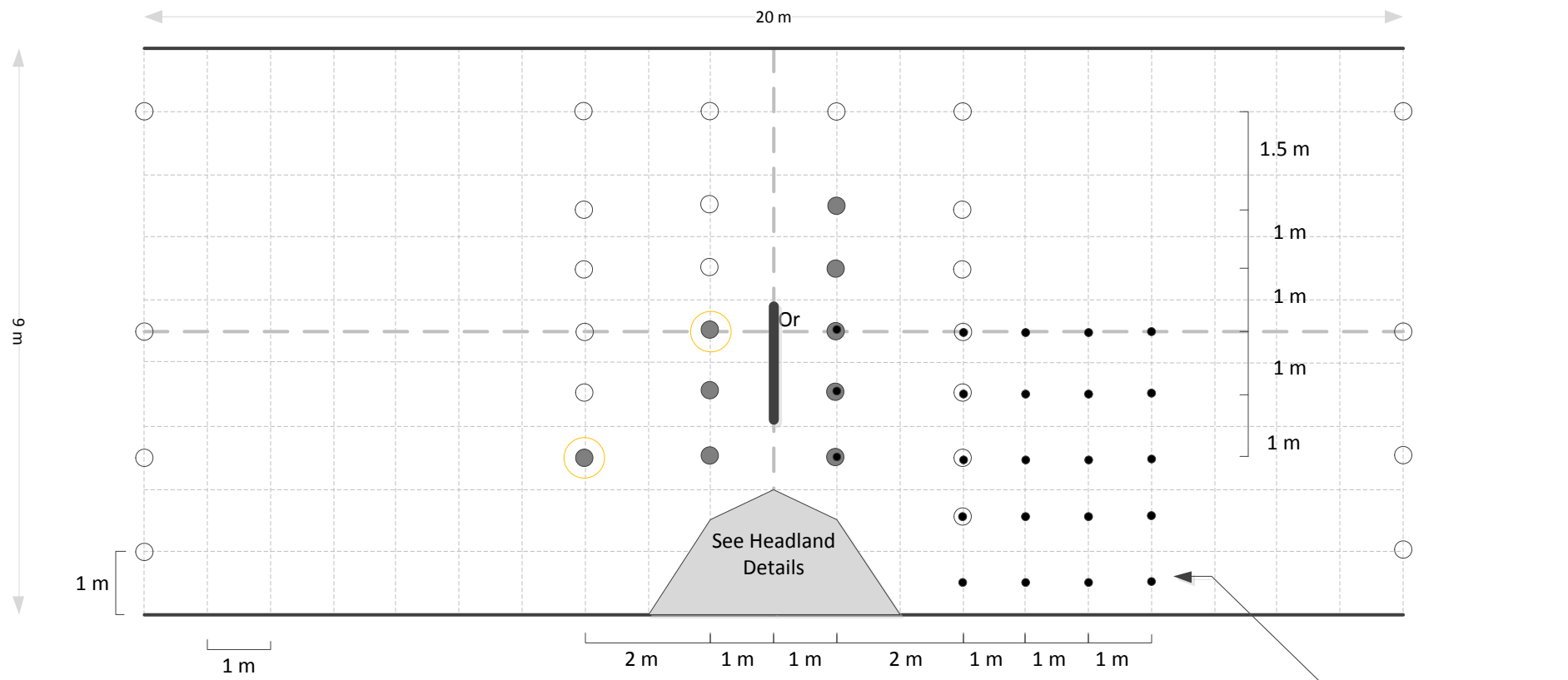


Key

- ADV point measurement
- ⊗ ADV depth profile (minimum 5 locations spaced evenly throughout depth)
- Propeller meter measurement
- ▬ Turbine Fence

NOTE: (1) Wave probes to be placed at all locations where velocity measurements are made
 (2) Or denotes the origin
 (3) All fences are 1.8 m long: Fence centres at (0,0)

Test 9: Turb 1	
PerAWAT	Date: 15/12/2011



○ This could be changed to propeller meter if not enough ADVs

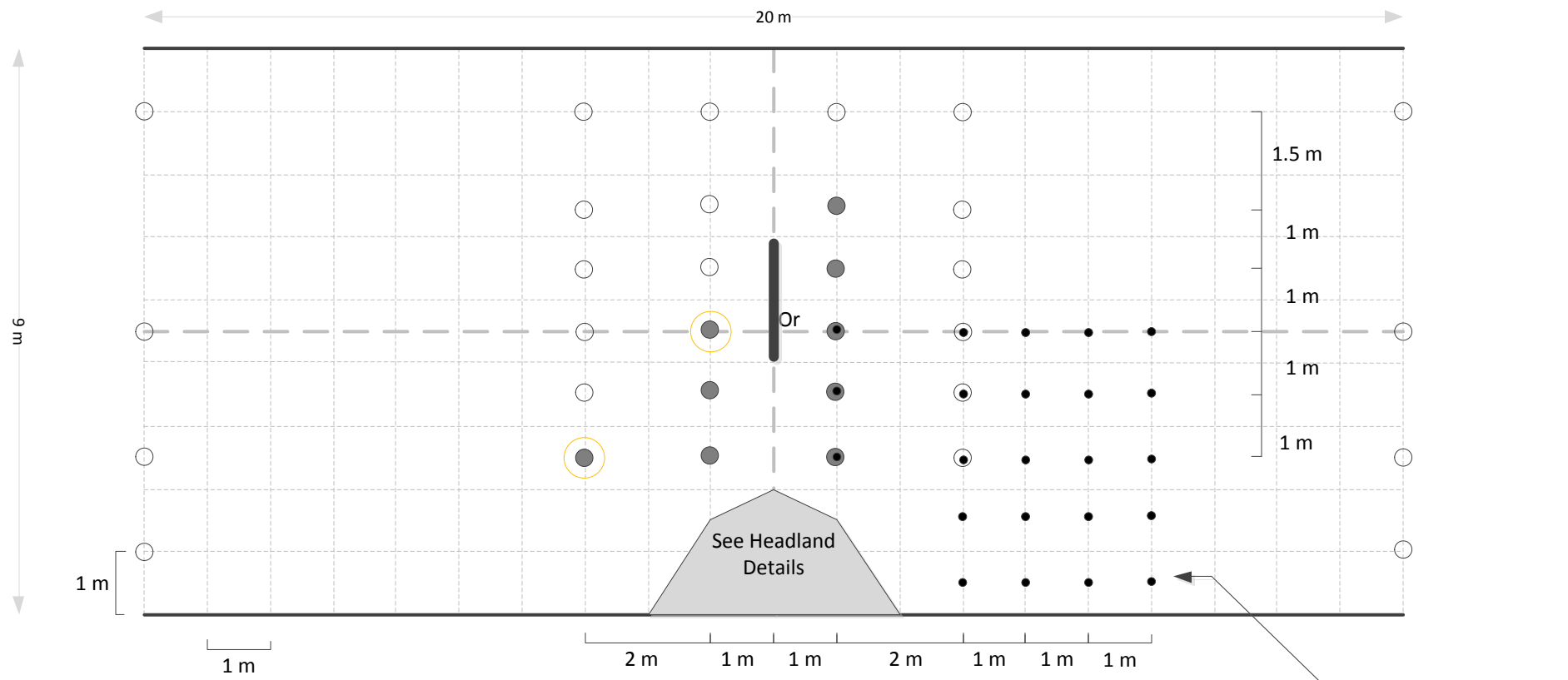
Points in Second Measurement

Key

- ADV point measurement
- ⊗ ADV depth profile (minimum 5 locations spaced evenly throughout depth)
- Propeller meter measurement
- ▬ Turbine Fence

NOTE: (1) Wave probes to be placed at all locations where velocity measurements are made
 (2) Or denotes the origin
 (3) All fences are 1.8 m long: Fence centres at (0,-0.5)

Test 10: Turb 2	
PerAWAT	Date: 15/12/2011

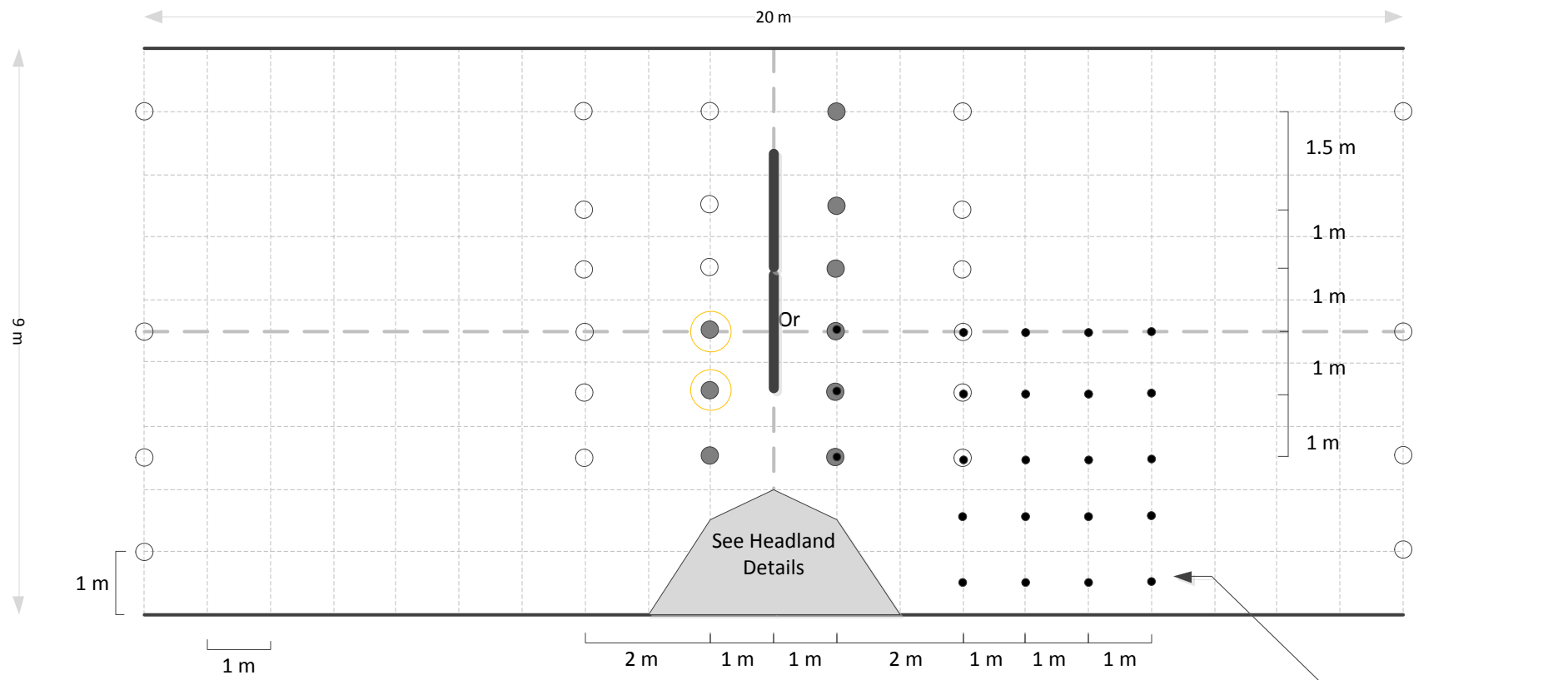


Key

- ADV point measurement
- ⊗ ADV depth profile (minimum 5 locations spaced evenly throughout depth)
- Propeller meter measurement
- ▬ Turbine Fence

NOTE: (1) Wave probes to be placed at all locations where velocity measurements are made
 (2) Or denotes the origin
 (3) All fences are 1.8 m long: Fence centres at (0,+0.5)

Test 11: Turb 3	
PerAWAT	Date: 15/12/2011

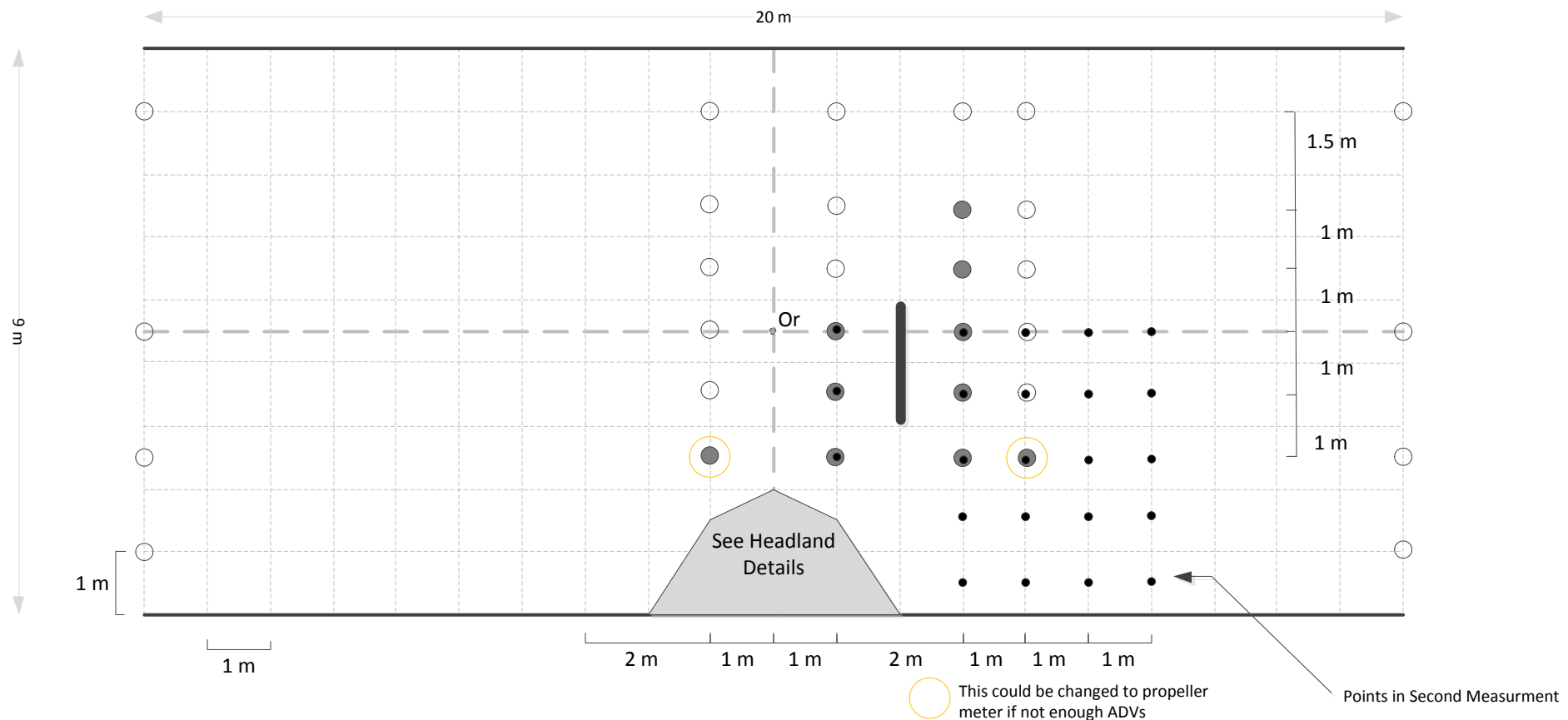


Key

- ADV point measurement
- ⊗ ADV depth profile (minimum 5 locations spaced evenly throughout depth)
- Propeller meter measurement
- ▬ Turbine Fence

NOTE: (1) Wave probes to be placed at all locations where velocity measurements are made
 (2) Or denotes the origin
 (3) All fences are 1.8 m long: Fence centres at (0,0), (0,1.8)

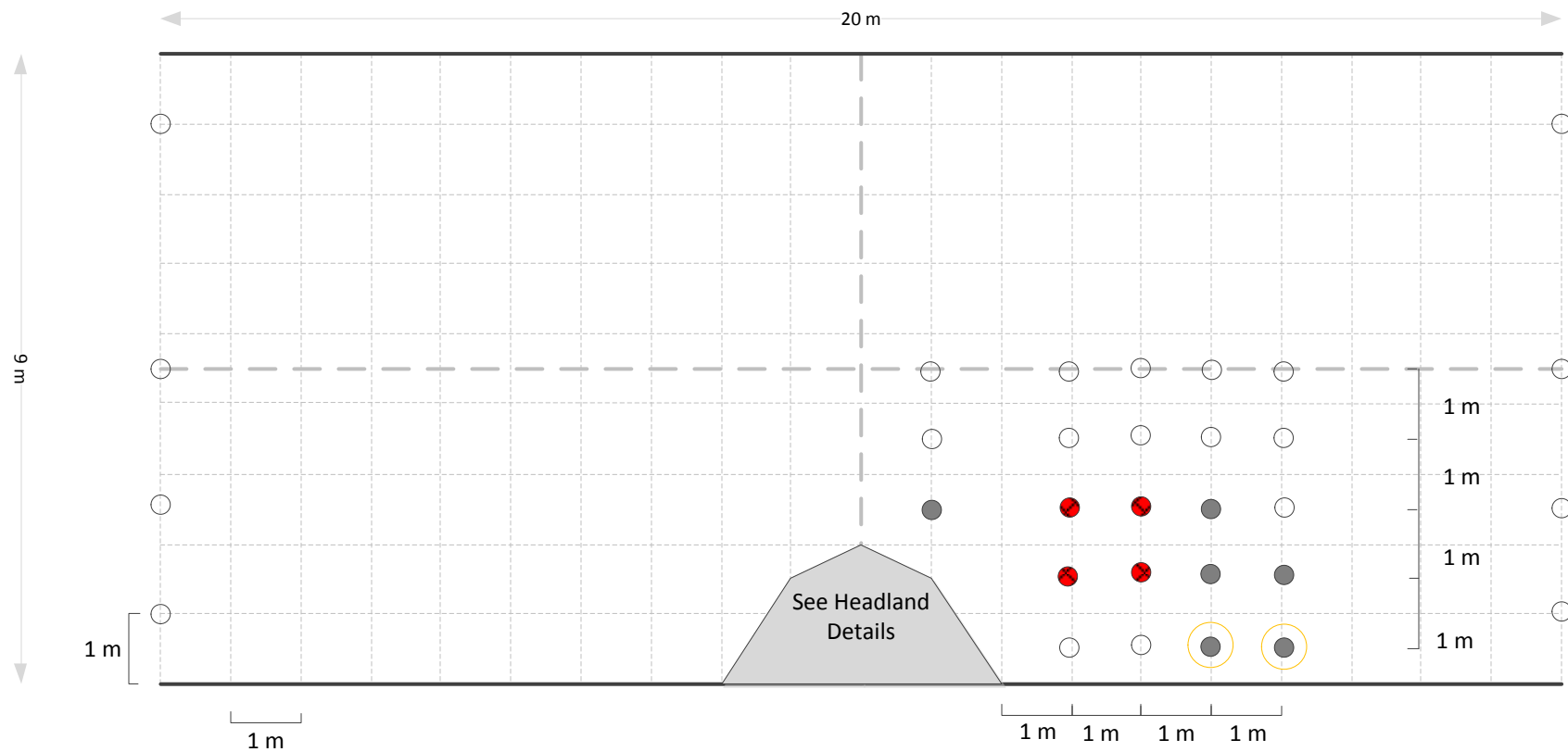
Test 12: Turb 4	
PerAWAT	Date: 15/12/2011



- Key**
- ADV point measurement
 - ⊗ ADV depth profile (minimum 5 locations spaced evenly throughout depth)
 - Propeller meter measurement
 - ▬ Turbine Fence

NOTE: (1) Wave probes to be placed at all locations where velocity measurements are made
 (2) Or denotes the origin
 (3) All fences are 1.8 m long: Fence centres at (-2,-0.5)

Test 13: Turb 5	
PerAWAT	Date: 15/12/2011



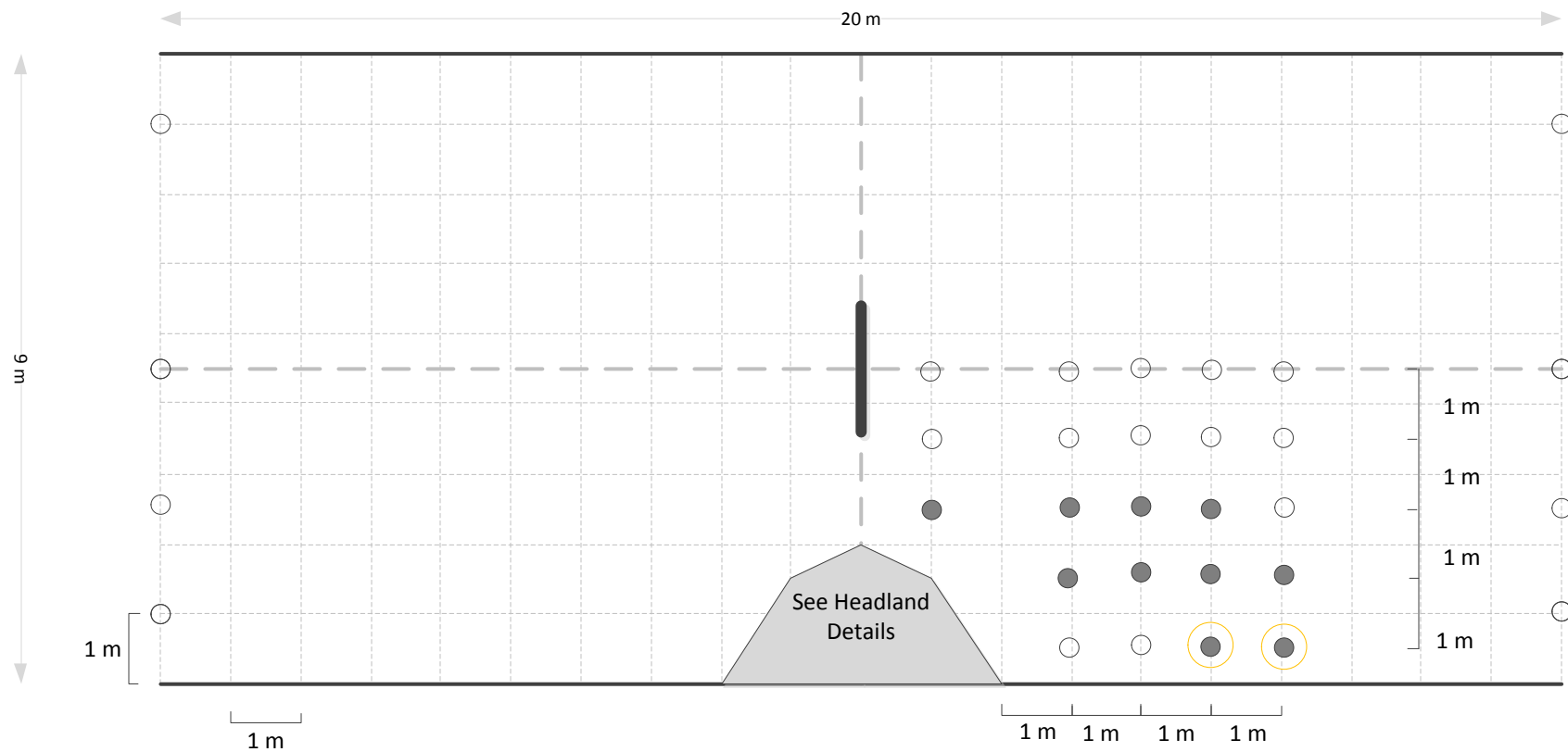
○ This could be changed to propeller meter if not enough ADVs

Key

- ADV point measurement
- ⊗ ADV depth profile (minimum 5 locations spaced evenly throughout depth)
- Propeller meter measurement
- Turbine Fence

NOTE: (1) Wave probes to be placed at all locations where velocity measurements are made
 (2) Or denotes the origin
 (3) All fences are 1.8 m long

Test 14: Base Case 2	
PerAWAT	Date: 15/12/2011



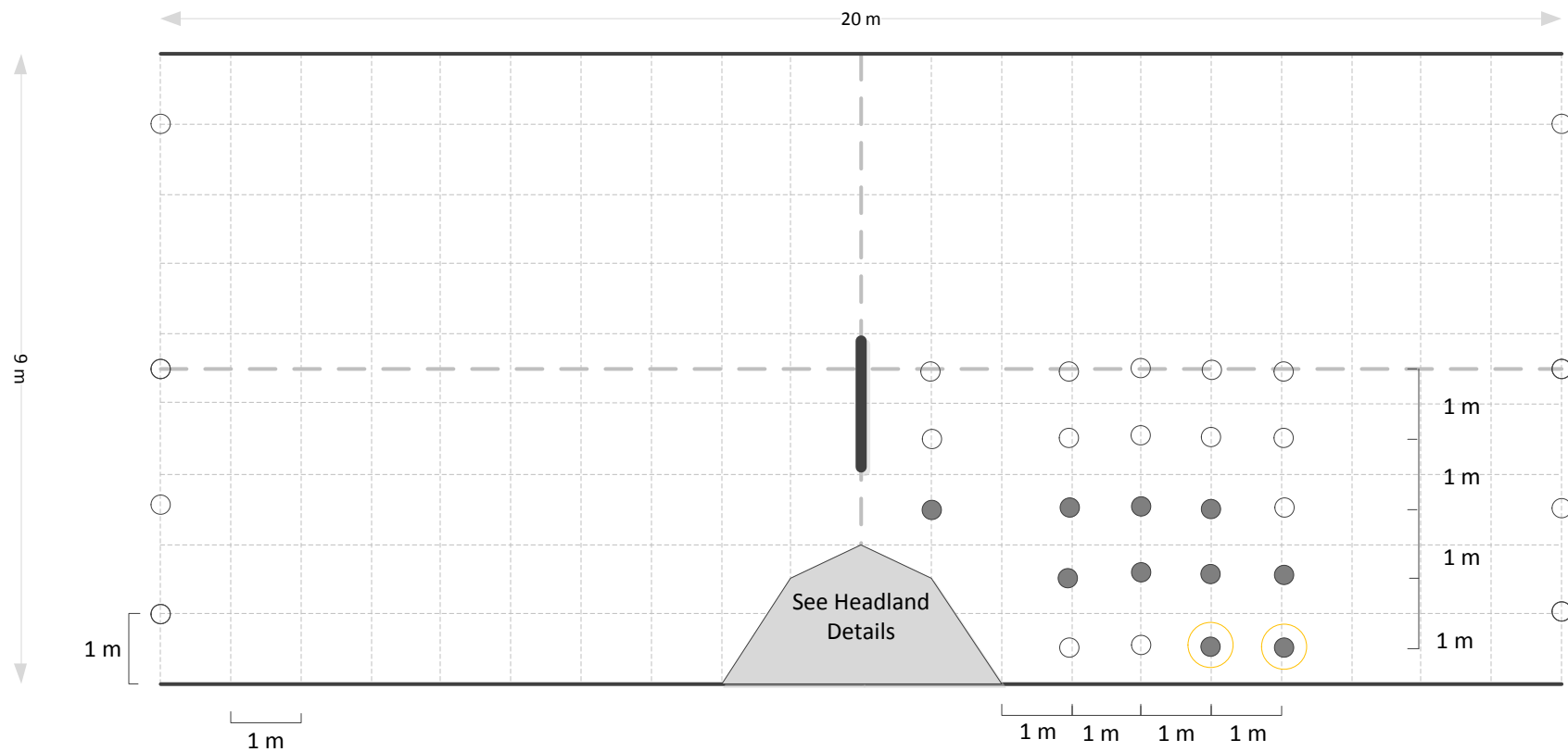
○ This could be changed to propeller meter if not enough ADVs

Key

- ADV point measurement
- ⊗ ADV depth profile (minimum 5 locations spaced evenly throughout depth)
- Propeller meter measurement
- ▬ Turbine Fence

NOTE: (1) Wave probes to be placed at all locations where velocity measurements are made
 (2) Or denotes the origin
 (3) All fences are 1.8 m long: Fence centres at (0,0)

Test15: Turb 1, wake meas.	
PerAWAT	Date: 15/12/2011



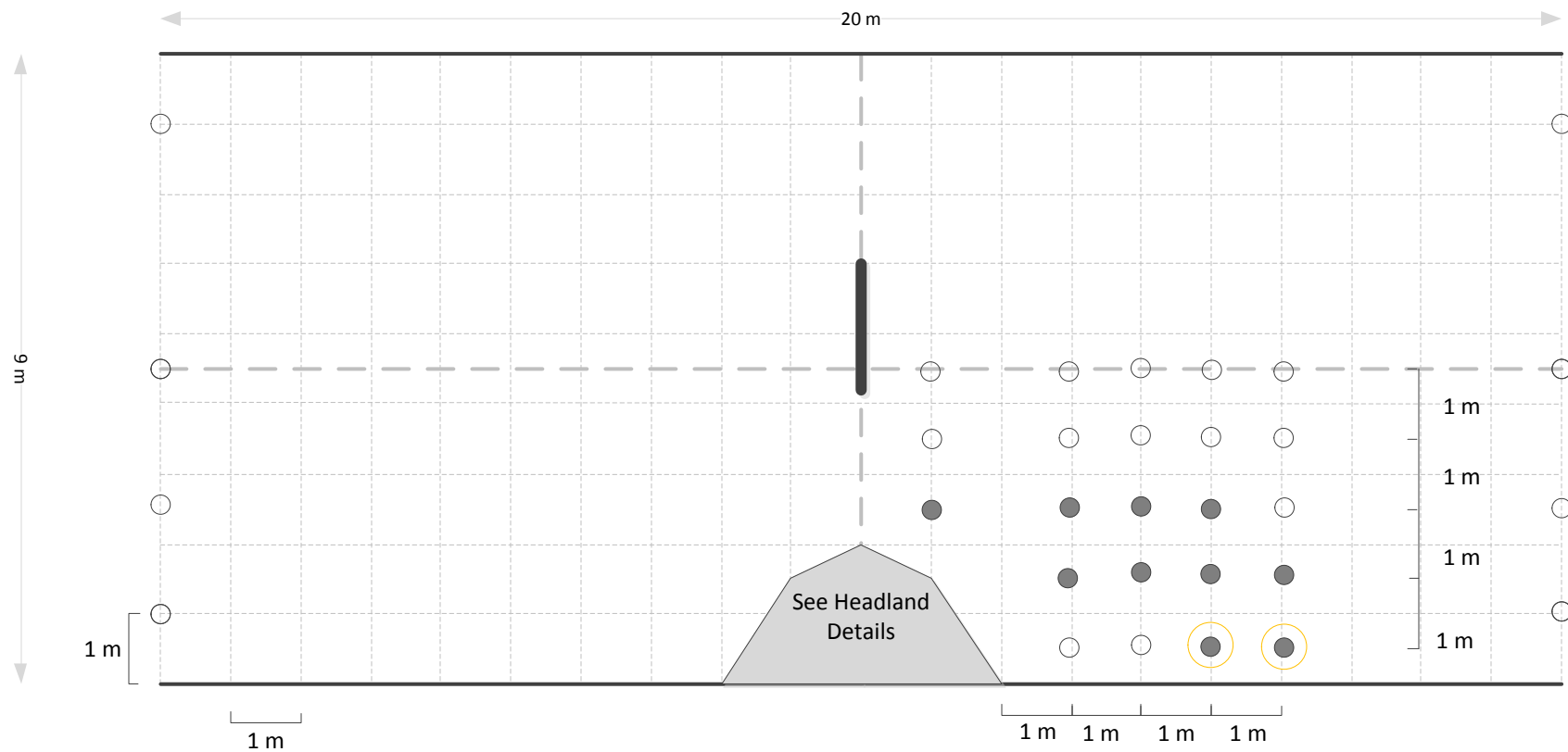
○ This could be changed to propeller meter if not enough ADVs

Key

- ADV point measurement
- ⊗ ADV depth profile (minimum 5 locations spaced evenly throughout depth)
- Propeller meter measurement
- ▬ Turbine Fence

NOTE: (1) Wave probes to be placed at all locations where velocity measurements are made
 (2) Or denotes the origin
 (3) All fences are 1.8 m long: Fence centres at (0,-0.5)

Test15: Turb 2, wake meas.	
PerAWAT	Date: 15/12/2011



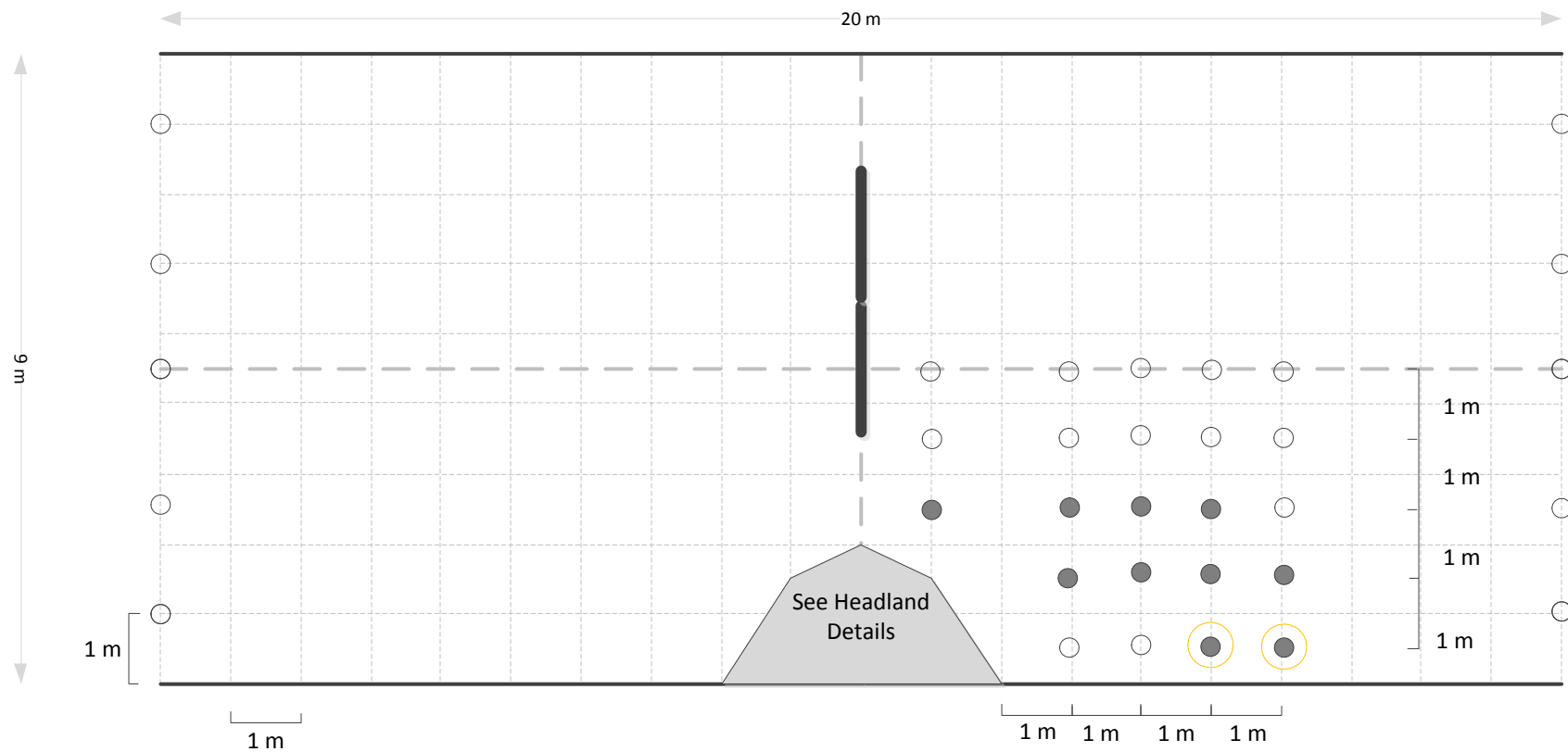
○ This could be changed to propeller meter if not enough ADVs

Key

- ADV point measurement
- ⊗ ADV depth profile (minimum 5 locations spaced evenly throughout depth)
- Propeller meter measurement
- ▬ Turbine Fence

NOTE: (1) Wave probes to be placed at all locations where velocity measurements are made
 (2) Or denotes the origin
 (3) All fences are 1.8 m long: Fence centres at (0,0.5)

Test15: Turb 3, wake meas.	
PerAWAT	Date: 15/12/2011



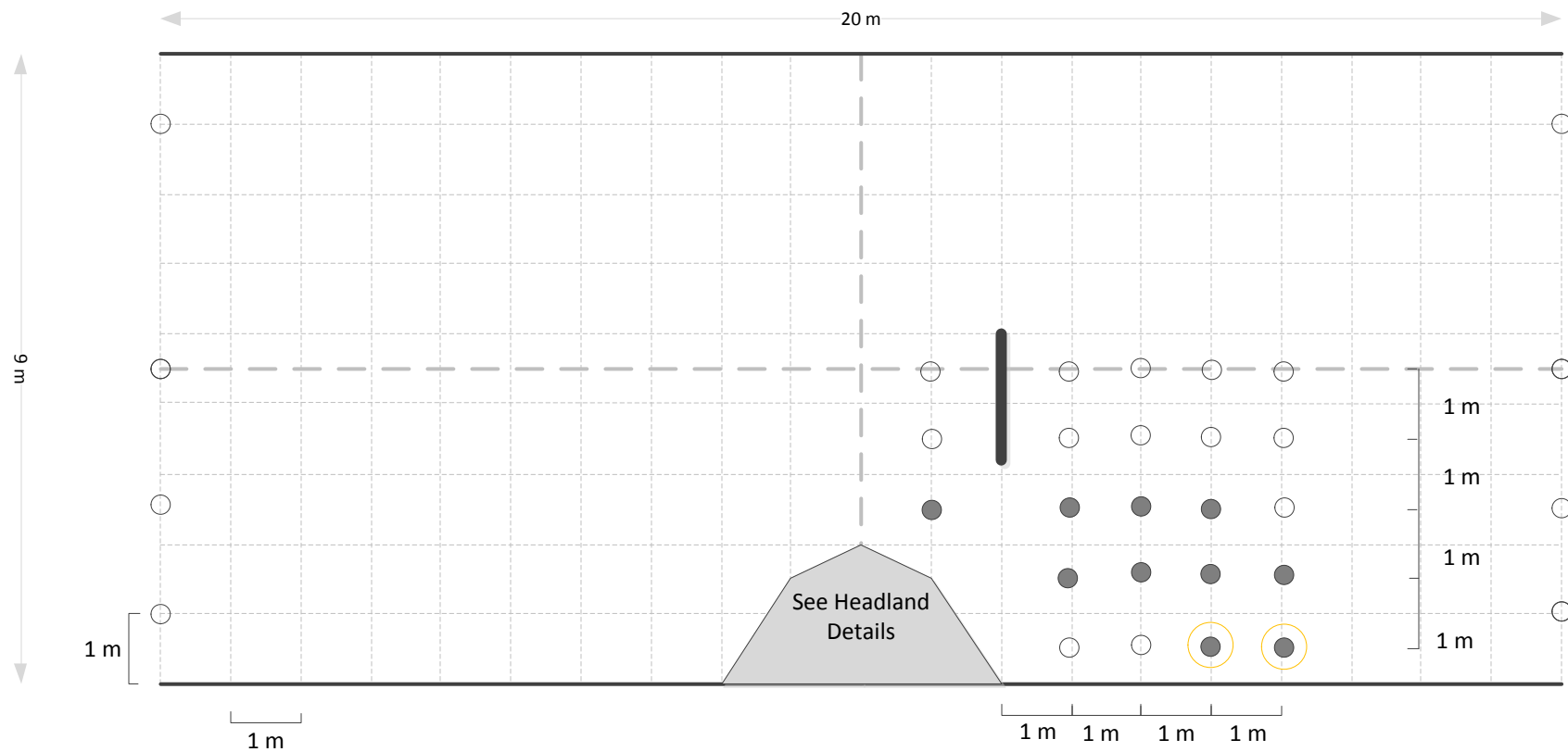
○ This could be changed to propeller meter if not enough ADVs

Key

- ADV point measurement
- ⊗ ADV depth profile (minimum 5 locations spaced evenly throughout depth)
- Propeller meter measurement
- Turbine Fence

NOTE: (1) Wave probes to be placed at all locations where velocity measurements are made
 (2) Or denotes the origin
 (3) All fences are 1.8 m long: Fence centres at (0,0), (0,1.8)

Test18: Turb 4, wake meas.	
PerAWAT	Date: 15/12/2011



○ This could be changed to propeller meter if not enough ADVs

Key

- ADV point measurement
- ⊗ ADV depth profile (minimum 5 locations spaced evenly throughout depth)
- Propeller meter measurement
- ▬ Turbine Fence

NOTE: (1) Wave probes to be placed at all locations where velocity measurements are made
 (2) Or denotes the origin
 (3) All fences are 1.8 m long: Fence centres at (-2,-0.5)

Test19: Turb 5, wake meas.	
PerAWAT	Date: 15/12/2011



THE UNIVERSITY OF
WESTERN AUSTRALIA
Achieving International Excellence

PERAWAT

WG4WP4, MILESTONE 1: SPECIFICATION FOR PHYSICAL SCALE MODELLING

Report to Garrad Hassan & Partners Ltd

January 2012

UWA Job No: 11600

DOCUMENT INFORMATION SUMMARY

Item	Description			
Client name	Garrad Hassan & Partners Ltd			
Client contact	Mat Thomson St Vincent's Works Silverthorne Lane Bristol, BS2 0QD UNITED KINGDOM			
Client reference	Purchase Order			
Date of issue	25/01/2012			
Report title	WG4WP4: Physical Scale Modelling Specification			
Report number	11600			
Version	Date of issue	Prepared	Verified	Comments
V0	24/12/2011	SD	MT, SW	Draft for review
V1	25/01/2012	SD		Revised draft for review

TABLE OF CONTENTS

1	Summary	6
2	Introduction	6
2.1	Background.....	6
2.2	Objectives of Work Package 4 (WG4 WP4).....	7
2.3	Aims of this Report: Milestone 1 (M1)	8
3	Preliminaries.....	8
3.1	Experimental Facilities at HR Wallingford.....	8
3.1.1	Previous experiments in the wave and current tank at HR Wallingford.....	9
3.1.2	Timing Constraints of the Experimental Program	9
3.2	Review of Coastal Sites around the UK.....	9
3.3	Similitude arguments in model scale tidal flows.....	10
3.3.1	Close to the devices.....	10
3.3.2	Far from the devices.....	11
3.3.3	Froude Scaling.....	11
3.3.4	Laboratory Effects.....	12
3.4	Problems with producing a model scale of the Pentland Firth.....	12
3.5	Arguments for scale model of an idealized coastal headland and tidal channel	13
3.5.1	Prototype Headland and Channel Scales.....	14
4	Numerical Simulations of tidal flow	14
4.1	Background.....	14
4.2	Turbine Fence modeled	16
4.3	Boundary Conditions Used in the Numerical Model	16
4.3.1	Numerical Boundary Conditions: Comparison to Model Experiments	16
4.3.2	Model Experiment Boundary Conditions: Comparison to Prototype	17
4.4	Numerical and Physical Accuracy of the Numerical Model Predictions	18
5	Model Geometry	19

5.1	Tidal Channel	19
5.1.1	Summary and Comparison to Prototype	20
5.2	Coastal Headland	20
5.2.1	Appropriate Bed Roughness	21
5.2.2	Velocity and Headland Plan Dimensions	22
5.2.3	Bathymetry surrounding the headland	23
5.2.4	Summary and Comparison to Prototype	24
6	Location of Tidal Fence	24
6.1	Tidal Channel	24
6.1.1	Discussion on Results	25
6.1.2	Variation in Boundary Condition	27
6.1.3	Conclusions and Measurement Locations	29
6.2	Coastal Headland	29
6.2.1	Discussion on Results	30
6.2.2	Conclusions and Measurement Locations	31
7	Summary and Specification of Experiments	31
7.1	Geometry	31
7.2	Flow Conditions	32
7.2.1	Note on Depth-Averaged Velocities	33
7.2.2	Calculating In-situ Roughness Length, z_0	33
7.3	Measurements and Measurement Locations	34
8	Conclusions	34
9	References	36
Appendix A – Scale Analysis		37
A1.	Introduction	38
A2.	Similitude arguments close to tidal devices	38
A3.	Similitude arguments far from tidal devices	39

Annex 1: Channel and Headland Geometry

Annex 2: Experimental measurement locations and tidal fence locations.

TABLES AND FIGURES ARE LISTED AT THE END OF DOCUMENT

PERAWAT

WG4 WP4: PHYSICAL SCALE MODELLING SPECIFICATION

1 SUMMARY

This report documents the work undertaken to select model scale geometries, and model turbine fence placement, for the physical scale tests to be conducted in WG4 WP4.

The choice of geometries and fence locations was determined from (i) a survey of sites around the UK, (ii) past experience in physical model testing and (iii) numerical simulations at model scale.

The model and fence location selection are summarised (in Section 7) in terms of:

- Specification of model geometry
- Specification of the inflow and outflow model tidal current boundary conditions
- Specification of the scale, thrust characteristic and layout of the array emulators
- Specification of the location for flow measurement devices for model comparison purposes

A scope of work for HR Wallingford to undertake these tests has been authored by Garrad Hassan & Partners with input from the project team. The scope of work is consistent with this report.

2 INTRODUCTION

2.1 Background

Garrad Hassan & Partners Ltd is leading a consortium of universities and utilities engaged in the Energy Technologies Institute (ETI) funded project: Performance Assessment of Wave and Tidal Array Systems (PerAWaT). The purpose of the project is to reduce the risk and uncertainty presently faced by marine energy device developers and investors, through the development of validated numerical tools and models to predict the potential energy extraction of different devices and arrays of devices at actual coastal locations.

The PerAWaT project considers both wave and tidal stream energy devices. The tidal work stream is focused on two principal activities

- (1) Numerical modeling (denoted as Working Group 3 WG3) and
- (2) Physical scale modeling (denoted as Working Group 4 WG4).

Both of these activities aim to build understanding of tidal energy extraction by separately investigating the performance of (i) individual tidal energy devices, (ii) arrays of tidal energy devices and (iii) devices deployed at a realistic coastal site. (A more complete breakdown of the organization of PerAWaT and the associated work packages are given in Rawlinson-Smith (2010)).

This report forms part of Work Package 4 (WP 4), which is concerned solely with physical scale modeling (i.e. WG4) of the performance of devices deployed at a coastal site (i.e. at the basin scale). The report supports the first deliverable (D1) in WP 4, which is to design and document a physical scale model test specification.

2.2 Objectives of Work Package 4 (WG4 WP4)

WP 4 is concerned solely with undertaking physical model scale experiments to simulate tidal energy devices deployed at a coastal site. Experiments will be conducted at HR Wallingford. The work package is distinct from other work packages in WG4, which have focused on physical modeling of devices (WP 1, WP 3) and arrays of devices (WP 2, WP 3, WP 5), but do not account for the surrounding geometry of a realistic coastal site.

The objective of WP4 is to investigate the impact of devices on the global flow field (e.g. the change in flow speed and elevation at regional/basin scale). Two outcomes are anticipated:

- (1) Validation of the basin scale numerical modeling of energy extraction (in WG3).
- (2) Critical evidence for stakeholders assessing the viability of large scale energy extraction.

The work package is split into three milestones and associated deliverables:

- Milestone 1: Developing a physical scale modelling specification.
 - Deliverable 1: Design and test specification
- Milestone 2: Characterisation of tidal device arrays, to be used in the coastal basin models, in a controlled environment.
 - Deliverable 2: Construction, testing and characterisation of device arrays
- Milestone 3: Construction and calibration of test equipment, undertake physical scale experiments and the documentation of experimental data.
 - Deliverable 3: Construction, calibration, testing and reporting of coastal basin scale experiments.

This report is only concerned with Milestone 1 and documents a test specification together with the design process that was used to form it.

2.3 Aims of this Report: Milestone 1 (M1)

The aim of this report is to outline an experimental schedule for a series of model scale tests (in accordance with Milestone 1 and Deliverable 1, listed in Section 2.2). To form this schedule work (including numerical simulations) has been undertaken to choose:

1. The most appropriate coastal site geometry
2. Location of model scale energy extractors within the coastal site: Including (i) the dimensions of the devices and (ii) the best location to place the devices.
3. The most appropriate measurements and recordings to be taken during each model scale experiment

Following some preliminaries, each of these areas of work is discussed in detail in the remainder of this report. The resulting experimental schedule is then documented and described.

3 PRELIMINARIES

3.1 Experimental Facilities at HR Wallingford

The experiments will be undertaken in the wave and current basin at HR Wallingford. The basin has plan dimensions of approximately 54 m by 27 m. A design wave field can be simulated within the basin through the control of 0.5 m wide paddles and, more importantly for the experiments proposed in this work package, tidal flows can also be simulated using four computerized pumps and fine tuning discharge rates through 40, 0.5 m wide inlet channels at each end of the basin. The range of operating water depths are believed to be between 0.3 m to 0.8 m.

A range of different coastal bathymetries can be constructed within the basin to model a particular coastal site. The material used to construct the bathymetry is dependent on the bathymetric form and detail required, and may include concrete barriers, hollow core blocks, etc.

Equipment for measuring water surface elevation and flow velocities are available (a detailed list of the measurement apparatus is given in Table 1). It is understood that 5 ADVs can be sourced in addition to the three listed in Table 1, giving a total of 8 (2 more may also be

sourced, but this is unlikely). Only 25, of the 34 listed in Table 1, of the miniature propeller current meters are believed to be available.

A computerized carriage can cover a 20 m by 20 m area (which will be used to support tidal devices). Care must be taken in avoiding significant variation in measurement locations between tests to ensure that the carriage is used efficiently.

3.1.1 Previous experiments in the wave and current tank at HR Wallingford

A previous experimental study concerning sand mounds in oscillatory flows has been undertaken in the wave and current basin at HR Wallingford (see Stansby et al. (2009)). In that study idealised channel geometry was constructed (see Figure 1) and oscillatory tidal currents having amplitude of approximately 0.5 m/s and period 1200 s were modelled. This previous study provides a very useful example of what can be achieved in the experimental facility.

3.1.2 Timing Constraints of the Experimental Program

It is anticipated that 3.5 weeks should be available for the experiments. Of this time, approximately 1 week is needed to set-up the coastal models and establish an experimental procedure (1 week assumes that a simple channel or headland geometry is adopted, consistent with that proposed in the experimental schedule outlined in Section 6).

3.2 Review of Coastal Sites around the UK

For the present work package it was initially suggested that model scale experiments would be undertaken for the Pentland Firth, Scotland. However, as discussed in Section 3.3, there are expected to be significant difficulties in reproducing representative tidal currents at model scale for a site such as the Pentland Firth. Consequently, to select more appropriate coastal (prototype) geometries for model scale experiments other locations around the UK have been reviewed.

Early studies by Black and Veatch (2004) and Black and Veatch (2005) suggest that there are up to approximately 57 locations, or ‘hot spots’, around the UK where natural tidal streams could be of sufficient size to support economical tidal stream energy extraction. Each of the hot spots have Spring tidal currents above approximately 2 m/s. The hot spots notably include the Pentland Firth, Bristol Channel and Anglesey, which are being studied in WG3 WP3 of PerAWaT.

Importantly, reviewing many of the coastal hot spots listed in Black and Veatch (2005) it is apparent that the majority of spots have geometries resembling coastal headlands (for example, Duncansby Head, Mull of Kintyre, Angelsey, Mull of Galloway and Portland Bill) and tidal channels (for example, Yell Sound, Pentland Firth, Papa Westray and Fall of Warness). In terms of tidal forcing mechanisms, the large tidal currents are observed close to coastal headlands because tidal streams are forced to accelerate around the headland, whereas large tidal currents exist in tidal channels because there is a difference of amplitude and/or phase in tidal elevation either side of the channel.

Based on the Black and Veatch summary of hot spots around the UK, it would thus appear to be advantageous, from the perspective of understanding the UK tidal resource, to investigate tidal stream energy extraction, and the effects of energy extraction on the natural flow field, in the context of tidal devices deployed within tidal channels and close to coastal headlands.

3.3 Similitude arguments in model scale tidal flows

For a model scale experiment to give a valuable representation of a larger coastal system (denoted as the prototype) all the major factors influencing the fluid mechanics must be in proportion between the prototype and model, while the factors which are not in proportion must have a negligible influence on the fluid mechanical behavior.

Appendix A identifies the factors (defined in terms of dimensionless numbers) expected to be important to the fluid mechanics in the model and prototype. A distinction is made between the flow field close to the tidal devices and far from the devices, where the flow field is locally three-dimensional, and horizontally two-dimensional, respectively.

3.3.1 Close to the devices

In a three dimensional free surface flow, applicable close to the tidal devices, it is well known that a geometrically undistorted model is required to achieve similitude in the advective accelerations and turbulent dissipative processes (Hughes, 1991). Assuming a geometrically undistorted model, dynamic similitude requires equality of the following dimensionless numbers (see Appendix A):

- Froude Number: $V/(gL)^{1/2}$
- Reynolds Number: VL/ν
- Keulegan-Carpenter Number: VT/L

where V is a characteristic velocity, L is a single characteristic length scale in all three directions, ν is viscosity, T is a characteristic time scale, and g is acceleration due to gravity.

3.3.2 *Far from the devices*

Far from the tidal devices the flow field is almost horizontal, and therefore two dimensional rather than three dimensional. The key dimensionless numbers include (see Appendix A):

- Froude Number: $V/(gH)^{1/2}$
- Horizontal Reynolds Number: VL/ν_t
- Kuelegan-Carpenter Number: VT/L
- Rossby number $Ro = V/Lf$, and
- Stability number $St = C_d L/H$.

where C_d is the depth averaged drag coefficient (this can be related to a roughness length at the seabed; see Equation 10, Section 7.2), ν_t is a depth-averaged eddy viscosity and, H and L now form two different length scales characterizing the vertical and horizontal directions, respectively. These two length scales are allowed for (see Hughes, 1991 and Appendix A). It should also be noted that the Froude number is based on the vertical dimension for depth-averaged flow, applicable far from the devices.

3.3.3 *Froude Scaling*

Traditionally Froude number scaling is undertaken in coastal model experiments, and the far field dynamics take precedence over any locally three dimensional small scale features (thus the scaling in Section 3.3.2 is adopted). The Froude number based on the depth is therefore set equal in the model and prototype:

$$\frac{g_m H_m}{V_m^2} = \frac{g_p H_p}{V_p^2}, \quad (1)$$

and the ratio of horizontal scale between the model and prototype (L_m/L_p) is allowed to differ from the vertical scale (H_m/H_p). In (1) the subscripts p and m denote the prototype and model, respectively. The adoption of a distorted model implies that the Reynolds stresses and the relative importance of vertical to horizontal diffusion is no longer in similitude between the model and prototype.

Pursuing the Froude scaling implied by (1), and noting that in almost all cases $g_m = g_p$, implies the velocity scale: $V_m/V_p = (H_m/H_p)^{1/2}$. The time scale then follows from the

Keulegan-Carpenter number and the horizontal length scale: $T_m/T_p = (L_m/L_p)^{1/2}$. The ratio of bed friction coefficient at model and prototype scale follows from the relative distortion of the model geometry: $(C_D)_m/(C_D)_p = (H_m/H_p) \cdot (L_p/L_m)$.

The remaining dimensionless numbers relevant for shallow water flow are the Rossby number and the horizontal Reynolds. The Rossby number cannot be matched in at model scale in the wave and current tank. Similarity of the Reynolds number cannot usually be achieved simultaneously with Froude similarity since the ratio between model and prototype horizontal Reynolds numbers (Hughes, 1992). Generally, however, incorrect modeling of the horizontal Reynolds number is expected to have little effect on shallow water flow over smooth bathymetry if eddy viscosity is sufficiently small that depth-averaged horizontal diffusion is negligible compared with the effects of, for example, the frictional processes parameterized by bed friction (Signell and Geyer, 1990).

Lastly, in addition to the conditions discussed above, there is a final important requirement in coastal basin models that the flow remains everywhere turbulent. This is necessary to ensure that the parameterization of bed friction and the interaction of the flow with the porous plate are appropriate in the model (the flow around the fence and the forces on the fence will change significantly if the flow becomes laminar). Turbulent flow is generally achieved when the Reynolds number, based on the vertical length scale and kinematic viscosity ($Re = VH/\nu$), is sufficiently greater than 10^3 (Jirka, 2001).

It is worth noting that if a distorted model is adopted in the model, the local field around the fence, including the geometry of the wake, may not be an ideal representation of the prototype based on the scaling arguments outlined in Section 3.3.1 and the associated appendix A.

3.3.4 Laboratory Effects

It is important to note that there are also often laboratory effects at model scale which affect the ability of a model to replicate the prototype. These may include the tidal boundary forcing conditions in the model and resolution of model bathymetry.

3.4 Problems with producing a model scale of the Pentland Firth

It was initially anticipated that $\sim 1/1000^{\text{th}}$ scale model of the Pentland Firth would be examined in this work package. However, modeling at this scale cannot be achieved easily for several reasons. These reasons include:

- Viscous Forces, Distorted Geometry and Model design: A $\sim 1/1000$ scale model of the Pentland Firth (with channel dimension ~ 30 km x 10 km) would fit into the HR Wallingford wave and current tank. However, for an undistorted model, depths of 60 m in the prototype translate to 6 cm in the model, and an average prototype velocity of 1.5 m/s scales to ~ 4.5 cm/s using Froude scaling. For these model conditions the depth Reynolds number is not sufficiently greater than 10^3 to ensure turbulent flow and so a carefully designed distorted model would be needed. The distortion is also needed to ensure adequate depth to place a model tidal fence.

Consequently, assuming a model depth of 20 cm is required to represent a 60 m prototype water depth (to fit the devices) would give a vertical scale of $\sim 1/300$. At this scale the model must be very carefully constructed because an error of 1 cm will equal 3 m in the prototype and could considerably alter, for example, the locations of maximum currents. To achieve good model accuracy would therefore require very careful (and time consuming) construction.

- Tidal Driving Boundary Conditions: To provide useful estimates of, for example, the Pentland Firth's tidal maximum energy potential using a physical model requires that the boundary forcing mechanisms to simulate the tide are correctly simulated at model scale. Within the HR Wallingford wave and current tank, tidal currents will be reproduced via computer controlled pumps which will produce a specific flow rate. However particular care is needed with these model boundary conditions because fixing the flow rate is fundamentally different to the prototype tide, which effectively fixes the tidal elevations on both sides of the Pentland Firth (due a phase lag in the propagation of the tides around the Orkney Islands) and not flow rate through the channel. A consequence of fixing the flow rate in the model experiments is that introducing many devices within the model will not reduce the flow rate (thus the power extracted must always increase with the addition of devices), whereas in the prototype the flow rate will reduce with the addition of devices (limiting power extraction).

3.5 Arguments for scale model of an idealized coastal headland and tidal channel

The preceding subsections have shown that modeling of a specific site such as the Pentland Firth is difficult due to the required detail in the model bathymetry, and it may not be possible to explore the maximum power potential at model scale unless the boundary conditions are carefully constructed (i.e. pump flow speed is varied). Because of this it has been decided that

idealized coastal geometries resembling a tidal channel and a coastal headland will be pursued instead. Several reasons for pursuing these idealized geometries include:

1. The idealized models can have a very simple bathymetry, reducing cost and construction times.
2. For coastal headlands and tidal channels the interactions of the devices with each other and the geometry will provide significant useful information on the performance of tidal devices in coastal basin. There is no need to pursue the maximum power potential of the sites and so the devices can have small resistance relative to the natural geometry (to be proven numerically in this report) such that boundary forcing is not important in the experiments.
3. The investigation of idealized sites is fundamental research and more general than analysis of a particular site.

3.5.1 Prototype Headland and Channel Scales

To determine the appropriate model scale for the idealized geometries, the typical prototype scales of tidal channels and coastal headlands around the UK are illustrated in Figure 2 and Figure 3. These figures summarise three of the five non-dimensional numbers for shallow water flows outlined in Section 3.3, namely the Froude number, Keulegan-Carpenter number and Stability number. For the tidal channel the horizontal length scale is the channel length, whereas for the coastal headland it is the headland breadth.

The remaining two non-dimensional numbers, the Reynolds and Rossby numbers cannot be matched at model scale simultaneously for any model geometry, see Section 3.3. However, previous studies have suggested that the first order tidal dynamics in tidal channels and close to coastal headlands can be well explained at the prototype scale by Froude number, Keulegan-Carpenter number and Stability number alone (for example, see Garrett and Cummins (2005) for tidal channels and Signell and Geyer (1991) for coastal headlands). A scale model of a headland or channel should therefore have similar non-dimensional values to those given in Figure 2 and Figure 3.

4 NUMERICAL SIMULATIONS OF TIDAL FLOW

4.1 Background

Numerical modeling is used in the remainder of this report to help choose the scale model dimensions of the idealized coastal headland and tidal channel, and to predict the flow fields

formed around the tidal devices. The numerical modeling approximates the shallow water equations (8) and (9), neglecting Coriolis forces, using the Discontinuous Galerkin Finite Element Method (see Draper (2011) for more information). Eddy viscosity is assumed to be constant throughout the domain, and is estimated as (Fischer et al. (1979)):

$$v_t = 0.2u_f h, \quad (2)$$

where $u_f = U_* C_d^{1/2}$ and U_* is the depth-averaged velocity. For $C_D = 0.008$ and a depth-averaged velocity of 0.3-0.5 m/s in 0.2 m of water depth, this leads to an eddy viscosity of $\sim 0.001-0.002 \text{ m}^2/\text{s}$.

To introduce tidal energy extraction into the numerical model it is assumed that tidal devices can be represented in the model as a porous strip, occupying a fraction of the water depth and extending laterally over a distance of several times the water depth. The near field surrounding the tidal devices in the numerical model is therefore approximated using actuator disc theory (see Draper (2011)), which amounts to the introduction of a thrust per unit width, along a line coinciding with the porous strip, of

$$T = \rho \frac{C_T B}{2} h U_* |U_*|, \quad (3)$$

where U_* is the depth-averaged velocity component passing normal to the strip, h is the fluid depth, C_T is the thrust coefficient and ρ is the fluid density. For a given Froude number the term C_T can be related via actuator disc theory to the geometry of the devices and their porosity (Draper et al. (2010)). Functionally it can be written as:

$$C_T = C_T(B, Fr, \alpha_4), \quad (4)$$

where Fr is the Froude number, B is the blockage ratio of the devices (for a porous strip this is given by the vertical width of the strip divided by the depth of the flow) and α_4 is related to the velocity in the wake of the strip. It should be noted that α_4 varies monotonically with the device porosity and the thrust coefficient is weakly dependent on Froude number.

The power extracted by the devices, per unit width, follows from equation (4) as:

$$P_E = \rho g U_* h \Delta h \left(1 - Fr^2 \frac{1 - \Delta h/(2h)}{\left(1 - \frac{\Delta h}{h}\right)^2} \right), \quad (5)$$

and the depth change Δh is related to the thrust coefficient via

$$\frac{1}{2}\left(\frac{\Delta h}{h}\right)^3 - \frac{3}{2}\left(\frac{\Delta h}{h}\right)^2 + \left(1 - Fr^2 + \frac{C_T B Fr^2}{2}\right)\left(\frac{\Delta h}{h}\right) - \frac{C_T B Fr^2}{2} = 0. \quad (6)$$

Alternative representations for the thrust term C_T are possible. For instance, an empirical relationship for the thrust coefficient, given as a function of the upstream velocity and device emulator characteristics, could be used.

4.2 Turbine Fence modeled

A schematic of the turbine fence to be used in the experiment is given in Figure 4. The length of the fence is 1.826 m, consisting of 14 circular porous discs with diameter 110 mm, spaced 1.2 diameters center to center. Similar emulators have been used in WG4 WP3. Previous characterization results from previous research in WG4 WP3 suggests that a thrust coefficient for each disc, based on the disc area, can be achieved in the range $C_T = 0.3 - 1.0$. The fence length has been chosen so that a fence can fit within the localized regions of higher velocity near the tip of the model headland (See Section 5.2) and to ensure that two fences fit easily within the channel when a headland is also present.

In terms of modeling the devices according to the theory outlined in Section 4.1, the fence in Figure 4 has been converted to a fence with equivalent blockage ratio and an equivalent α_4 for a given thrust coefficient. It has been assumed in the final simulations that a $C_T = 1.0$ can be achieved in the experiment (earlier calculations were also undertaken for a $C_T = 0.9$, these are listed clearly in Section 6).

Consequently, taking the flow depth to be 0.2 m the blockage ratio of the fence has been modeled as 0.36 (equal to that of the discs within the fence). To achieve a thrust coefficient of $C_T = 1.0$ at this blockage ratio requires a wake velocity coefficient of $\alpha_4 = 0.7$ when $Fr = 0$, and $\alpha_4 = 0.73$ for $Fr = 0.3$ (see Draper (2011) for details on this calculation). Given the negligible variation in α_4 with Froude number, a constant value of $\alpha_4 = 0.7$ is used to represent a fence with $C_T = 1.0$ in the numerical simulations ($\alpha_4 = 0.73$ is used for $C_T = 0.9$).

4.3 Boundary Conditions Used in the Numerical Model

4.3.1 Numerical Boundary Conditions: Comparison to Model Experiments

In most of the numerical simulations undertaken in this report a fixed depth-averaged velocity time series is specified at the left hand boundary of the channel to represent time varying or steady flow, and a fixed water depth of 0.2 m is specified at the right hand boundary of the channel. These boundary conditions are not identical to those expected in the experiments, which will use pumps which will circulate a volume of water at a fixed time varying flow rate whilst achieving a water depth within the channel of approximately 0.2 m.

Despite the differences, the numerical boundary conditions used in this report are expected to give very good predictions of the experiment (i.e. flow field around the headland, forces on the fences etc.) because the variation in depth along the channel is expected to be small in the experiments. Consequently a fixed upstream velocity (in the numerical model) is similar to a fixed flow rate (in the experiment) and a fixed downstream depth (in the numerical model) is very similar to a small variation in water depth (in the experiment).

A more accurate representation of the experimental boundary conditions in the numerical simulations was not possible because fluctuations in water depth at either end of the channel in the experiments, although small, will be dependent on the reservoir constructed either side of the channel and are therefore very hard to predict and incorporate into a predictive numerical model. However, it should be noted that measurement of the experimental elevations and velocities are planned at either end of the channel (see Annex 2). This will allow retrospective numerical simulations to specify identical boundary conditions to the experiment.

4.3.2 Model Experiment Boundary Conditions: Comparison to Prototype

The typical boundary conditions used in the numerical simulations are very similar to those expected in the model experiments. However, there is a question mark as to whether the model scale boundary conditions are representative of the prototype boundary conditions.

More specifically, as discussed in the previous subsection and in Section 3.4, the flow within the HR Wallingford wave and current tank will be reproduced via computer controlled pumps which will produce a fixed steady or time varying flow rate in the experiments both with and without turbine fences. However, in prototype channels the flow rate through the channel is often driven effectively by the difference in tidal elevations on both sides of the channel, and these elevations, as opposed to the flow rate, remain (almost) fixed with the introduction of turbine fences (see Garrett and Cummins, 2005).

A consequence of the different boundary conditions in the experiment and prototype is that, with the addition of fences in the model the flow rate will remain fixed and the power extracted by the fences (and the forces on the fences) will increase. In contrast, in the prototype the addition of fences will increase the net resistance of the channel and therefore slow the flowrate through the channel, leading to less power extraction (and lower forces on the fence) than if the flowrate remained fixed. The discrepancy between the two boundary condition cases is greatest when the fences increase the net resistance of the channel by a significant amount.

It is believed that in the model scale experiments the resistance of the fences is small relative to that of the channel bed friction itself (this is borne out in Sections 5 and 6). As a result the fences should lead to only a small increase in net resistance in the channel, and consequently the power they extract (and the forces on them) will be very similar regardless of the adoption of fixed flow rate boundary conditions or fixed elevation boundary conditions. Numerical simulations confirming this conclusion are given in Section 6.1.2.

4.4 Numerical and Physical Accuracy of the Numerical Model Predictions

Numerical accuracy of the numerical model predictions is very good (detailed validation and numerical convergence of the numerical code used is well documented in Draper (2011)). In terms of physical accuracy, the numerical simulations will provide useful predictions of the model if:

1. The model flow satisfies the assumptions of shallow water flow, and
2. The representation of the tidal devices using the thrust coefficient is appropriate.

The first of these requirements may not be met if:

- Secondary flows are significant for the headland geometry as flow passes around the headland. The magnitude of secondary flows, assuming a logarithmic stream-wise velocity profile and a parabolic vertical eddy viscosity distribution is given by $u_s \sim u_c(6h/r_c)$, where u_s is the magnitude of the secondary flow, u_c is the magnitude for the stream wise flow, h is the depth and r_c is the radius of curvature of the headland (Kalkwijk and Booij, 1986). For a model depth of 0.2 m and a headland radius of curvature of ~ 2.5 m, secondary flows are expected to be ~ 48 % of the magnitude of stream wise flow. However, if the depth reduces near the headland (as will occur with a sloping bathymetry) to a depth of 0.1 m, the secondary flows are expected to be just ~ 24 % of the magnitude of the stream wise flow. Measurement of

the velocity with depth is suggested in the experiments to determine if secondary flows are significant.

- The bathymetry surrounding the headland is sufficiently steep so that separation may occur in the vertical plane. Using a 2D non-hydrostatic numerical model Stansby and Zhou (1999) have shown that for bathymetric slopes of less than 10° , separation in the vertical plane is unlikely.
- There are spatial variations in effective bed friction coefficient: The bed shear stress enters the shallow water equations via the bottom boundary condition and assumes that the shear stress at the seabed is in phase, and a constant fraction of, the square of the depth-averaged horizontal velocity. Stansby (2003) has, however, shown that for wake flows with recirculation this assumption may be violated in some cases.

The second requirement will be met if the effect of the devices is to simply introduce a concentrated momentum sink into the flow well defined by the assumptions of actuator disc theory. No allowance is made in the numerical simulations to introduce an additional source of turbulence to the representation the tidal devices.

5 MODEL GEOMETRY

5.1 Tidal Channel

The geometry of the tidal channel has been chosen to match the idealised channel used successfully in Stansby et al. (2009). The remaining parameters of still water depth, bed friction coefficient, channel velocities and flow period (for sinusoidal cases) have been selected based on the following arguments:

1. Still water depth: a still water depth of 0.2 m has been chosen to (i) give a similar value to that used successfully in the experiments of Stansby et al. (2009); (ii) accommodate the tidal headland experiments, which require a sufficiently shallow depth to increase the effects of bed friction on the recirculating flow in the wake of the headland (see Section 5.2); and (iii) maintain turbulent flow over the range of velocities to be modelled.
2. Bed friction: Bed friction in the channel has been chosen to accommodate the tidal headland experiments (see Section 5.2) and is to be composed of a seabed with sediment grain diameter of 1.2 cm, so as to give an effective roughness length z_o of 1 mm (or a Nikuradse roughness of 30 mm).

The bed friction drag coefficient in the channel can be calculated as $C_d = 0.4^2 / (\ln(h/z_o) - 1)^2$. For a roughness length of $z_o = 1$ mm and a channel depth of 0.2 m this gives $C_d = 0.009$. This is consistent with a depth change between both ends of the 20 m channel of approximately 2.3 cm in the case of steady flow and up to 2.3 cm in sinusoidal flow (assuming a steady current of 0.5 m/s and a maximum oscillatory current of 0.5 m/s, respectively).

3. Velocities: A depth-averaged velocity of 0.5 m/s has been adopted to ensure that (i) turbulent flow is simulated over the 0.2 m deep channel flow and across the porous discs representing the tidal devices, and (ii) the force on the turbine fences, and the difference in force between turbine fences, will be easy to measure.
4. Flow period: A period of 1200 s has been selected for the oscillatory currents. This is the same velocity adopted in Stansby (2009) and will ensure that the velocity within the channel is sinusoidal and not polluted by seiching effects.

5.1.1 Summary and Comparison to Prototype

The idealised channel has a Froude number of 0.35, Keulegan-Carpenter number (based on the channel length) of 30 and Stability number of 0.9. Figure 2 summarises how these non-dimensional ratios compare with the numerous (prototype) tidal channels found around the UK. The Keulegan-Carpenter number and Stability number are clearly within the scatter. The Froude number of the channel is slightly higher than the prototype channels, but is sufficiently small to ensure that flow remains everywhere subcritical when tidal fence are introduced (see the numerical simulations in Section 6).

The model channel depth to length ratio is 0.1, which is larger than that in the prototype channels which have a depth to length ratio of $\sim 0.01 \pm 0.005$. This implies a slight distortion of geometry in the model. Based on the length scale, the idealised channel represents a 1:150-350 scale model of a prototype channel measuring between 3 to 7 km in length.

The final channel geometry is given in Annex 1.

5.2 Coastal Headland

The geometry of the coastal headland has been selected to approximate a Gaussian shaped headland, which is a headland shape that has been well studied in the literature without tidal energy extraction (see, for example, Signell and Geyer, 1991). The Gaussian shape also provides a useful approximation to various headlands observed around the UK.

A sloping seabed around the headland is adopted to better represent a realistic coastal boundary layer and to provide the realistic result that the maximum natural kinetic flux occurs some distance away from the tip of the headland.

Figure 5 outlines the basic dimensions of the idealised headland. Numerical experiments have been undertaken to determine the most appropriate values for these dimensions. In particular numerical simulations have been undertaken to select:

- (i) Appropriate model bed roughness
- (ii) Appropriate model flow velocity and headland plan dimensions (L_5 and L_6)
- (iii) Appropriate model slope and extent of sloping bathymetry (L_6 and D_1)

Each of the simulations is undertaken on a longer numerical domain $(x, y) \in (-20, 20) \text{ m} \times (0, 9) \text{ m}$, than in the experiment, so as to investigate the length of the recirculation zone behind the headland. An example mesh is given in Figure 6. Third order polynomial basis functions are used in each test (equivalent to fourth order accuracy in space). A fixed velocity time series is prescribed on the left hand boundary ($x = -20 \text{ m}$) and the right hand boundary ($x = 20 \text{ m}$) has a fixed depth of 0.2 m, as discussed in Section 4.3.

5.2.1 *Appropriate Bed Roughness*

Numerous simulations were undertaken with different bed roughness coefficients C_d . Figures 7 and 8 present two particular example simulations that illustrate the effects of varying the bed roughness between values of $C_d = 0.009$ and $C_d = 0.004$, respectively, for a headland with $L_6 = 1.5 \text{ m}$, $L_5 = 2.5 \text{ m}$, $L_4 = 2 \text{ m}$, and $D_1 = 0.1 \text{ m}$. The upstream velocity is 0.3 m/s and the depth averaged eddy viscosity is taken to be $0.001 \text{ m}^2/\text{s}$. Each figure shows four snapshots of the depth-averaged velocity vectors at times of $0T$, $0.1T$, $0.2T$ and $0.25T$ (point of maximum currents).

Comparing Figure 7 and 8 it is clear that the length of the recirculation zone at the point of maximum currents is longer in Figure 8, which has the lower drag coefficient C_d . Since it is ideal to achieve simple boundary conditions in the experiments at $x = \pm 10 \text{ m}$, it is undesirable for the recirculation zone to extend beyond 10 m, and hence the higher friction velocity of $C_d = 0.009$ is clearly preferred. (It should be noted that although an even higher friction factor may further shorten the length of the recirculation zone and guarantees simple boundary conditions at either end of the channel, a value of $C_d = 0.009$ is believed to be the largest that can be practically achieved in the experiments.)

Out of interest, Figure 9 presents an identical case to Figure 7, but with a depth-averaged eddy viscosity of $0.002 \text{ m}^2/\text{s}$. It is clear that the flow field is indistinguishable from Figure 7, suggesting that the bed friction factor and, not the eddy viscosity, effectively governs the length of the recirculation zone for a given upstream velocity.

In summary $C_d = 0.009$ is recommended in the experiments to ensure the headland recirculation zone lies within the channel extents.

5.2.2 *Velocity and Headland Plan Dimensions*

The desired headland plan dimensions were chosen to ensure that elevated velocities result close to the tip of the headland whilst the recirculation zone in the wake of the headland does not extend beyond the channel exit. Numerous experiments were undertaken for different headland dimensions. A subset of these tests are given in Table 2. Table 2 also lists the force exerted by (and the drag force on) a tidal fence located at $(x, y) = (0, 0)$. This indicates the effect of the elevated tidal currents on the drag force experienced by a fence in-line with the headland (it was originally thought that the force on the fence needed to be of the order of 20 N to get an accurate measurement).

Figures 10-33 illustrate the flow field for the headland geometry listed in Table 2. Each figure shows four snapshots of the depth-averaged velocity vectors at times of $0 T$, $0.1 T$, $0.2 T$ and $0.25 T$ (point of maximum currents).

With reference to Table 2 and Figures 10-33, it is evident that for a $2 \times 2.5 \text{ m}$ headland (tests 1-6) the wake length is approximately 10 m, with the longest wake when the upstream velocity is 0.35 m/s and the shortest when the upstream velocity is 0.25 m/s . The results for the $2 \times 4.5 \text{ m}$ headland (tests 7-12) are similar to the $2 \times 2.5 \text{ m}$ headland.

For the 2.5×2.5 headland (tests 13-18) the wake is longer than 10 m, consistent with a larger velocity above the headland due to the greater contraction offered by the headland in the channel. In contrast, for the 1.5×2.5 headland (tests 19-24) the wake is within 10 m, consistent with the headland offering a smaller contraction.

In summary the following general statements can be made concerning Figures 10-33 and Table 2:

- For a fixed upstream velocity the offshore extent of the headland determines the force on the fence, simply because it forces the flow through a tighter constriction, leading to increased velocity at the fence.

- There is very little change in thrust, for a given headland extent and upstream velocity, when the fence width and aspect ratio changes.

In summary, after consultation with members of the project team it was decided to adopt the 1.5 x 2.5 m headland and a velocity of 0.35 m/s. This gives a recirculation zone less than 10 m and a force on the fence of approximately 10-15 N/fence. It was confirmed by HR Wallingford that their load cells could accurately measure loads in this range with good resolution (of the order of 0.01-0.1 N).

5.2.3 Bathymetry surrounding the headland

With respect to Figure 5, two parameters control the bathymetry surrounding the headland; the extent L_6 and the depth at the coastline D_1 . These values should be determined to ensure that (i) the flow remains sub-critical close to the tip of the headland, (ii) the kinetic flux is a maximum some distance from the exact tip of the headland (as is believed to be realistic in the prototype), and (iii) to ensure that the beach slope is less than 1:10 so that the flow is less likely to separate in the vertical plane.

Figures 34, 36 and 38 present the instantaneous kinetic flux directed in the x -direction at four points in a tidal cycle - $0 T$, $0.1 T$, $0.2 T$ and $0.25 T$ – for a headland with dimensions 1.5 x 2.5 m headland and upstream velocity 0.35 m/s (these dimensions and velocity match the findings from Section 5.2.2). The depth at the coastline is varied between the three figures, taking values of 5 cm (Figure 34), 10 cm (Figure 36) and 15 cm (Figure 38). In each case the beach extent is set to $L_6 = 1.5$ m to ensure that a slope of less than 1:10 is achieved for each case.

Comparing Figures 34, 36 and 38 it is evident that the location of highest kinetic flux is very close to the tip of the headland when $D_1 = 15$ cm (Figure 38). This is believed to be unrealistic for most prototype headlands and undesirable because it is not possible to place a model fence at the location close to the tip of the headland since the depth is too shallow. For $D_1 = 5$ cm and $D_1 = 10$ cm (figures 34 and 36) the location of highest kinetic flux is approximately 1 m from the tip of the headland and in deeper water were a fence can be placed.

Figures 35, 37 and 39 display the same headland geometry as Figures 34, 36 and 38, respectively, but present the Froude number at each point in time. Comparing Figure 35 ($D_1 = 5$ cm), Figure 37 ($D_1 = 10$ cm) and Figure 39 ($D_1 = 15$ cm), it is evident that in the former case the Froude number approaches (if not exceeds) unit, whereas in the remaining cases the

Froude number remains well below unit. Since super-critical flow is unlikely in the prototype a shallow depth of $D_1 = 5$ cm is undesirable in the experiments.

In summary, it therefore appears evident that a deep coastline ($D_1 = 15$ cm) may lead to an unrealistic location of maximum kinetic flux, whereas a shallow coastline ($D_1 = 5$ cm) may lead to unrealistically high Froude numbers near the tip of the headland. Consequently a value of $D_1 = 10$ cm has is recommended. A headland extent of $L_6 = 1.5$ m will ensure that the slope (1:15) is not likely to lead to separation in the vertical plane.

At this stage it is also of interest to note for the chosen headland bathymetry that the width (in the y-direction) at the upstream side of the region of elevated kinetic flux in Figure 36 is approximately 1.5-2 m. A fence 1.82 m long, as outlined in Section 4.2, therefore appears to be a suitable length to occupy the region of elevated flux.

5.2.4 Summary and Comparison to Prototype

Taking $C_d = 0.009$, $L_4 = 1.5$ m, $L_5 = 2.5$ m and the upstream flow velocity to be 0.35 m/s, the idealised headland will have an upstream Froude number of 0.25, Keulegan-Carpenter number (based on the headland width of L_5) of 160 and Stability number of 0.11. Figure 3 summarises how these non-dimensional ratios compare with the numerous (prototype) tidal channels found around the UK. The Froude number and Stability number are clearly within the scatter. The Keulegan-Carpenter number is higher than the prototype channels, due to constraints on the minimum model tidal period to avoid seiching, minimum velocity to ensure turbulent flow and maximum model size.

The offshore depth to headland width (L_5) is 0.08, which is larger than that in the prototype headlands which have a depth to width of approximately 0.001-0.02. This implies a slight distortion in geometry. Based on the headland width, the idealised headland represents a 1:100-600 scale model of a prototype headland of breadth 0.4 to 1.5 km in width.

The final headland geometry is given in Annex 2.

6 LOCATION OF TIDAL FENCE

6.1 Tidal Channel

Following consultation with the project team a number of fence locations were selected for experimentation in the tidal channel. To investigate these locations the simulation tests cases summarized in Table 3 were undertaken.

Table 4 summaries the results from these simulations, listing the predicted force on the fence, power extracted by the fence and power removed in the channel (due to bed friction and the fence) for each configuration. Figures 40-49 present flow fields (in the form of streamlines, Froude number and velocity vectors) for a subset of the fence locations listed in Table 3.

In summary the simulations cover the following fence layouts which are represented in the final fence locations listed in Annex 2:

- Layout 1 (see experiment 2 in Annex 2): Tests 500a considers the simplest case of a single fence in the center of the channel. Test 503a and 504a consider two variations of fence thrust for the same placement.
- Layout 2 (see experiment 4 in Annex 2): Test 501a considers three turbines completely across the channel.
- Layout 3 (see experiment 6 in Annex 2): Test 502a considers a two-fence asymmetric placement.
- Layout 4 (see experiment 7 in Annex 2): Tests 505a-506a investigates placement of an asymmetric staggered arrangement.
- Layout 5 (see experiment 5 in Annex 2): Tests 507a-509a investigates placement for an asymmetric staggered arrangement.

Tests with the final character of ‘b’ and ‘c’ are identical to those with ‘a’, but have different flow velocity. In the case of ‘b’ the upstream velocity is 0.3 m/s. In the case of ‘c’ a sinusoidal velocity of amplitude 0.5 m/s is modeled.

6.1.1 Discussion on Results

The following general conclusions can be made regarding the results in Table 4 and the flow fields illustrated in Figures 40-49:

In general:

1. For each of the steady flow numerical runs in Table 3 and 4 the maximum loads on the fences occur for a 0.5 m/s flow and are close to 20 N/fence when $C_T = 0.9$. At a lower steady velocity of 0.3 m/s the thrust is smaller (less than 6 N/fence). In the oscillatory flow tests (‘c’ tests) the time averaged thrust is of the order of 14 N/fence, and the maximum thrust is also close to 20 N/fence in the worst case.

It is suggested (see point 4) that at a $C_T = 1.0$ (highest practical value) is used in the experiments. With that thrust coefficient the loads on the fence will be higher than in Table 4, but will not exceed the 50 N/fence limit of the HR Wallingford load cells.

2. For the tests with multiple fences the difference in force between fences is generally between 0-2 N/fence at 0.5 m/s flow, and between 0-1 N/fence at 0.3 m/s. The difference in forces illustrates the ‘blockage’ effect of using multiple devices and the effect of the fence layout on power extraction. Importantly, the resolution of the HR Wallingford load cell (of 0.01 N) will be capable of measuring the differences in fence load in the experiments. However it is also recommended that the higher flow velocity of 0.5 m/s be used to ensure a larger measureable difference between fence loads.
3. For all test results the power extracted by the fence in the numerical simulations is less than 10% of that due to bed friction (and the fence) in the channel (i.e. the total dissipated power). This indicates that the addition of turbines has little effect on the net resistance of the channel. Consequently boundary conditions resembling a fixed tidal flow rate (to be adopted in the model) or a fixed elevation difference across the channel (expected in the prototype) would be expected to lead to similar turbine thrust and power extraction.

All of the layouts appear to give interesting results worthy of experimentation. In particular some notes on the simulation results, and the justification for the final fence placement in layouts 4 and 5 in particular, are given below:

4. Layout 1: Comparison of tests 500a, 503a and 504a and their respective flow fields illustrate that a higher thrust coefficient has a much larger wake deficit. Consequently, when more than one turbine fence is introduced the blockage effects within the channel will be more pronounced and the arrangement of staggered fences will lead to more variation in force per fence. Based on this finding it is suggested that the largest realistic thrust coefficient should be used in the experiments, which is believed to be $C_T = 1.0$. Using a large thrust coefficient will also lead to the largest effects of fence deployment on the natural flow field around the headland (see Section 6.2).
5. Layout 2: Comparison of test 500a with 501a illustrates that the force on the fences are higher in the latter case, simply because they introduce a greater blockage. It will be interesting to confirm this experimentally.
6. Layout 3: Tests 502a and 502b illustrate that a slightly higher load is experienced by the fence towards the top of the channel owing to blockage effects. Thus layout 3

begins to explore optimal fence placement and will provide very useful experimental results.

7. Layout 4: In both test 506a,b and 505a,b the largest thrust is felt by the single isolated fence, which is exposed to the flow accelerating around the two adjacent fences. This is also true for flow from left to right in oscillatory flow (not shown), but the opposite results (in that the single turbine experiences less load) when the flow is from right to left. Despite this the total load (across all fences) is similar to Layout 2. It will be interesting to confirm this experimentally.

Furthermore, the tests results show that there is almost negligible difference when the fences are staggered by 1m (test 505) or 1.5 m (test 506). Consequently 1 m spacing is suggested in the experiments, simply to keep the measurement gird compact about the fence.

8. Layout 5: Comparing tests 507-509, the maximum thrust is again on the most downstream fence, similar to the result in Layout 4, owing to the fact that the downstream fence experiences the accelerated flow bypassing the upstream fences.

Furthermore, the test results shown that there is minimal difference in forces on the fences when the fences are staggered by 1 m along the channel (test 507), 1.5 m along the channel (test 508) or with some lateral spacing across the channel (test 509). Consequently 1 m spacing along the channel and no lateral spacing is suggested in the experiments (see Annex 2 Experiment 5), simply to keep the measurement gird compact about the fence.

6.1.2 Variation in Boundary Condition

It was mentioned in Section 4.3.2 that the prototype tidal channel boundary conditions are more representative of a fixed elevation difference, where the elevations are fixed at either end of the channel with the introduction of fences. In contrast, in the model tidal channel the boundary conditions will effectively fix the flow rate with the introduction of fences. To compare what affect these different boundary conditions may have on the experimental results (i.e. the flow field and the forces on the fence) two numerical tests have been conducted to mimic the prototype and model conditions for the fence placement examined in Test 501a (see Table 3). This particular test has been chosen for the comparison because it is the case in which the resistance offered by the turbine fence is largest and, consequently, (see the discussion in Section 4.3.2) the effects of the different boundary conditions are expected to be

largest (see Table 4). In both tests the flow is held constant in time; thus steady flow is modeled.

In the first of the numerical tests the depth along the upstream boundary has been fixed to 21.35 cm and the depth along the downstream boundary has been fixed to 18.8 cm, to mimic prototype conditions. In the second numerical test the flowrate has been fixed along the upstream boundary to be 0.5 m/s, whereas the depth at the downstream boundary has been fixed to 18.8 cm, to mimic model conditions. Both tests are performed with zero eddy viscosity, i.e. $\nu_T = 0.0 \text{ m}^2/\text{s}$.

Without turbine fence, Figures 68 and 69, together with Table 7, illustrate that in both tests the boundary conditions lead to almost identical depth-averaged velocity and depth throughout the channel, and the same flow rate through the location where the fences will be placed. It should also be noted that the velocity is approximately 0.5 m/s at the center of the channel and the depth is approximately 20 cm, which are the conditions which are specified for the actual model experiments (see Section 7).

Following confirmation that the flow fields were very similar without turbine fence, the boundary conditions were subsequently held constant and turbine fence were introduced. Thus comparison of the resulting flow fields and forces on the fence can be used to investigate the effect of the different boundary conditions.

Following the introduction of the turbine fence, the resulting flow fields in both tests are illustrated in Figures 70-73. In both tests the variations in the flow field, visualized in terms of the Froude number (Figures 70 and 71) and streamlines (Figures 72 and 73), are very similar. Table 7 summarizes the forces on the fence for both test conditions and the total flow rate through the fences. The central fence experiences a force of 17.2 N in the test with constant flow rate, whilst it experiences a force of 15.7 N in the test with constant elevation. As expected, the force is higher for the test with constant flowrate (see Section 4.3.2 for a discussion why) but the difference is only 9 %. This small difference is consistent with the finding that the power extracted by the fence, relative to the total power dissipated in the channel, was also small in Test 501a (see Table 4).

In summary the effects of using model boundary conditions comprising of a fixed flowrate, as opposed to a fixed elevation difference, are believed to be manageably small. More specifically, the general flow field is expected to be very similar regardless of the boundary

conditions, and similar forces (at most approximately 10% larger with the proposed model boundary conditions) are expected.

6.1.3 Conclusions and Measurement Locations

The forces on the fence for the locations in Table 3 and adopted in Annex 2 can be measured by the apparatus available to HR Wallingford. For 0.5 m/s upstream steady, or maximum oscillatory, velocity there is also expected to be sufficient variation in the forces on the fences, when multiple fences are used, to allow for accurate measurement of the force difference in the experiments. The power extracted by the fence is small compared to that dissipated due to bed friction such that the boundary conditions of fixed flow rate in the model are expected to be satisfactory.

To record the flow field about the fence a number of measurement locations are suggested (see Annex 1). The total number of measurement locations is limited by the number of ADVs and propeller meters available in the experiments (see Section 3.1). The locations form a grid around the fence, spaced a minimum of 1 m behind the fence (where vertical mixing is expected to be complete). The ADVs have been positioned to exploit symmetry (both about the x-axis for fence placement and the y-axis to account for bi-directional flow) in the arrangement where possible.

Depth profiles are requested in the wake of a device in Experiment 2 to validate that the flow field is mixed. Depth profiles are requested in Experiment 1 and 3 to document natural flow conditions in the channel.

Measurement locations and fence locations are given in Annex 2.

6.2 Coastal Headland

Following consultation with the project team a number of fence locations were selected for experiments with the coastal headland. These locations are summarized in the top half of Table 5. The locations have been chosen to explore the following points in the experiment:

- Experiments 9, 10, 11 and 13 explore the variation in power that can be removed by a fence at different strategically placed locations around the headland. The range of experiments will test the hypothesis that the location of maximum flux is the best location to place a fence and how important fence placement is to the force on the device and, indirectly, power extraction.

- Experiment 9 and 12 have been chosen to allow (with comparison to experiments 1 and 6, respectively) comparison of the performance of fence at given locations in a channel both with and without a headland present.

To predict the forces on the fence and the flow field for the fence location in Table 5 a series of numerical simulations modeling oscillatory and steady flow have been undertaken for the headland dimensions selected in Section 5.2 (Tests 620-625). A fence with $C_T = 1.0$ has been adopted for these tests. Table 6 summaries the results from these simulations, listing the predicted force on the fence, power extracted by the fence and power removed in the channel (due to bed friction and the fence). Figures 50-67 present flow fields (in the form of streamlines, Froude number and velocity vectors) for a subset of the fence locations listed in Table 5.

In addition to the fence locations listed in table 5 for the chosen headland, a number of simulations were also performed for fence locations near to an earlier headland geometry with dimensions $L_4 = 2.5$ m, $L_5 = 2.5$ m, $L_6 = 2$ m and $D_1 = 0.05$ m. A fence with $C_T = 0.9$ was modeled in each test. The results, in terms of fence force and power, together with channel power, are also given in Table 6.

6.2.1 Discussion on Results

The following conclusion/observations can be made concerning the results in Table 6:

- For the 1.5 x 2.5 m headland (Tests 620-625), which will be used in the experiments, the maximum force on the fences ranges from 15.9 to 20.7 N/fence in oscillatory flow. This is within the capabilities of the load cells confirmed by HR Wallingford.
- Across all the tests in Table 6 it is evident that the maximum force on a fence in oscillatory flow is similar to that in uniform flow, suggesting close to quasi-steady conditions in the oscillatory tests. Furthermore, as an example, the flow field at time of maximum currents ($0.25T$) in the bottom right of Figures 50-52, and the flow field for identical headland geometry and fence place, but in steady flow depicted in Figure 65-67, are similar.
- Both for the adopted 1.5 x 2.5 m headland and the earlier headland results summarised in Table 6, the power extracted by the fence in the numerical simulations is less than 10% of that due to bed friction (and the fence) in the channel (i.e. the total dissipated power). This indicates that the addition of turbines has little effect on the net resistance of the channel. Consequently boundary conditions resembling a fixed tidal flow rate

(to be adopted in the model) or a fixed elevation difference across the channel (expected in the prototype) would be expected to lead to similar turbine thrust and power extraction.

- Figures 50-67 indicate that the wake structure behind the headland is similar for all fence locations. This suggests that the turbine fence has minimal effect on the natural recirculating flow behind the headland. This is an interesting results and one that would be nice to confirm experimentally. Using a fence with a large thrust coefficient (consistent with that preferred in Section 6.1) will provide most interesting results in this regard.

6.2.2 *Conclusions and Measurement Locations*

The forces on the fence for the locations in Table 5 can be measured by the apparatus available to HR Wallingford. There is also good variation in the forces on the fence for the difference fence locations, and the power extracted by the fence is small compared to that dissipated due to bed friction such that the boundary conditions of fixed flow rate in the model are expected to be satisfactory.

To accurately record the flow field about the turbines and headland a number of flow measurement locations will need to be recorded (see Annex 2). Given the limited number of ADVs and propeller meters these measurements will need to be conducted in two sets (Set 1: Experiments 8-13; Set 2: Experiments 14-19). The first set will measure the velocities in the wake of the fence and close to the tip of the headland. The second set will measure the velocities in the recirculation zone for comparison to undisturbed conditions.

Depth profiles are requested close to the tip of the headland in Experiment 8 and in the wake of the headland in Experiment 14 to investigate secondary flows and if depth-averaged flow, with a self-similar log law velocity profile, is applicable in locations of strong recirculation.

Measurement locations and fence locations are given in Annex 2.

7 SUMMARY AND SPECIFICATION OF EXPERIMENTS

7.1 Geometry

Based on the simulations conducted in Section 5, Annex 1 outlines the channel geometry and headland geometry.

A friction factor of $C_d=0.009$ should be achieved on the seabed of the model channel and the sloping sides of the headland. In practice, for a 0.2 m deep flow, this friction factor is equivalent to a roughness length z_o of approximately 1 mm (See Equation 10), which corresponds to a Nikuradse roughness (assuming a hydrodynamically rough flow) of 30 mm or a median particle grain size of the model seabed of 12 mm. The vertical walls of the channel can be smooth.

It should be noted that grains of diameter greater than 6 mm (with density ~ 2500 kg/m³ or above) would be expected to have a threshold velocity of greater than 1 m/s (Soulsby, 1997), referenced at 0.1 m above the seabed, and are thus expected to remain stationary in the model flow conditions.

7.2 Flow Conditions

The requirements for steady and oscillatory flow include:

Tidal Channel

- Steady flow: Uniform flow rate across the channel, providing depth-averaged velocities of 0.5 m/s and a water depth of 20 cm at the centre of the channel (i.e. location $(x, y) = (0,0)$). The surface elevations at either end of the channel should be $20 \pm < 3$ cm.
- Oscillatory flow: For the oscillatory flow conditions a peak flow rate across the channel, providing depth-averaged velocity magnitude ranging between 0-0.5 m/s and a mean water depth of 20 cm, with a range of $\pm < 1$ cm, at the centre of the channel (i.e. location $(x, y) = (0,0)$). The velocity should vary sinusoidally with time from the peak flow rate with a period of 1200 s. The surface elevations at either end of the channel should be $20 \pm < 3$ cm throughout.

Coastal Headland

- Steady flow: Uniform flow rate across the upstream entrance to the channel, providing depth-averaged velocities of 0.35 m/s and a water depth of approximately 21.5 cm at the upstream end of the channel (i.e. location $(x, y) = (-10, y)$). (Note the additional 1.5 cm depth at the upstream end accounts for surface slope across the channel).
- Oscillatory flow: For the oscillatory flow conditions a uniform peak flow rate across the upstream entrance to the channel, providing depth-averaged velocity magnitude ranging between 0-0.35 m/s and a mean water depth of 20 cm, with a range of $\pm < 3$

cm, at the upstream end of the channel (i.e. location $(x, y) = (-10, y)$). The velocity should vary sinusoidally with time from the peak flow rate with a period of 1200 s.

7.2.1 Note on Depth-Averaged Velocities

It should be noted that the velocities quoted above are depth-averaged values. These can be determined from point velocity measurements with the ADV once the in-situ roughness height z_o has been determined (Section 7.2.2 discusses how the roughness could be calculated). If a roughness length cannot be determined easily during testing, a good approximation is $z_o = d_{50}/12$, where d_{50} is the median particle size of the gravel used on the bed of the channel (back calculation following the experiments can confirm the exact depth-averaged velocities).

Once z_o has been calculated or estimated, the depth-averaged velocity U_* can be computed from (i) a single ADV velocity measurement at a height z above the seabed and (ii) a wave probe measurement of the water depth h at the same points, using the relationship

$$u(z) = U_* \frac{\ln(z/z_o)}{\ln(h/z_o) - 1} \text{ or } U_* = u(z) \frac{\ln(h/z_o) - 1}{\ln(z/z_o)}. \quad (7)$$

This relationship is expected to be appropriate for both steady flow and time-averaged unsteady flow; the latter expectation being formed due to the long time period (20 minutes) of the unsteady oscillations (analysis of the time-averaged velocity unsteady profiles made in the experiments will need to be undertaken to confirm this.)

7.2.2 Calculating In-situ Roughness Length, z_o

Following the measurement of a velocity profile within the tidal channel (when no turbines or headland are present) the roughness length can be determined by ‘best fitting’ the following equation to the measured velocity at several points through the water depth (this assumes that the measured profile will be consistent with a logarithmic profile):

$$u(z) = \frac{u_f}{0.4} \ln\left(\frac{z}{z_o}\right). \quad (8)$$

The friction velocity in the above expression is given by

$$u_f = (gh_a S)^{1/2}, \quad (9)$$

where S is the slope of the free surface in the along-stream direction (which can be computed from the wave probe readings at either end of the channel) and h_a is the averaged depth along the channel.

7.3 Measurements and Measurement Locations

The measurements that will be required include elevation measurements (via wave probes), point velocity measurements (by propeller current meters and ADVs) and forces on the fence (via load cells). The wave probes will need to measure a fluctuation of up to 5 cm, with a resolution of approximately 0.1 cm. The ADV measurements should be significantly long to characterise turbulent fluctuations and Reynolds stresses at a flow velocity up to at least 0.5 m/s (recorded anywhere in the upper half of the water column). The load cells should measure up to (peak) 50 N/fence with a resolution of approximately 0.01-0.1 N/fence.

Detailed locations and further information on device placement is given in Annex 2.

8 CONCLUSIONS

- Physical scale models of the Pentland Firth, or an equivalent site, would be difficult because:
 1. The scale is large and so accurate bathymetric representation of the prototype in the model would be time consuming and expensive.
 2. Investigation and experimental results of the maximum model power potential would be difficult to scale to the prototype because of differences in the boundary forcing conditions at model and prototype scale.
- Physical scale model tests of an idealised headland and tidal channel have the following advantages:
 1. Many hot spots for tidal energy around the UK resemble tidal channels or headlands.
 2. The idealised models have simple bathymetry and are easy to construct.
 3. The effect of power extraction on the natural tidal flows and other tidal fence can be investigated without the need to explore maximum power extraction which would require far more complicated model boundary conditions.
- Based on previous work and numerical simulation idealised model scale geometry of a headland and channel have been documented (see Annex 1). The following notes can be made about the geometry:

1. The idealised model geometries relate to approximately 1:150-350 and 1:100-600 scale reproductions of a typical prototype channel and headland, respectively.
 2. The idealised model channel has similar Keulegan-Carpenter number and stability number to prototype channels. The Froude number is slightly higher than prototype values, but is everywhere subcritical with and without model fences.
 3. The idealised headland has similar Stability number and Froude number to prototype headlands. The model tidal excursion (velocity multiplied by tidal period) relative to the dominant model length scale, is higher than prototype values – however this was unavoidable in the model because the model period needed to be sufficiently high to avoid seiching in the wave and current tank, the length scale was confined to the geometry of the wave and current tank and the velocity needed to be sufficiently high to ensure turbulent flow over the depth and over the diameter of the devices.
- Based on expectations, and backed up by numerical analysis, a priority list of tidal fence locations have been formed (see Annex 2). The following predictions have been formed
 1. The force per fence is expected to be significantly less than 50 N/fence (the limit of the load cells to be used). Numerical simulations indicate a maximum force of approximately 20 N/fence in the channel tests and lower than 20 N/fence in the headland tests, depending on the location of the fence.
 2. For the porosity of the turbines selected for use in the experiments, and the fence extents, the ratio of resistance offered by the fences to the resistance naturally offered due to bed friction will remain small in all experiments. More specifically, in all cases the power extracted by the fence in numerical simulations was less than 10% of that due to bed friction in the channel. Consequently tidal forcing with a fixed flow rate is not expected to augment power extraction or the forces on the fence by a significant amount, compared with tidal forcing by a fixed elevation difference across the channel (which may be more representative of a prototype channel). This has been confirmed with numerical analysis mimicking the prototype and model boundary conditions.

9 REFERENCES

- Black and Veatch (2004) Phase I: UK tidal stream energy resource assessment. Carbon Trust Marine Energy Challenge.
- Black and Veatch (2005) Phase II: UK tidal stream energy resource assessment. Carbon Trust Marine Energy Challenge.
- Draper, S. (2011) Tidal Stream Energy Extraction in Coastal Basins. DPhil University of Oxford, UK.
- Fischer, H.B., Imberger, J., List, E.J., Koh, R.C.Y and Brooks, N.H. (1979) Mixing in Inland and Coastal Waters. Academic Press, UK.
- Garrett, C. and Cummins, P. (2005) The power potential of tidal currents in channels. Proc. R. Soc. Lon. A, 461: 2563-2572.
- Hughes, S.A. (1993): Physical models and laboratory techniques in coastal engineering, World Scientific.
- Jirka, G.H. (2002) Large scale flow structures and mixing processes in shallow flows. Journal of Hydraulic Research, 39(6): 567-573.
- Kalkwijk, J.P.T. and Booij, R. (1986) Adaption of secondary flow in nearly-horizontal flow. Journal of Hydraulic Research, 24: 19-37.
- Rawlinson-Smith, R. (2010) Performance Assessment of Wave and Tidal Array Systems (PerAWAT). Seminar to the BWEA, March. Available at <http://www.renewable-uk.com/events/wave-tidalconference/>.
- Signell, R.P. and Geyer, W.R. (1991) Transient eddy formation around headlands. Journal of Geophysical Research, 96: 2561-2575.
- Signell, R.P. (1989) Tidal dynamics and dispersion around coastal headlands. PhD thesis, MIT.
- Stansby, P.K., Huang, J., Apsley, D.D., Garcia-Hermosa, M.I., Borthwick, A.G.L., Taylor, P.H. and Soulsby, R.L. (2009) Fundamental study for morphodynamic modelling: Sand mounds in oscillatory flows. Coastal Engineering, 56: 408-418.
- Stansby, P.K. (2003) A mixing-length model for shallow turbulent wakes. Journal of Fluid Mechanics, 495: 369-384.

APPENDIX A – SCALE ANALYSIS

A1. Introduction

In this appendix the important non-dimensional equations outlining the similitude requirements between model and prototype are derived from the underlying differential equations that describe the fluid flow. A distinction is made between (i) the flow field very close to the tidal devices, which is locally three-dimensional, and (ii) the nearly horizontal flow field far from the devices.

A2. Similitude arguments close to tidal devices

Close to the tidal devices the flow is locally three dimensional. Ignoring surface tension and compressibility effects the basic physics can be well explained by the continuity equation and the Navier Stokes equations:

$$\nabla \mathbf{u}_* = 0, \quad \text{and} \quad (\text{A1})$$

$$\frac{\partial \mathbf{u}_*}{\partial t_*} + \mathbf{u}_* \cdot \nabla \mathbf{u}_* = -g\mathbf{k} - \frac{1}{\rho} \nabla p_* + \nabla \cdot (\nu \nabla \mathbf{u}_*) - \overline{\nabla \mathbf{u}_*'^2}. \quad (\text{A2})$$

In these equations \mathbf{u}_* is the vector of velocities $(u_*, v_*, w_*)^T$, p is pressure, ν is kinematic viscosity, $\mathbf{k} = (0,0,1)^T$, g is the acceleration due to gravity, and the primes denote turbulent fluctuating components of velocity which lead to the Reynolds stresses (the over bar indicating time average). Equations (A1)-(A2) are supplemented by the usual non-slip boundary conditions at the seabed and the kinematic condition at the free surface.

In both prototype and model the magnitudes of the various physical parameters in (1) and (2) can be scaled and made non-dimensional:

$$(u, v, w) = \frac{(u_*, v_*, w_*)}{V}, (x, y, z) = \frac{(x_*, y_*, z_*)}{L}, t = \frac{t_*}{T}, p = \frac{p_*}{P}, \quad (\text{A3})$$

The assumption in (A3) is that in both model and prototype, all three directions have just one scale, and all three velocity components have just one scale, respectively. For the directions this implies that the model must be a geometrically undistorted replica of the prototype (Hughes, 1991). For example, the scale on all directions in the model relative to the prototype, say L_m/L_p , is the same (where the subscript m denotes the model and p the prototype).

With (A3), (A1) and (A2) become:

$$\nabla \mathbf{u} = 0, \quad \text{and} \quad (\text{A4})$$

$$\left(\frac{L}{VT}\right) \frac{\partial \mathbf{u}}{\partial t} + \mathbf{u} \cdot \nabla \mathbf{u} = -\left(\frac{gL}{V^2}\right) \mathbf{k} - \left(\frac{P}{\rho V^2}\right) \nabla p + \left(\frac{\nu}{LV}\right) \nabla^2 \mathbf{u} - \nabla \overline{\mathbf{u}'^2}, \quad (\text{A5})$$

Both the model and prototype are governed by the non-dimensional equations (A4) and (A5) close to the turbines. Consequently the solution in terms of the non-dimensional parameters must be identical in the model and prototype if the dimensionless ratios in the brackets of equation (5) are the same. Matching the different ratio's effectively ensures that the contribution of the different forces, per unit mass, represented by the terms in the momentum equations are in the same proportion between the model and prototype.

The coefficients in brackets in (5) describe four dimensionless numbers

1. Froude number $Fr = gL/V^2$,
2. Reynolds number $Re = VL/\nu$,
3. Euler number $Eu = P/\rho V^2$, and
4. Keulegan-Carpenter number $Kc = VT/L$.

As a result of pursuing an undistorted model it is clear that, provided the five coefficients above are matched, the advective accelerations and Reynolds stress are automatically in similitude. The Euler number is also satisfied automatically for an undistorted model.

A3. Similitude arguments far from tidal devices

Away from the tidal devices the flow resembles a shallow water flow, so that the vertical velocities (and their fluctuations) can be neglected and the pressure distribution becomes almost hydrostatic with depth. Assuming that the horizontal velocities are independent of the vertical direction (except close to the seabed), the continuity and momentum equations can be integrated over the depth to give (Dean and Dalrymple, 1984)

$$\frac{\partial \eta_*}{\partial t_*} + \nabla \cdot [\bar{\mathbf{u}}_*(h_* + \eta_*)] = 0, \quad \text{and} \quad (\text{A6})$$

$$\frac{\partial \bar{\mathbf{u}}_*}{\partial t} + \bar{\mathbf{u}}_* \cdot \nabla \bar{\mathbf{u}}_* + f(\mathbf{k} \times \bar{\mathbf{u}}_*) = -g \nabla \eta_* - \frac{C_D \bar{\mathbf{u}}_* |\bar{\mathbf{u}}_*|}{h_* + \eta_*} + \nabla \cdot (\nu_t \nabla \bar{\mathbf{u}}_*). \quad (\text{A7})$$

In (A6) and (A7) $\bar{\mathbf{u}}_*$ is the vector of horizontal depth-averaged velocities $(\bar{u}_*, \bar{v}_*)^T$, f is the Coriolis parameter, h_* is the still water depth, η_* is free surface elevation above still water, ν_t is now the depth averaged eddy-viscosity, and C_D is introduced via the bottom boundary condition

$$v \frac{\partial \mathbf{u}_*}{\partial z} = C_D \bar{\mathbf{u}}_* |\bar{\mathbf{u}}_*| \text{ at } z_* = -h_* \quad (\text{A8})$$

In a similar fashion to Section A.2, the following scales can be introduced

$$(\bar{u}, \bar{v}) = \frac{(\bar{u}_*, \bar{v}_*)}{V}, z = \frac{z_*}{H}, (x, y) = \frac{(x_*, y_*)}{L}, t = \frac{t_*}{T}, \eta = \frac{\eta_*}{H}, \quad (\text{A9})$$

where we have now allowed for, but not forced, different scales in the vertical and horizontal directions. The scales in (A9) lead to the non-dimensional equations

$$\left(\frac{L}{VT}\right) \frac{\partial \eta}{\partial t} + \nabla \cdot [\bar{\mathbf{u}}(h + \eta)] = 0, \text{ and} \quad (\text{A10})$$

$$\left(\frac{L}{VT}\right) \frac{\partial \bar{\mathbf{u}}}{\partial t} + \bar{\mathbf{u}} \cdot \nabla \mathbf{u} + \left(\frac{fL}{V}\right) (\mathbf{k} \times \bar{\mathbf{u}}) = -\left(\frac{gH}{V^2}\right) \nabla \eta - \left(\frac{C_D L}{H}\right) \frac{\bar{\mathbf{u}} |\bar{\mathbf{u}}|}{h + \eta} + \left(\frac{\nu_t}{LV}\right) \nabla^2 \bar{\mathbf{u}}. \quad (\text{A11})$$

Far from the turbines both the model and prototype are governed by the non-dimensional equations (A10) and (A11). Consequently the solution in terms of the non-dimensional parameters must be identical in the model and prototype if the dimensionless ratios in the brackets are the same. The terms in brackets define five dimensionless coefficients:

1. Froude number (but now with depth as the length scale)
2. Reynolds number
3. Keulegan-Carpenter number
4. Rossby number $Ro = V/Lf$, and
5. Stability number $St = C_D L/H$.

The shallow water flow must also remain turbulent in the model, such that the Reynolds number in the vertical dimension significantly exceeds 10^3 (Jirka, 2001).

TABLES

**Table 1. Instrumentation available for physical model studies at HR Wallingford.
Supplied by Tom Coates (HR Wallingford).**

Equipment and instrumentation	Quantity	Notes
Instrumentation		
Wave generation PC systems	10	
Data acquisition PC systems (64 channel or greater)	8	
Supplementary data acquisition systems	10	
Wave probes	150	
Water level followers	8	
Pitot tubes	10	
Miniature propeller current meters	34	
ADV current meters	3	
In line load cells	22	
6-axis force cells	4	
Pressure transducers	60	
Ship mooring line transducers	36	
Ship fender transducers	24	
Qualysis (non contact) motion measurement systems	4	With spare cameras
Bed profilers (2D)	2	
3D Laser scanners	2	
SLR cameras	6	With remote triggering
Camcorders	11	
Additional pumps		
Small capacity pumps	20	1 cusec or less
Large capacity pumps	20	1 to 20 cusecs

Table 2. Headland Geometry test cases.

Test	Offshore Extent of Headland (m)	Width (along beach) of headland (m)	Upstream velocity (m/s)	Turbine Fence Location (x,y)	Maximum Thrust
Test 1	2	2.5	0.3	-	-
Test 2	2	2.5	0.3	(0,0)	13.6 N/fence
Test 3	2	2.5	0.35	-	-
Test 4	2	2.5	0.35	(0,0)	20.2 N/fence
Test 5	2	2.5	0.25	-	-
Test 6	2	2.5	0.25	(0,0)	8.6 N/fence
Test 7	2	4	0.3	-	-
Test 8	2	4	0.3	(0,0)	13.9 N/fence
Test 9	2	4	0.35	-	-
Test 10	2	4	0.35	(0,0)	20.6 N/fence
Test 11	2	4	0.25	-	-
Test 12	2	4	0.25	(0,0)	8.7 N/fence
Test 13	2.5	2.5	0.3	-	-
Test 14	2.5	2.5	0.3	(0,0)	18.3 N/fence
Test 15	2.5	2.5	0.35	-	-
Test 16	2.5	2.5	0.35	(0,0)	28.2 N/fence
Test 17	2.5	2.5	0.25	-	-
Test 18	2.5	2.5	0.25	(0,0)	11.45 N/fence
Test 19	1.5	2.5	0.3	-	-
Test 20	1.5	2.5	0.3	(0,0)	10.7 N/fence
Test 21	1.5	2.5	0.35	-	-
Test 22	1.5	2.5	0.35	(0,0)	15.9 N/fence
Test 23	1.5	2.5	0.25	-	-
Test 24	1.5	2.5	0.25	(0,0)	6.85 N/fence

Table 3. Channel turbine fence test cases.

Test	Velocity	Turbine Fence 1 position	Turbine Fence 2 position	Turbine Fence 3 position	Fence thrust Coefficient C_T
Test 500a	0.5 m/s	-	(0,0)	-	0.9
Test 501a	0.5 m/s	(0,-1.8)	(0,0)	(0,+1.8)	0.9
Test 502a	0.5 m/s	-	(0,0)	(0,+2.7)	0.9
Test 503a	0.5 m/s	-	(0,0)	-	1.9
Test 504a	0.5 m/s	-	(0,0)	-	0.31
Test 505a	0.5 m/s	(1,-1.8)	(0,0)	(0,+1.8)	0.9
Test 506a	0.5 m/s	(1.5,-1.8)	(0,0)	(0,+1.8)	0.9
Test 507a	0.5 m/s	(1,-1.8)	(0,0)	(-1,1.8)	0.9
Test 508a	0.5 m/s	(1.5,-1.8)	(0,0)	(-1.5,+1.8)	0.9
Test 509a	0.5 m/s	(+1,-2.7)	(0,0)	(-1,+2.7)	0.9
Test 500b	0.3 m/s	-	(0,0)	-	0.9
Test 501b	0.3 m/s	(0,-1.8)	(0,0)	(0,+1.8)	0.9
Test 502b	0.3 m/s	-	(0,0)	(0,+2.7)	0.9
Test 503b	0.3 m/s	-	(0,0)	-	1.9
Test 504b	0.3 m/s	-	(0,0)	-	0.31
Test 505b	0.3 m/s	(1,-1.8)	(0,0)	(0,+1.8)	0.9
Test 506b	0.3 m/s	(1.5,-1.8)	(0,0)	(0,+1.8)	0.9
Test 507b	0.3 m/s	(1,-1.8)	(0,0)	(-1,1.8)	0.9
Test 508b	0.3 m/s	(1.5,-1.8)	(0,0)	(-1.5,+1.8)	0.9
Test 509b	0.3 m/s	(1,-2.7)	(0,0)	(-1,+2.7)	0.9
Test 500c	0.5 m/s, 1200 s	-	(0,0)	-	0.9
Test 501c	0.5 m/s, 1200 s	(0,-1.8)	(0,0)	(0,+1.8)	0.9
Test 502c	0.5 m/s, 1200 s	-	(0,0)	(0,+2.7)	0.9
Test 503c	0.5 m/s, 1200 s	-	(0,0)	-	1.9
Test 504c	0.5 m/s, 1200 s	-	(0,0)	-	0.31
Test 505c	0.5 m/s, 1200 s	(1,-1.8)	(0,0)	(0,+1.8)	0.9
Test 506c	0.5 m/s, 1200 s	(1.5,-1.8)	(0,0)	(0,+1.8)	0.9
Test 507c	0.5 m/s, 1200 s	(1,-1.8)	(0,0)	(-1,1.8)	0.9
Test 508c	0.5 m/s, 1200 s	(1.5,-1.8)	(0,0)	(-1.5,+1.8)	0.9
Test 509c	0.5 m/s, 1200 s	(1,-2.7)	(0,0)	(-1,+2.7)	0.9

Table 4a: Channel turbine fence test case results (steady flow).

Test	Channel Power dissipated	Fence Position 1		Fence Position 2		Fence Position 3	
		Power	Thrust	Power	Thrust	Power	Thrust
Test 500a	271 W	-	-	8.9 W	17.6 N	-	-
Test 501a	275 W	10.3 W	19.4 N	10.1 W	19.2 N	10.3W	19.4 N
Test 502a	275 W	-	-	9.4 W	18.2 N	9.8 W	18.5 N
Test 503a	275 W	-	-	16.6 W	35.3 N	-	-
Test 504a	269 W	-	-	3.3 W	6.3 N	-	-
Test 505a	276 W	11.5 W	21 N	9.5 W	18.3 N	10.1 W	19.2 N
Test 506a	275 W	11.5 W	21 N	9.5 W	18.3 N	10 W	19 N
Test 507a	272 W	11.4 W	20.9 N	10.0 W	19 N	9.1 W	17.8 N
Test 508a	272 W	11.7 W	21.2 N	9.7 W	19 N	8.9 W	17.5 N
Test 509a	277 W	11.3 W	20.8 N	10.0 W	20 N	9.7 W	18.6 N
Test 500b	48 W	-	-	1.5 W	5 N	-	-
Test 501b	50 W	1.7 W	5.5 N	1.65 W	5.4 N	1.7 W	5.5 N
Test 502b	50 W	-	-	1.5 W	5.2 N	1.65 W	5.4 N
Test 503b	50 W	-	-	2.8 W	10 N	-	-
Test 504b	50 W	-	-	0.6 W	1.95 N	-	-
Test 505b	49 W	1.8 W	5.8 N	1.6 W	5.3 N	1.7 W	5.5 N
Test 506b	50 W	1.8 W	5.8 N	1.6 W	5.3 N	1.7 W	5.4 N
Test 507b	50 W	1.8 W	5.8 N	1.7 W	5.5 N	1.5 W	5.3 N
Test 508b	50 W	1.8 W	5.8 N	1.7 W	5.4 N	1.5 W	5.3 N
Test 509b	50 W	1.8 W	5.8 N	1.6 W	5.4 N	1.7 W	5.4 N

Table 4b: Channel turbine fence test case results (oscillatory flow).

Test	Velocity, Period	Average Channel Power dissipated (W)	Maximum Average Power Extracted by fence	Maximum Instantaneous fence thrust
Test 500c	0.5 m/s, 1200 s	84.2	2.9 (7.1 N/m)	17 N/fence
Test 501c	0.5 m/s, 1200 s	84.6	6.4 (7.7 N/m)	18 N/fence
Test 502c	0.5 m/s, 1200 s	84.4	6.0 (7.4 N/m)	17 N/fence
Test 503c	0.5 m/s, 1200 s	85.0	5.3 (14 N/m)	34 N/fence
Test 504c	0.5 m/s, 1200 s	84.0	1.1 (2.6 N/m)	6 N/fence
Test 505c	0.5 m/s, 1200 s	84.6	3.2 (7.6 N/m)	19 N/fence
Test 506c	0.5 m/s, 1200 s	84.6	3.2 (7.6 N/m)	20 N/fence
Test 507c	0.5 m/s, 1200 s	84.6	3.2 (7.6 N/m)	19 N/fence
Test 508c	0.5 m/s, 1200 s	84.6	3.2 (7.6 N/m)	19 N/fence
Test 509c	0.5 m/s, 1200 s	84.6	9.4 (7.4 N/m)	18 N/fence

Table 5: Headland Geometry and turbine fence test cases.

Test	Type	Velocity (m/s)	Loc. fence 1	Loc. fence 2	Loc. fence 3
Tests on adopted headland of 1.5 x 2.5 m (Turbine with $\alpha_4 = 0.73$)					
Test 620	Oscilla	0.3 m/s	(0,0)	-	-
Test 621	Oscilla	0.3 m/s	(0,-0.5)	-	-
Test 622	Oscilla	0.3 m/s	(0,-1)	-	-
Test 623	Oscilla	0.3 m/s	(0,0)	(0,1.8)	-
Test 624	Oscilla	0.3 m/s	(2,-1)	-	-
Test 625	Steady	0.3 m/s	(0,0)	-	-
Previous tests on headland 2.5 x 2.5 m (Turbine with $\alpha_4 = 0.73$)					
Test 626	Steady	0.5 m/s	(0,0)	-	-
Test 627	Steady	0.5 m/s	(0,-0.5)	-	-
Test 628	Steady	0.5 m/s	(0,+0.5)	-	-
Test 629	Steady	0.5 m/s	(0,0)	(0,2.7)	-
Test 630	Steady	0.5 m/s	(0,0)	(0,1.8)	-
Test 631	Steady	0.5 m/s	(1.25,-0.5)	-	-
Test 632	Steady	0.5 m/s	(2.5,-0.5)	-	-
Test 633	Steady	0.3 m/s	(0,0)	-	-
Test 634	Steady	0.3 m/s	(0,-0.5)	-	-
Test 635	Steady	0.3 m/s	(0,+0.5)	-	-
Test 636	Steady	0.3 m/s	(0,0)	(0,2.7)	-
Test 637	Steady	0.3 m/s	(0,0)	(0,1.8)	-
Test 638	Steady	0.3 m/s	(1.25,-0.5)	-	-
Test 639	Oscilla	0.5 m/s; 1200s	(0,0)	-	-
Test 640	Oscilla	0.5 m/s; 1200s	(0,+0.5)	-	-
Test 641	Oscilla	0.5 m/s; 1200s	(0,0)	(0,2.7)	-
Test 642	Oscilla	0.5 m/s; 1200s	(0,0)	(0,1.8)	-
Test 643	Oscilla	0.5 m/s; 1200s	(2.5,-0.5)	-	-
Test 644	Oscilla	0.3 m/s; 1200s	(0,0)	-	-
Test 645	Oscilla	0.3 m/s; 1200s	(0,-0.5)	-	-
Test 646	Oscilla	0.3 m/s; 1200s	(0,+0.5)	-	-
Test 647	Oscilla	0.3 m/s; 1200s	(0,0)	(0,2.7)	-
Test 648	Oscilla	0.3 m/s; 1200s	(0,0)	(0,1.8)	-
Test 649	Oscilla	0.3 m/s; 1200s	(1.25,-0.5)	-	-
Test 650	Oscilla	0.3 m/s; 1200s	(2.5,-0.5)	-	-

Table 6: Headland Geometry and turbine fence test case results.

Test	Type	Fence 1: Maximum Power (and Thrust)	Fence 2: Maximum Power (and Thrust)	Max Total Channel dissipation
Tests on adopted headland of 1.5 x 2.5 m (Turbine with $\alpha_4 = 0.73$)				
Test 620	Oscilla	7.3 W (15.9 N/fence)	-	160 W
Test 621	Oscilla	8.4 W (17.5 N/fence)	-	170 W
Test 622	Oscilla	9.3 W (18.7 N/fence)	-	180 W
Test 623	Oscilla	8.3 W (17.3 N/fence)	7.0 W (15.4 N/fence)	176 W
Test 624	Oscilla	10.7 W (20.7 N/fence)	-	177 W
Test 625	Steady	7.6 W (16.3 N/fence)	-	173 W
Previous tests on headland 2 x 2 m (Turbine with $\alpha_4 = 0.73$)				
Test 626	Steady	67 W (83N/fence)	-	665 W
Test 627	Steady	80 W (95N/fence)	-	665 W
Test 628	Steady	45 W (56 N/fence)	-	665 W
Test 629	Steady	78 W (94 N/fence)	50 W (64 N/fence)	702 W
Test 630	Steady	80W (95 N/fence)	56W (71 N/fence)	705 W
Test 631	Steady	83W (98 N/fence)	-	665 W
Test 632	Steady	98 W (112 N/fence)	-	610 W
Test 633	Steady	3.4W (8.9 N/fence)	-	48 W
Test 634	Steady	3.8W (9.7 N/fence)	-	47 W
Test 635	Steady	3 W (8.2 N/fence)	-	48 W
Test 636	Steady	3.5 W (9.2 N/fence)	2.6 W (7.3 N/fence)	51 W
Test 637	Steady	3.65 W (9.4 N/m)	2.75 W (7.7 N/fence)	50 W
Test 638	Steady	4.6 W (11.2 N/m)	-	47 W
Test 639	Oscillatory	69 W (84 N/fence)	-	626 W
Test 640	Oscillatory	56 W (72 N/fence)	-	637 W
Test 641	Oscillatory	75 W (90.7 N/fence)	46 W (61 N/fence)	663 W
Test 642	Oscillatory	75 W (90 N/fence)	53 W (68 N/fence)	663 W
Test 643	Oscillatory	96 W (110 N/fence)	-	582 W
Test 644	Oscillatory	6.5 W (14 N/fence)	-	88 W
Test 645	Oscillatory	7.5 W (15.4 N/m)	-	88 W
Test 646	Oscillatory	5.7 W (12.8 N/fence)	-	89 W
Test 647	Oscillatory	7 W (14.86 N/fence)	5W (11.7 N/fence)	90.4 W
Test 648	Oscillatory	7 W (14.9 N/fence)	5W (14.9 N/fence)	89.5 W
Test 649	Oscillatory	9.1 W (17.9 N/fence)	-	87 W
Test 650	Oscillatory	9.1 W (17.8 N/fence)	-	88 W

Table 7: Flowrate through the location of turbine fence and forces on turbine fence for two different tidal channel boundary conditions: (i) boundary conditions fixing the flowrate in the channel, and (ii) boundary conditions fixing the elevation difference across the channel.

	Fixed Flowrate Boundary Conditions			Fixed Elevation Boundary Conditions		
	Total Flowrate through location of Fences	Force on Fence		Total Flowrate through location of Fences	Force on Fence	
		Middle Fence	End Fences		Middle Fence	End Fences
Without Turbine fence	0.54 m ³ /s	NA	NA	0.54 m ³ /s	NA	NA
With turbine fence	0.52 m ³ /s	17.4 N	17.2 N	0.494 m ³ /s	15.7 N	15.6 N

FIGURES

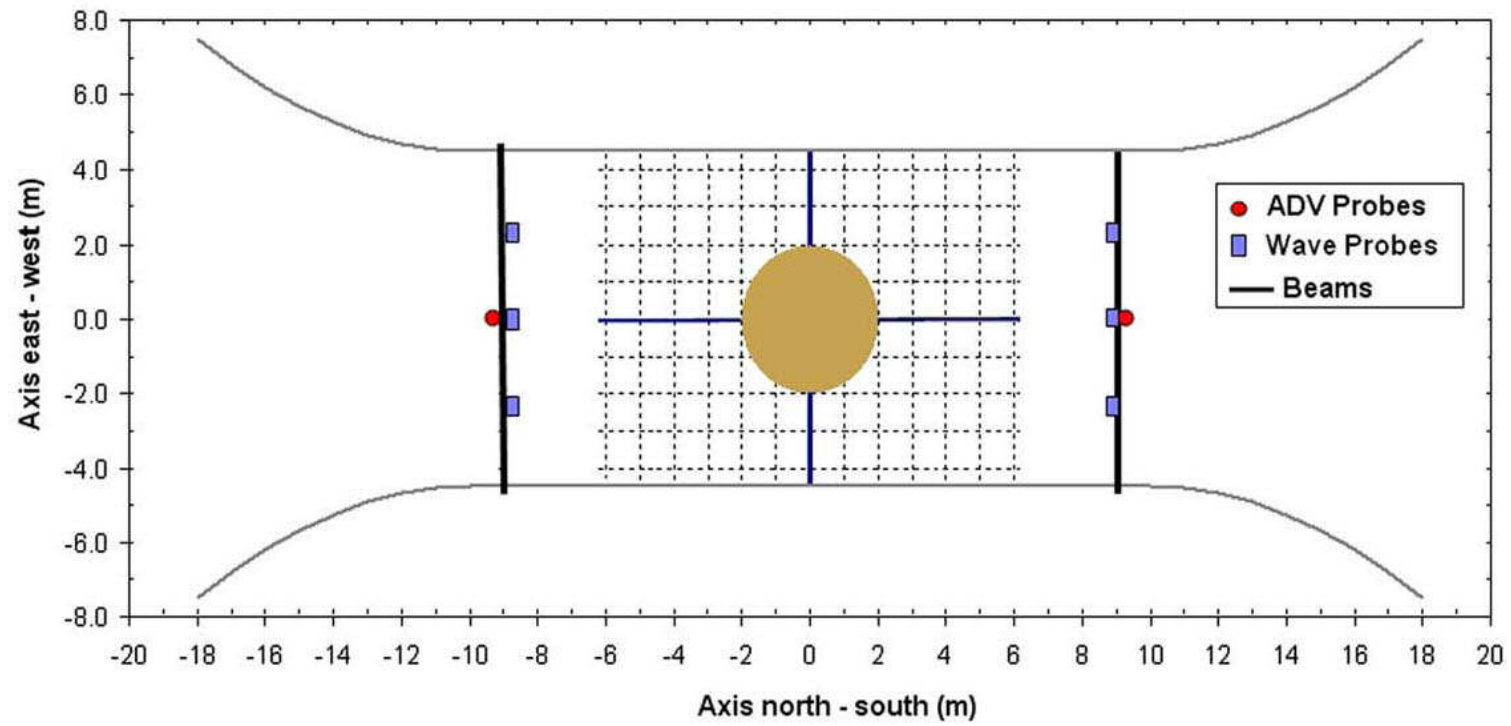


Figure 1. Previous channel geometry constructed at HR Wallingford. Picture from Stansby et al. (2009).

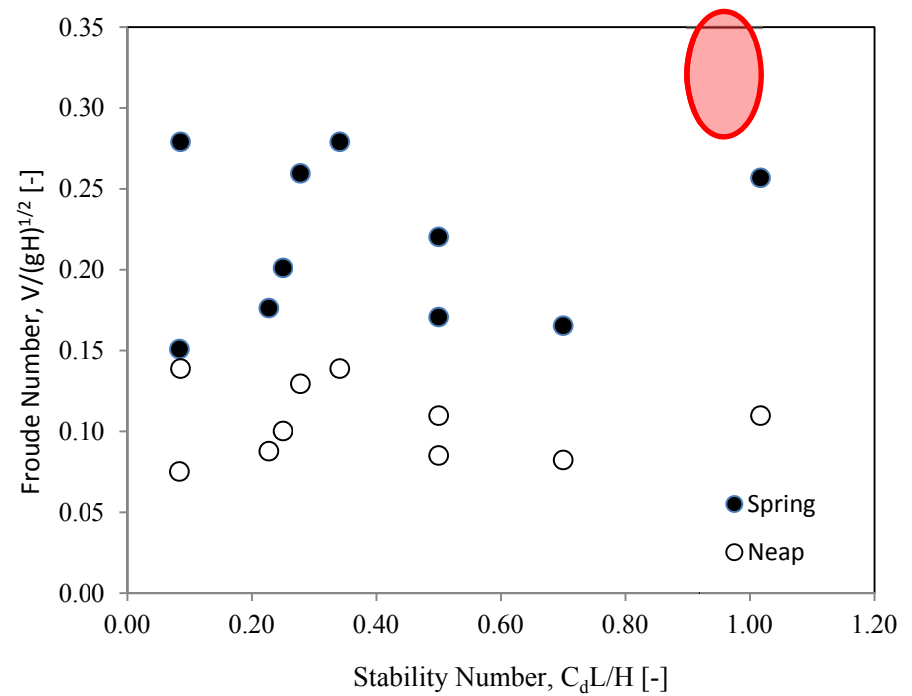
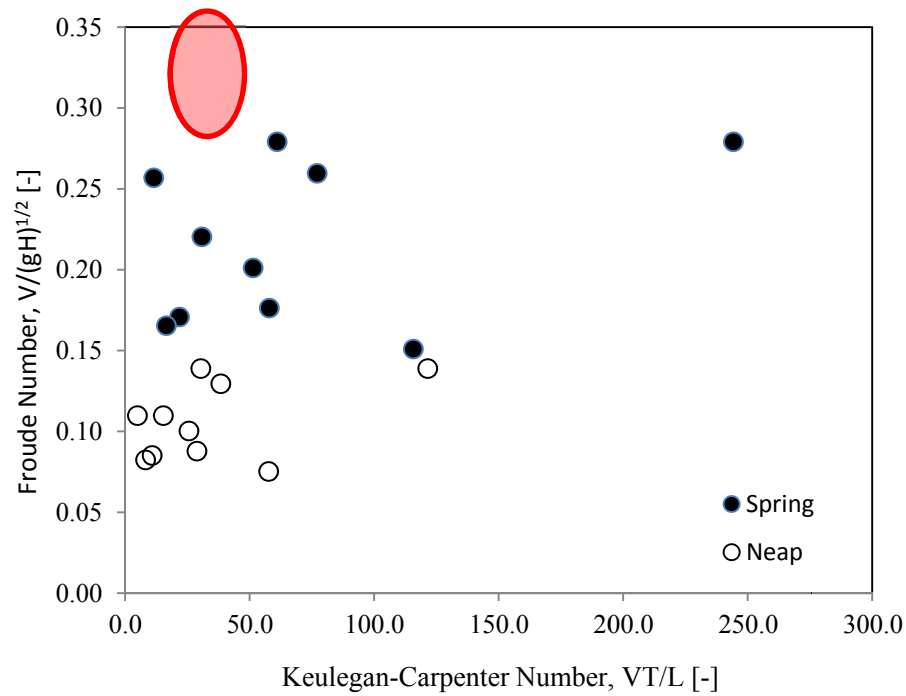


Figure 2. Tidal Channels in the UK, red ovals indicate model scales (Channels include: Yell Sound, Bluemull Sound, Pentland Firth, Papa Westray, Fers Nes, Gulf of Coryvreckan, Dorus Mor, Loche-Linnhe Corran and Kyle Rhea).

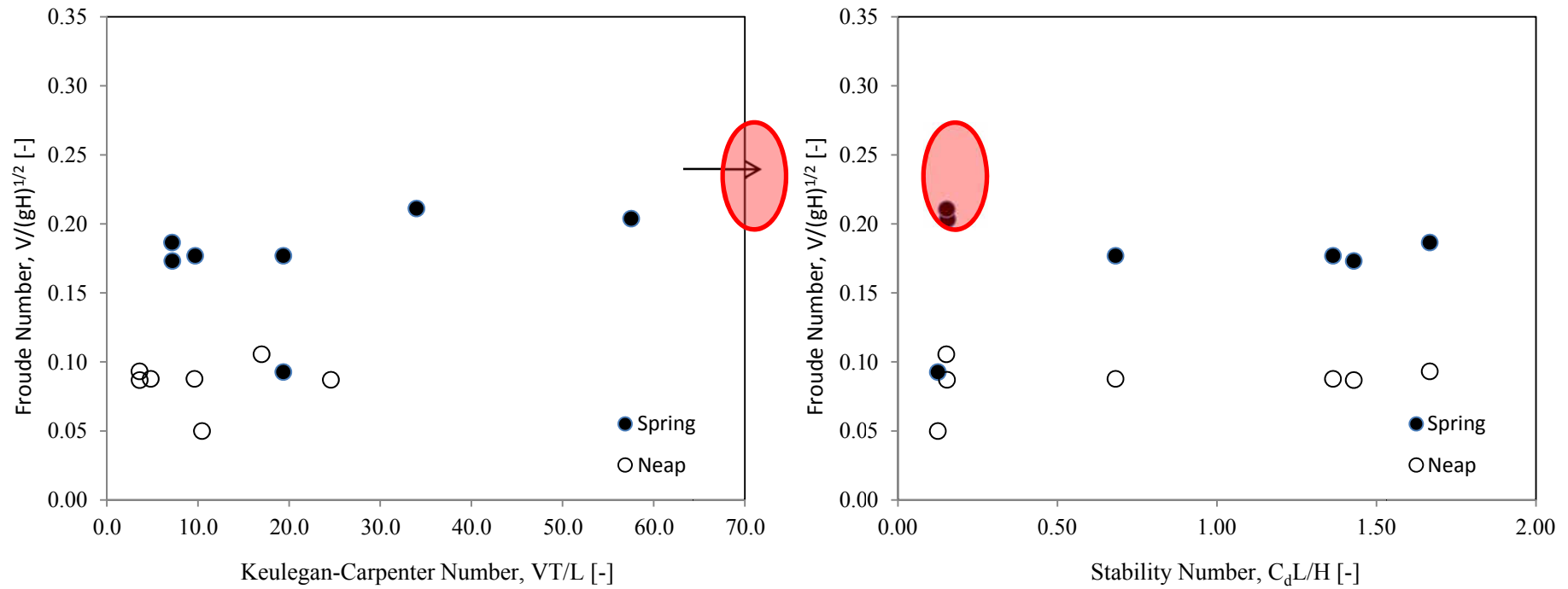


Figure 3. Coastal Headlands in the UK, red ovals indicate model scales (Headlands include: Duncansby Head, Mull of Kintyre, Mull of OA, Angelsey, Mull of Galloway, Isle of Wight and Portland Bill)

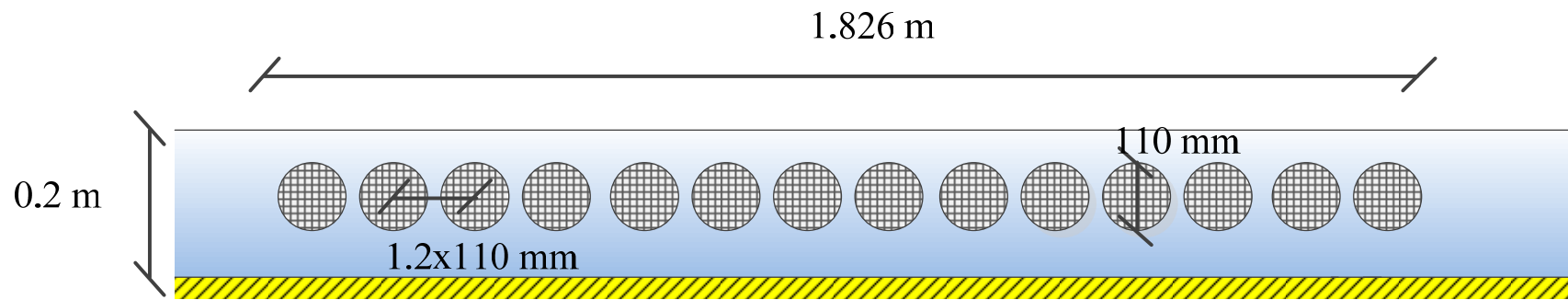
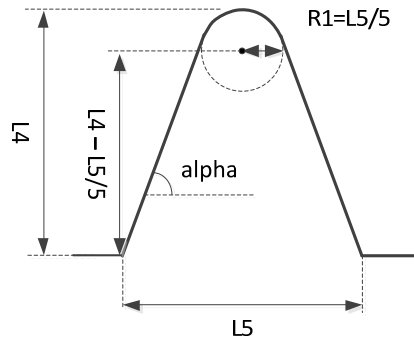
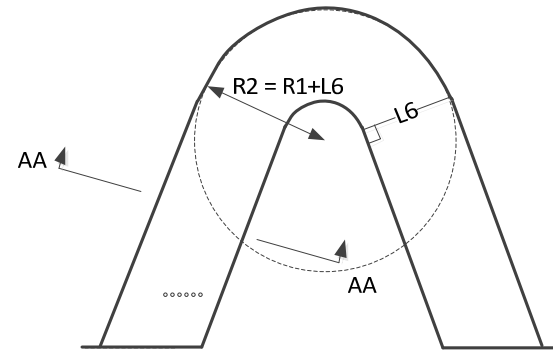


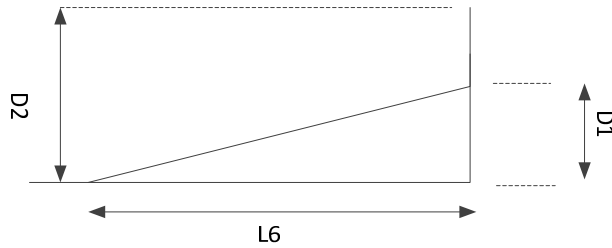
Figure 4. Schematic of model tidal fence



Top View: Headland Geometry



Top View: Extent of Bathymetry



Section AA

Figure 5. Basic Geometry of Coastal Headland

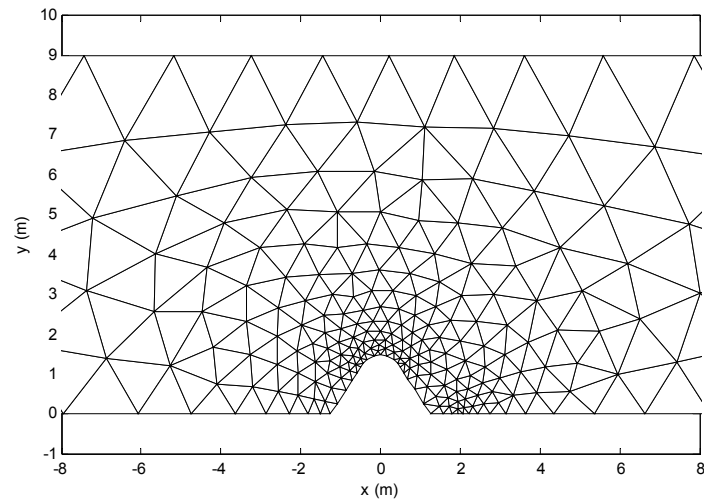
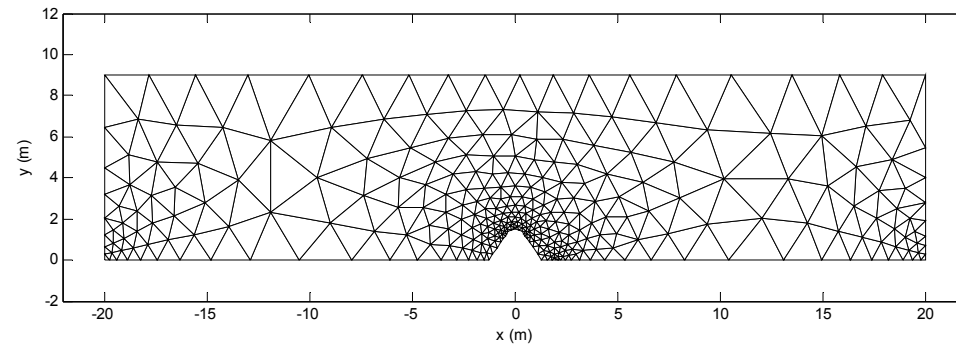


Figure 6. Example Numerical Mesh for Coastal Headland

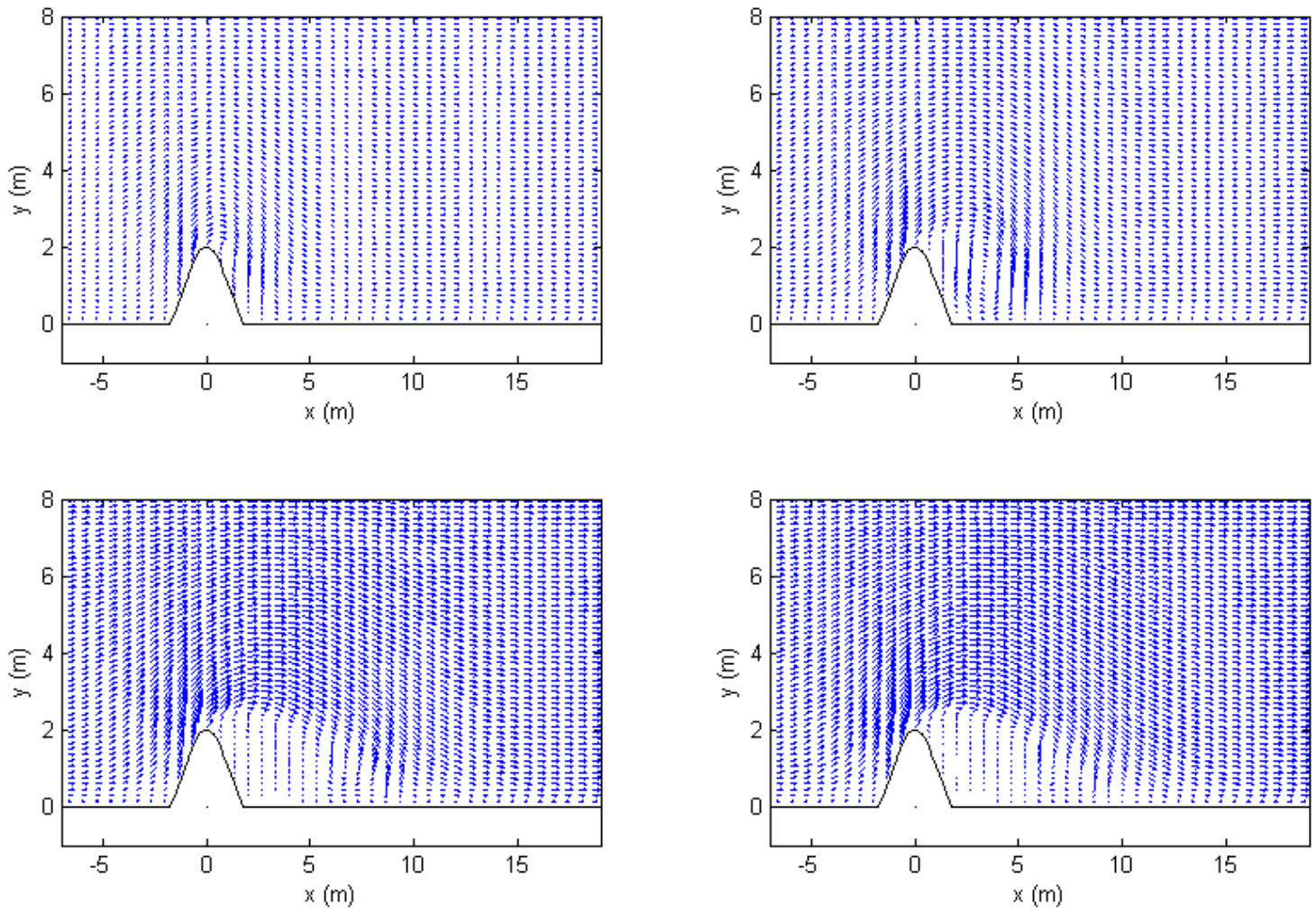


Figure 7. Vector flow field for headland with small C_d . Clockwise from top left of $0T$, $0.1T$, $0.2T$ and $0.25T$. See text for more details.

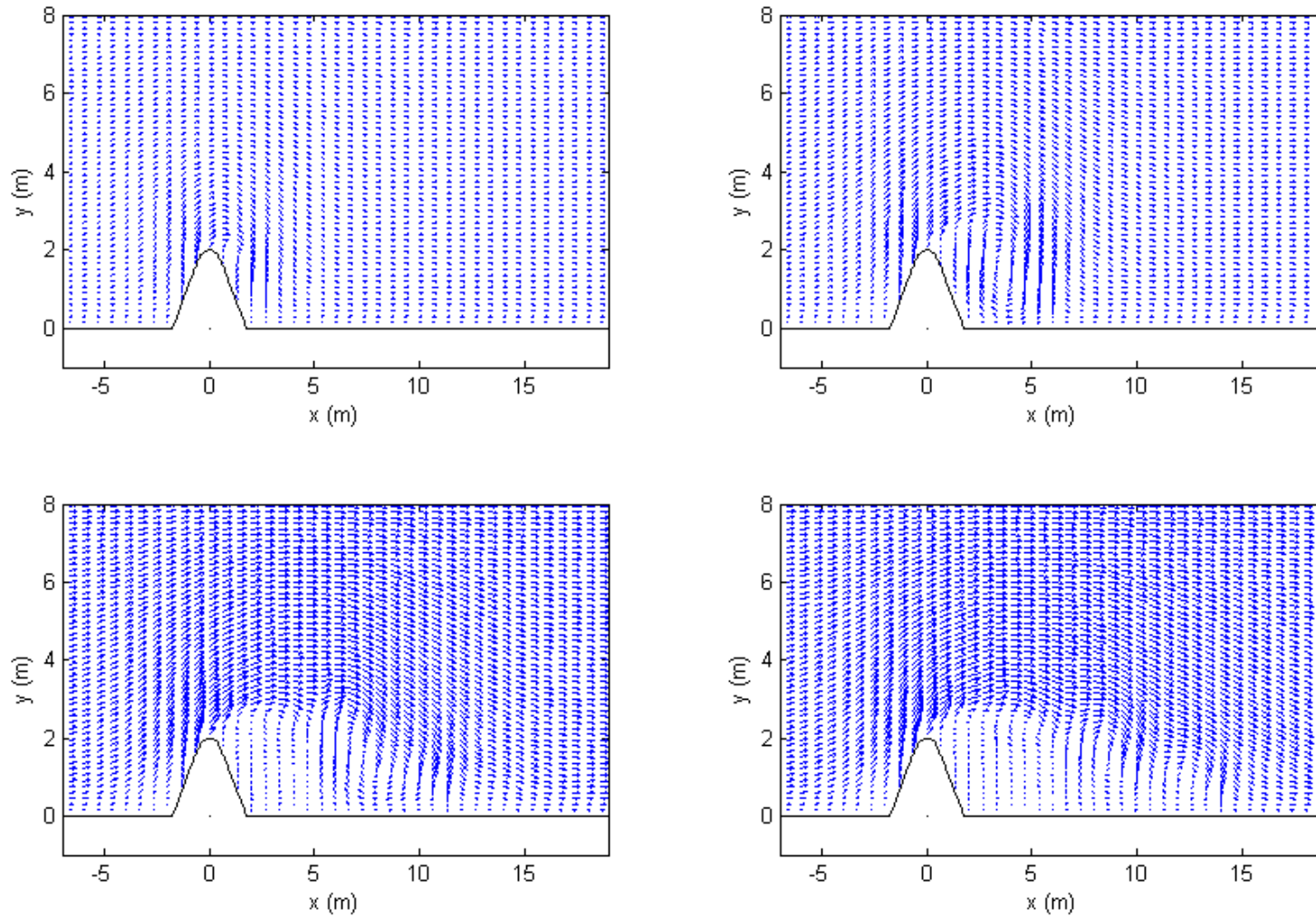


Figure 8. Vector flow field for headland with small C_d . Clockwise from top left of $0T$, $0.1T$, $0.2T$ and $0.25T$. See text for more details.

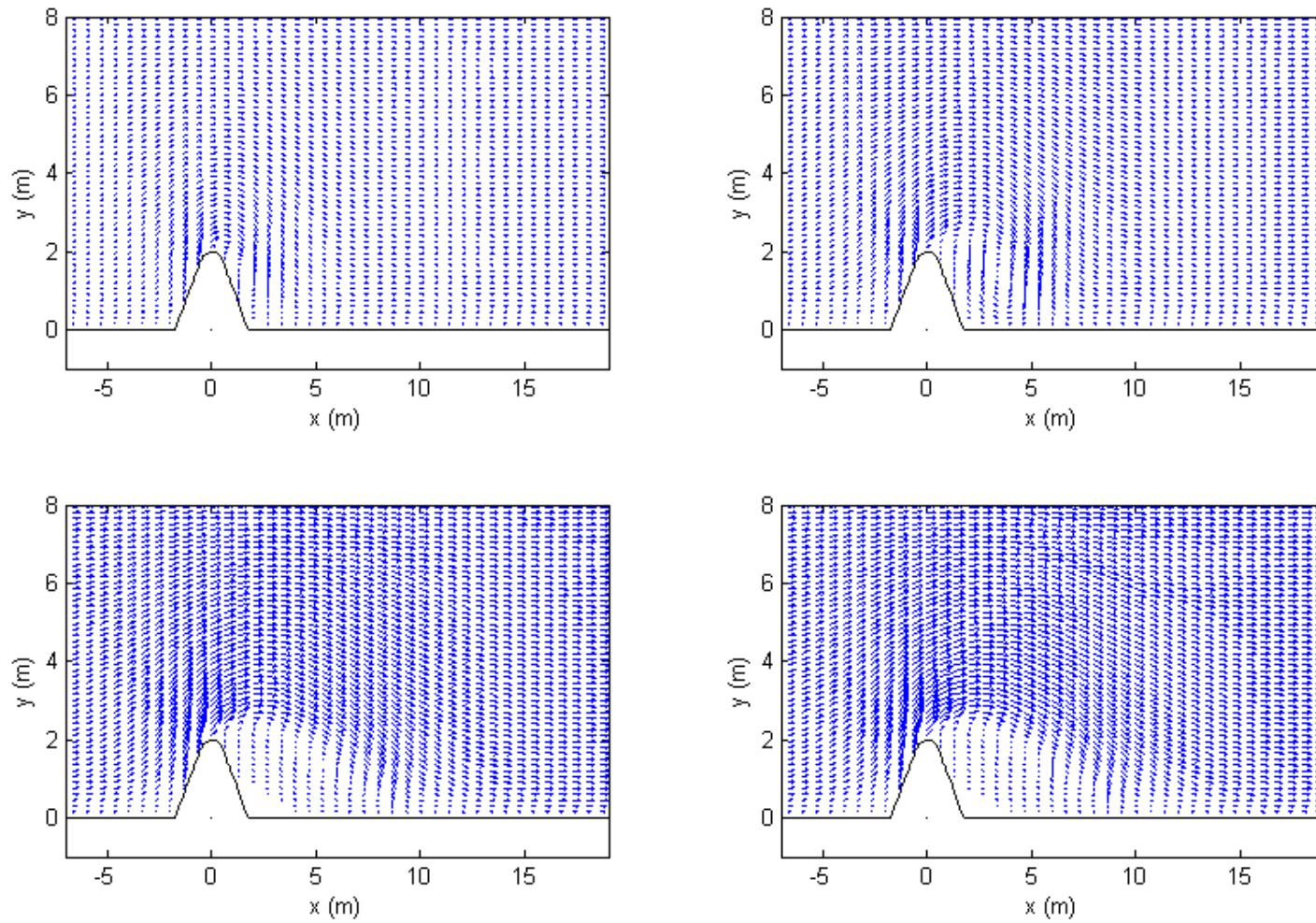


Figure 9. Vector flow field for headland with small C_d and eddy viscosity ν_T . Clockwise from top left of $0T$, $0.1T$, $0.2 T$ and $0.25 T$. See text for more details.

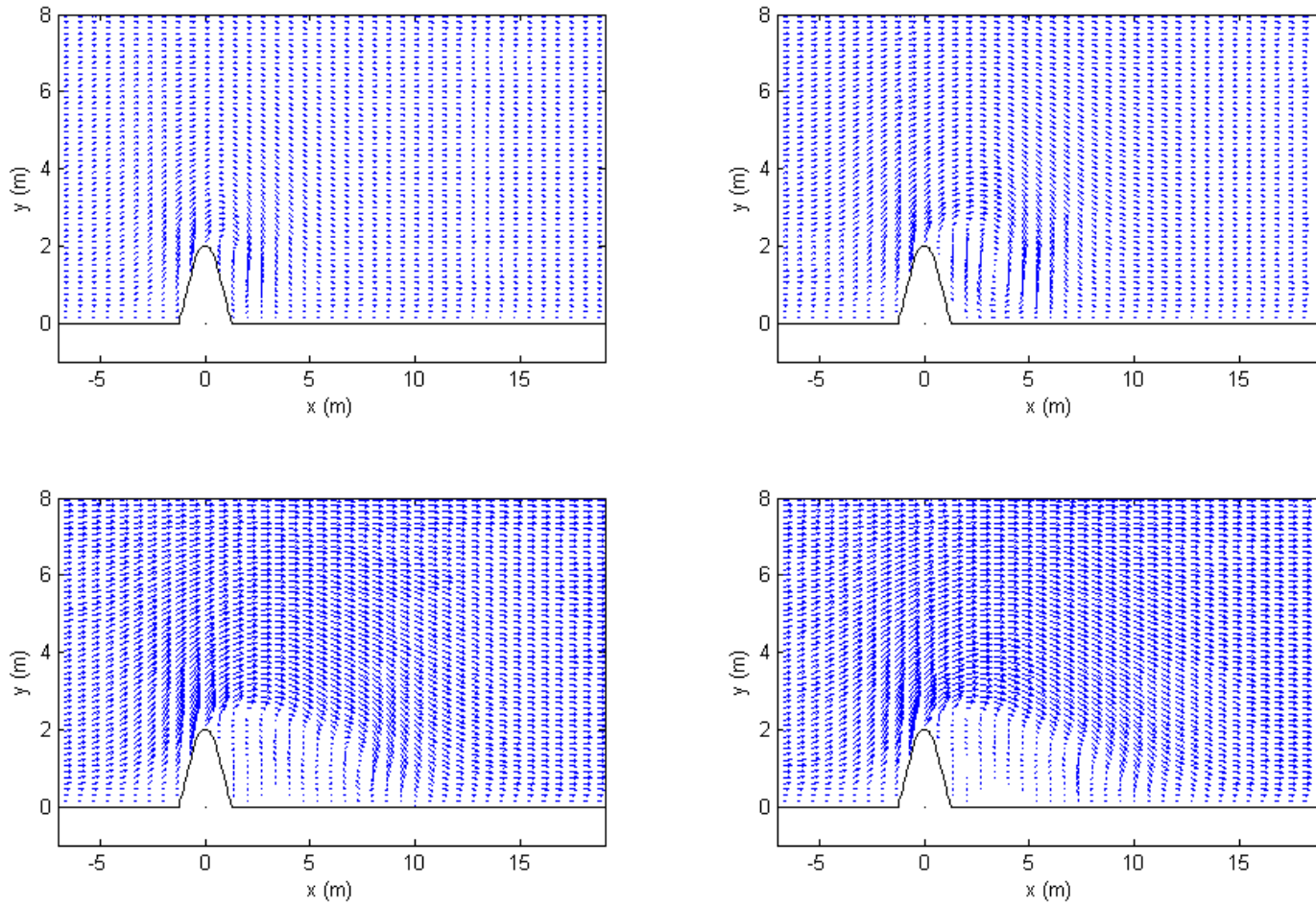


Figure 10: Test 1, 2x2.5 m headland, 0.3 m/s - Clockwise from top left: 0.05T, 0.1T, 0.2T, 0.25T. Without turbine fence.

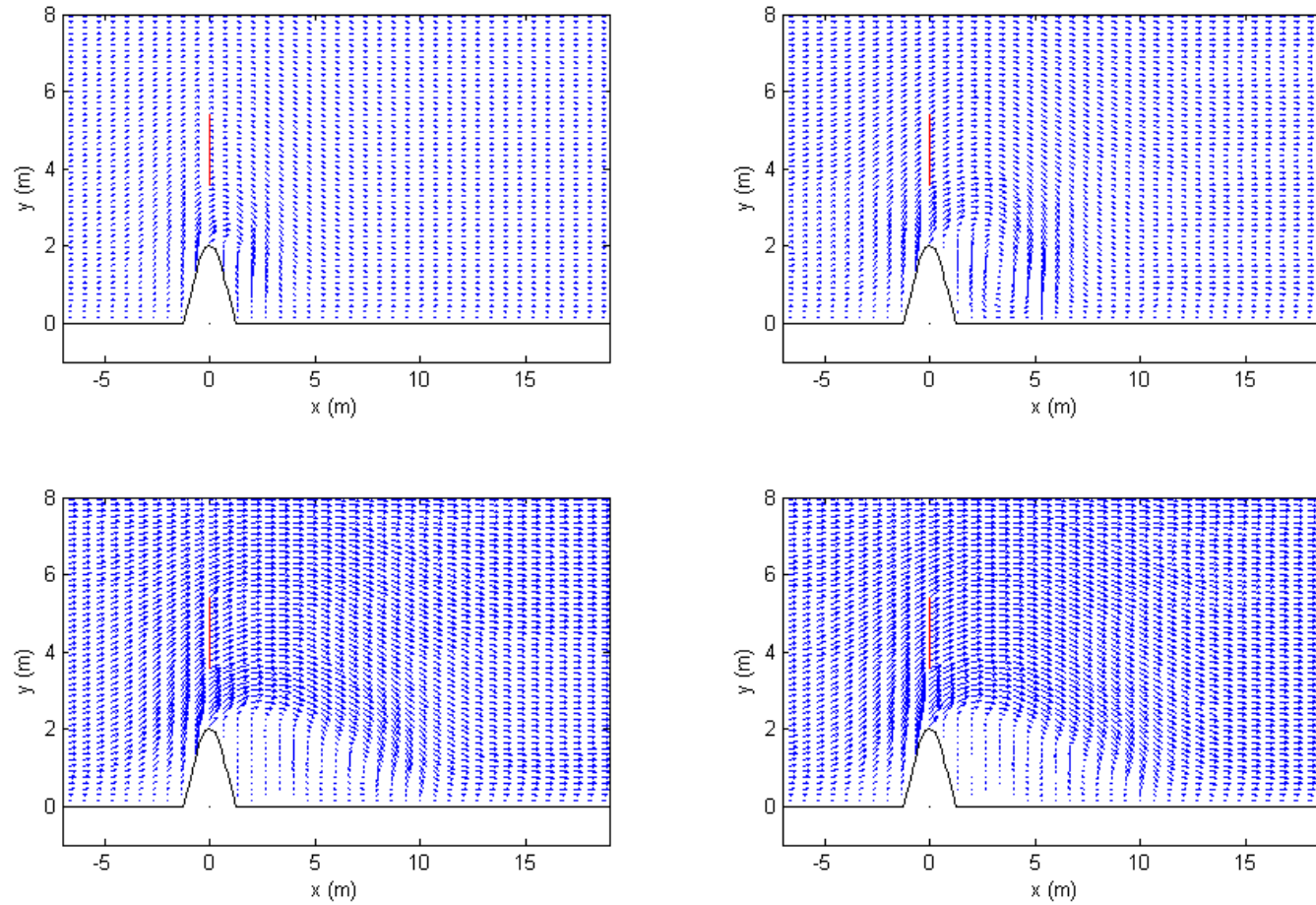


Figure 11: Test 2, 2x2.5 m headland, 0.3 m/s - Clockwise from top left: 0.05T, 0.1T, 0.2T, 0.25T. With turbine fence at (0,0).

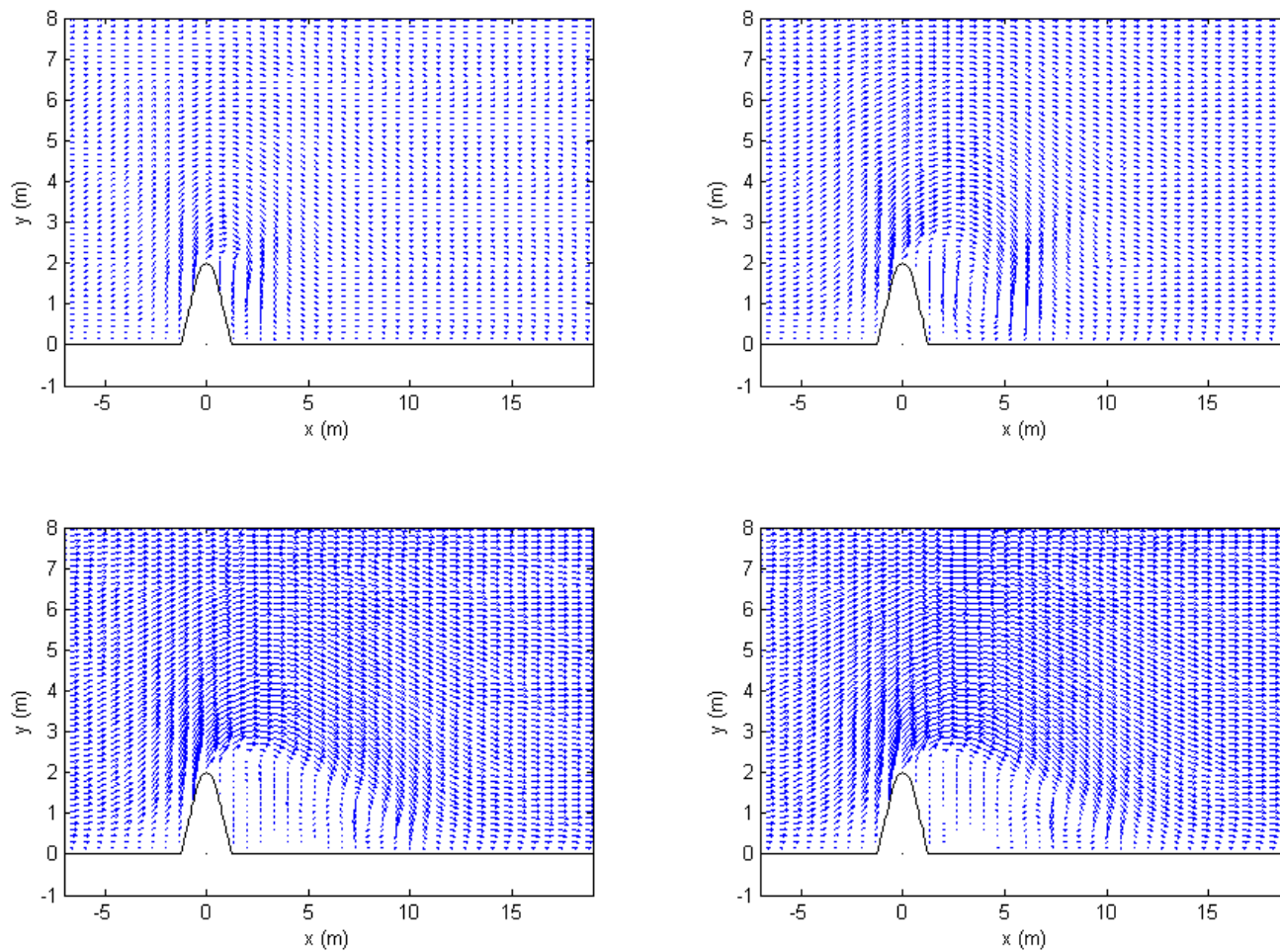


Figure 12: Test 3, 2x2.5 m headland, 0.35 m/s - Clockwise from top left: 0.05T, 0.1T, 0.2T, 0.25T. Without turbine fence.

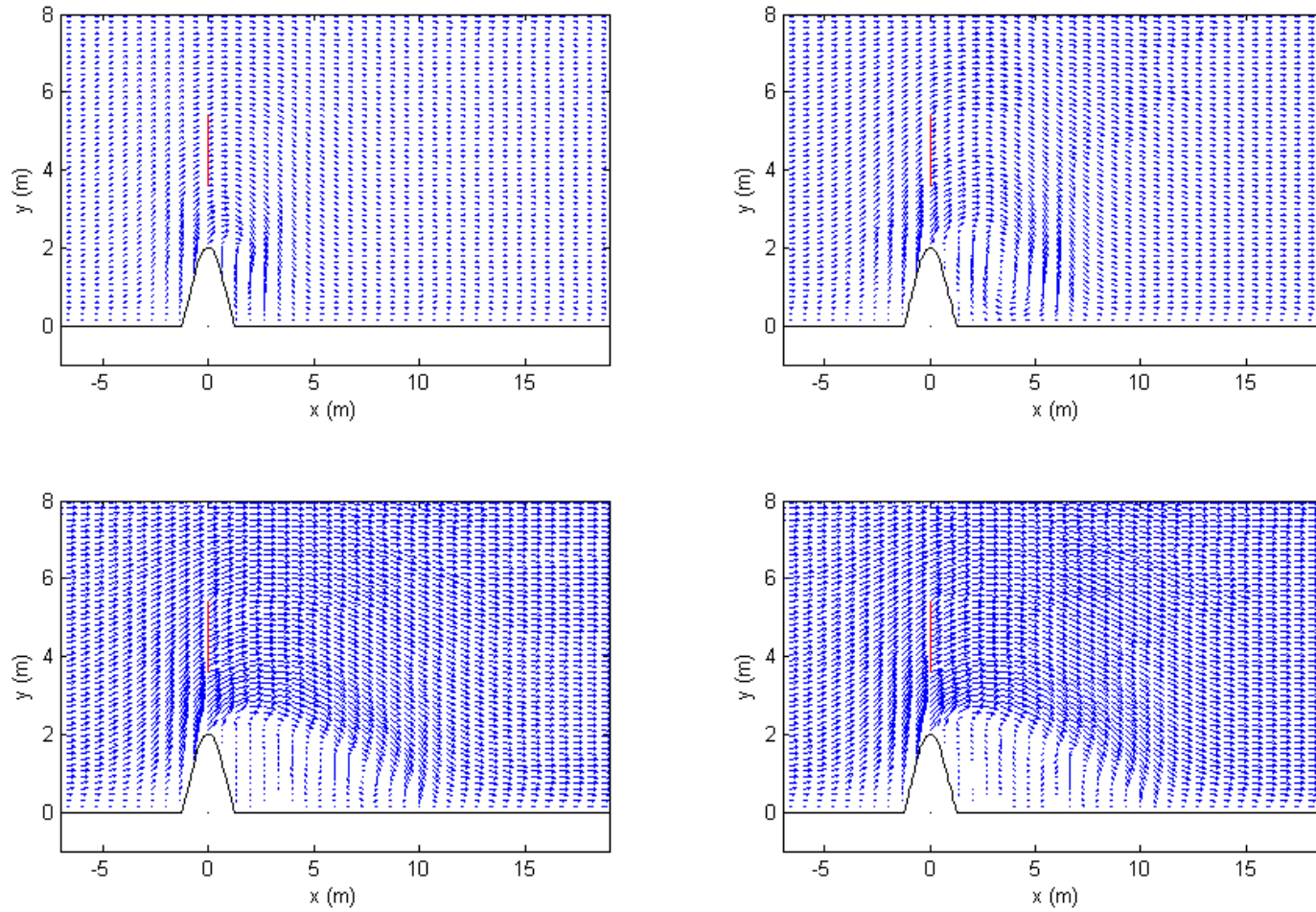


Figure 13: Test 4, 2x2.5 m headland, 0.35 m/s - Clockwise from top left: 0.05T, 0.1T, 0.2T, 0.25T. With turbine fence at (0,0).

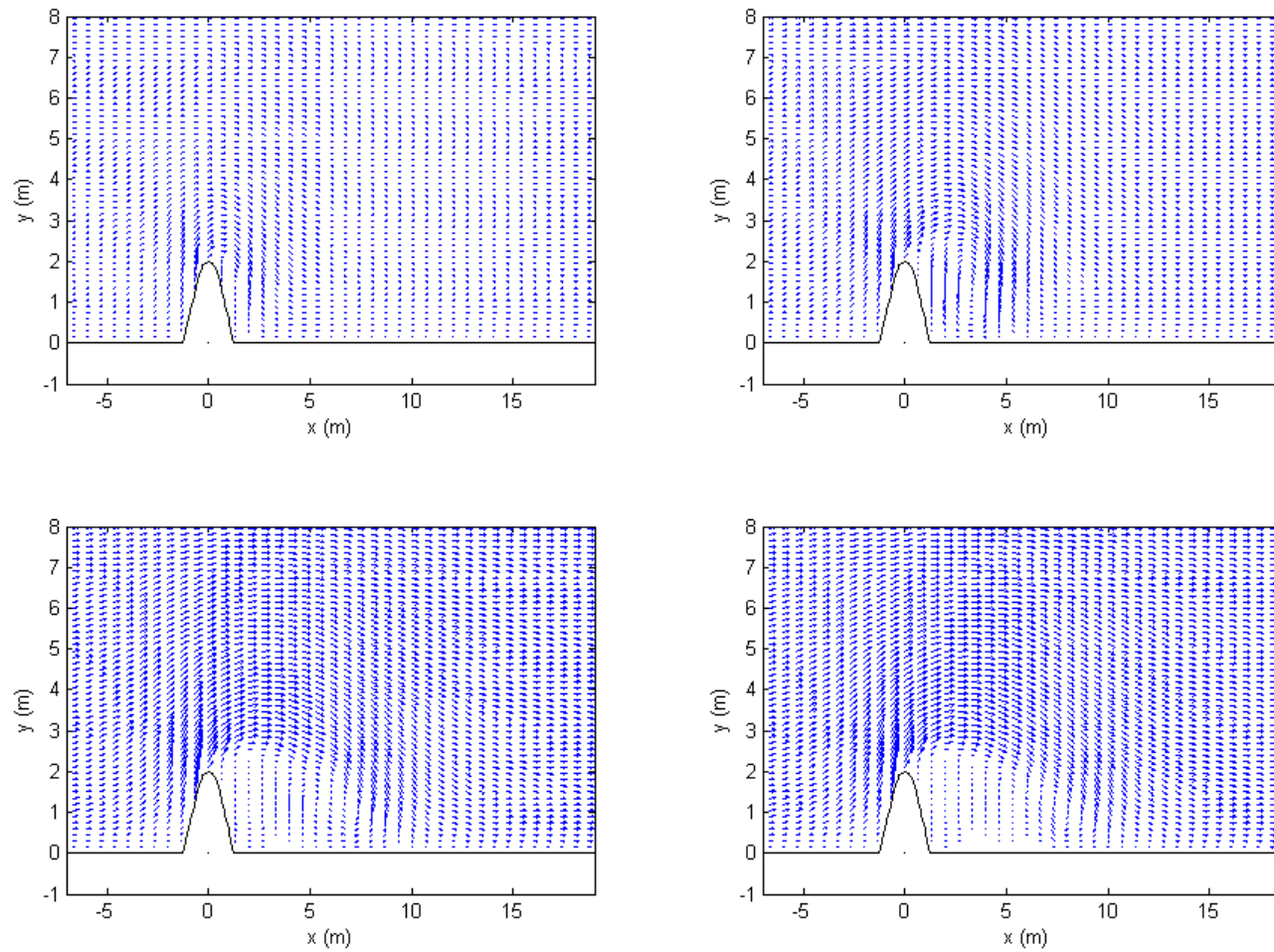


Figure 14: Test 5, 2x2.5 m headland, 0.25 m/s - Clockwise from top left: 0.05T, 0.1T, 0.2T, 0.25T. No turbine fence.

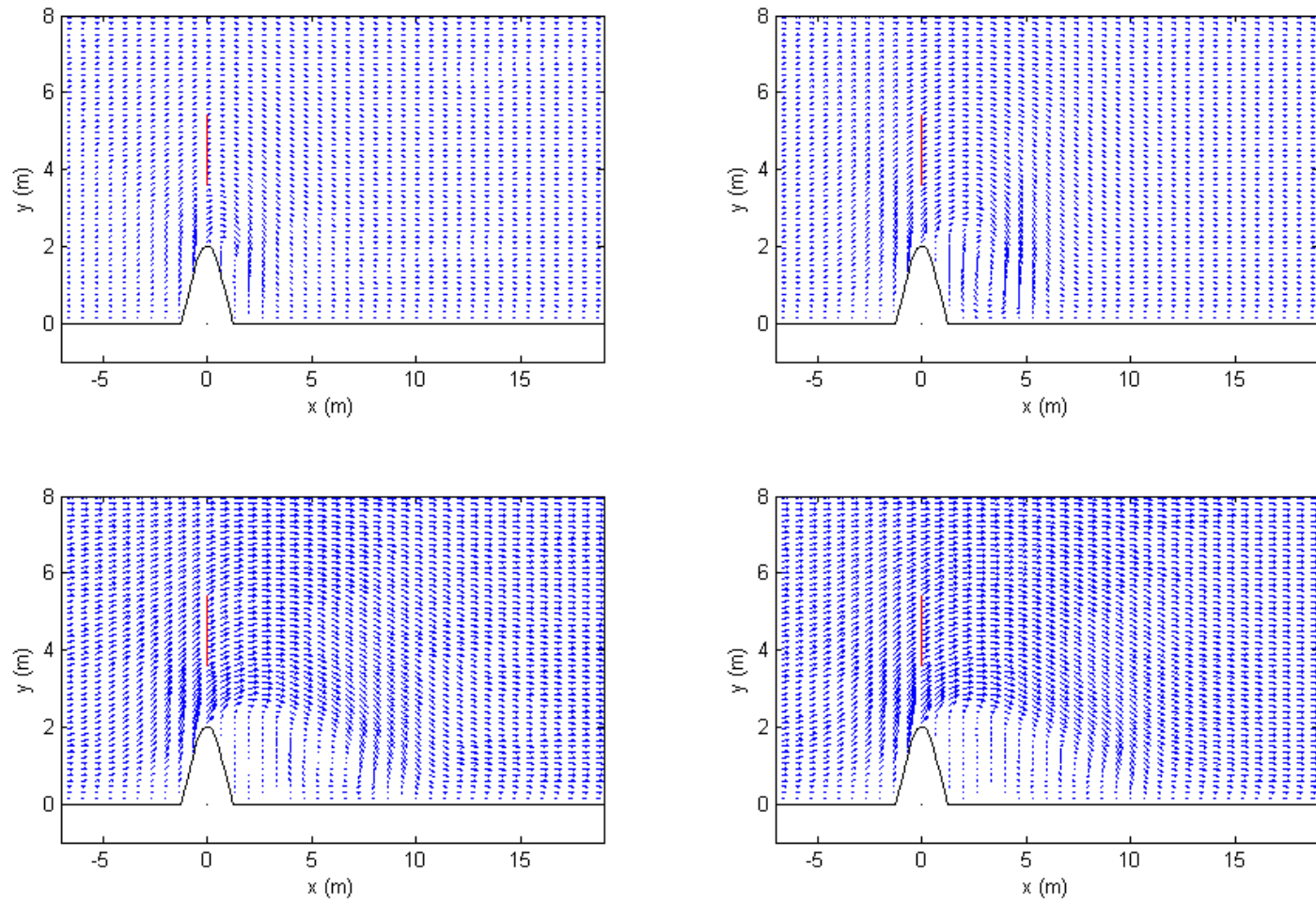


Figure 15: Test 6, 2x2.5 m headland, 0.25 m/s - Clockwise from top left: 0.05T, 0.1T, 0.2T, 0.25T. With turbine fence at (0,0).

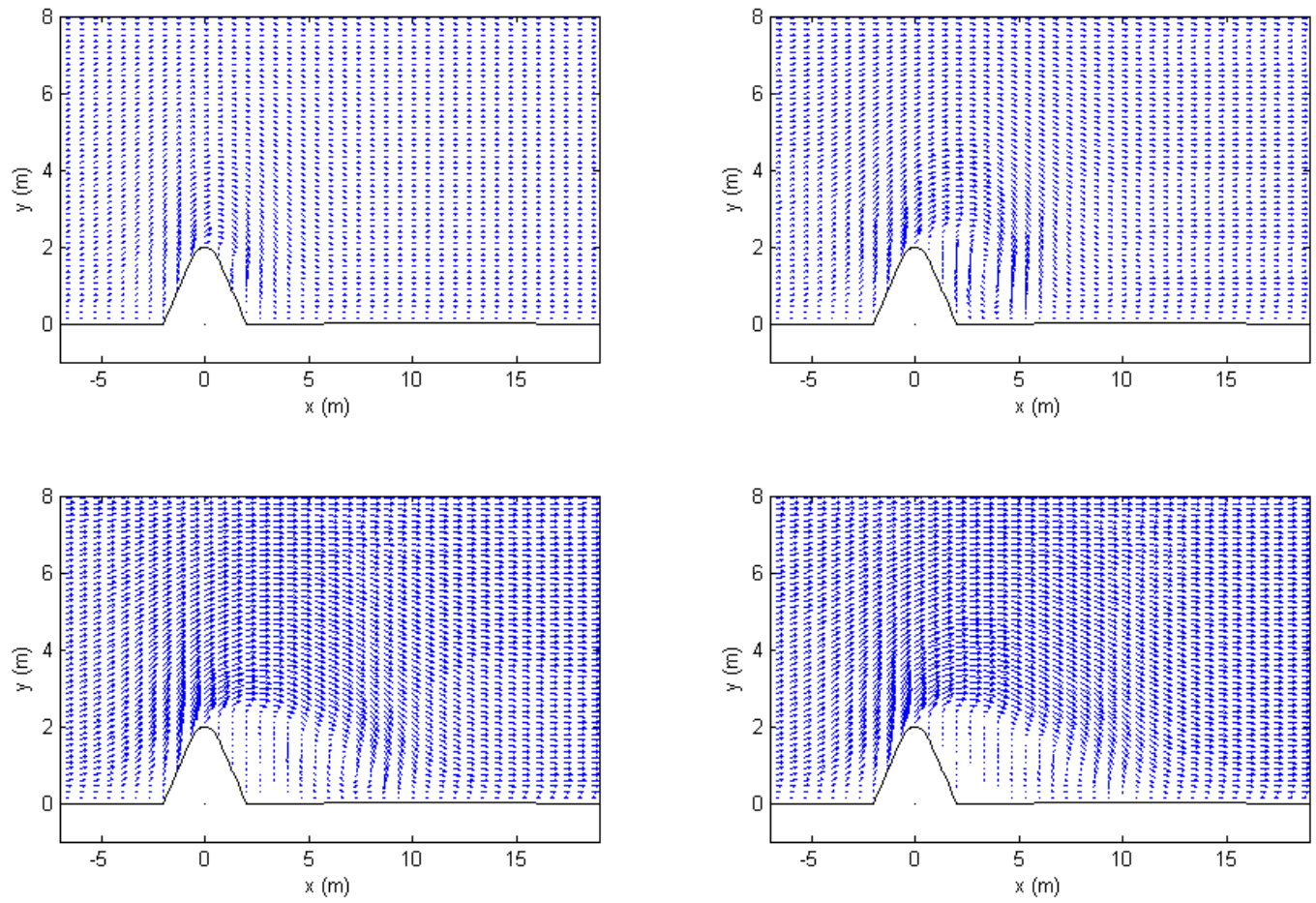


Figure 16: Test 7, 2x4 m headland, 0.3 m/s - Clockwise from top left: 0.05T, 0.1T, 0.2T, 0.25T. Without turbine fence.

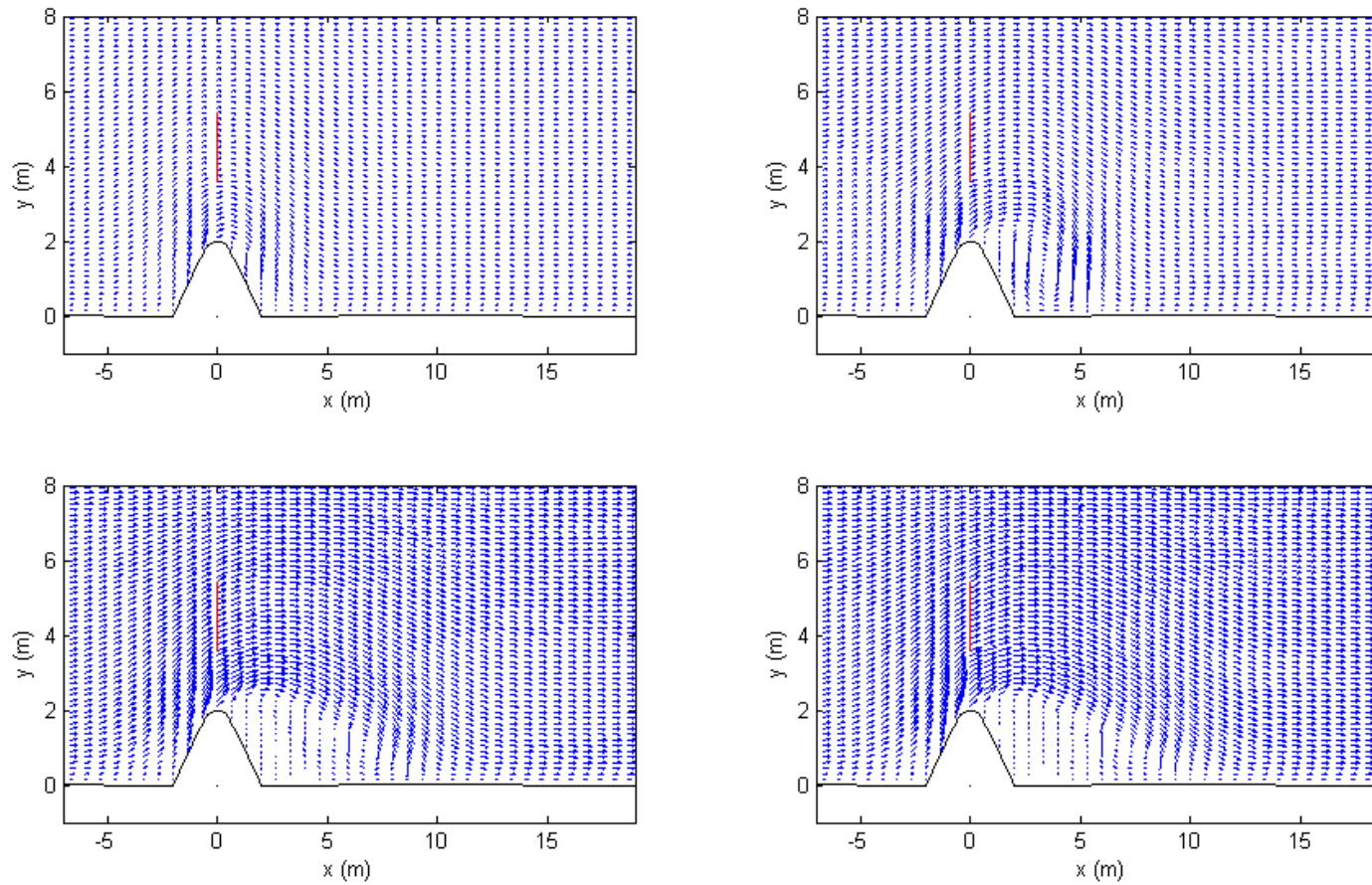


Figure 17: Test 8, 2x4 m headland, 0.3 m/s - Clockwise from top left: 0.05T, 0.1T, 0.2T, 0.25T. With turbine fence at (0,0).

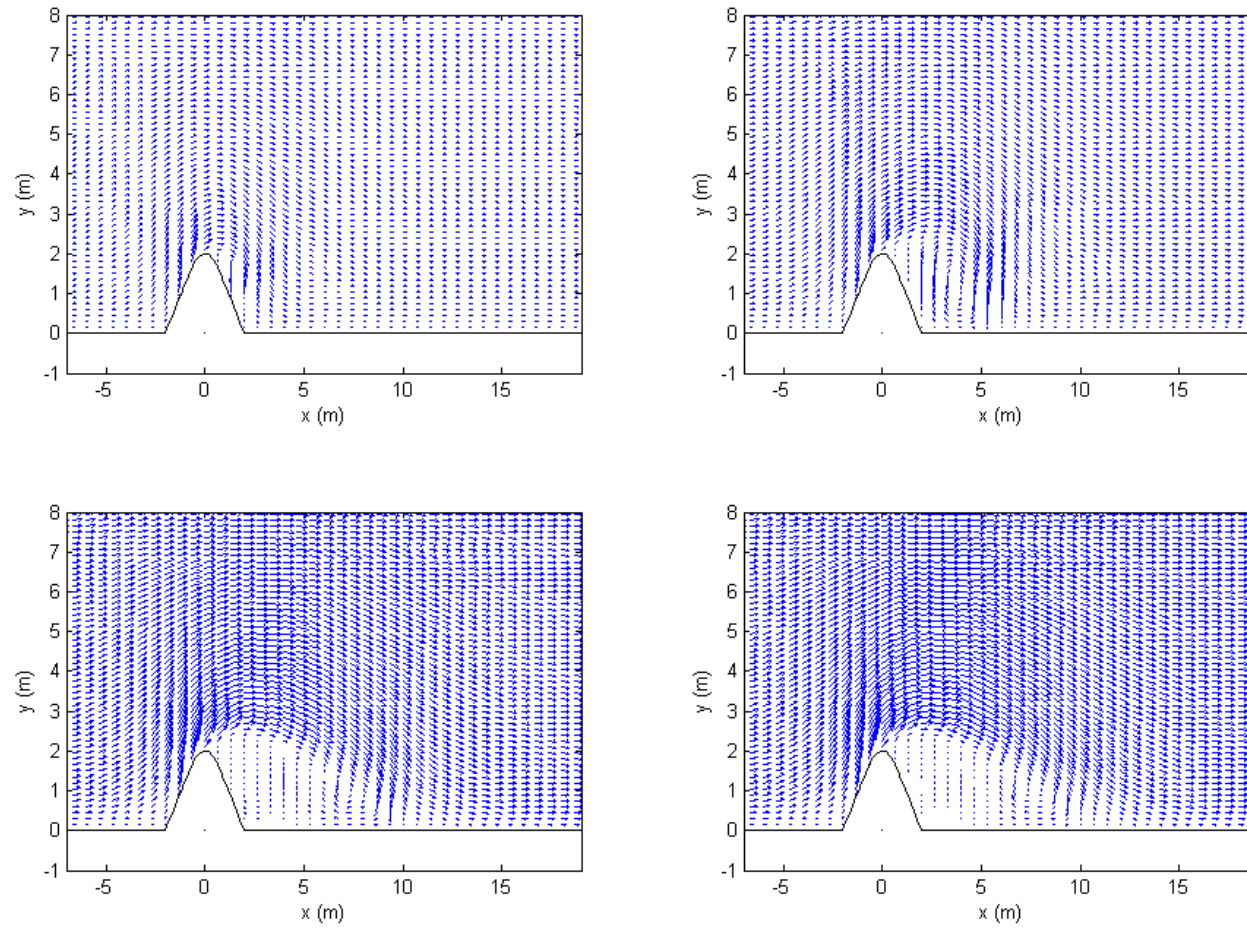


Figure 18: Test 9, 2x4 m headland, 0.35 m/s - Clockwise from top left: 0.05T, 0.1T, 0.2T, 0.25T. Without turbine fence.

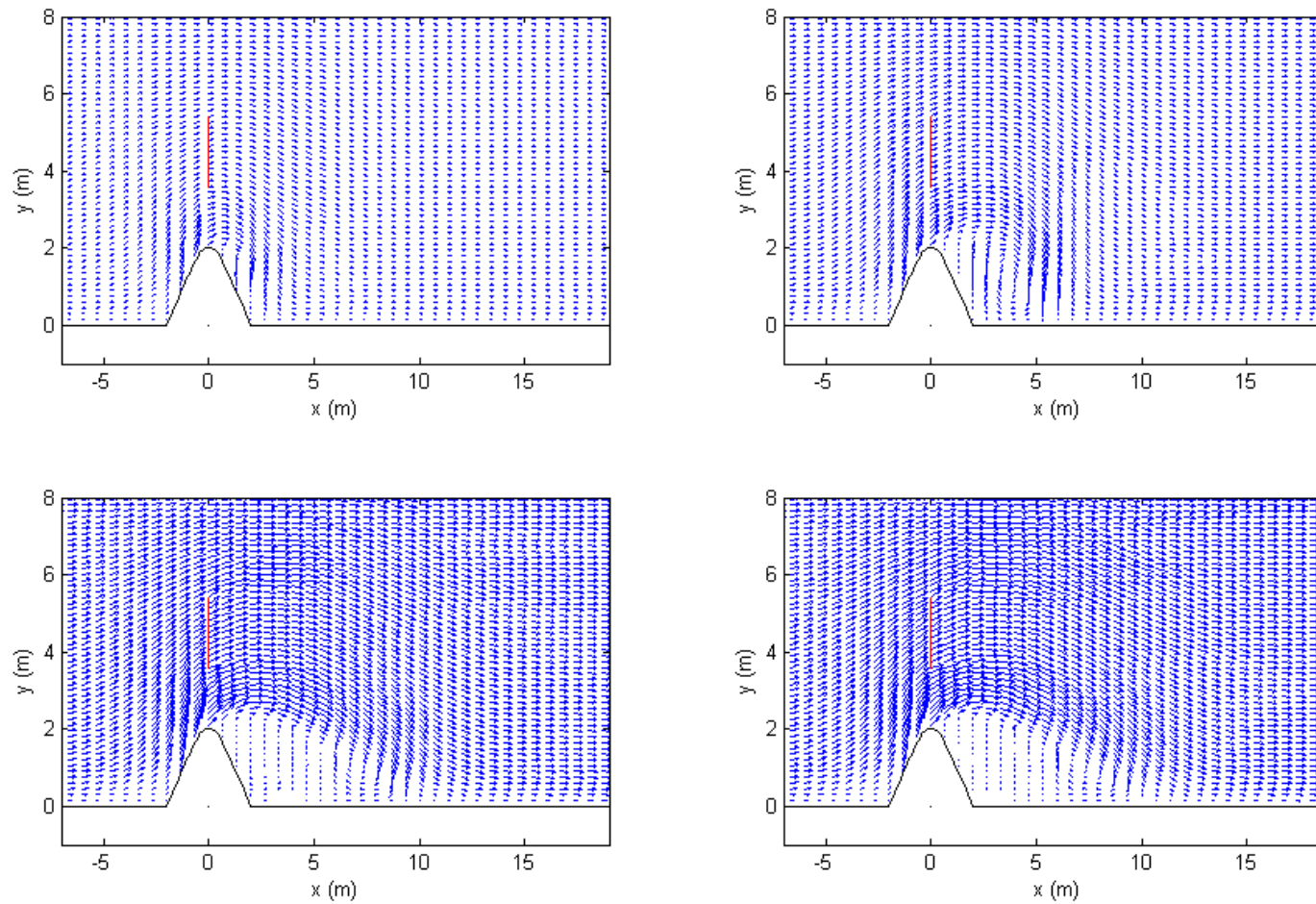


Figure 19: Test 10, 2x4 m headland, 0.35 m/s - Clockwise from top left: 0.05T, 0.1T, 0.2T, 0.25T. With turbine fence at (0,0).

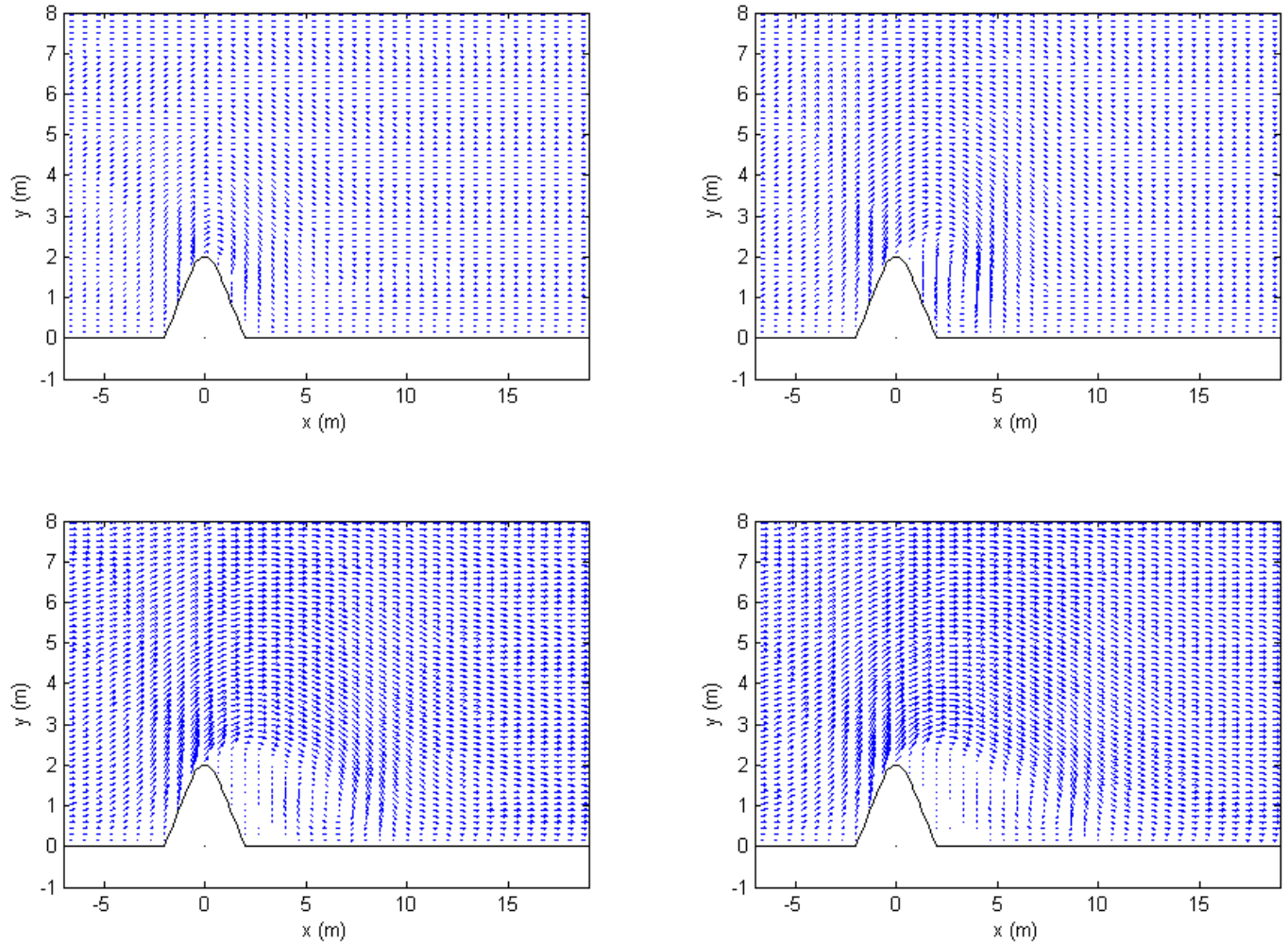


Figure 20: Test 11, 2x4 m headland, 0.25 m/s - Clockwise from top left: 0.05T, 0.1T, 0.2T, 0.25T. Without turbine fence.

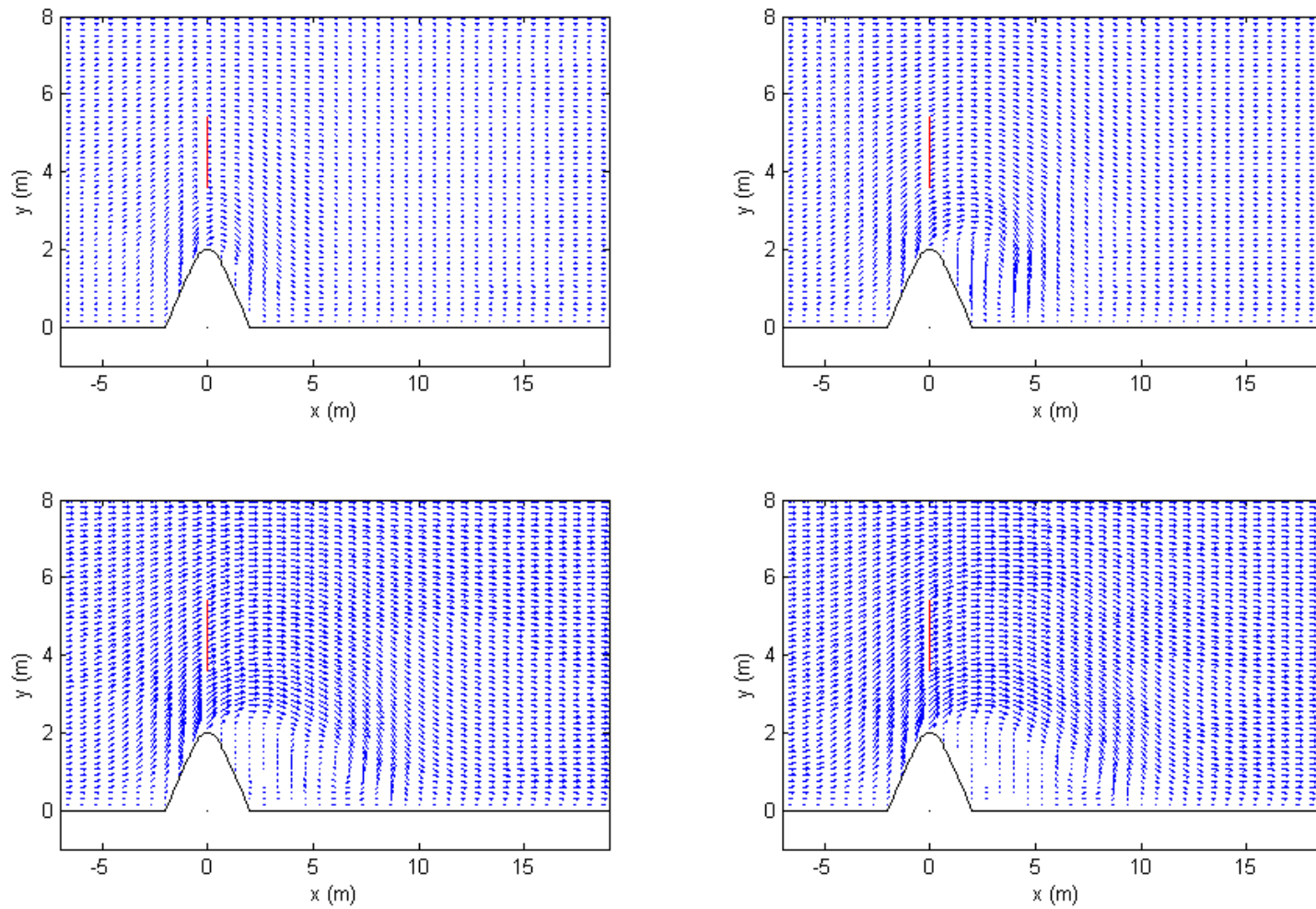


Figure 21: Test 12, 2x4 m headland, 0.25 m/s - Clockwise from top left: 0.05T, 0.1T, 0.2T, 0.25T. With turbine fence at (0,0).

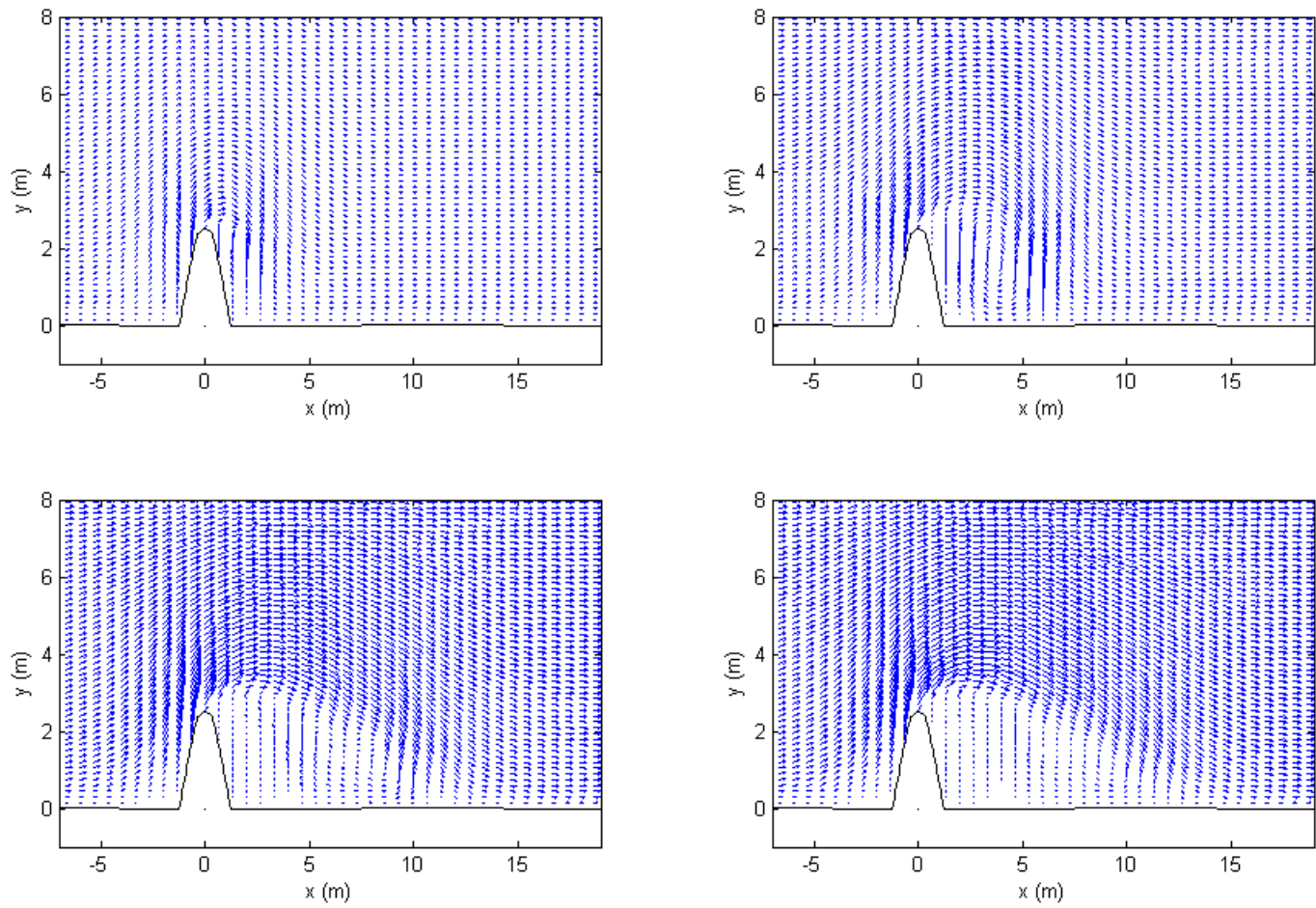


Figure 22: Test 13, 2.5x2.5m headland, 0.3 m/s - Clockwise from top left: 0.05T, 0.1T, 0.2T, 0.25T. Without turbine fence.

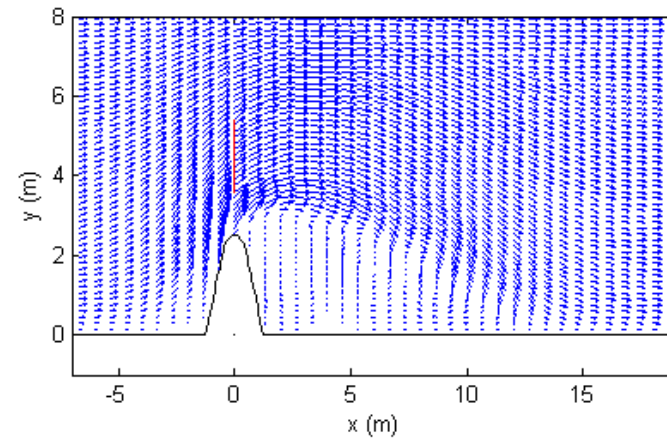
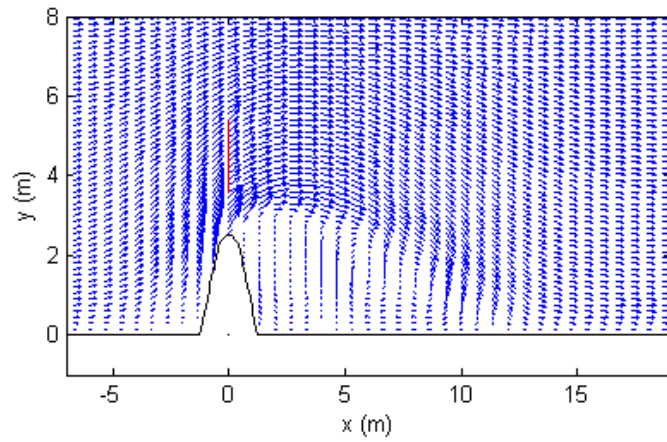
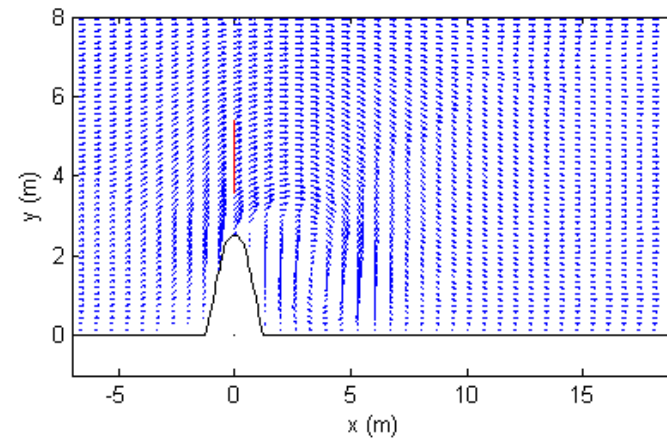
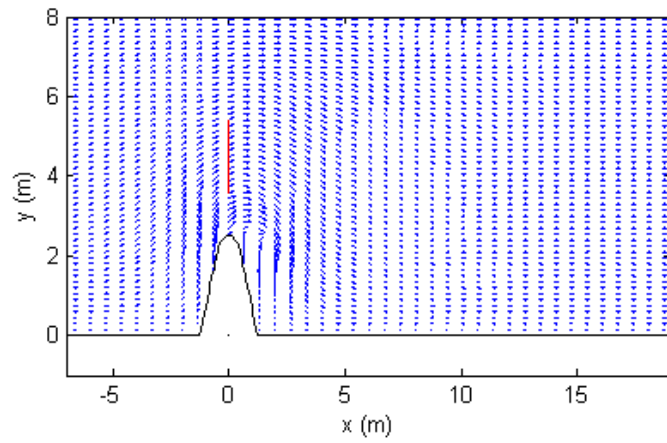


Figure 23: Test 14, 2.5x2.5 m headland, 0.3 m/s - Clockwise from top left: 0.05T, 0.1T, 0.2T, 0.25T. With turbine fence at (0,0).

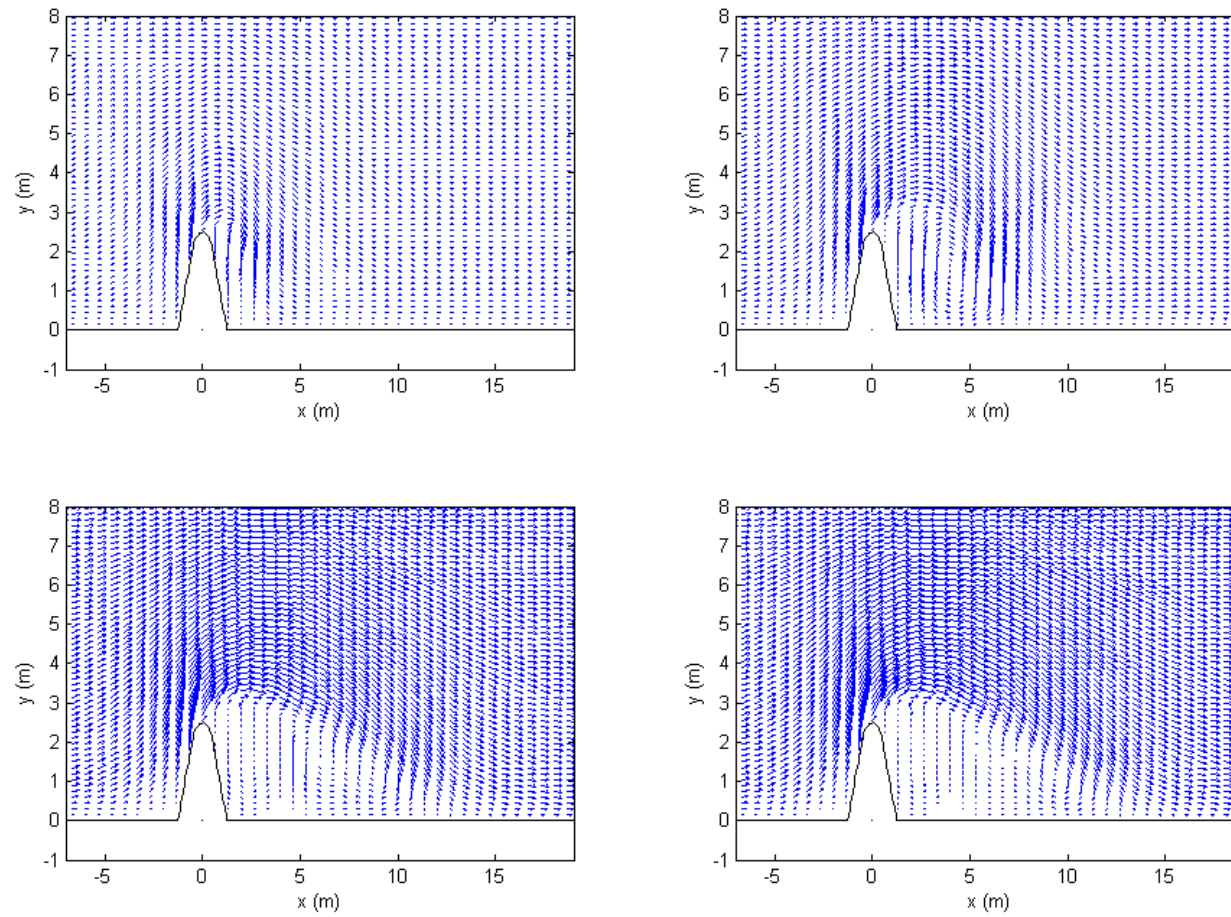


Figure 24: Test 15, 2.5x2.5m headland, 0.35 m/s - Clockwise from top left: 0.05T, 0.1T, 0.2T, 0.25T. Without turbine fence.

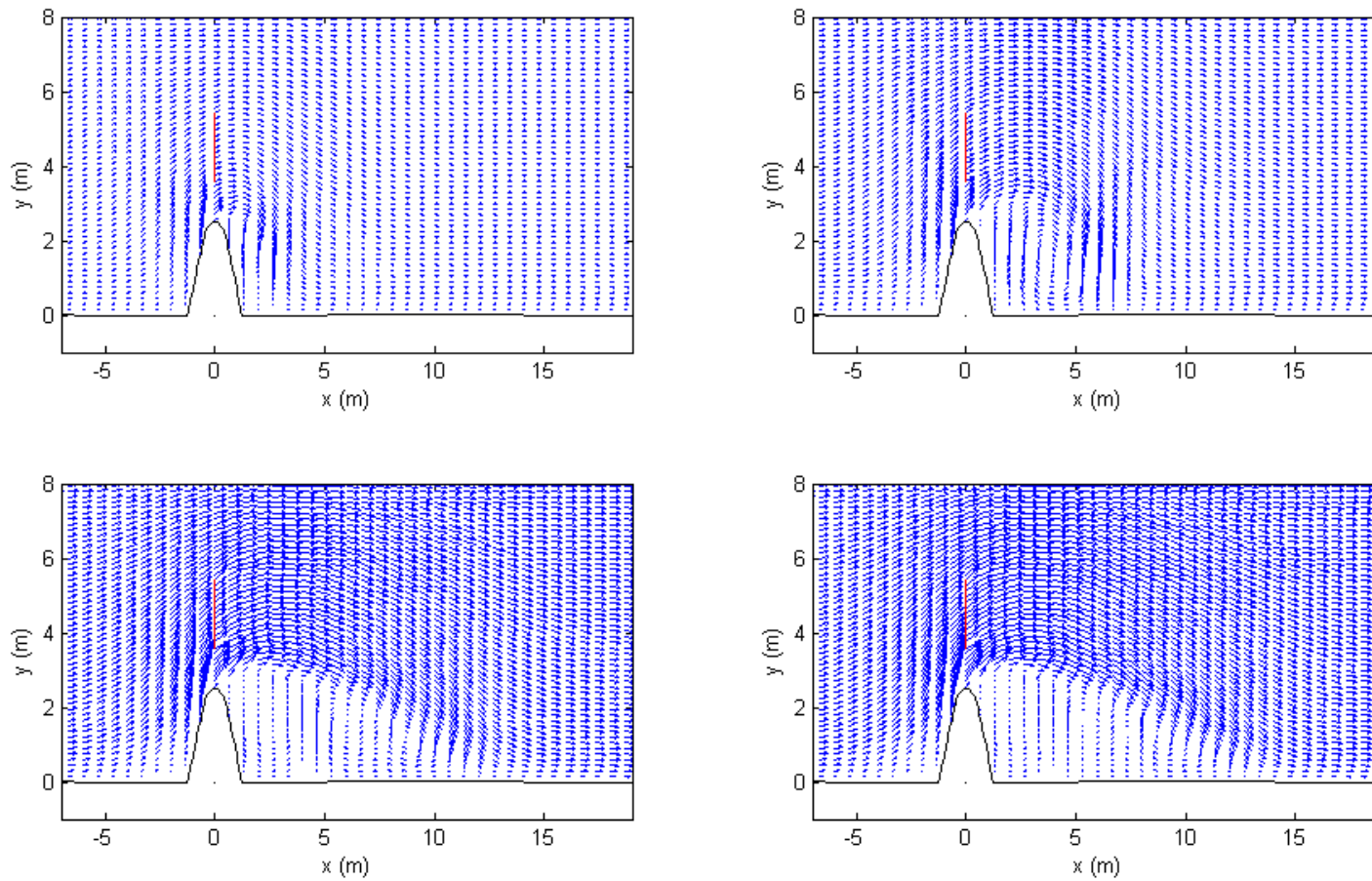


Figure 25: Test 16, 2.5x2.5 m headland, 0.35 m/s - Clockwise from top left: 0.05T, 0.1T, 0.2T, 0.25T. With turbine fence at (0,0).

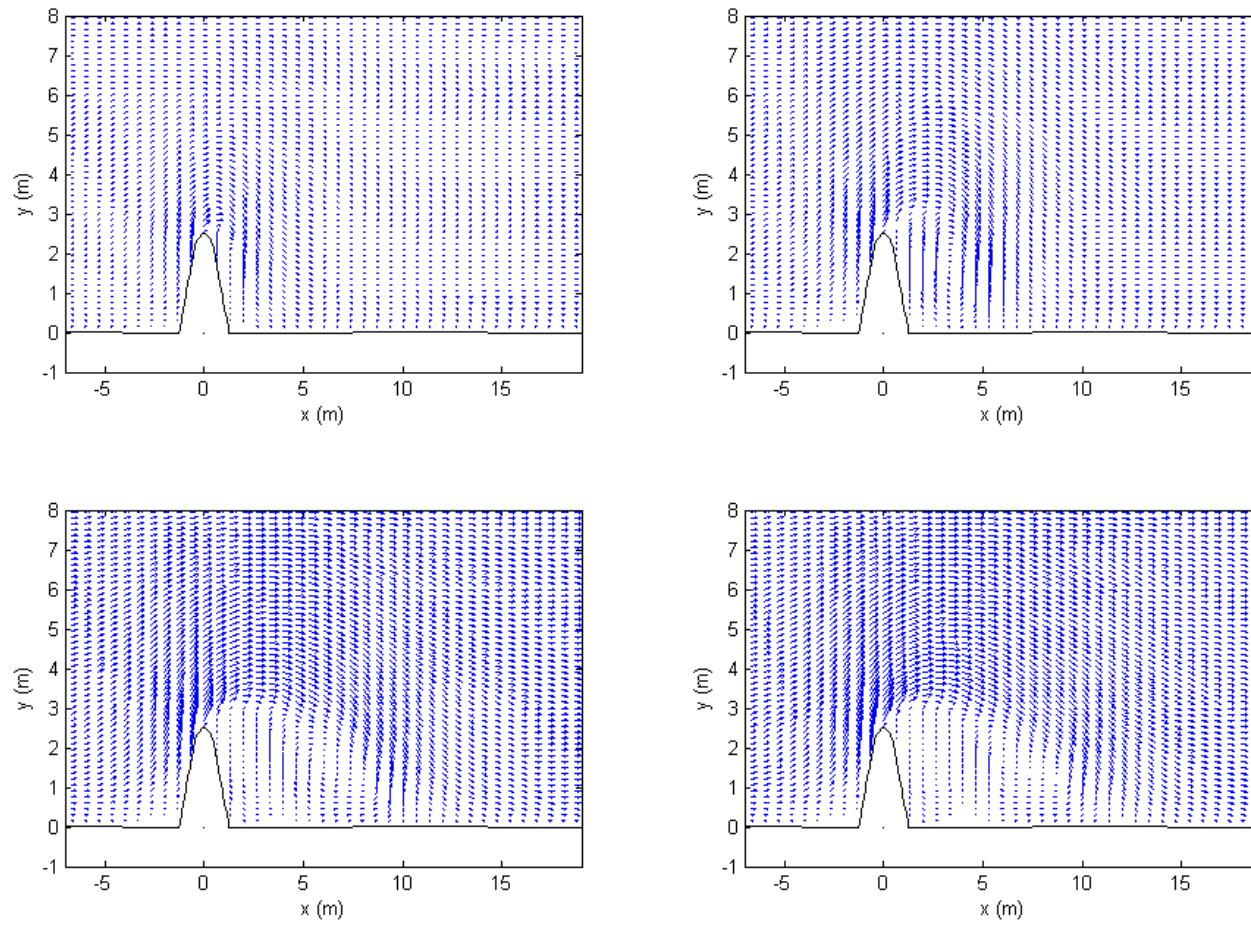


Figure 26: Test 17, 2.5x2.5m headland, 0.25 m/s - Clockwise from top left: 0.05T, 0.1T, 0.2T, 0.25T. Without turbine fence.

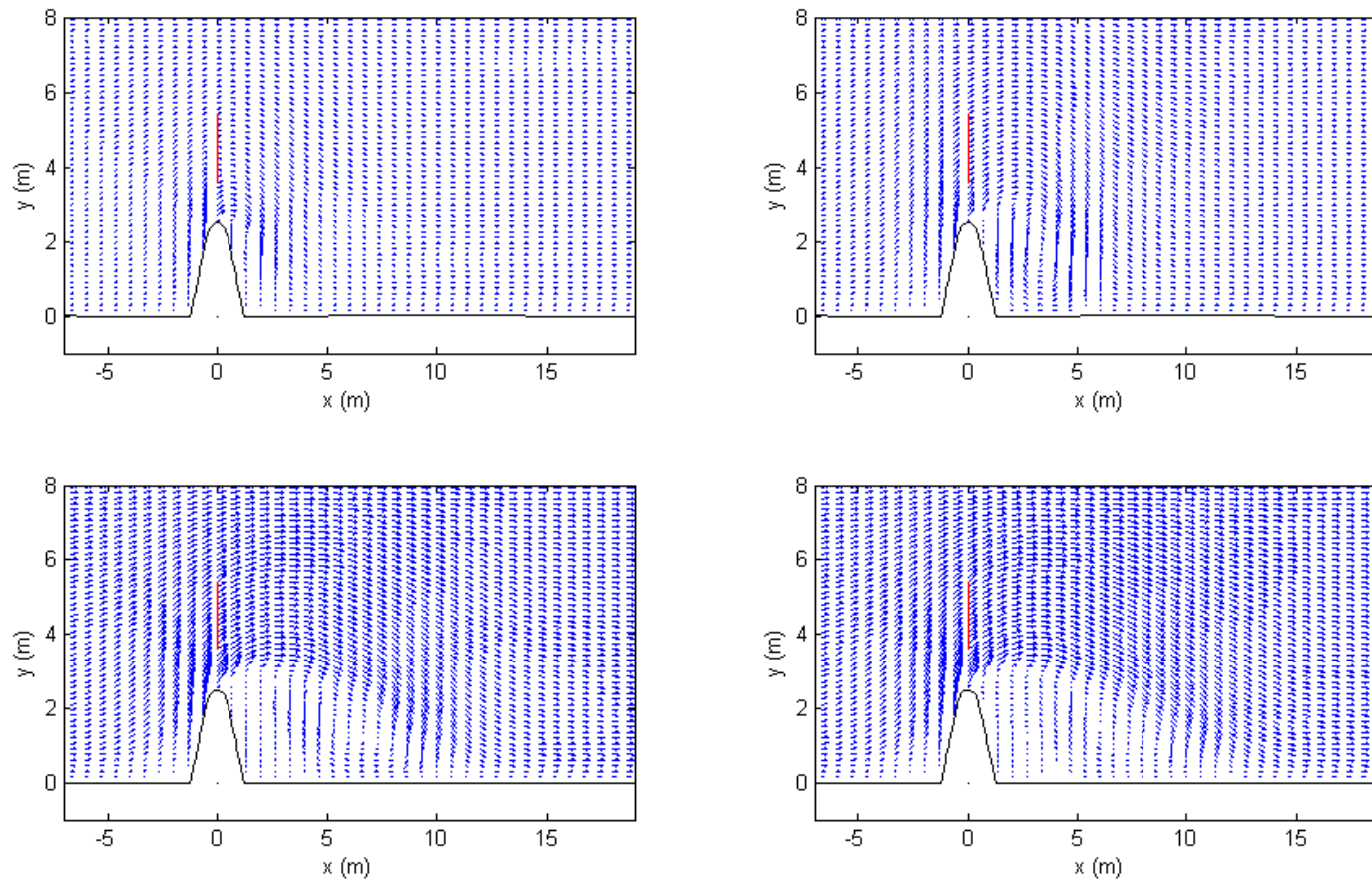


Figure 27: Test 18, 2.5x2.5 m headland, 0.25 m/s - Clockwise from top left: 0.05T, 0.1T, 0.2T, 0.25T. With turbine fence at (0,0).

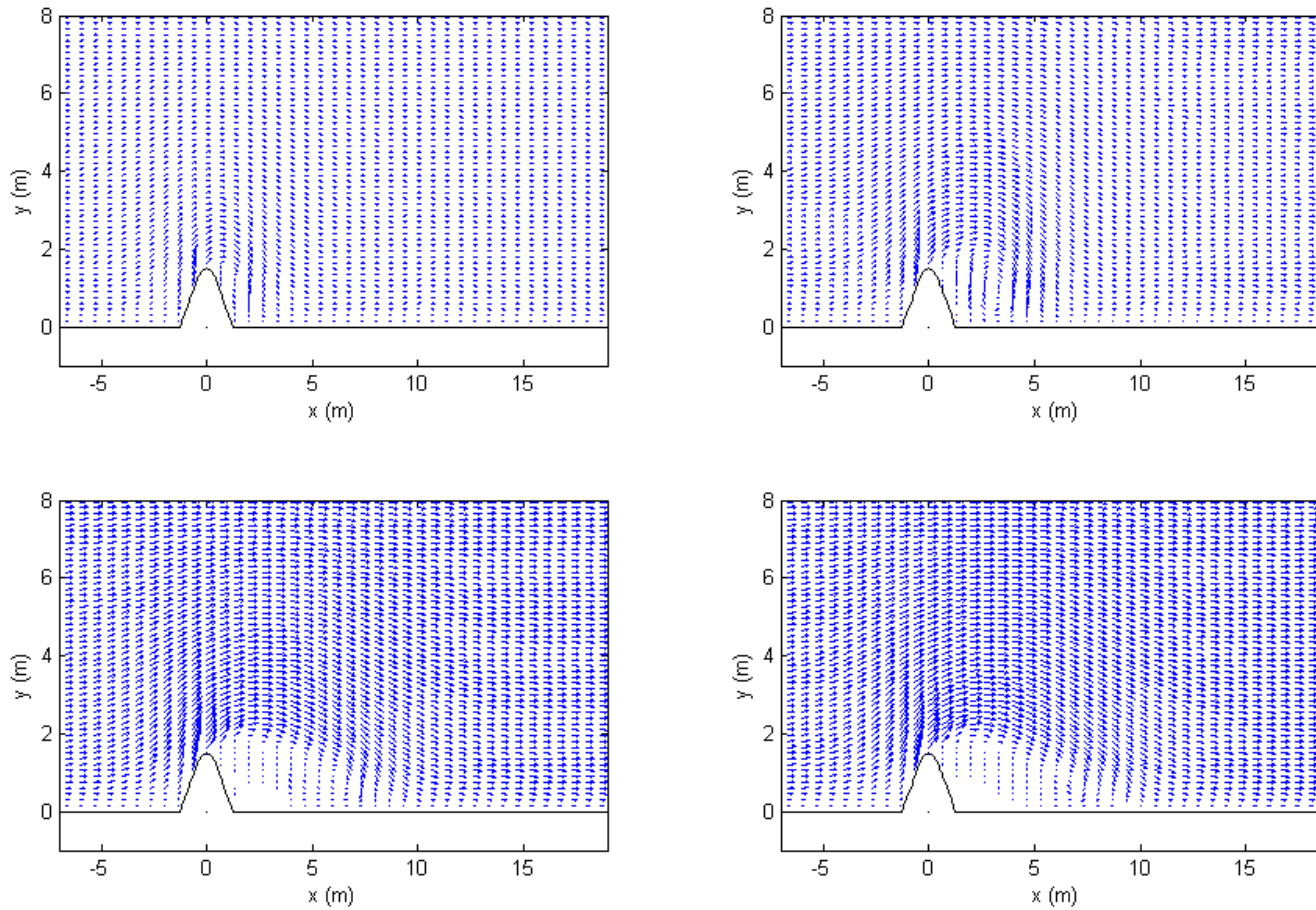


Figure 28: Test 19, 1.5x2.5m headland, 0.3 m/s - Clockwise from top left: 0.05T, 0.1T, 0.2T, 0.25T. Without turbine fence.

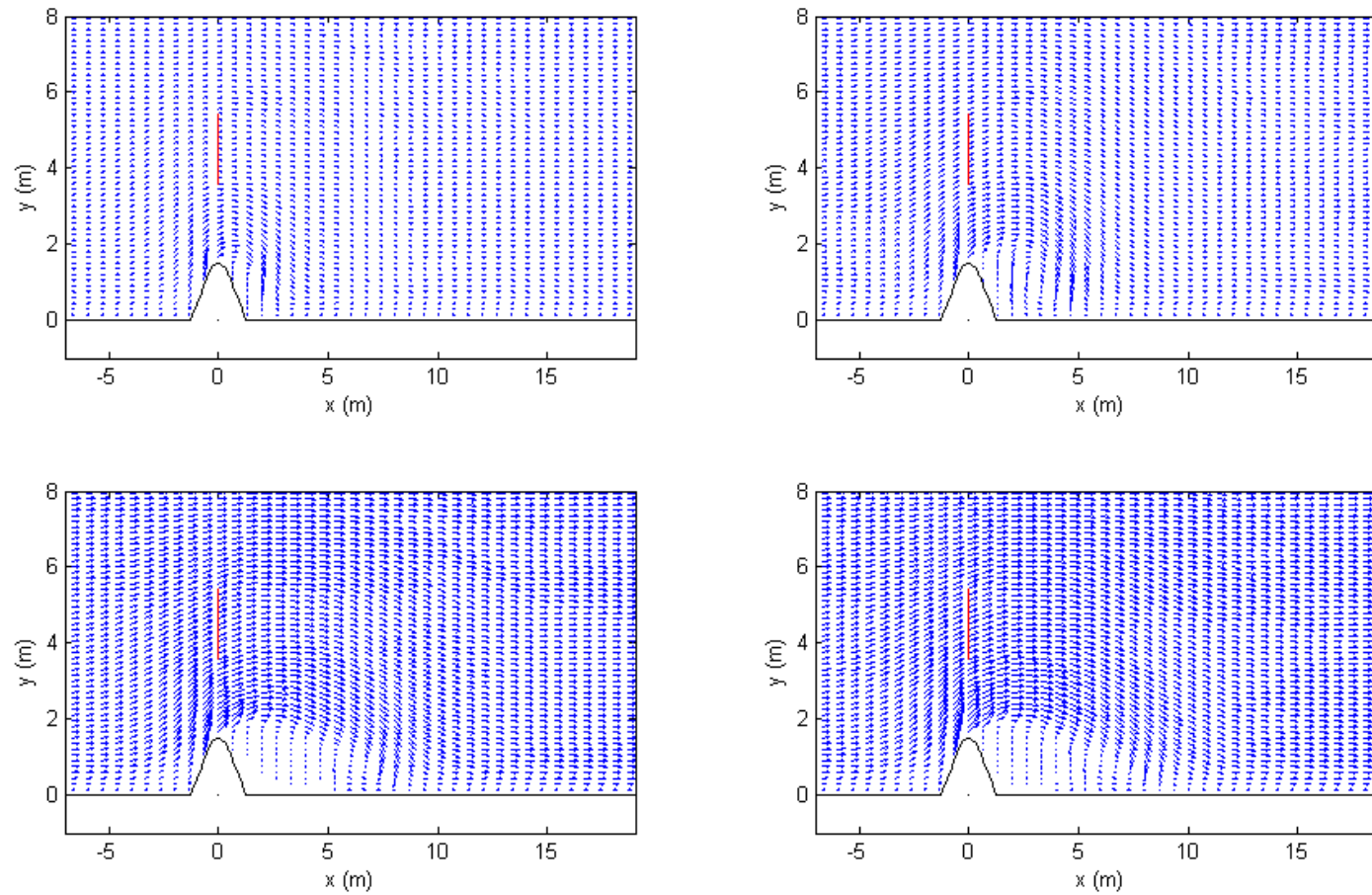


Figure 29: Test 20, 1.5x2.5 m headland, 0.3 m/s - Clockwise from top left: 0.05T, 0.1T, 0.2T, 0.25T. With turbine fence at (0,0).

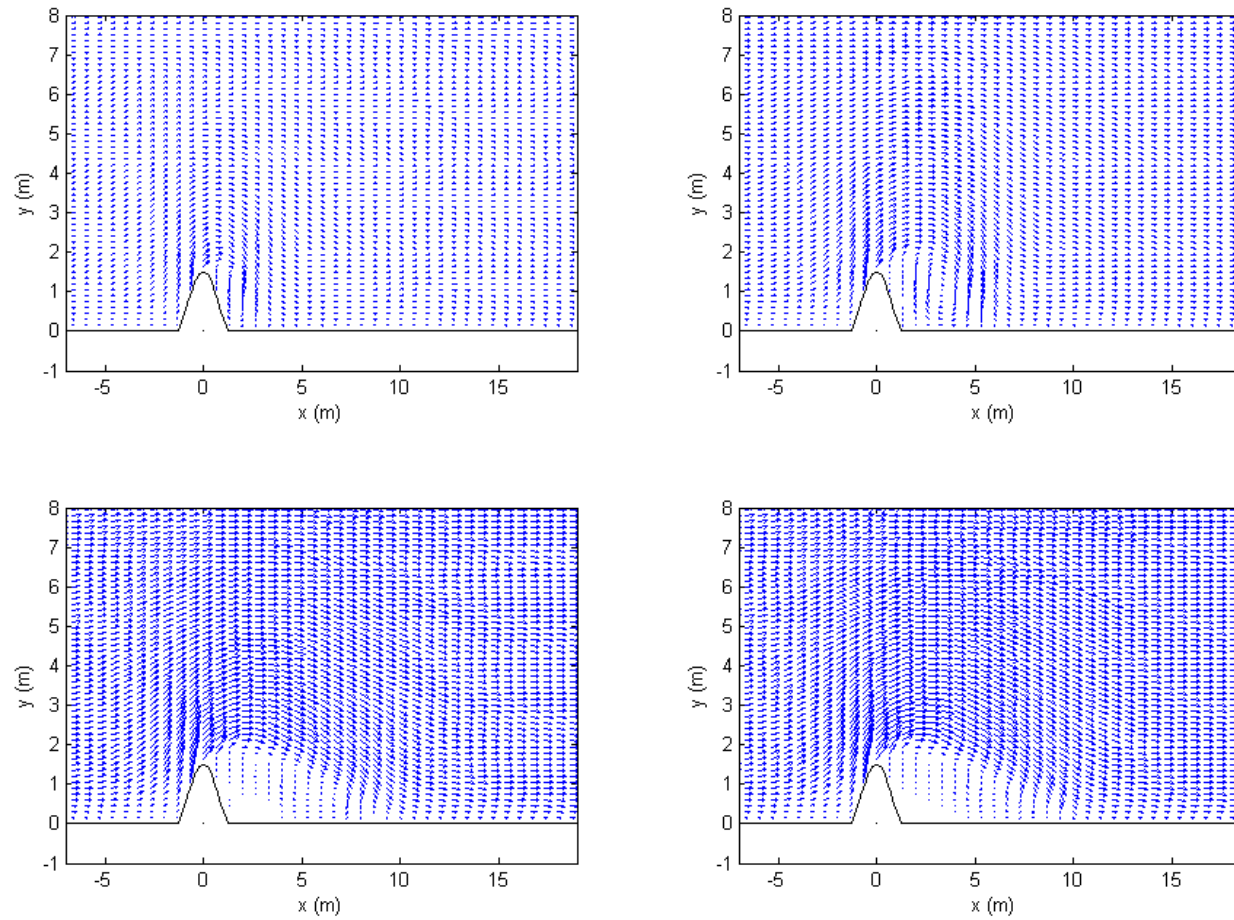


Figure 30: Test 21, 1.5x2.5m headland, 0.35 m/s - Clockwise from top left: 0.05T, 0.1T, 0.2T, 0.25T. Without turbine fence.

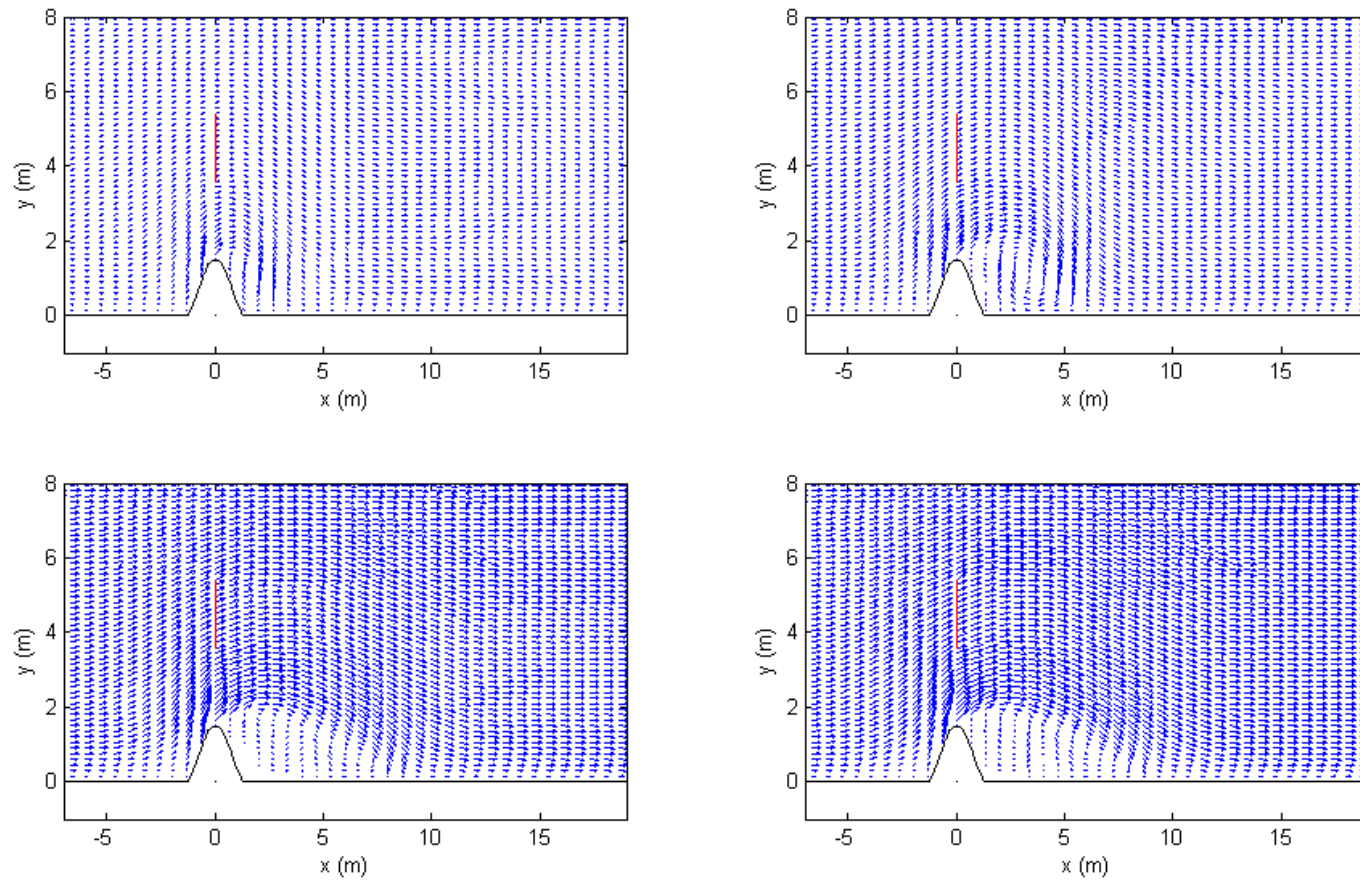


Figure 31: Test 22, 1.5x2.5 m headland, 0.35 m/s - Clockwise from top left: 0.05T, 0.1T, 0.2T, 0.25T. With turbine fence at (0,0).

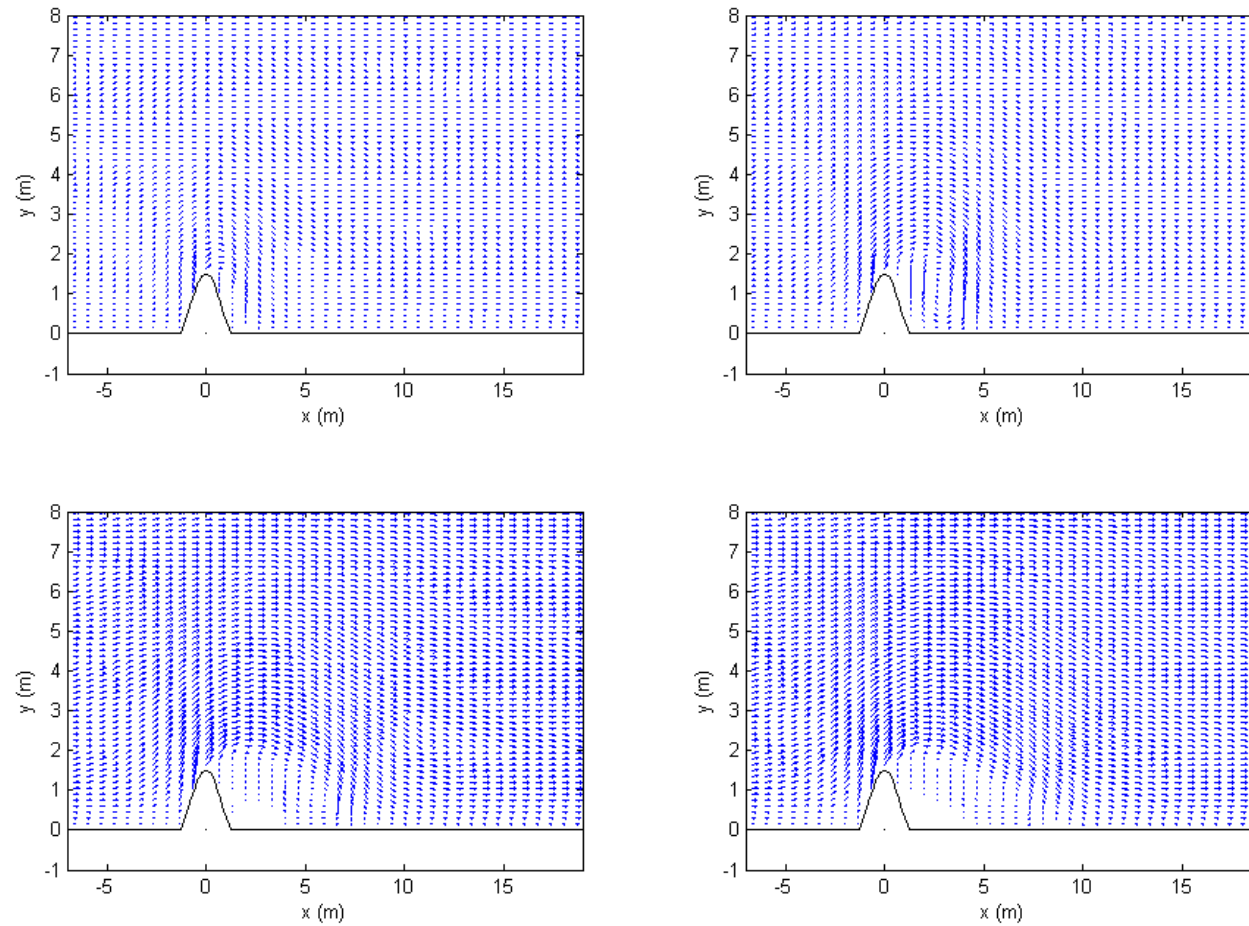


Figure 32: Test 23, 1.5x2.5m headland, 0.25 m/s - Clockwise from top left: 0.05T, 0.1T, 0.2T, 0.25T. Without turbine fence.

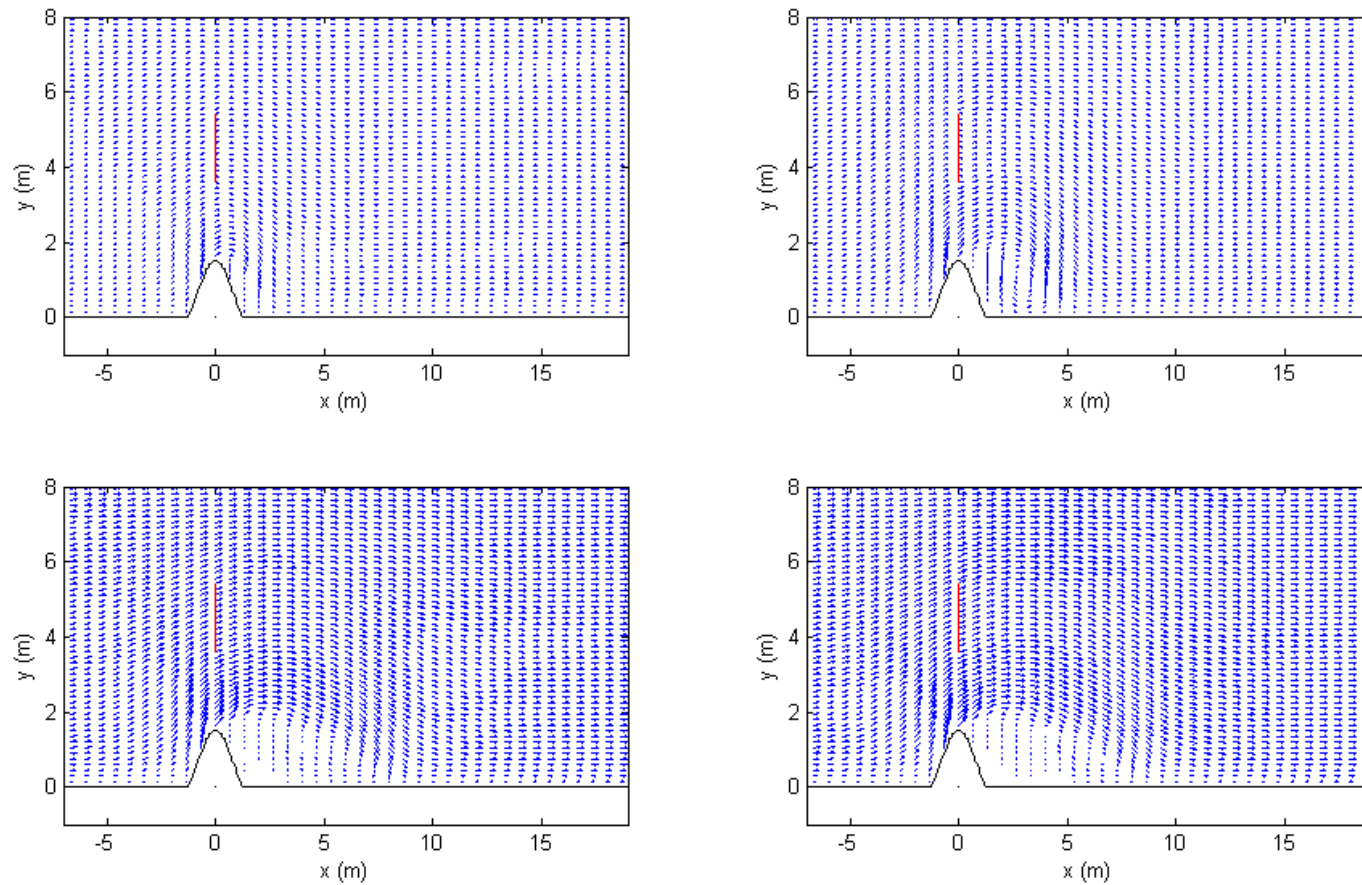


Figure 33: Test 24, 1.5x2.5 m headland, 0.25 m/s - Clockwise from top left: 0.05T, 0.1T, 0.2T, 0.25T. With turbine fence at (0,0).

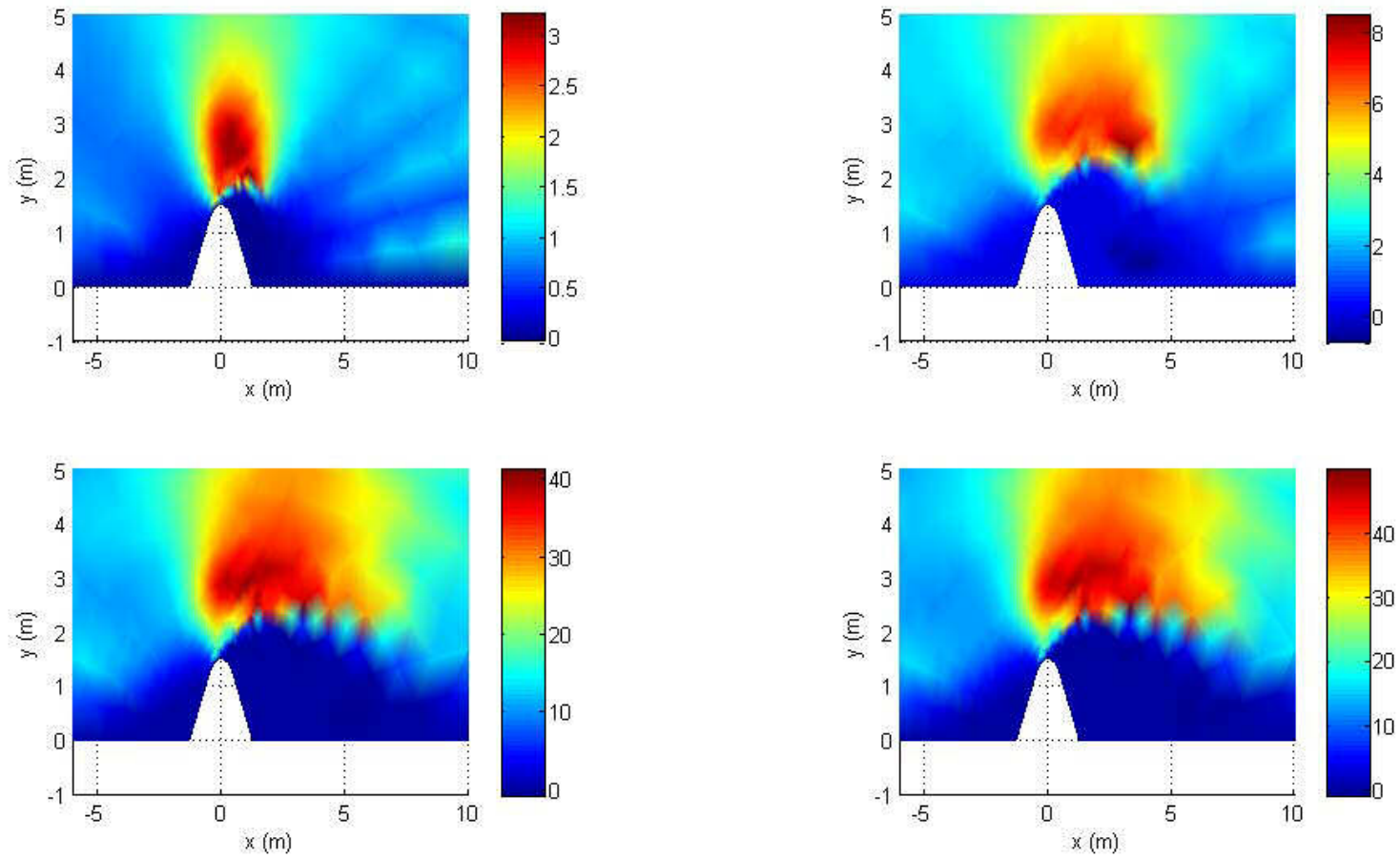


Figure 34: Kinetic flux directed in the x-direction for headland with $D_1=5$ cm. Clockwise from top left: 0.05T, 0.1T, 0.2T, 0.25T.

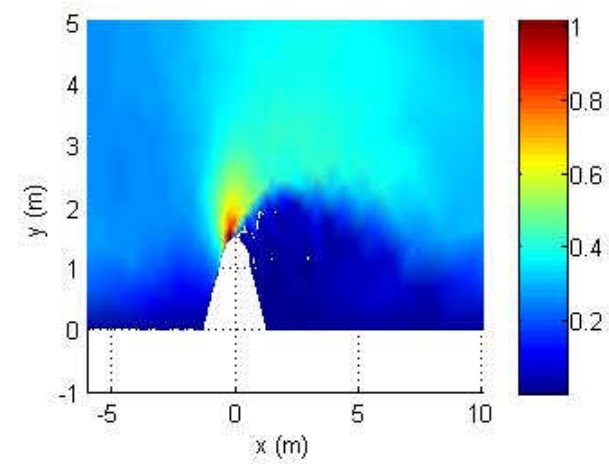
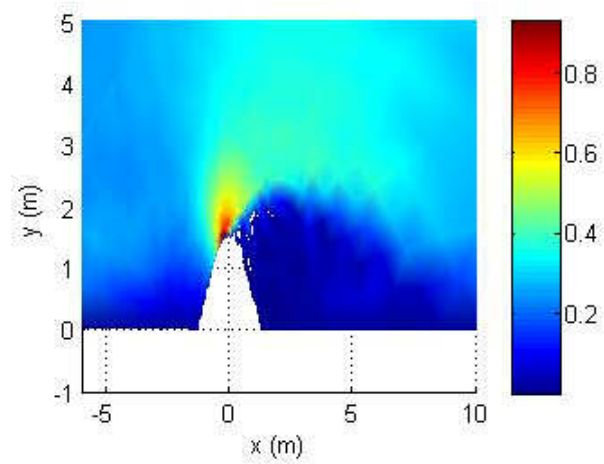
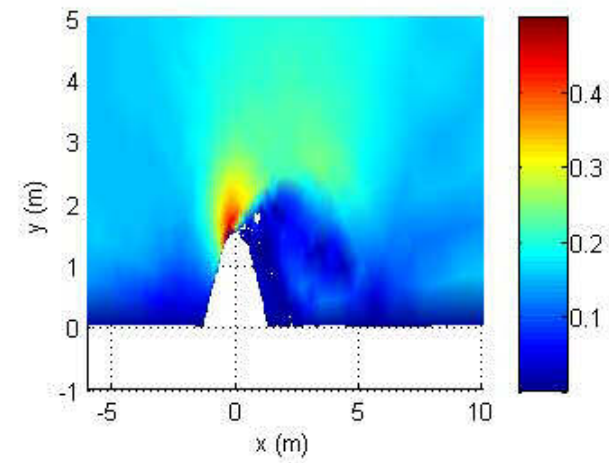
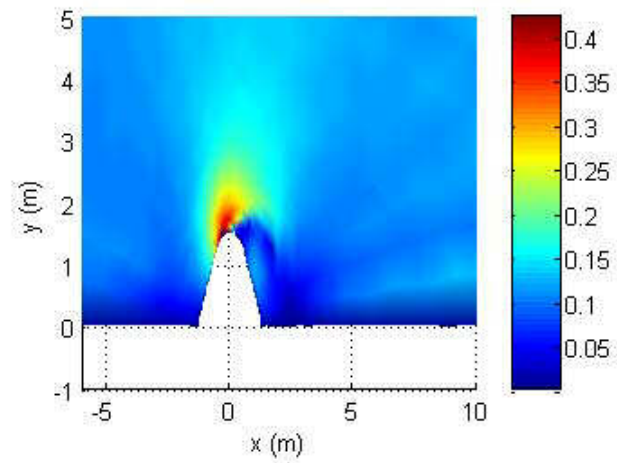


Figure 35: Froude number for headland with $D_1=5$ cm. Clockwise from top left: 0.05T, 0.1T, 0.2T, 0.25T.

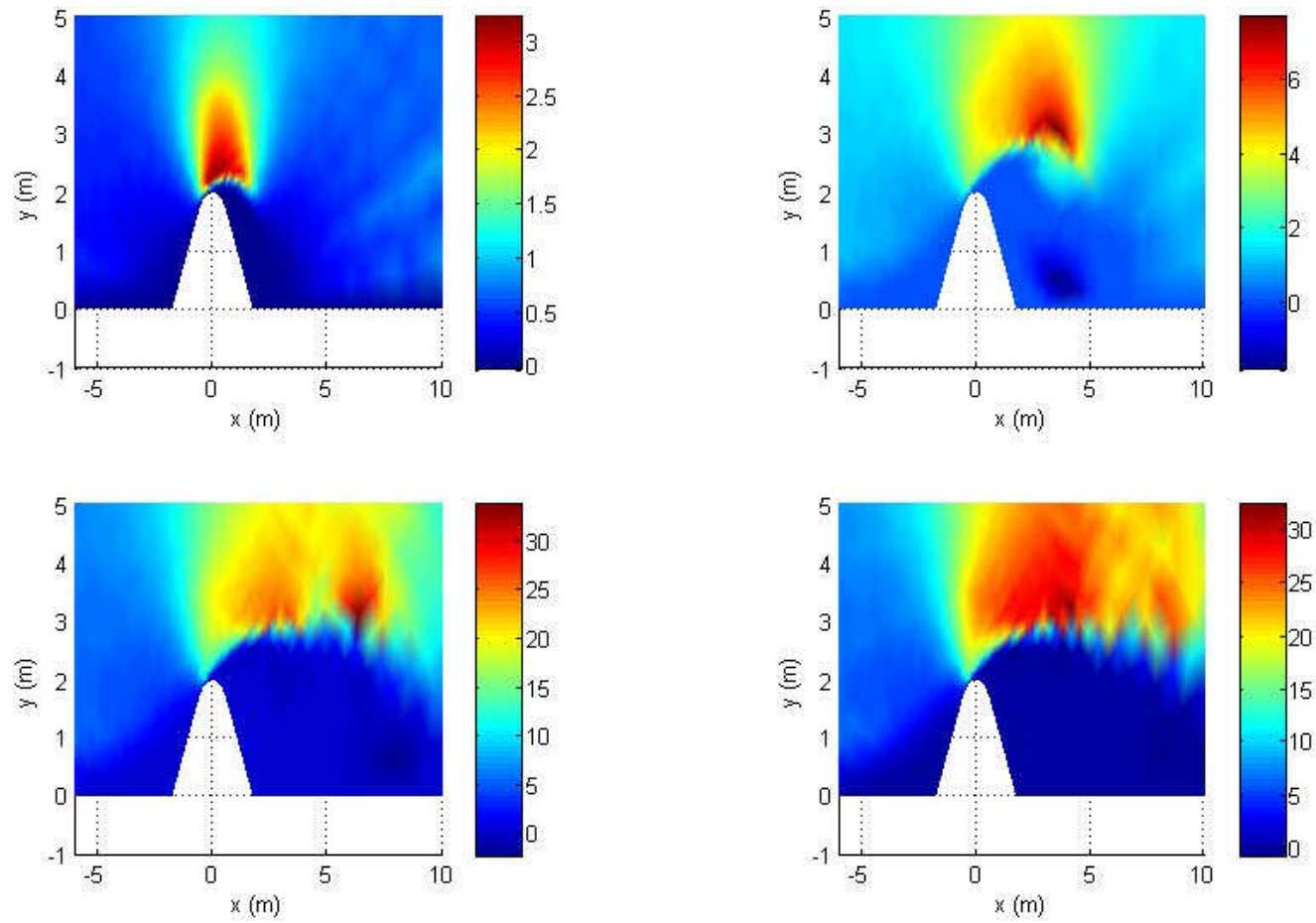


Figure 36: Kinetic flux directed in the x-direction for headland with $D_1=10$ cm. Clockwise from top left: $0.05T$, $0.1T$, $0.2T$, $0.25T$.

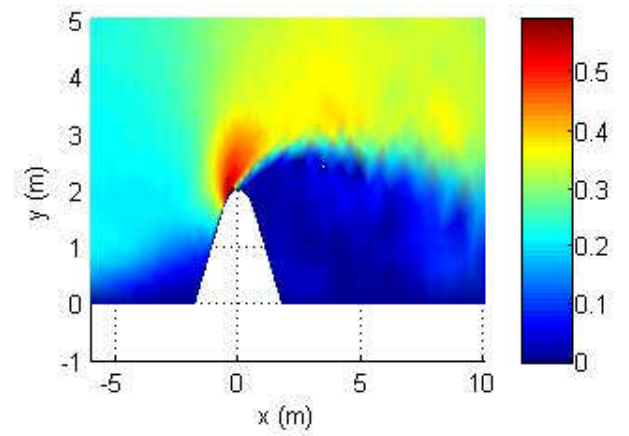
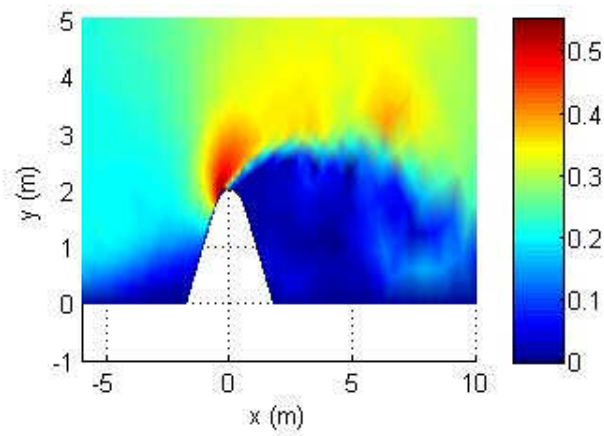
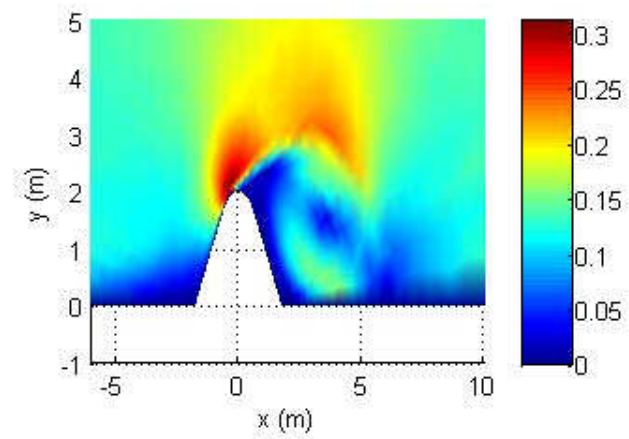
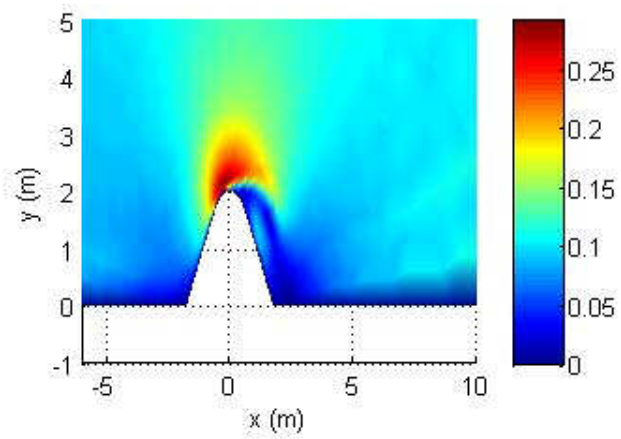


Figure 37: Froude number for headland with $D_1=10$ cm. Clockwise from top left: 0.05T, 0.1T, 0.2T, 0.25T.

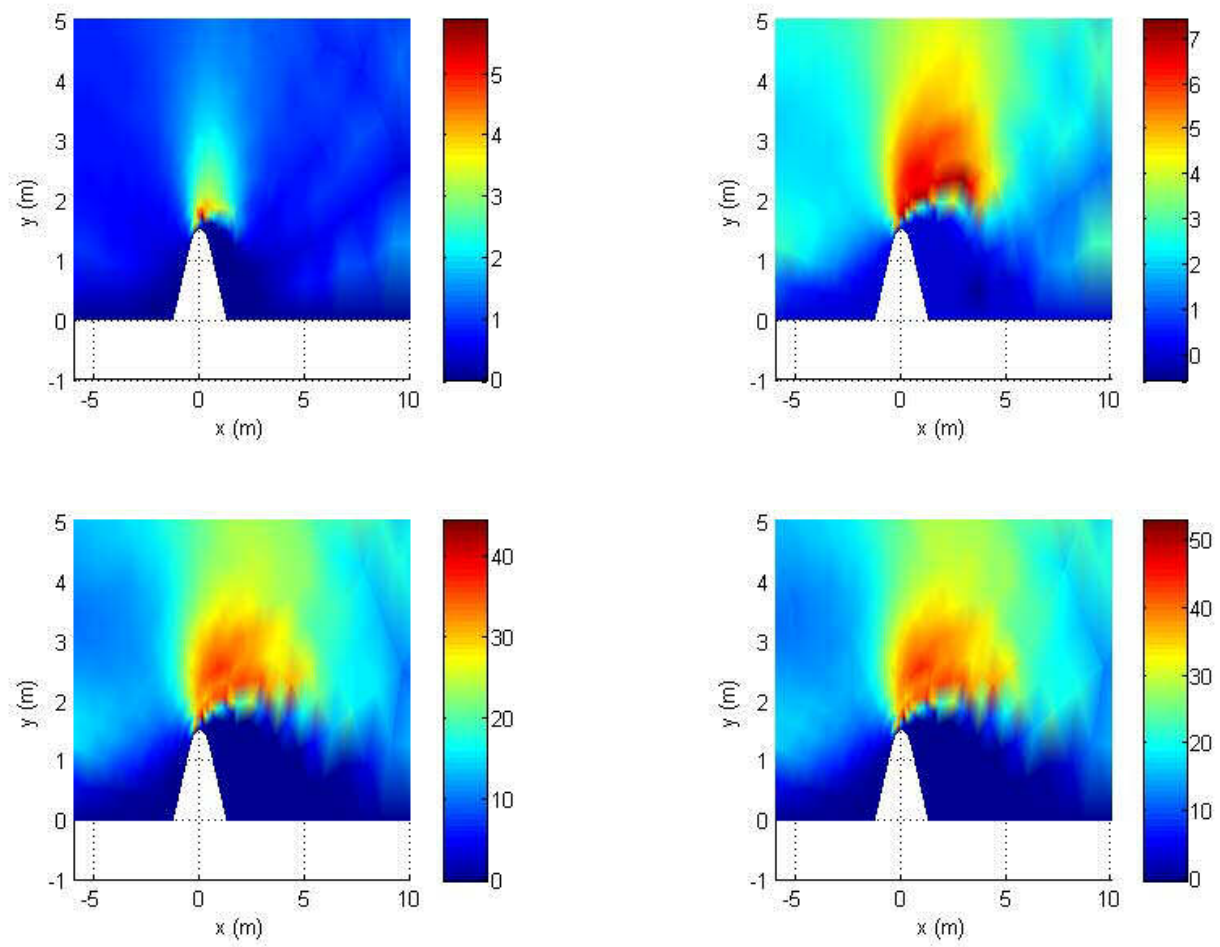


Figure 38: Kinetic flux directed in the x-direction for headland with $D_1=15$ cm. Clockwise from top left: 0.05T, 0.1T, 0.2T, 0.25T.

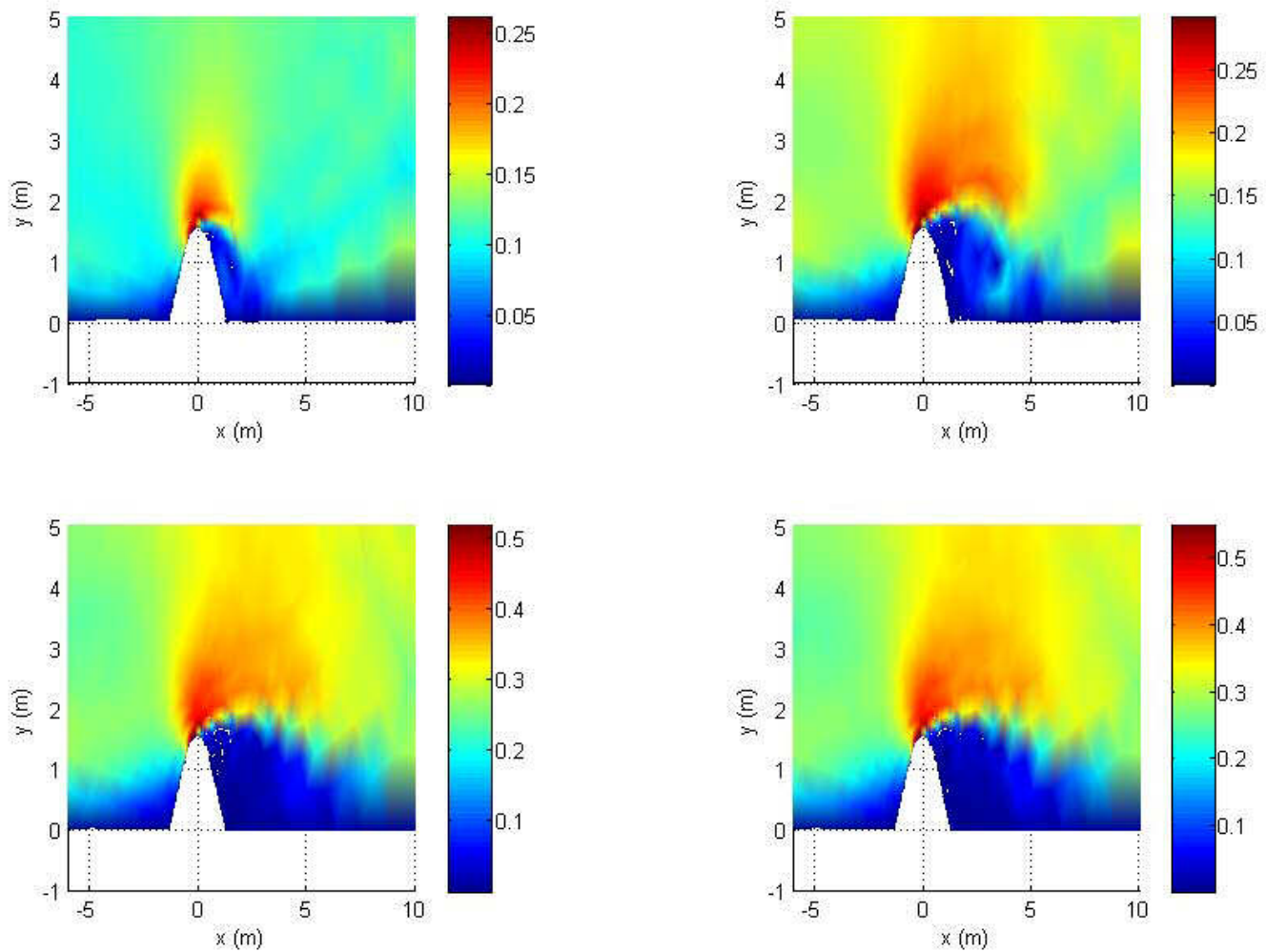


Figure 39: Froude number for headland with $D_1=15$ cm. Clockwise from top left: 0.05T, 0.1T, 0.2T, 0.25T.

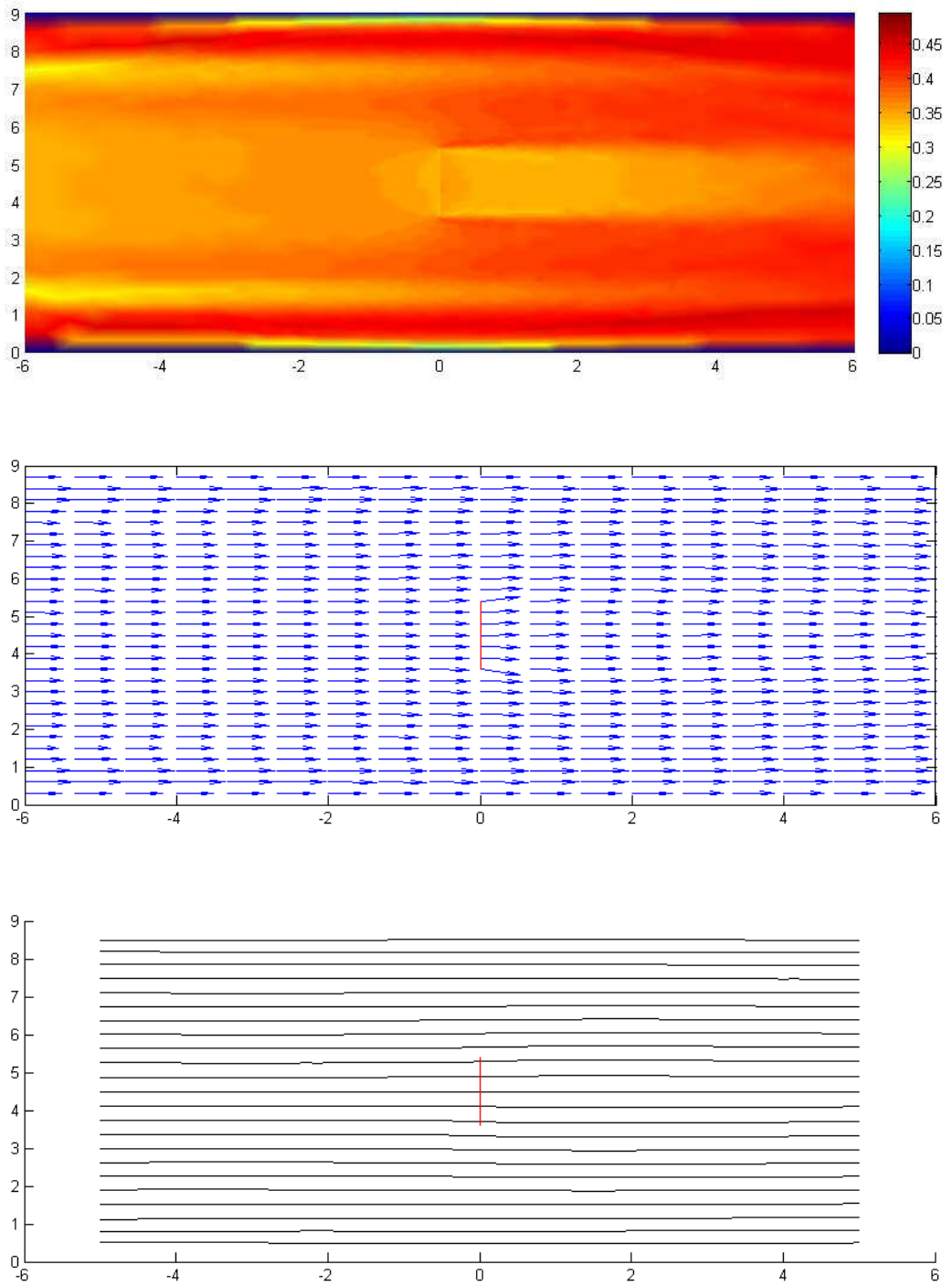


Figure 40: (top) Froude number, (middle) velocity vectors and (bottom) streamlines for Test 500.

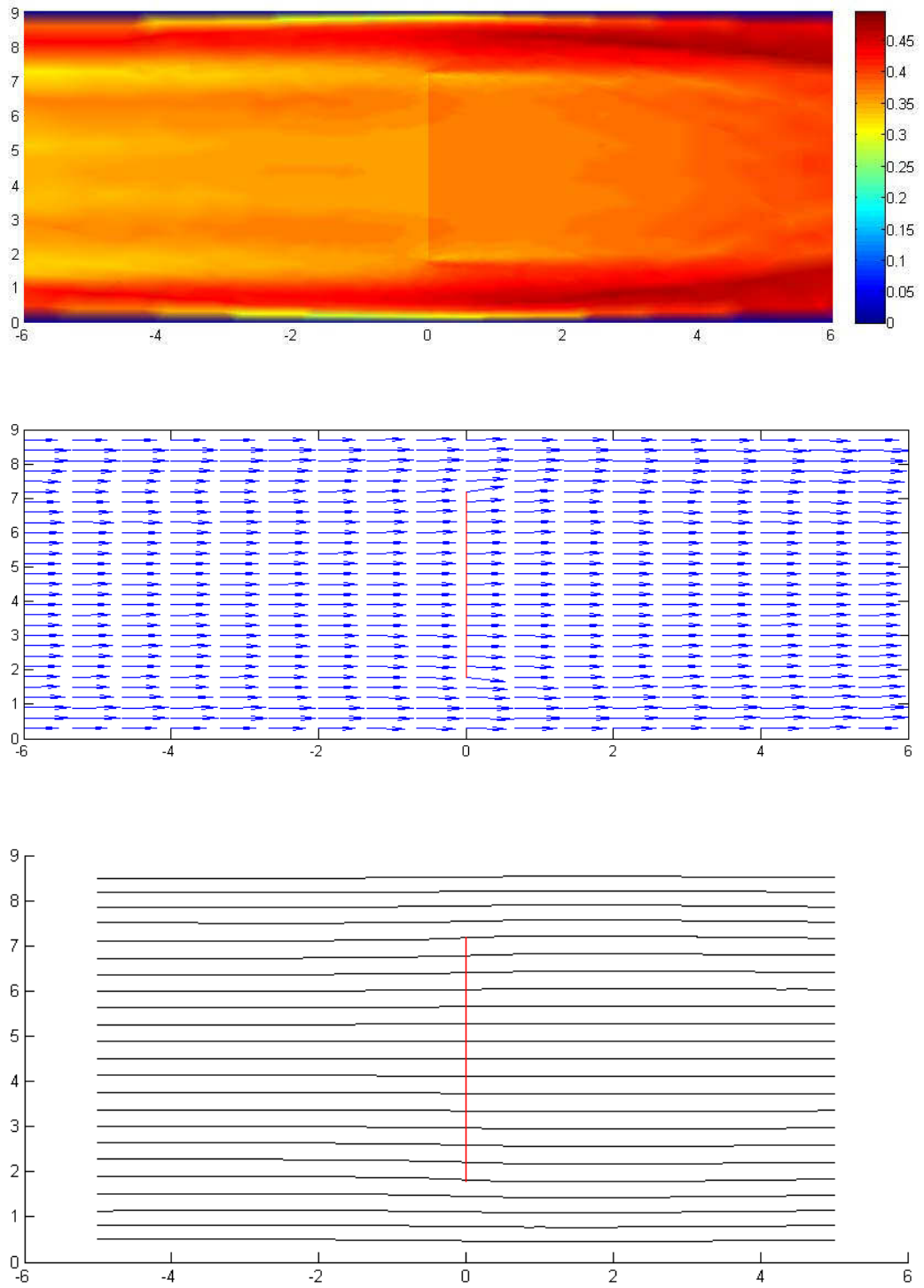


Figure 41: (top) Froude number, (middle) velocity vectors and (bottom) streamlines for Test 501.

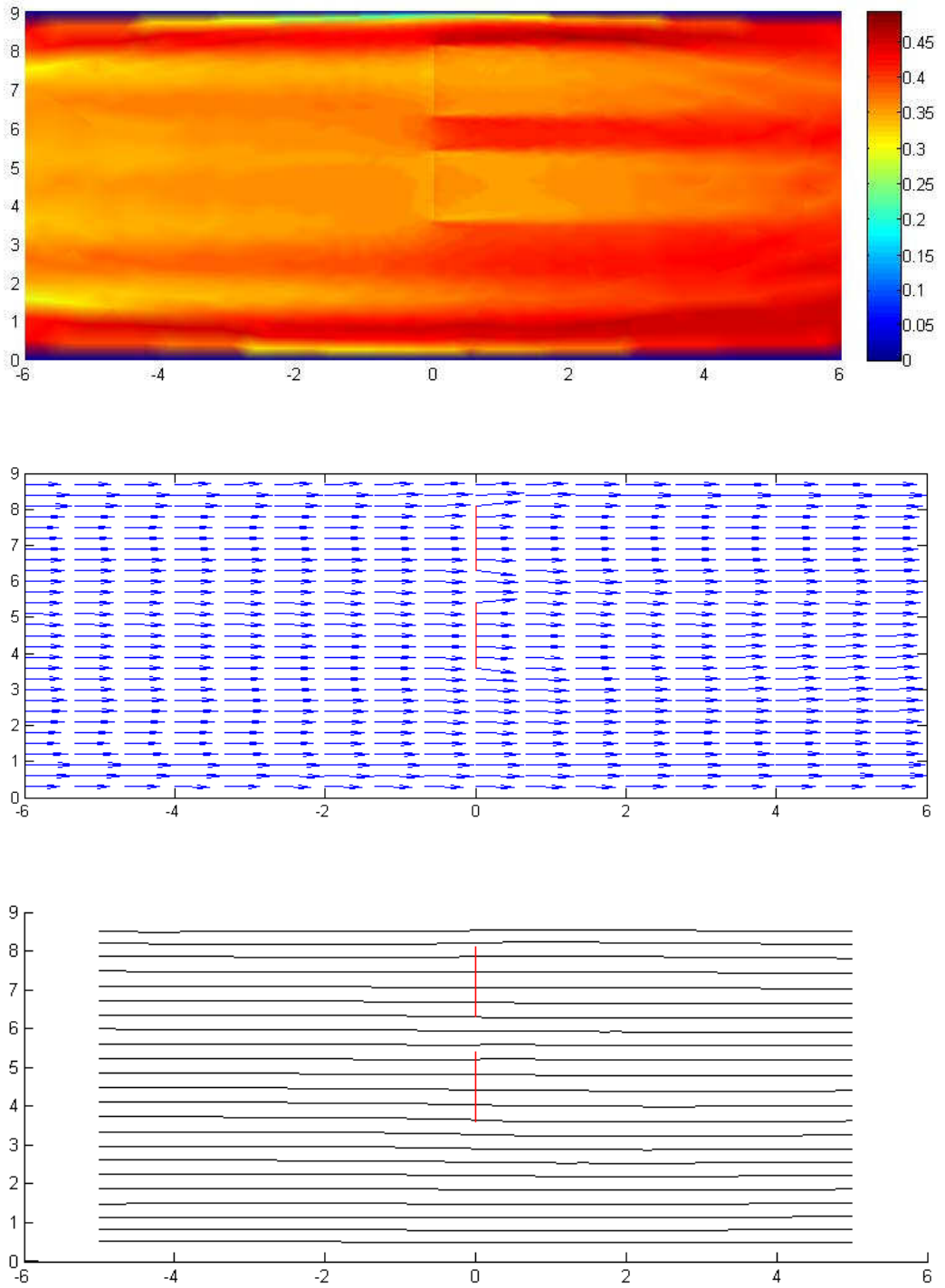


Figure 42: (top) Froude number, (middle) velocity vectors and (bottom) streamlines for Test 502.

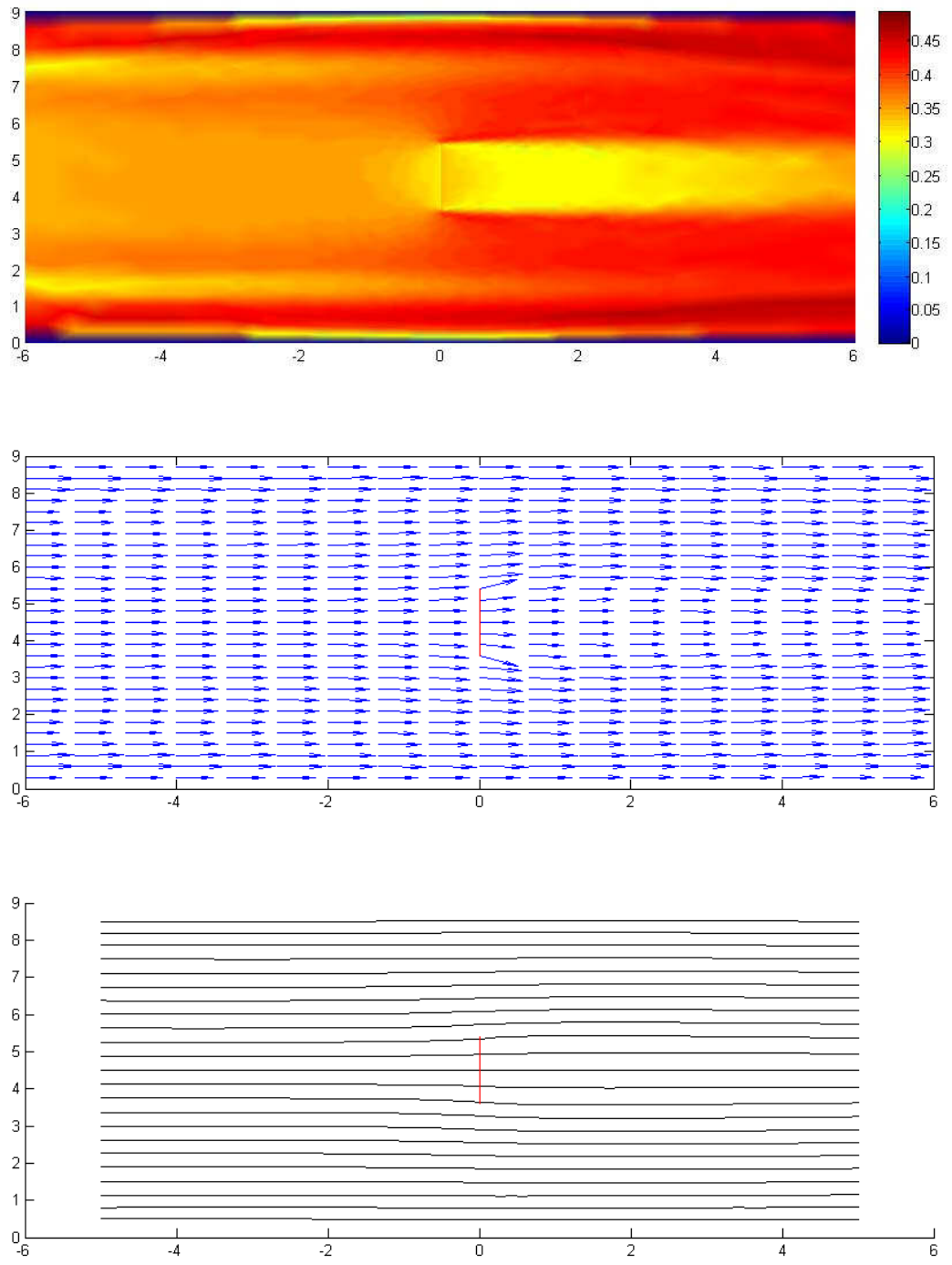


Figure 43: (top) Froude number, (middle) velocity vectors and (bottom) streamlines for Test 503.

Test 206x

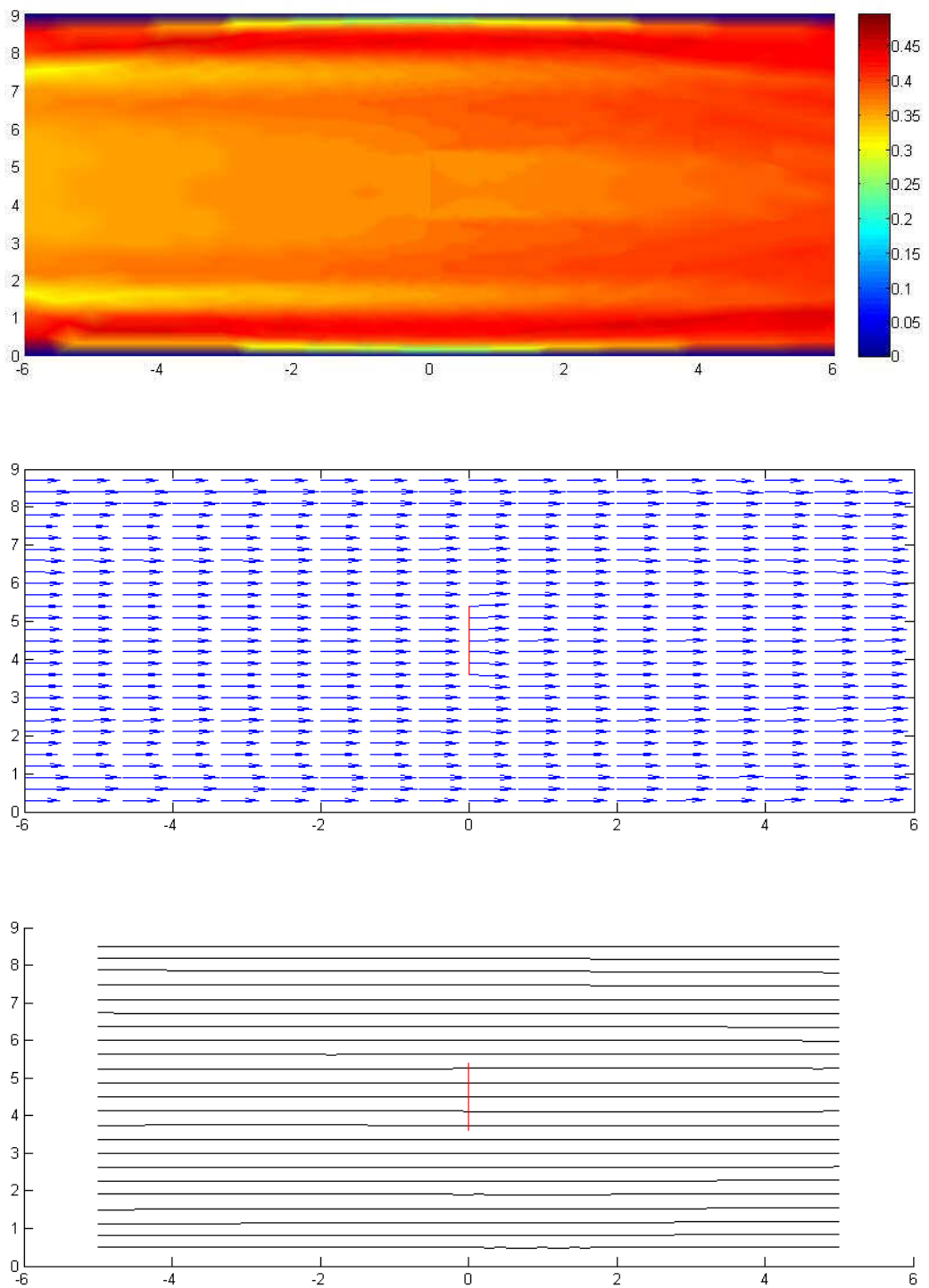


Figure 44: (top) Froude number, (middle) velocity vectors and (bottom) streamlines for Test 504.

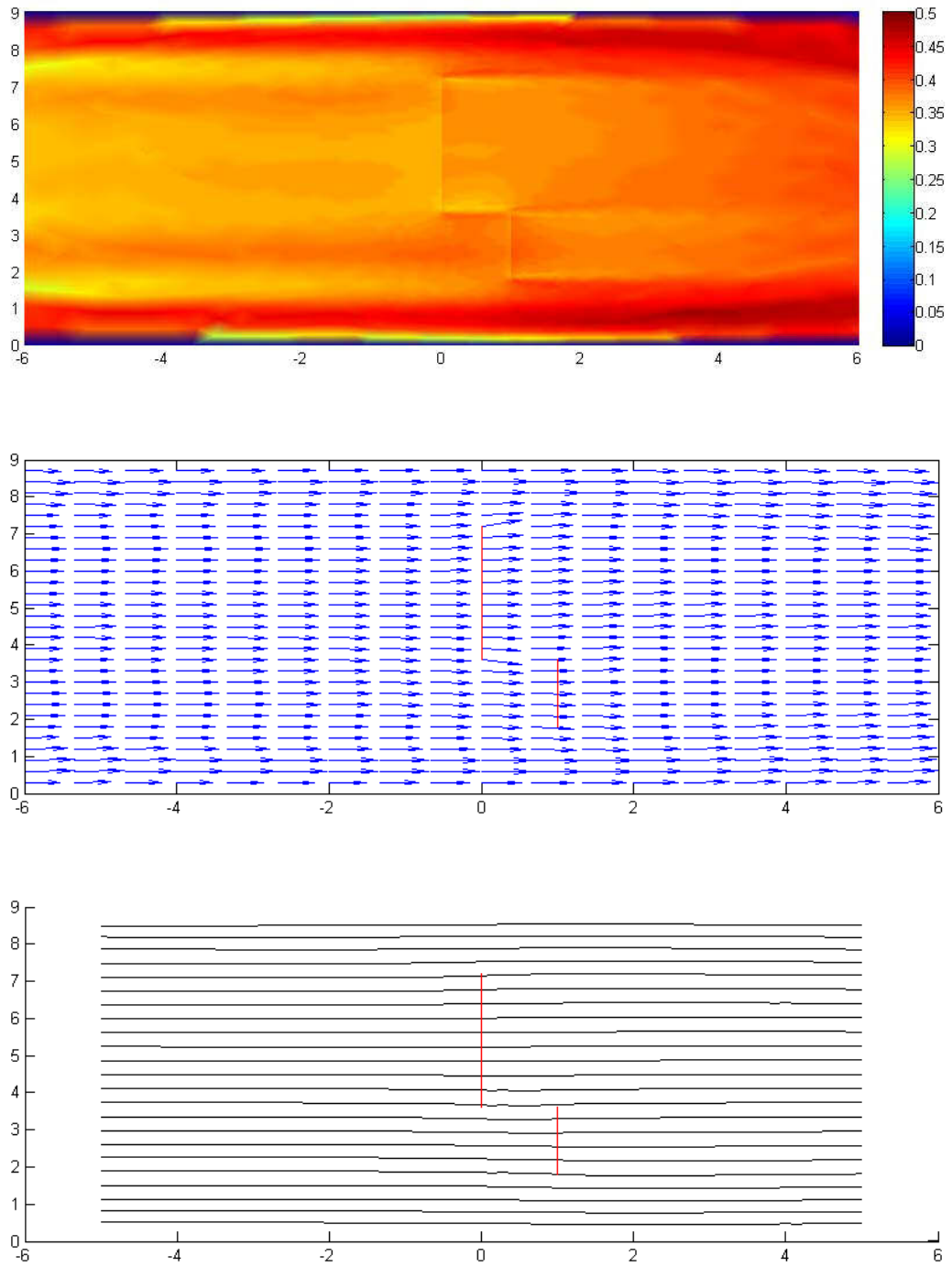


Figure 45: (top) Froude number, (middle) velocity vectors and (bottom) streamlines for Test 505.

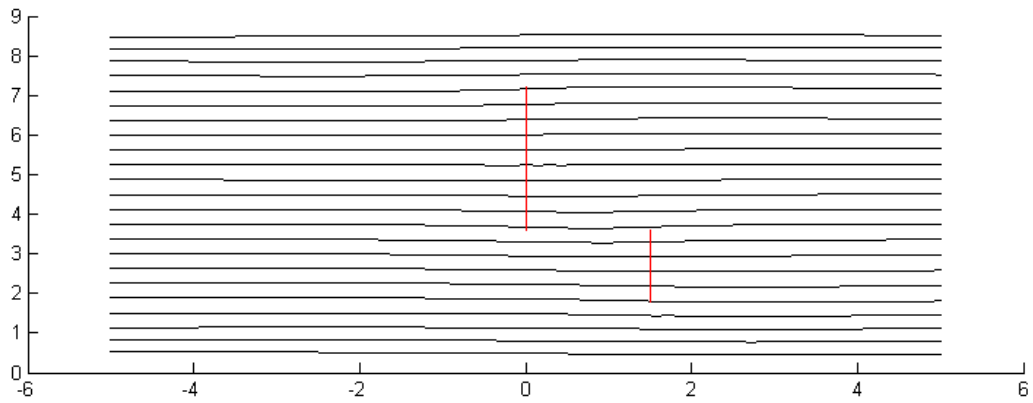
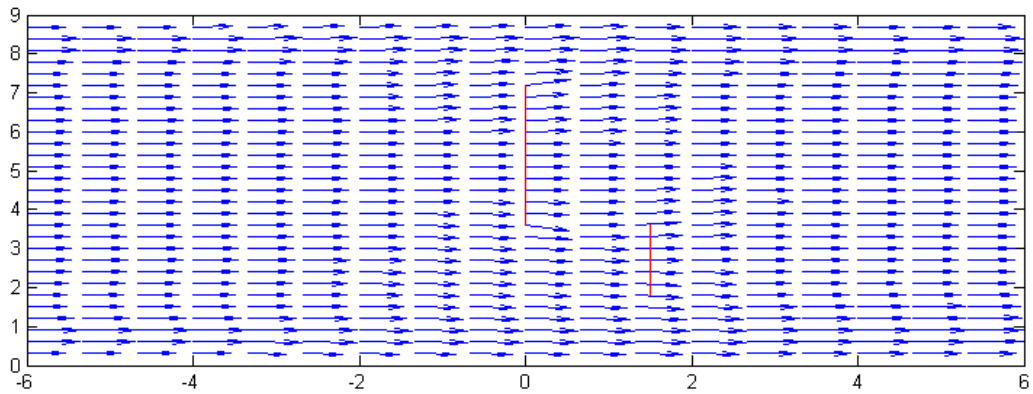
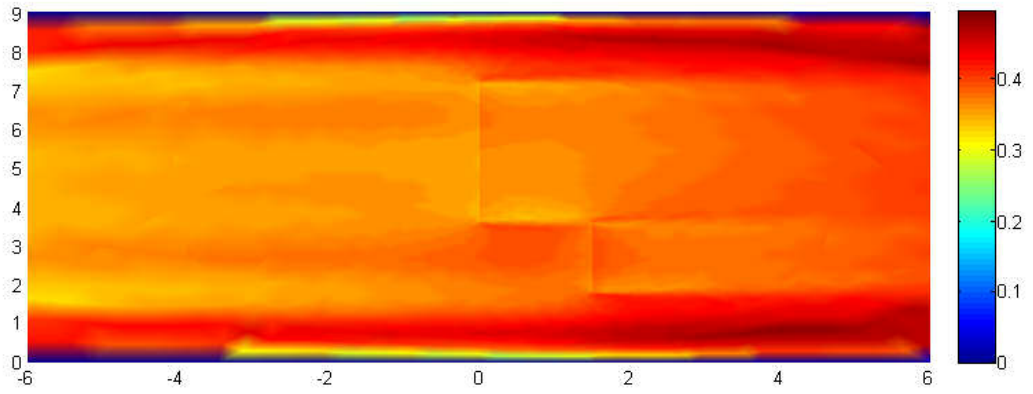


Figure 46: (top) Froude number, (middle) velocity vectors and (bottom) streamlines for Test 506.

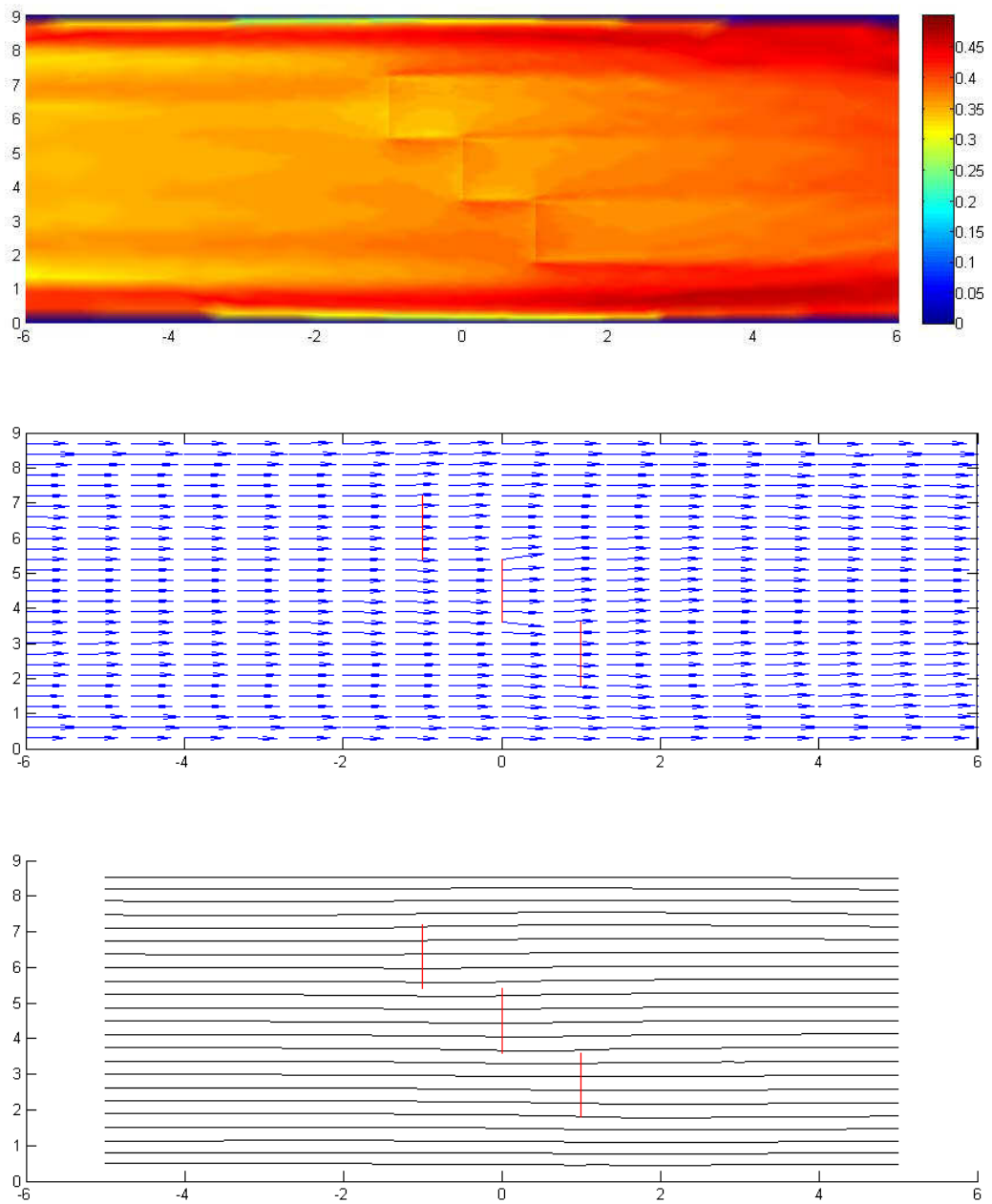


Figure 47: (top) Froude number, (middle) velocity vectors and (bottom) streamlines for Test 507.

Test 210x

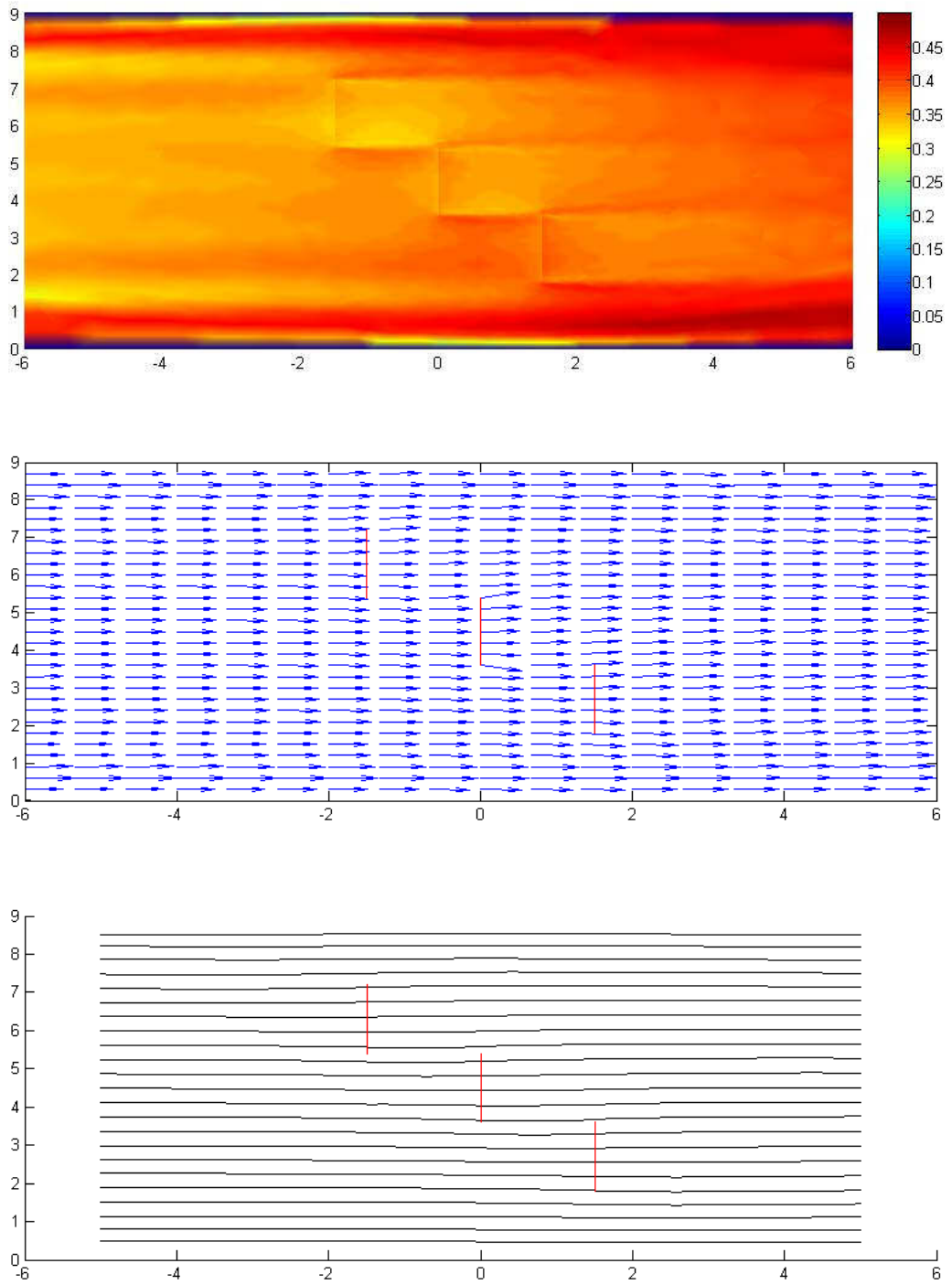


Figure 48: (top) Froude number, (middle) velocity vectors and (bottom) streamlines for Test 508.

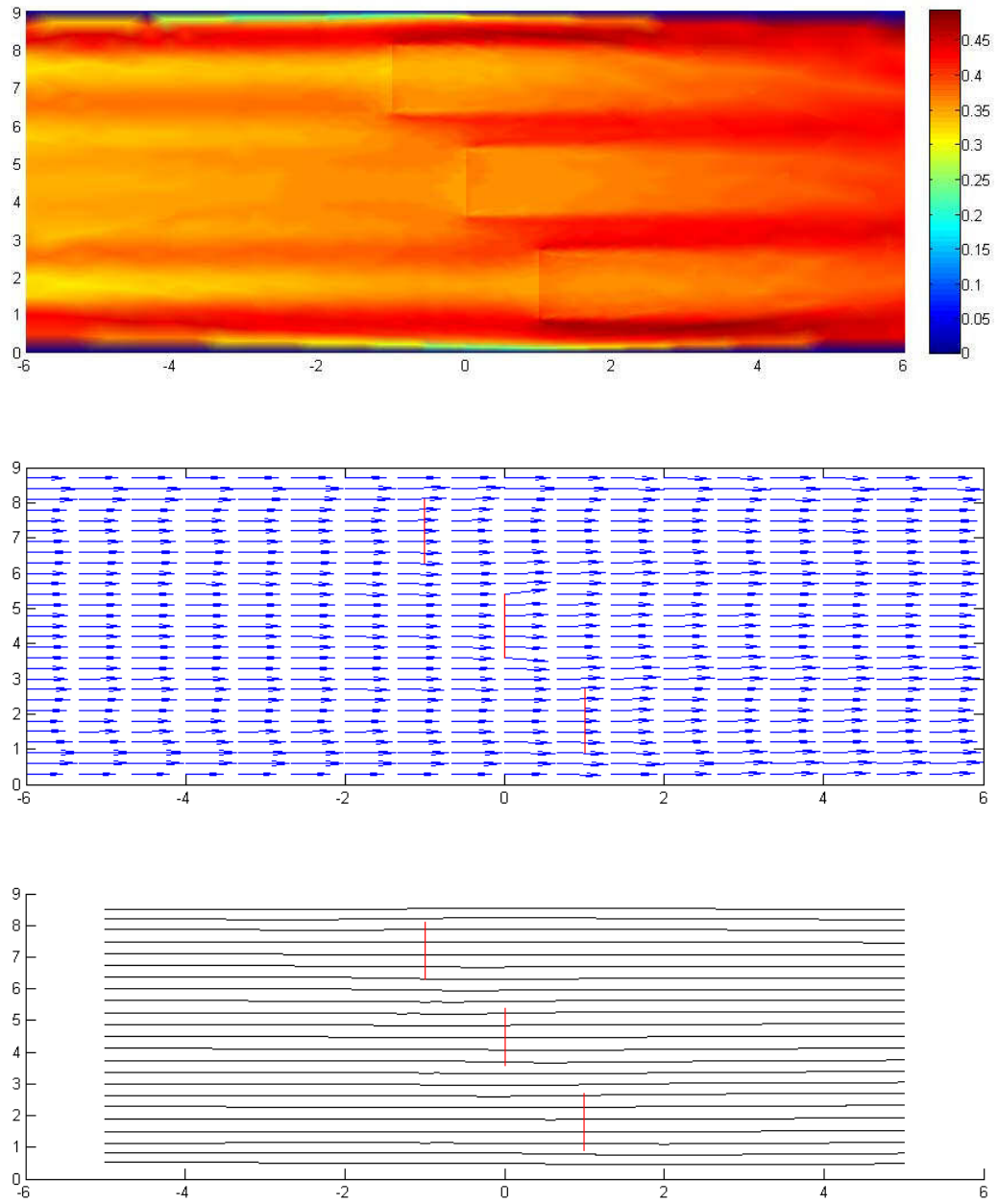


Figure 49: (top) Froude number, (middle) velocity vectors and (bottom) streamlines for Test 509.

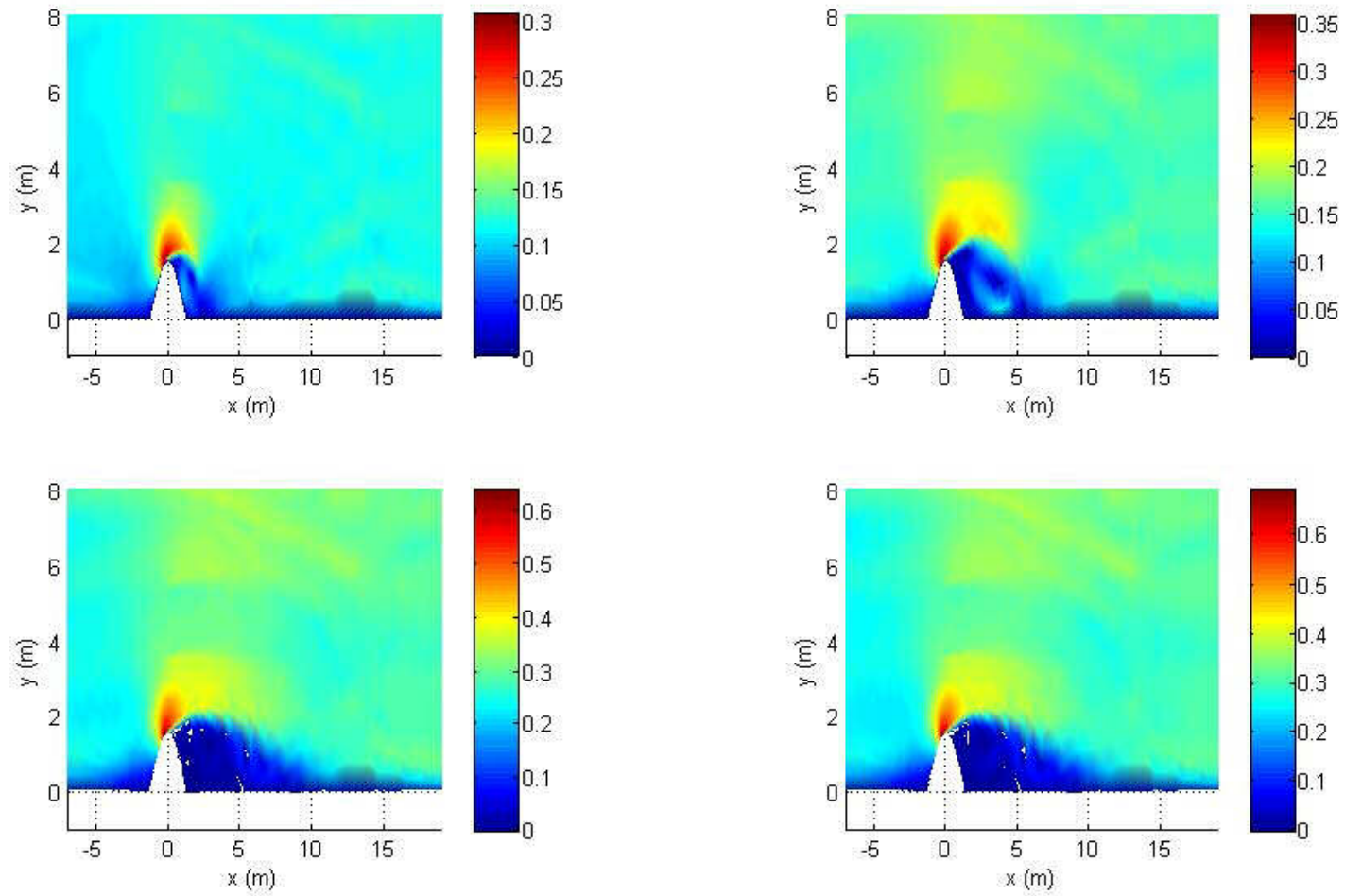


Figure 50: Test 620, Froude number. Clockwise from top left: 0.05T, 0.1T, 0.2T, 0.25T.

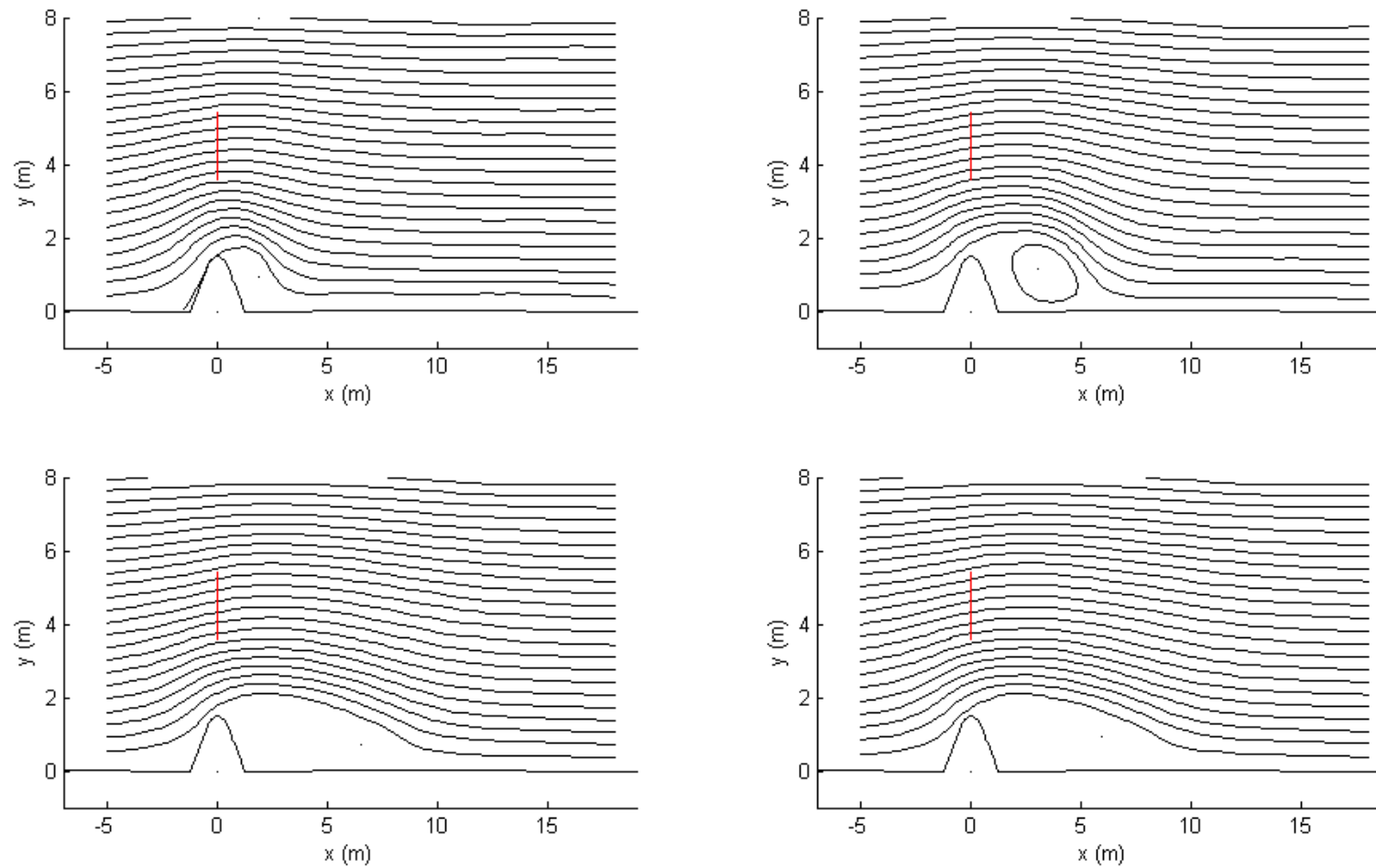


Figure 51: Test 620, Instantaneous Streamlines. Clockwise from top left: 0.05T, 0.1T, 0.2T, 0.25T.

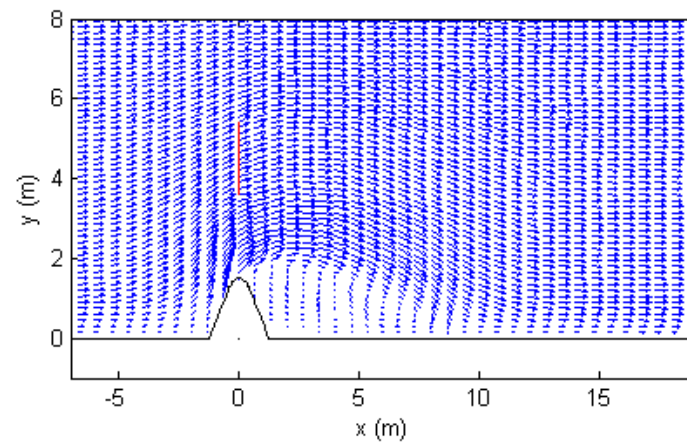
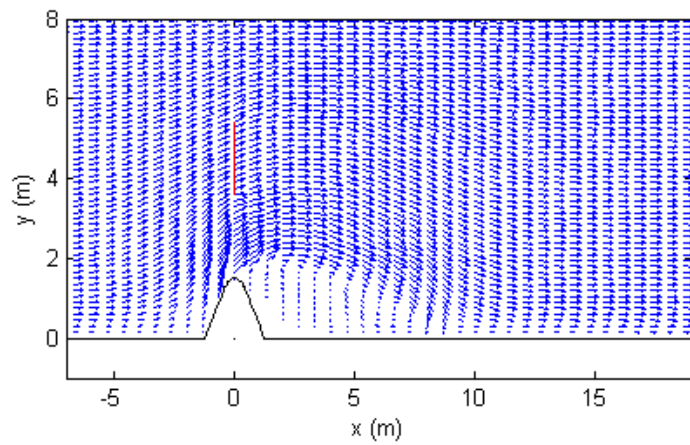
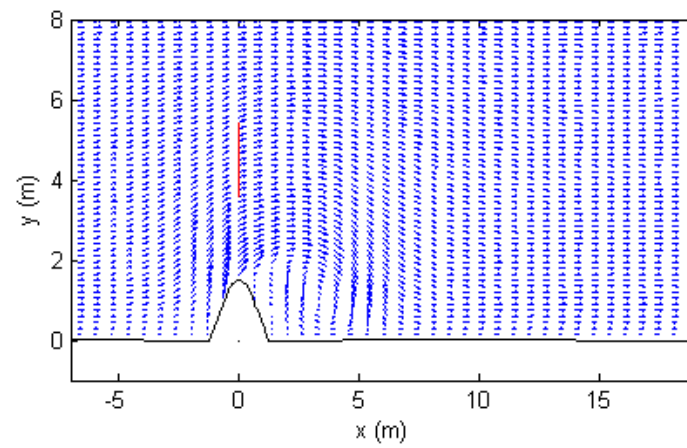
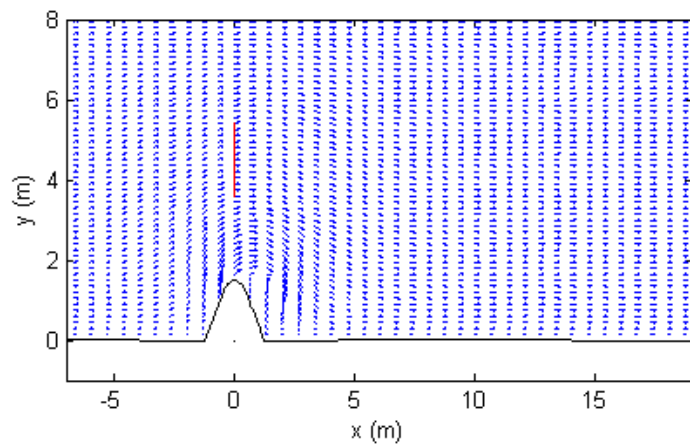


Figure 52: Test 620, Velocity Vectors. Clockwise from top left: 0.05T, 0.1T, 0.2T, 0.25T.

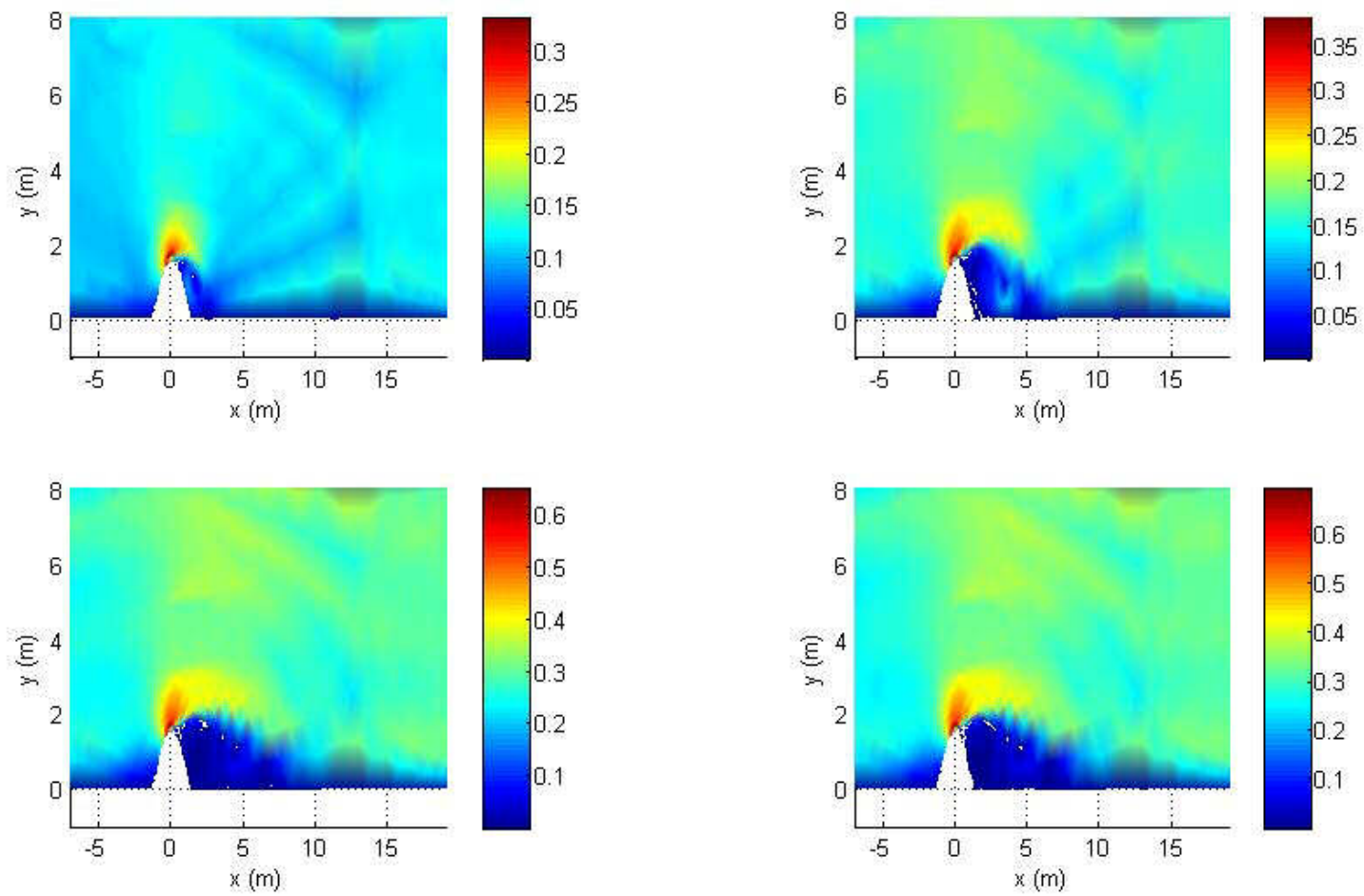


Figure 53: Test 621, Froude number. Clockwise from top left: 0.05T, 0.1T, 0.2T, 0.25T.

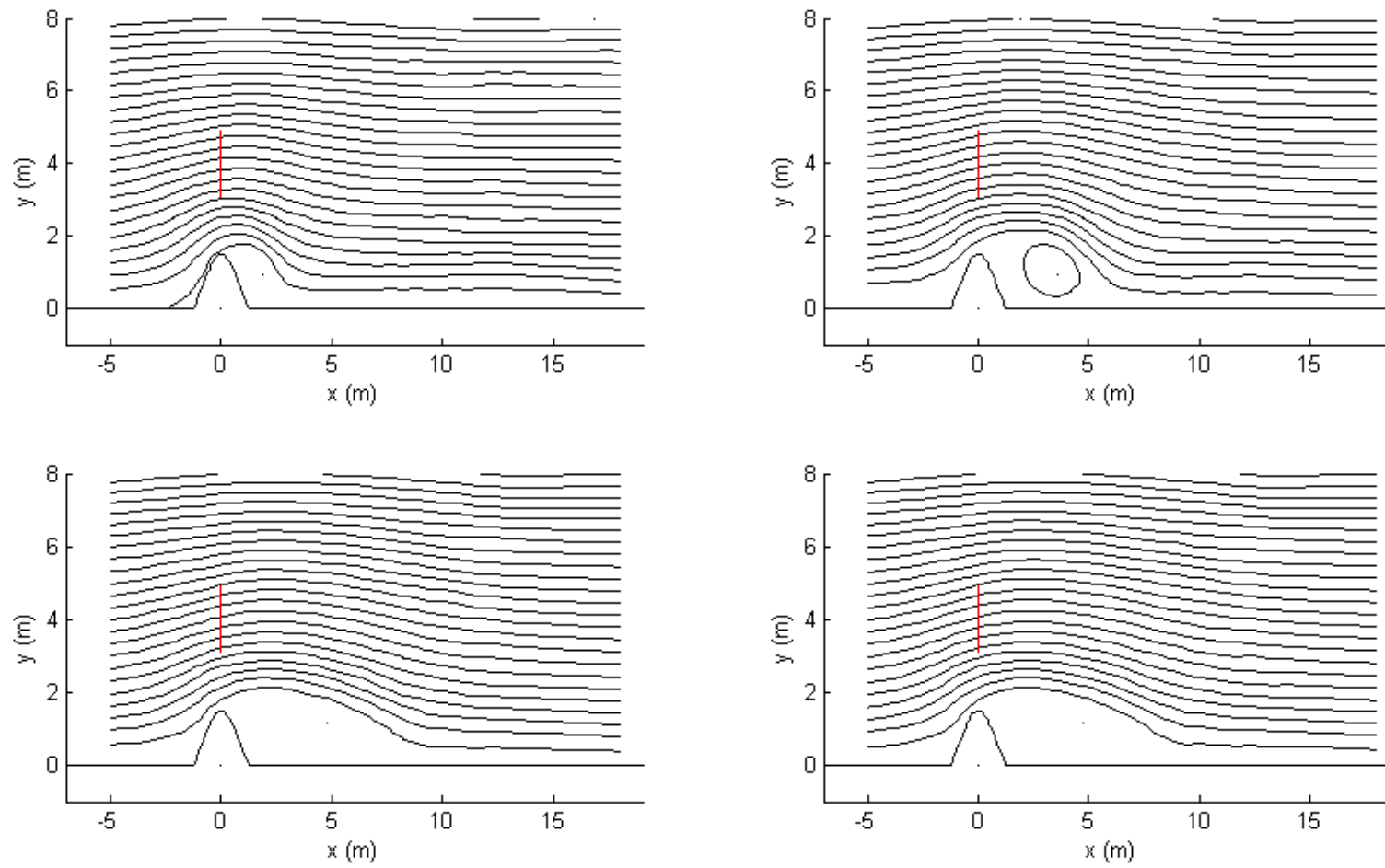


Figure 54: Test 621, Instantaneous Streamlines. Clockwise from top left: 0.05T, 0.1T, 0.2T, 0.25T.

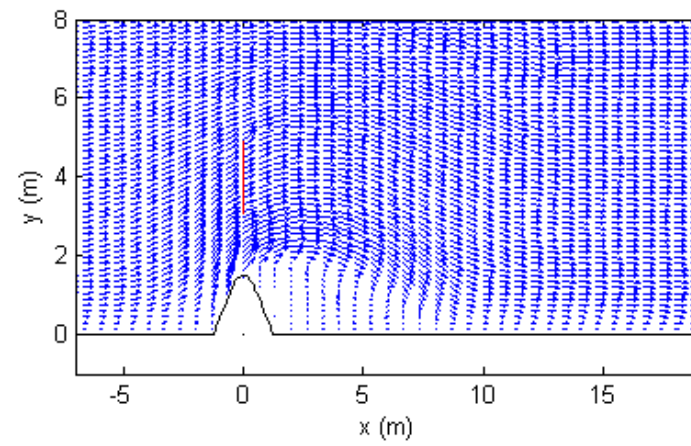
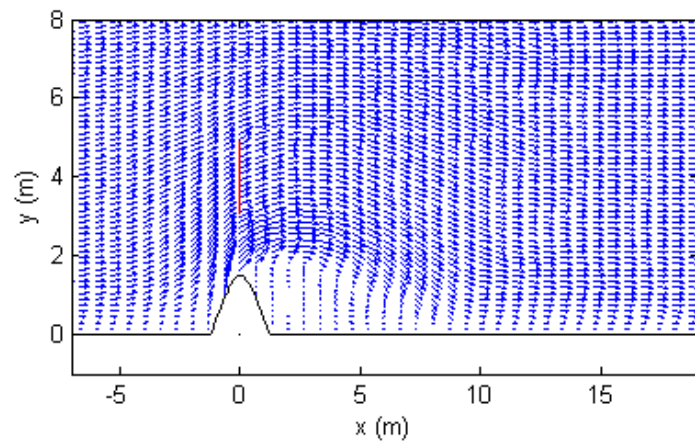
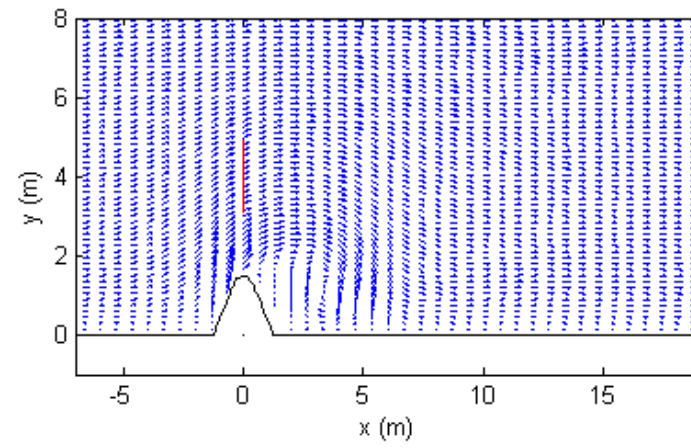
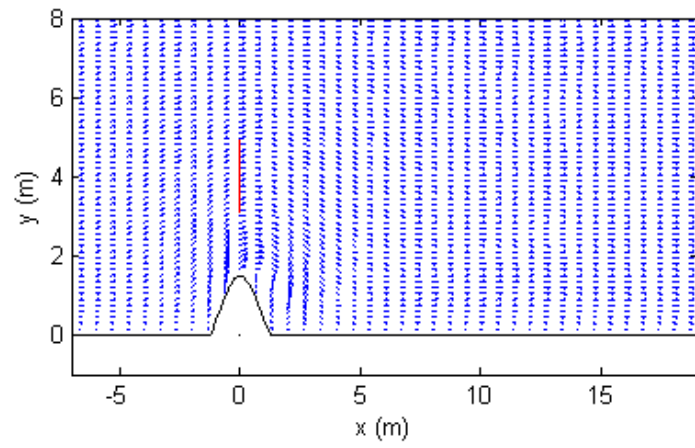


Figure 55: Test 621, Velocity Vectors. Clockwise from top left: 0.05T, 0.1T, 0.2T, 0.25T.

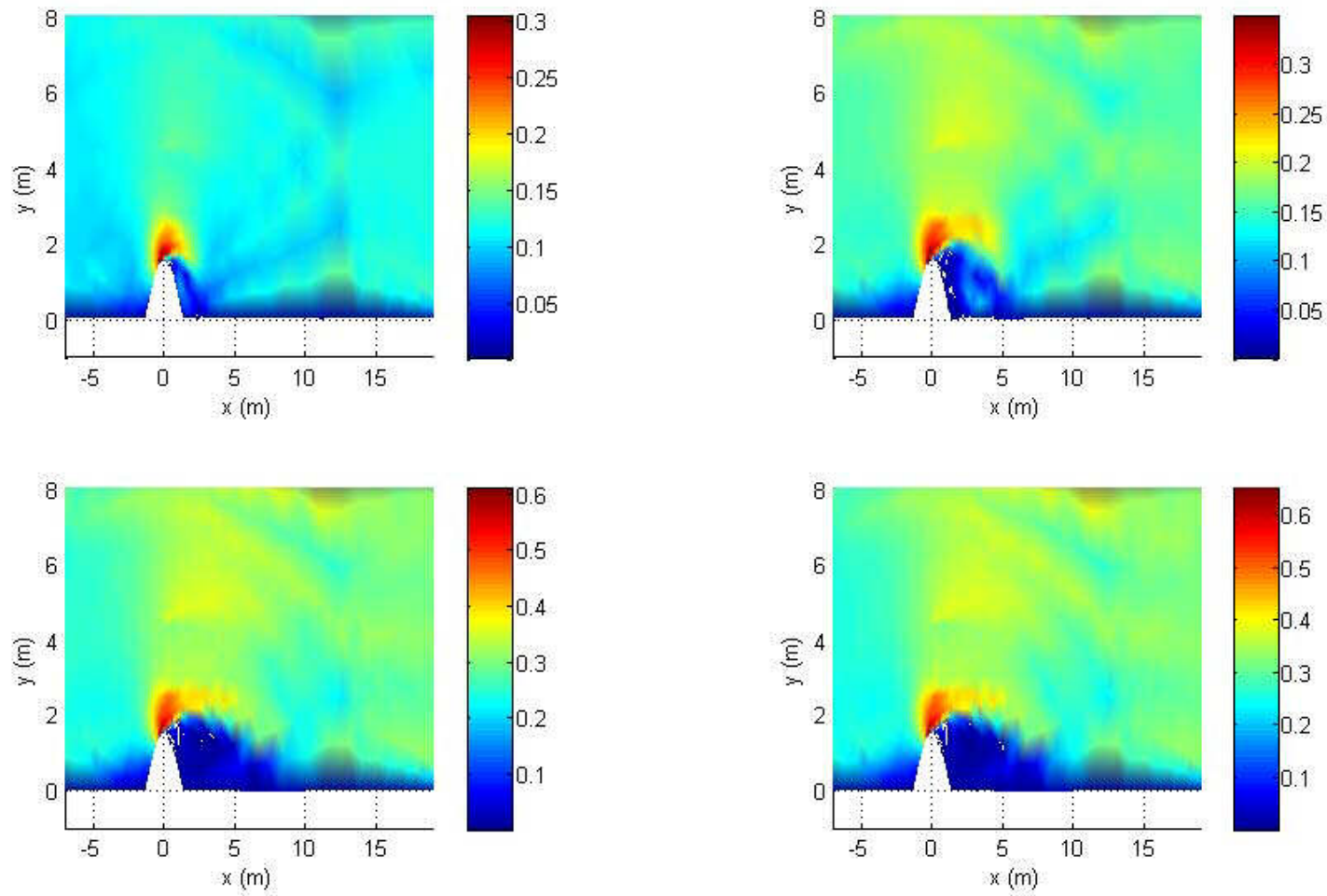


Figure 56: Test 622, Froude number. Clockwise from top left: 0.05T, 0.1T, 0.2T, 0.25T.

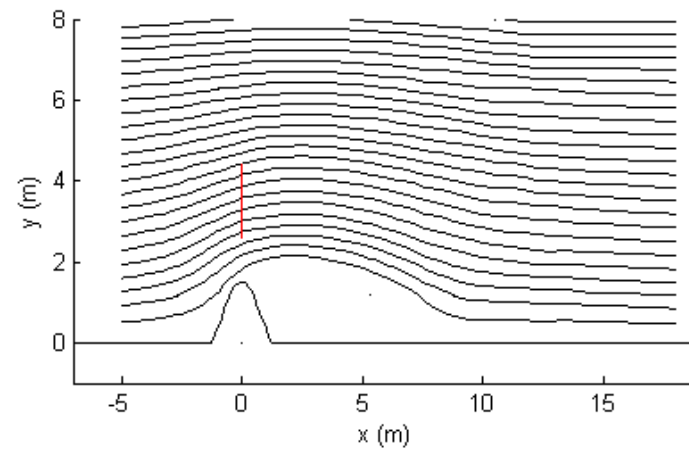
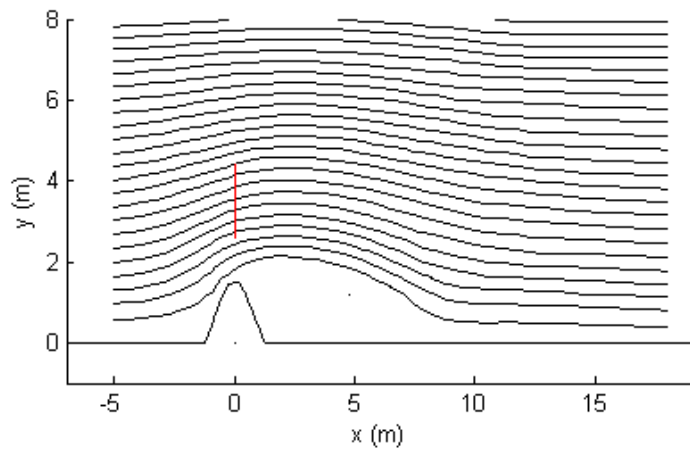
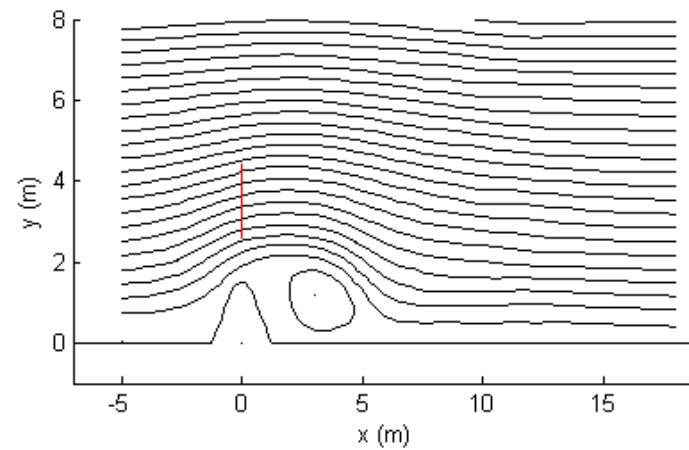
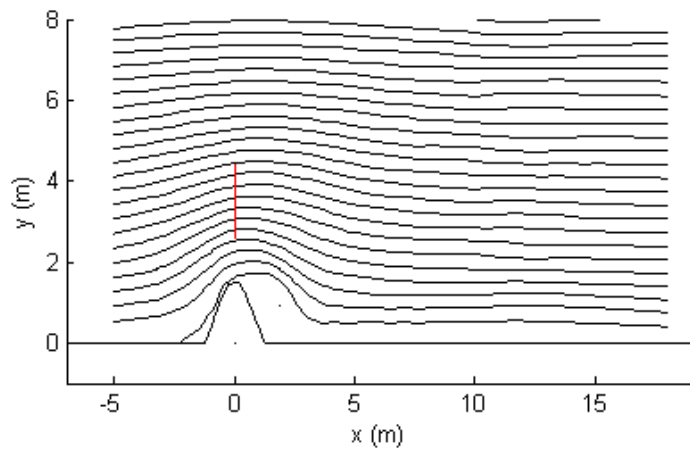


Figure 57: Test 622, Instantaneous Streamlines. Clockwise from top left: 0.05T, 0.1T, 0.2T, 0.25T.

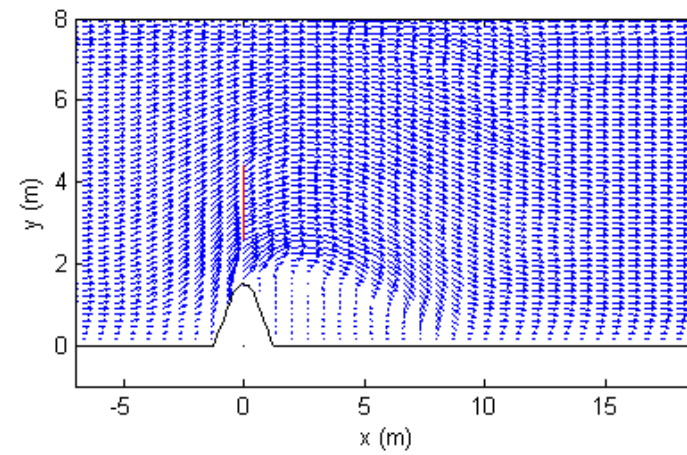
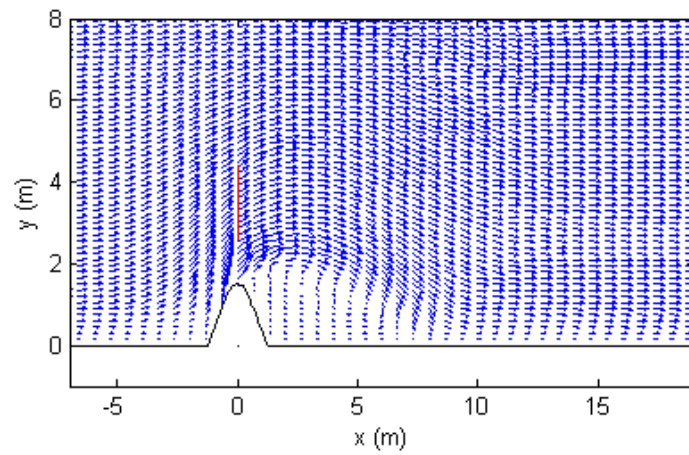
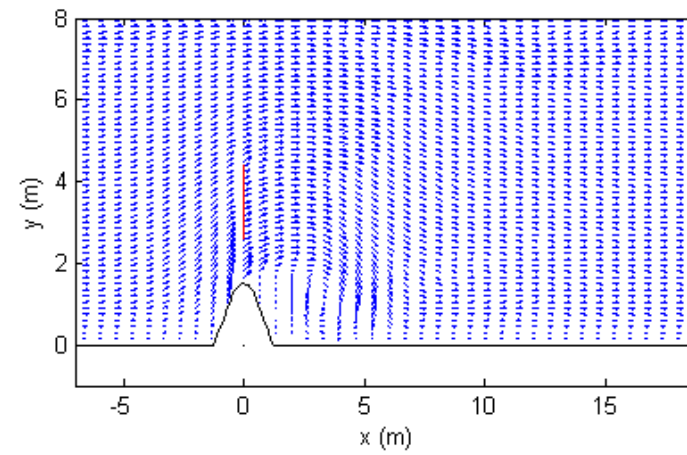
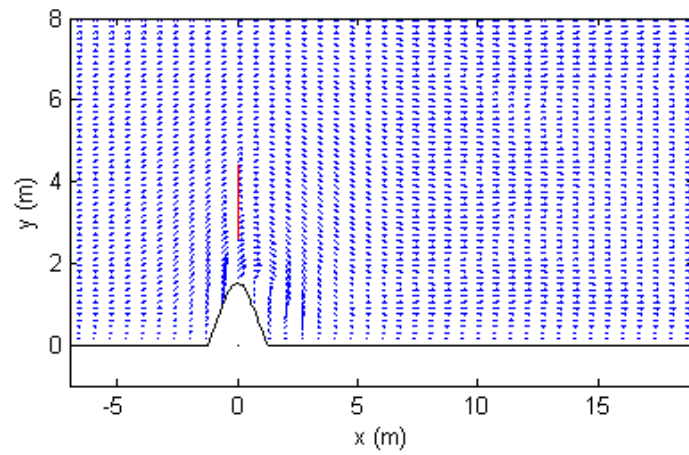


Figure 58: Test 622, Velocity Vectors. Clockwise from top left: 0.05T, 0.1T, 0.2T, 0.25T.

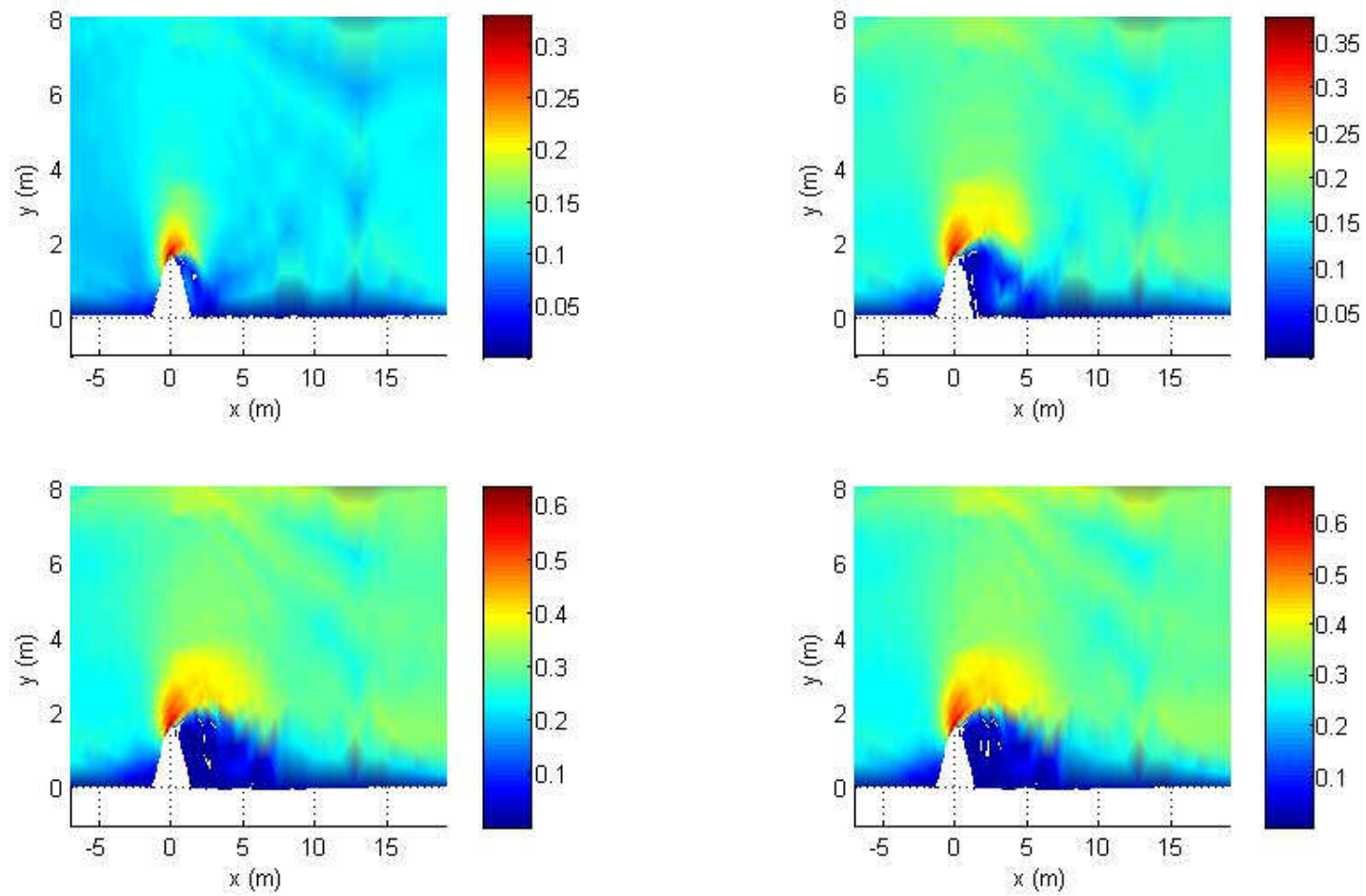


Figure 59: Test 623, Froude number. Clockwise from top left: 0.05T, 0.1T, 0.2T, 0.25T.

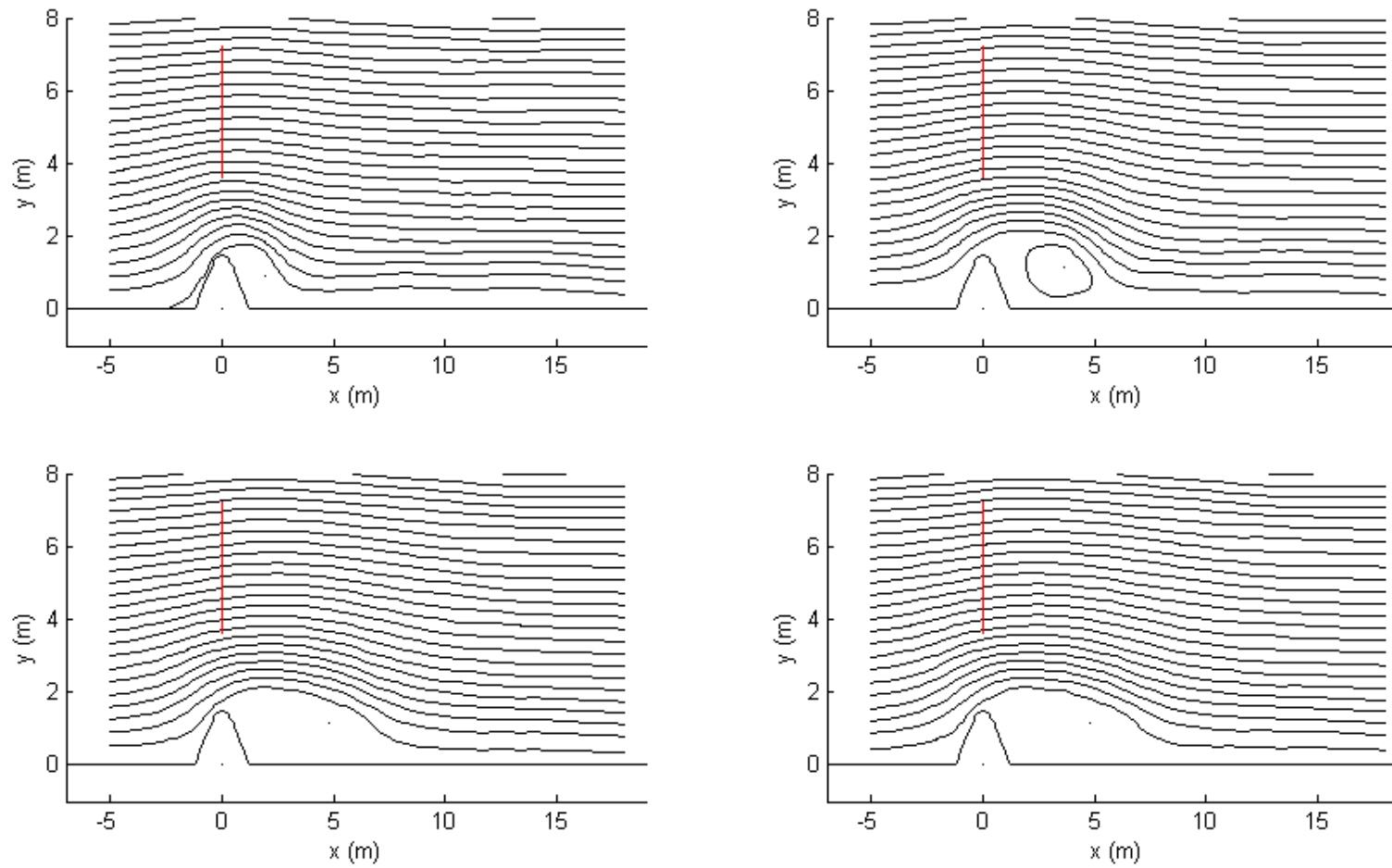


Figure 60: Test 623, Instantaneous Streamlines. Clockwise from top left: 0.05T, 0.1T, 0.2T, 0.25T.

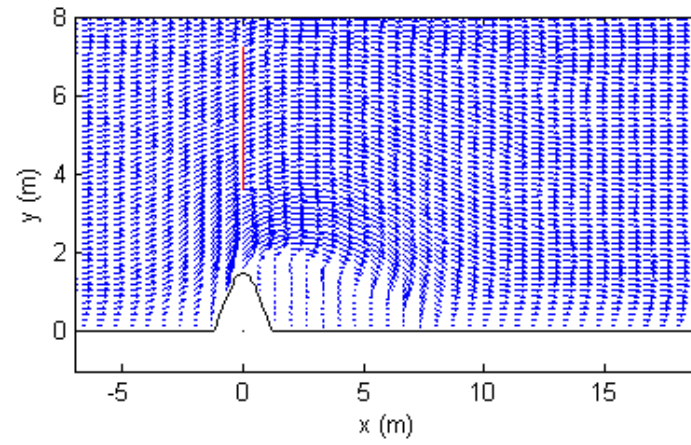
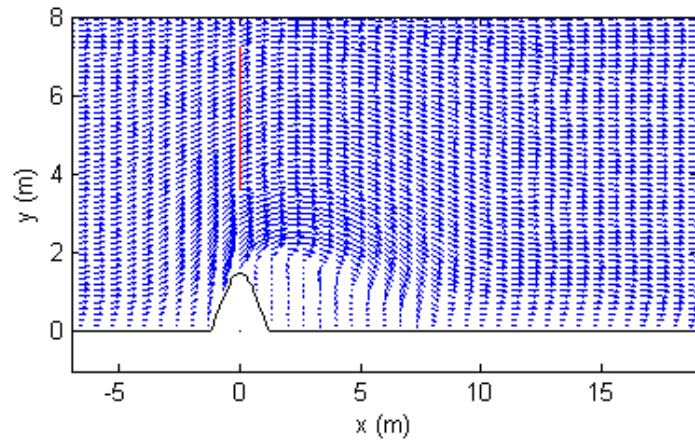
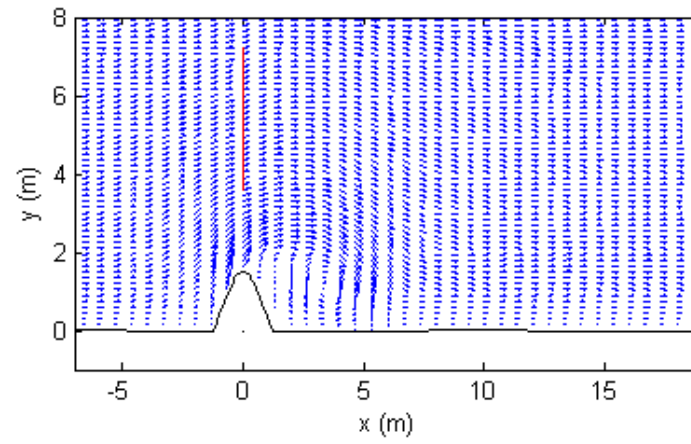
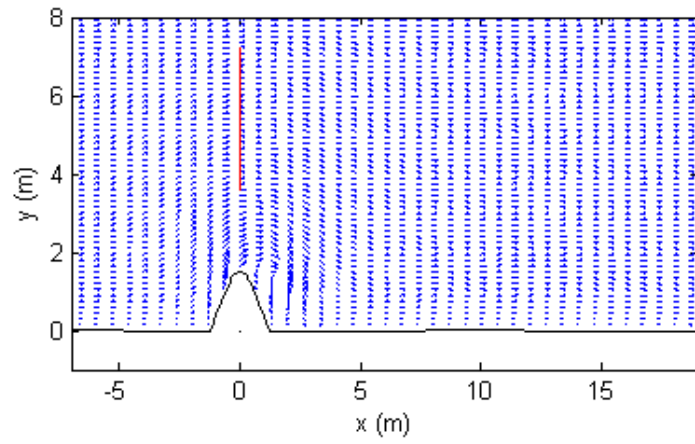


Figure 61: Test 623, Velocity Vectors. Clockwise from top left: 0.05T, 0.1T, 0.2T, 0.25T.

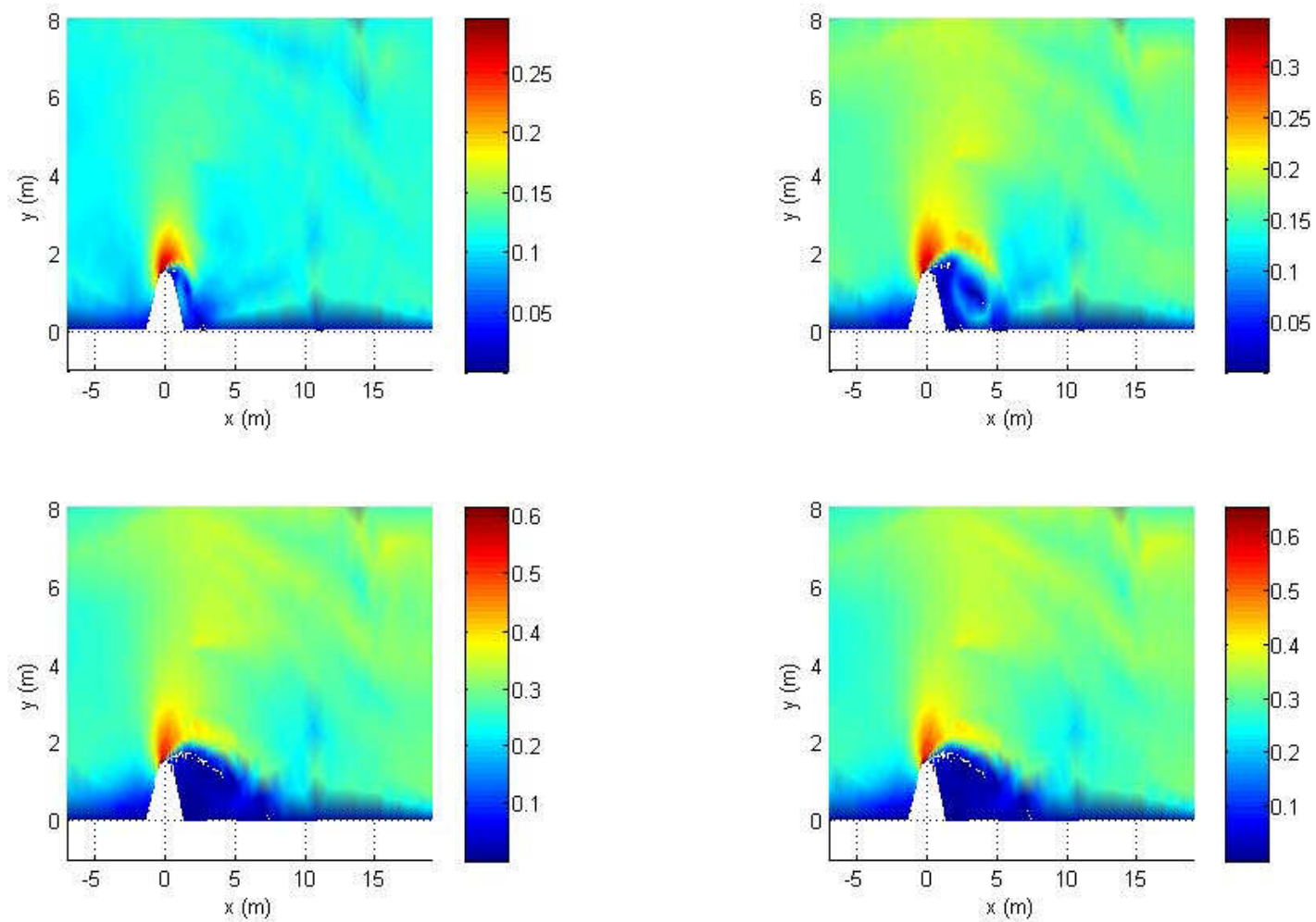


Figure 62: Test 624, Froude number. Clockwise from top left: 0.05T, 0.1T, 0.2T, 0.25T.

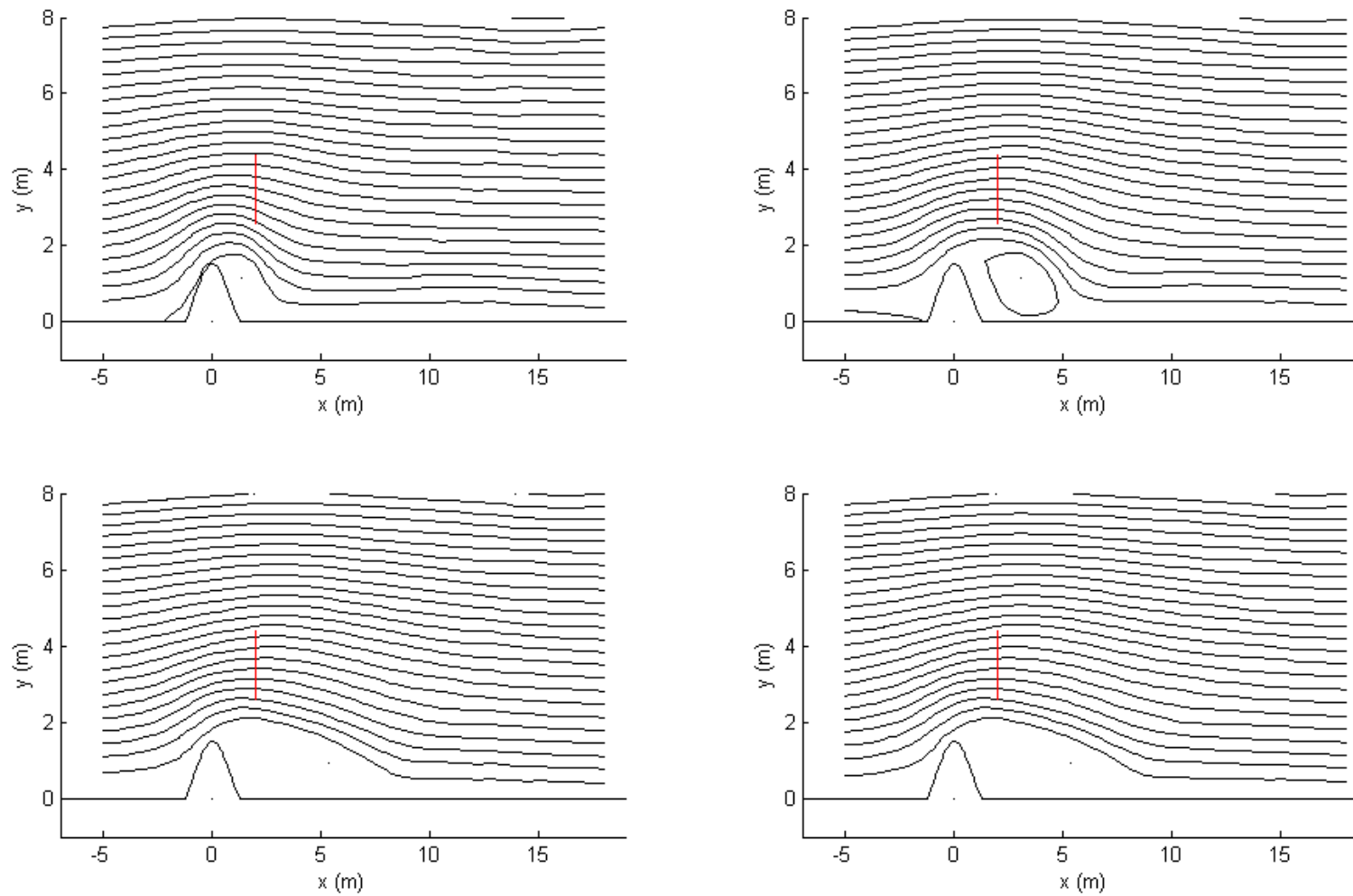


Figure 63: Test 624, Instantaneous Streamlines. Clockwise from top left: 0.05T, 0.1T, 0.2T, 0.25T.

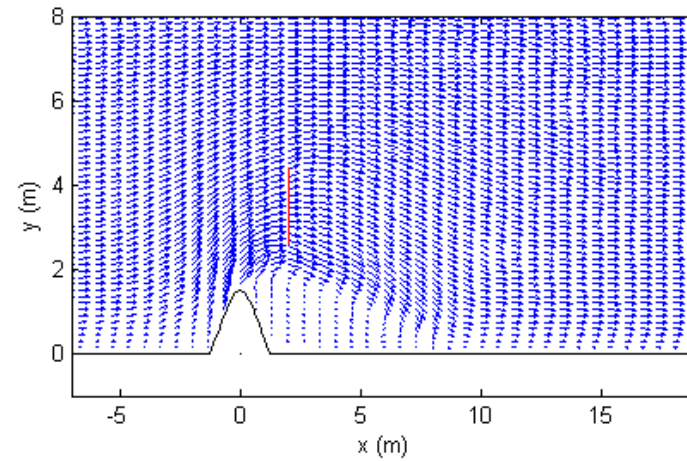
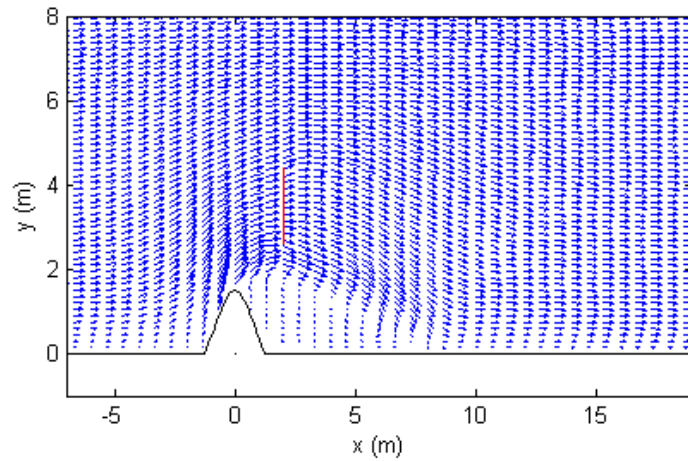
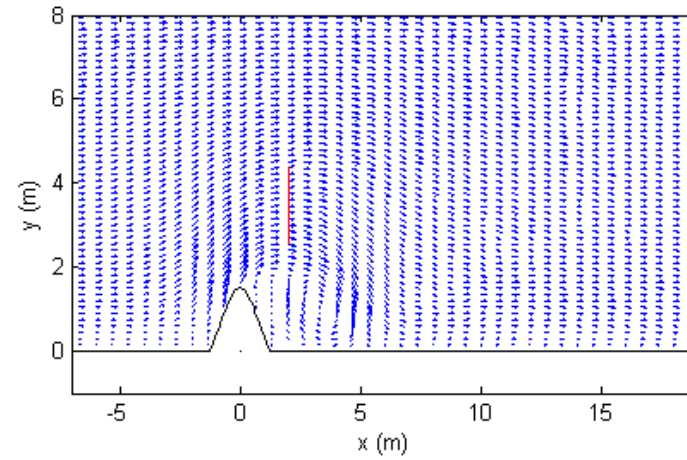
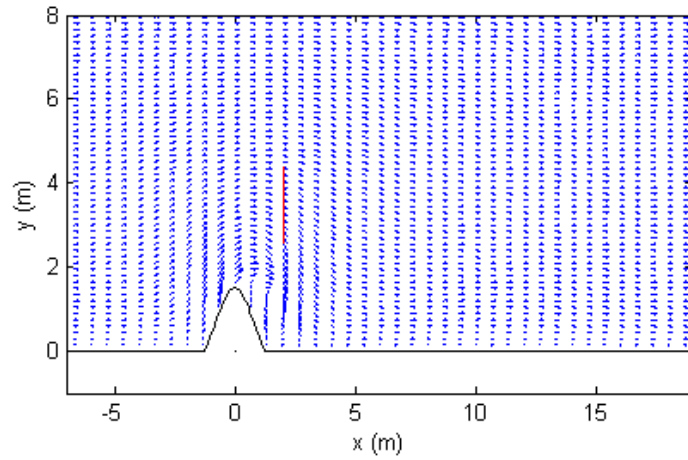


Figure 64: Test 624, Velocity Vectors. Clockwise from top left: $0.05T$, $0.1T$, $0.2T$, $0.25T$.

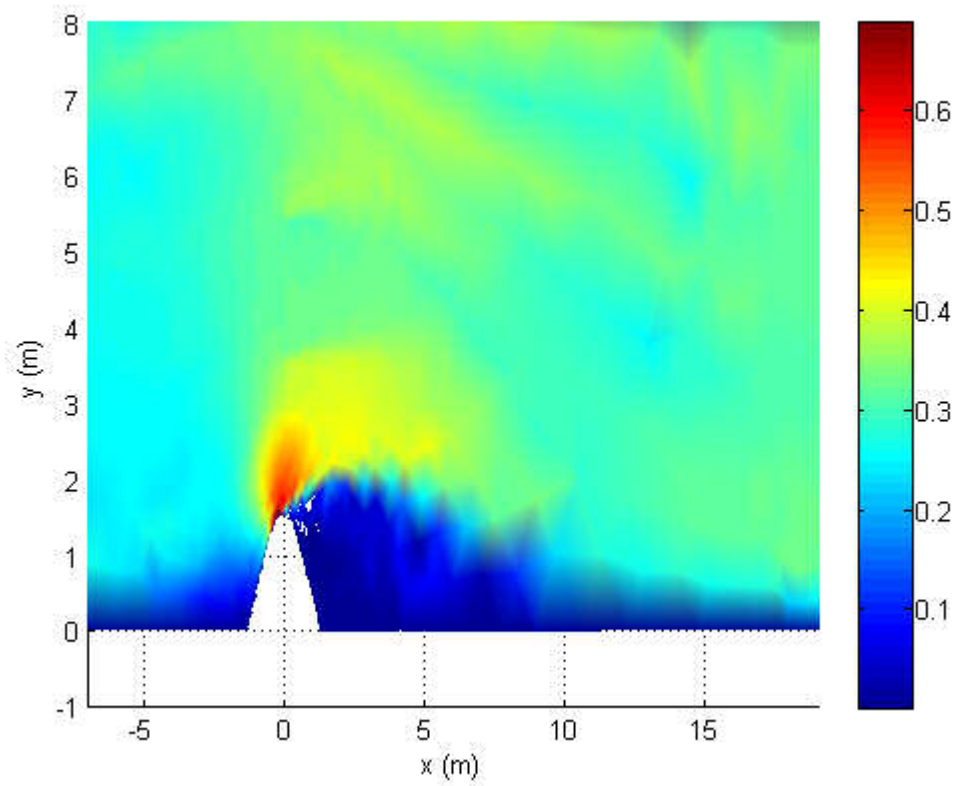


Figure 65: Test 620, Froude number. Clockwise from top left: 0.05T, 0.1T, 0.2T, 0.25T.

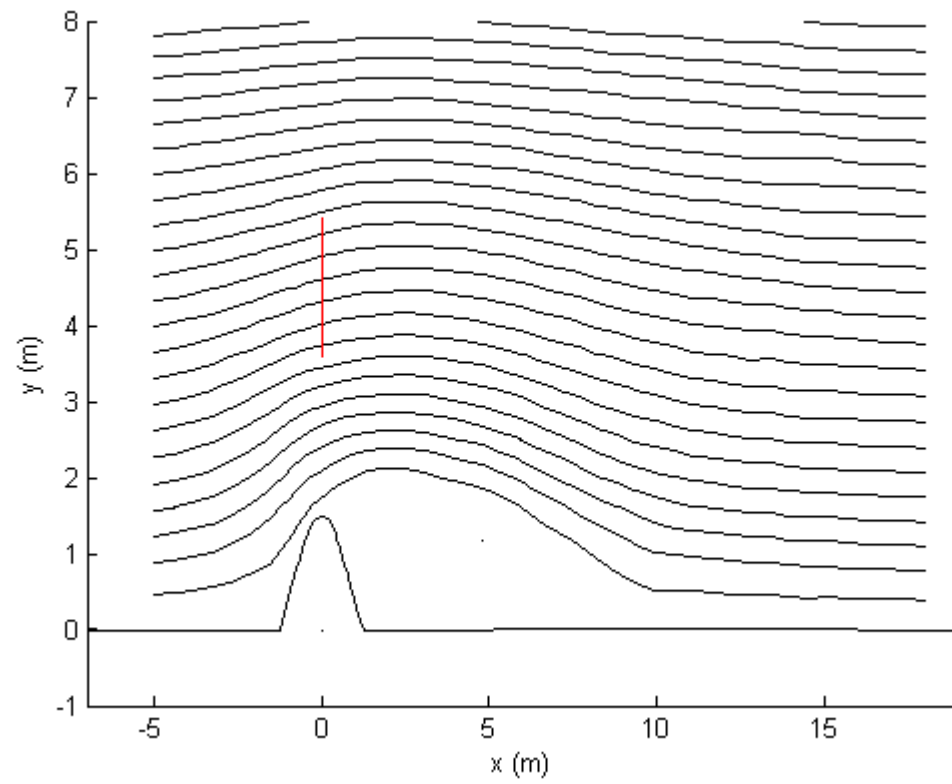


Figure 66: Test 620, Instantaneous Streamlines. Clockwise from top left: 0.05T, 0.1T, 0.2T, 0.25T.

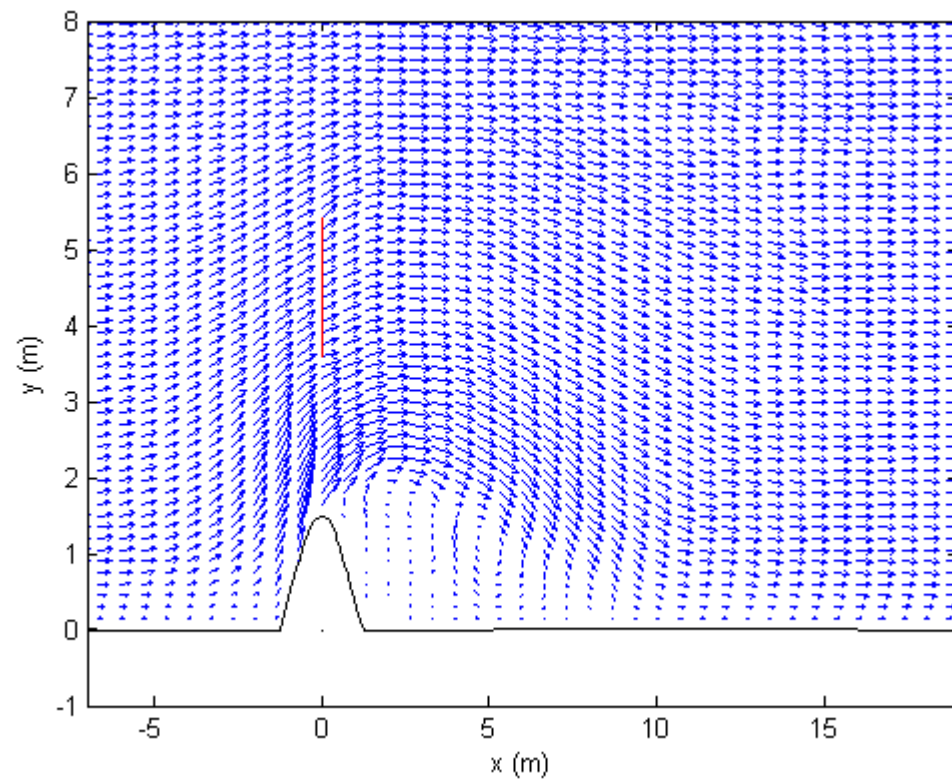


Figure 67: Test 620, Velocity Vectors. Clockwise from top left: 0.05T, 0.1T, 0.2T, 0.25T.

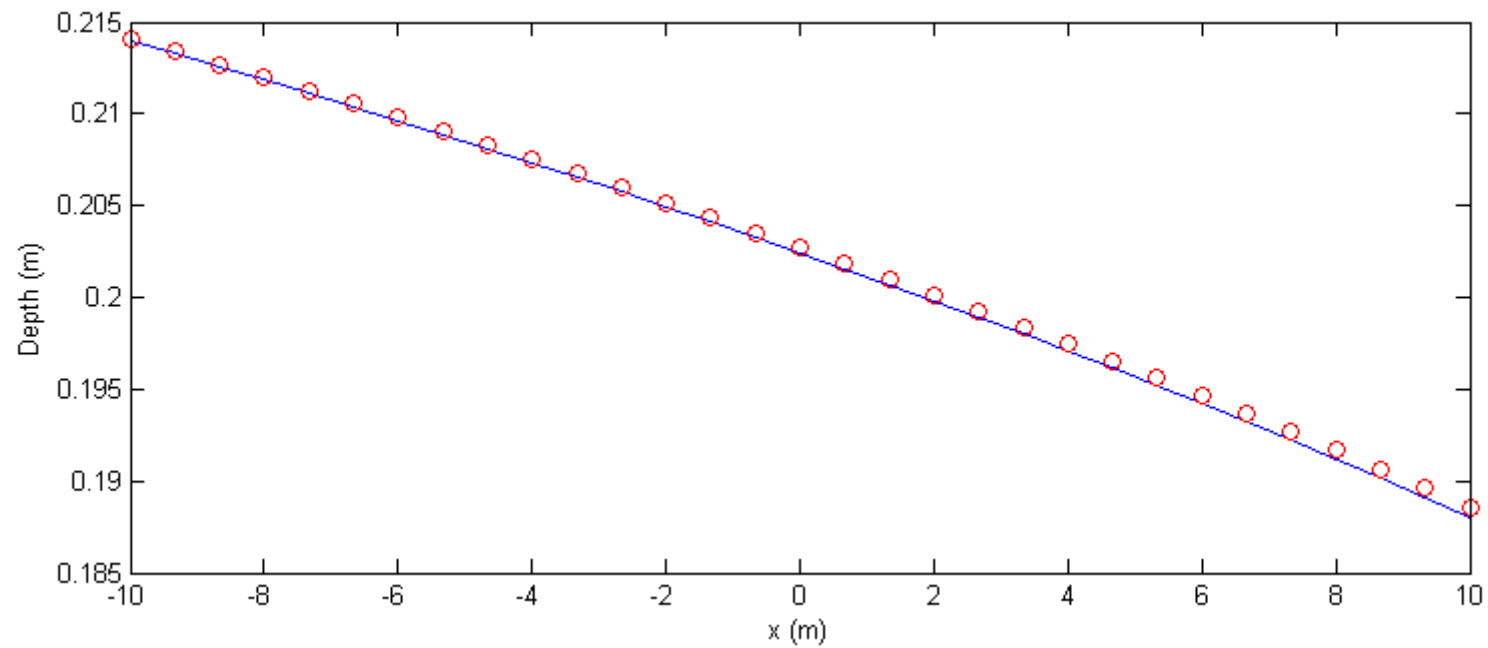


Figure 68: Elevation along the centre of the channel ($y=0$). Solid line represents fixed elevation boundary conditions without turbine fence. Circles represent fixed flow rate boundary conditions without turbine fence.

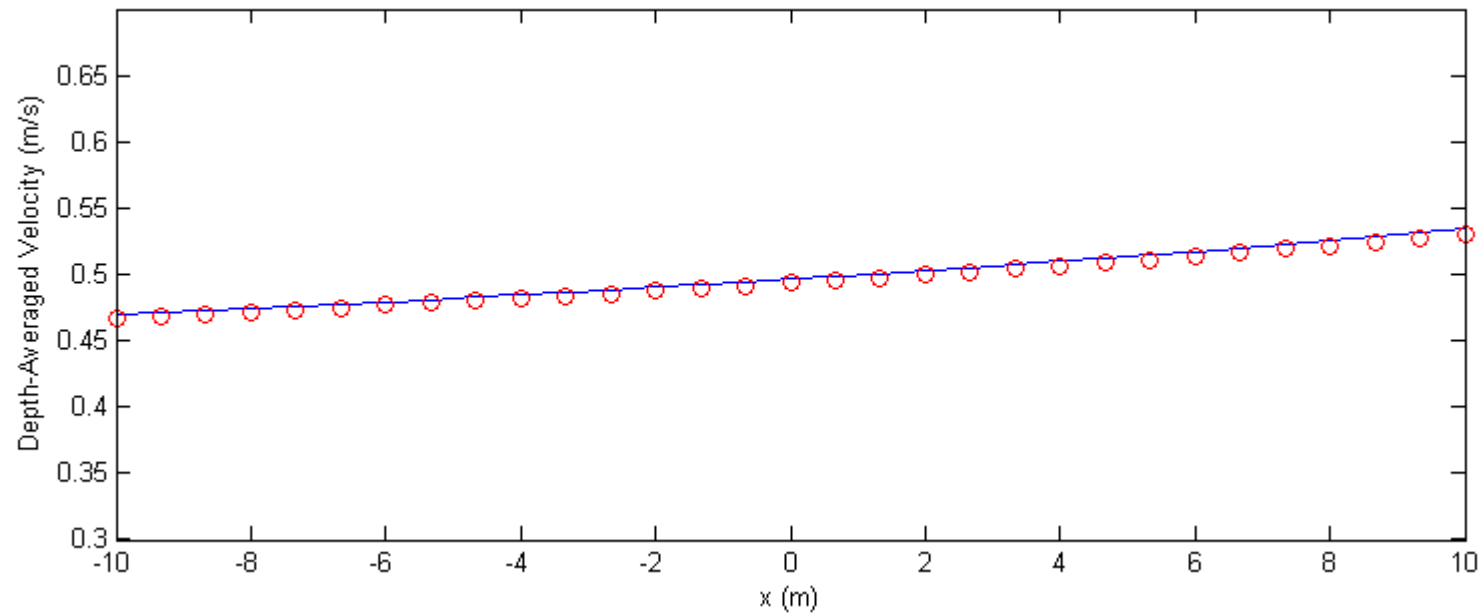


Figure 69: Along channel depth-average velocity along the centre of the channel ($y=0$). Solid line represents fixed elevation boundary conditions without turbine fence. Circles represent fixed flow rate boundary conditions without turbine fence.

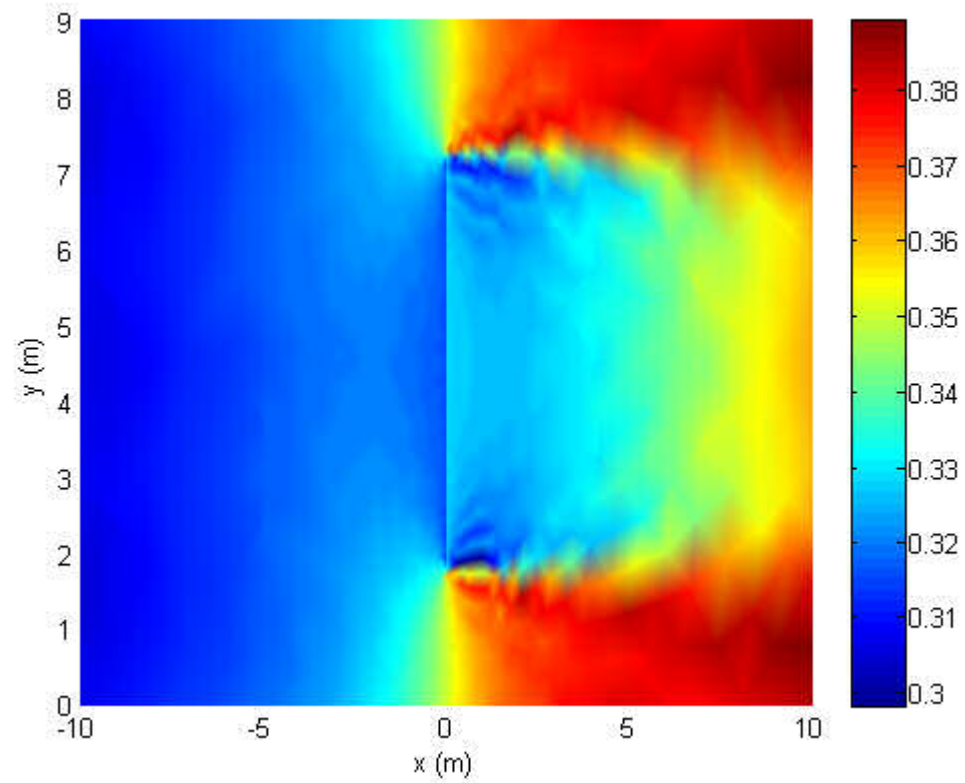


Figure 70: Flow field (represented by Froude number) with the addition of turbine fences for fixed elevation boundary conditions.

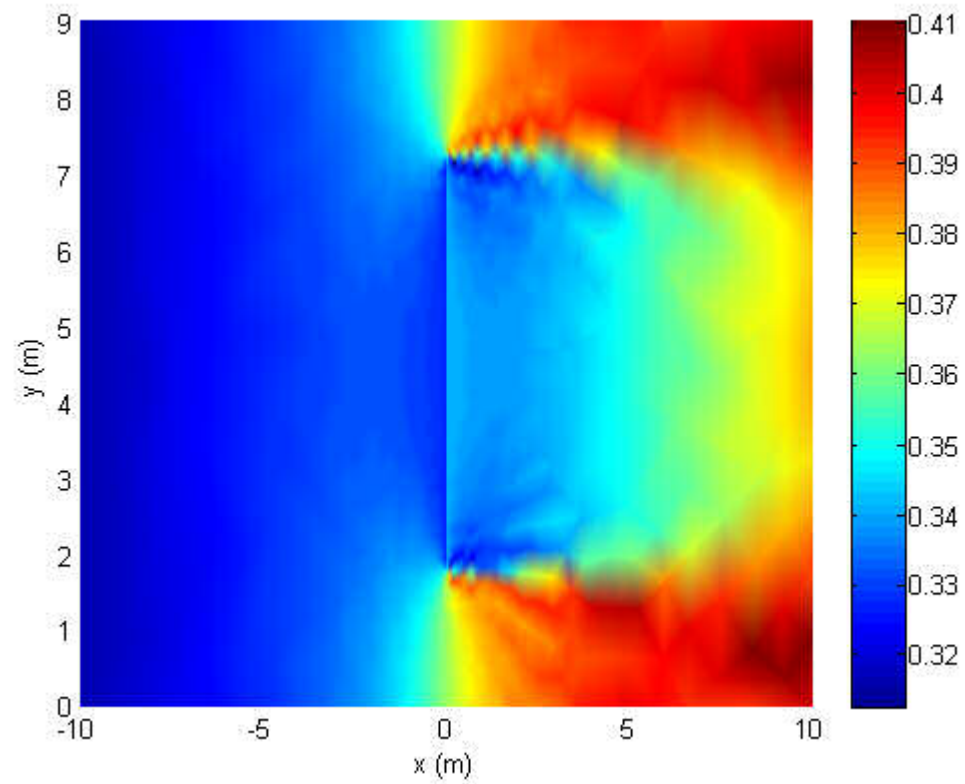


Figure 71: Flow field (represented by Froude number) with the addition of turbine fences for fixed flow rate boundary conditions.

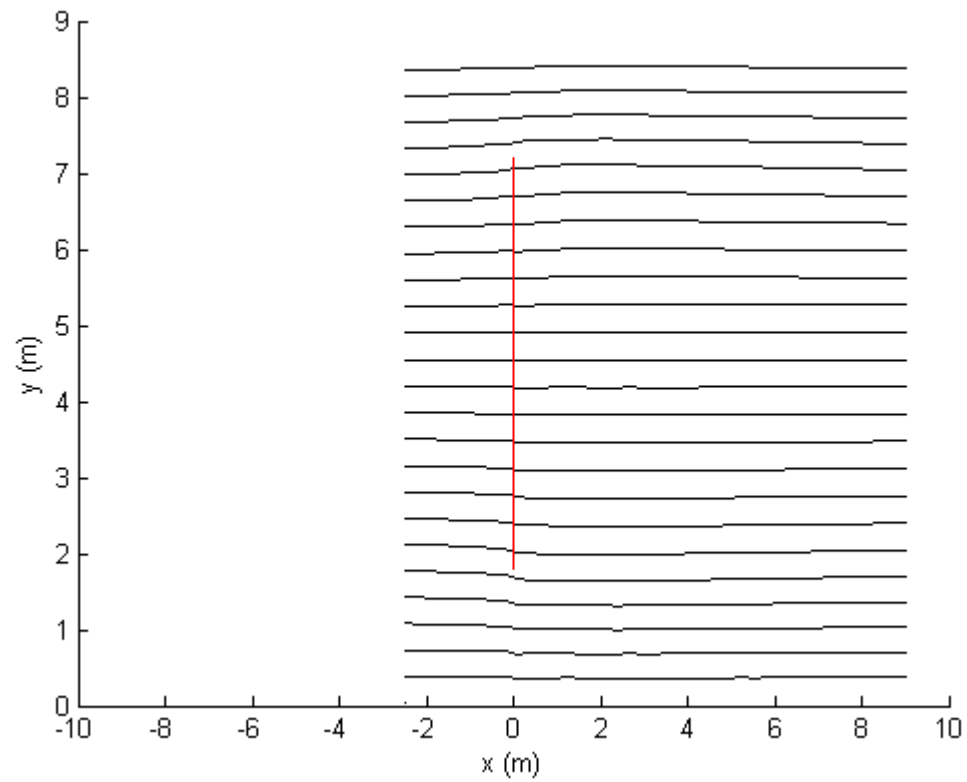


Figure 72: Flow field (represented by streamlines) with the addition of turbine fences for fixed elevation boundary conditions.

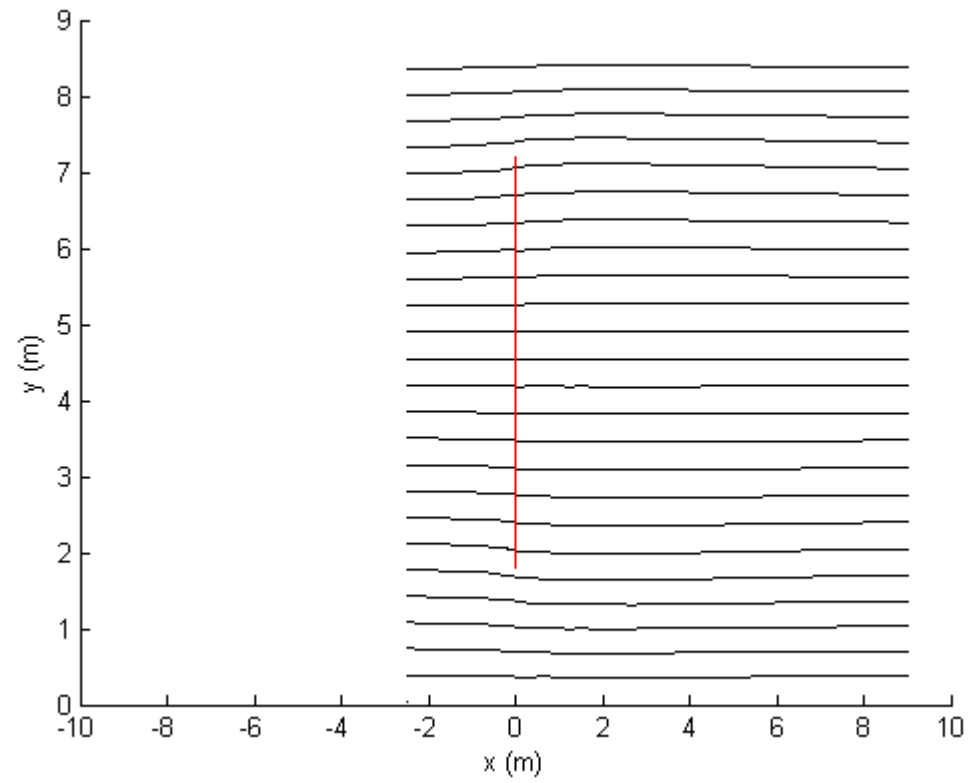
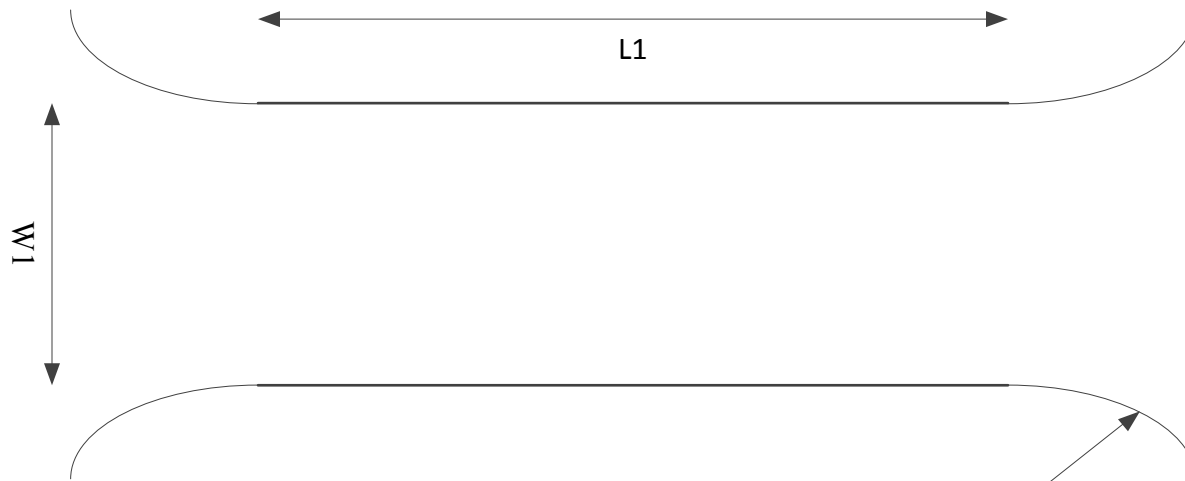


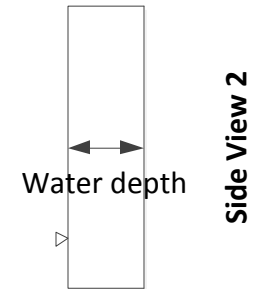
Figure 73: Flow field (represented by streamlines) with the addition of turbine fences for fixed flow rate boundary conditions.

ANNEX 1

Top View

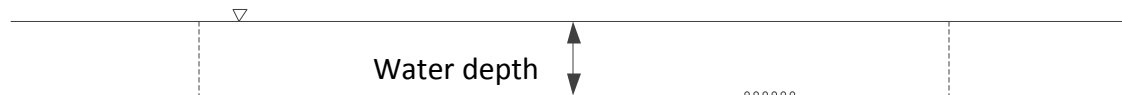


Inlets designed to ensure uniform inflow across width of channel



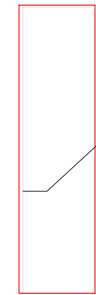
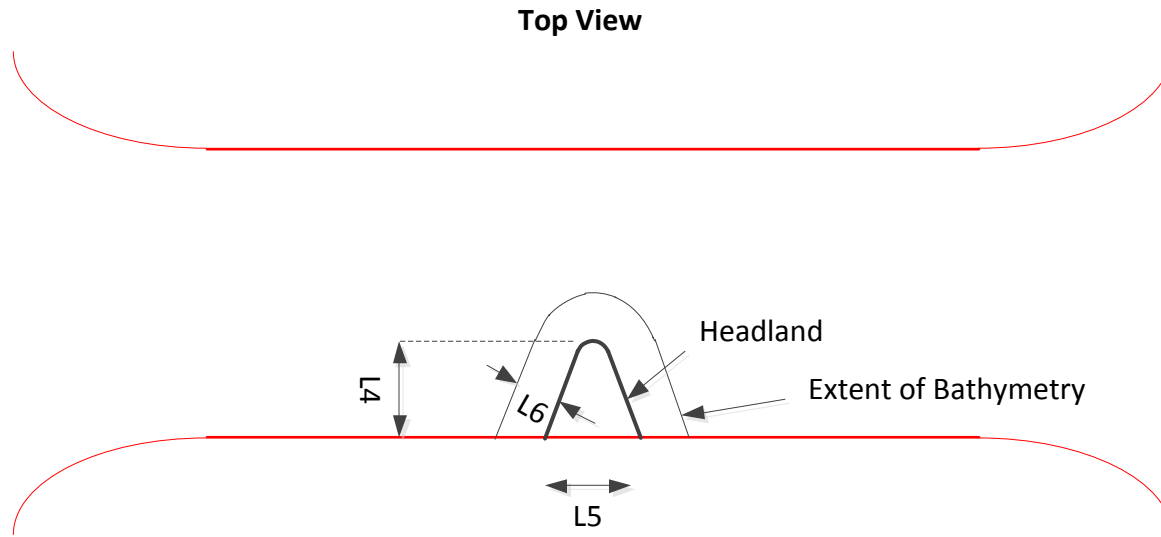
NOTES: (1) W1 = 9 m
(2) L1 = 20 m

Side View 1

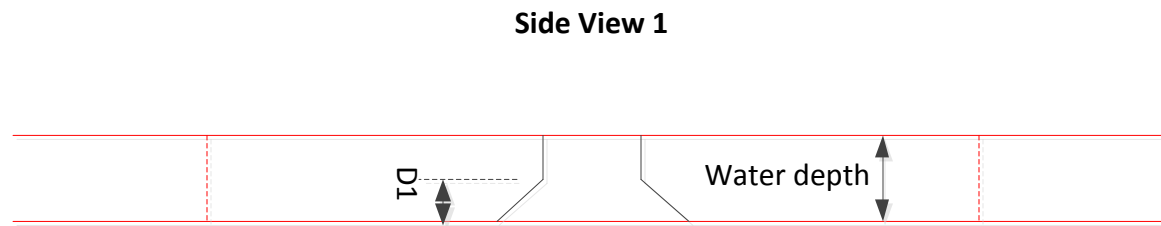


Bed to give $z_o = 1\text{mm}$,
i.e. grain size of
approximately 1.2 cm.

Channel Geometry	No. 1/1
PerAWAT	Date: 24/12/2011

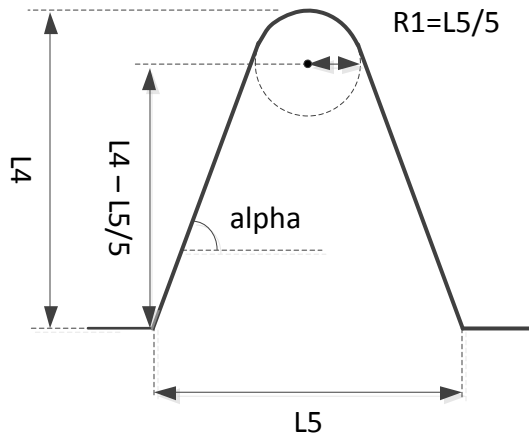


Side View 2

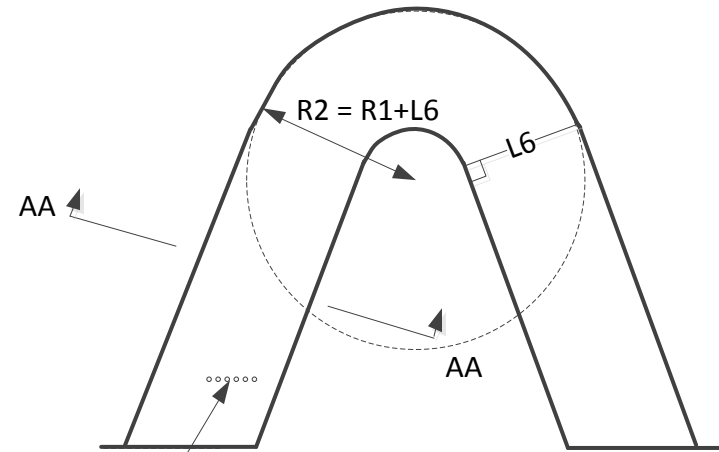


NOTES: (1) See Channel Geometry for channel outline
 (2) See Headland Geometry 2/2 for detailed headland geometry

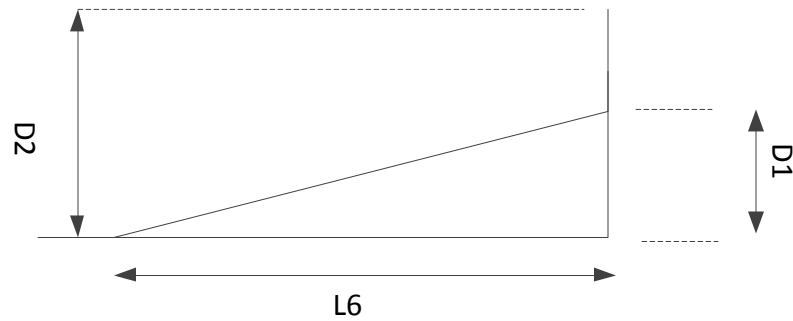
Headland Geometry		No. 1/2
PerAWAT	Date: 24/12/2011	



Top View: Headland Geometry



Top View: Extent of Bathymetry

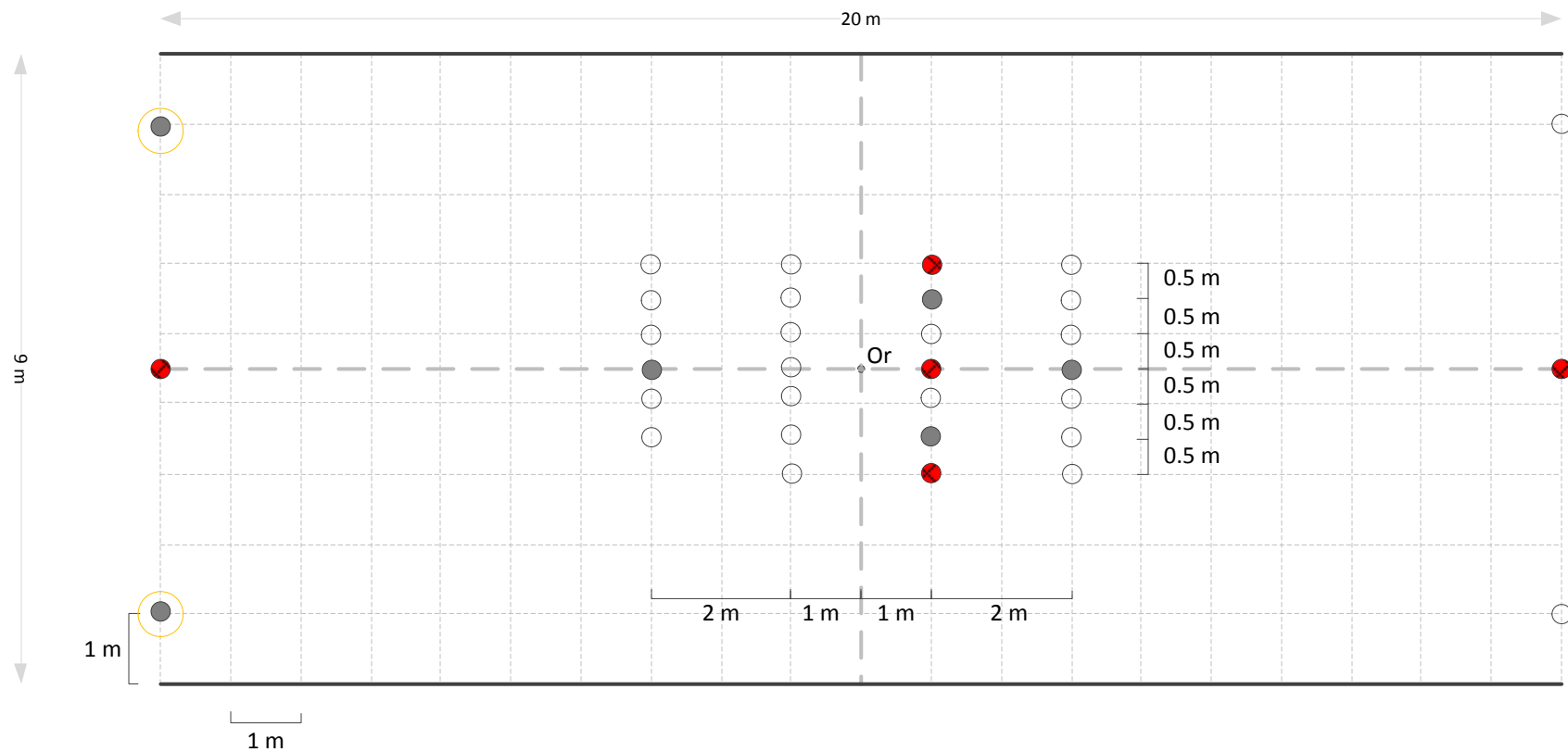



Section AA

- NOTES: (1) $L5 = 2.5$ m
 (2) $L4 = 1.5$ m
 (3) $D1 = 0.1$ m
 (4) $L6 = 1.5$ m
 (5) $\alpha = 56.8947$ degrees
 (6) $D2 > 0.2$ m





Headland Geometry		No. 2/2
PerAWAT	Date: 24/12/2011	

ANNEX 2



 This could be changed to propeller meter if not enough ADVs

Key

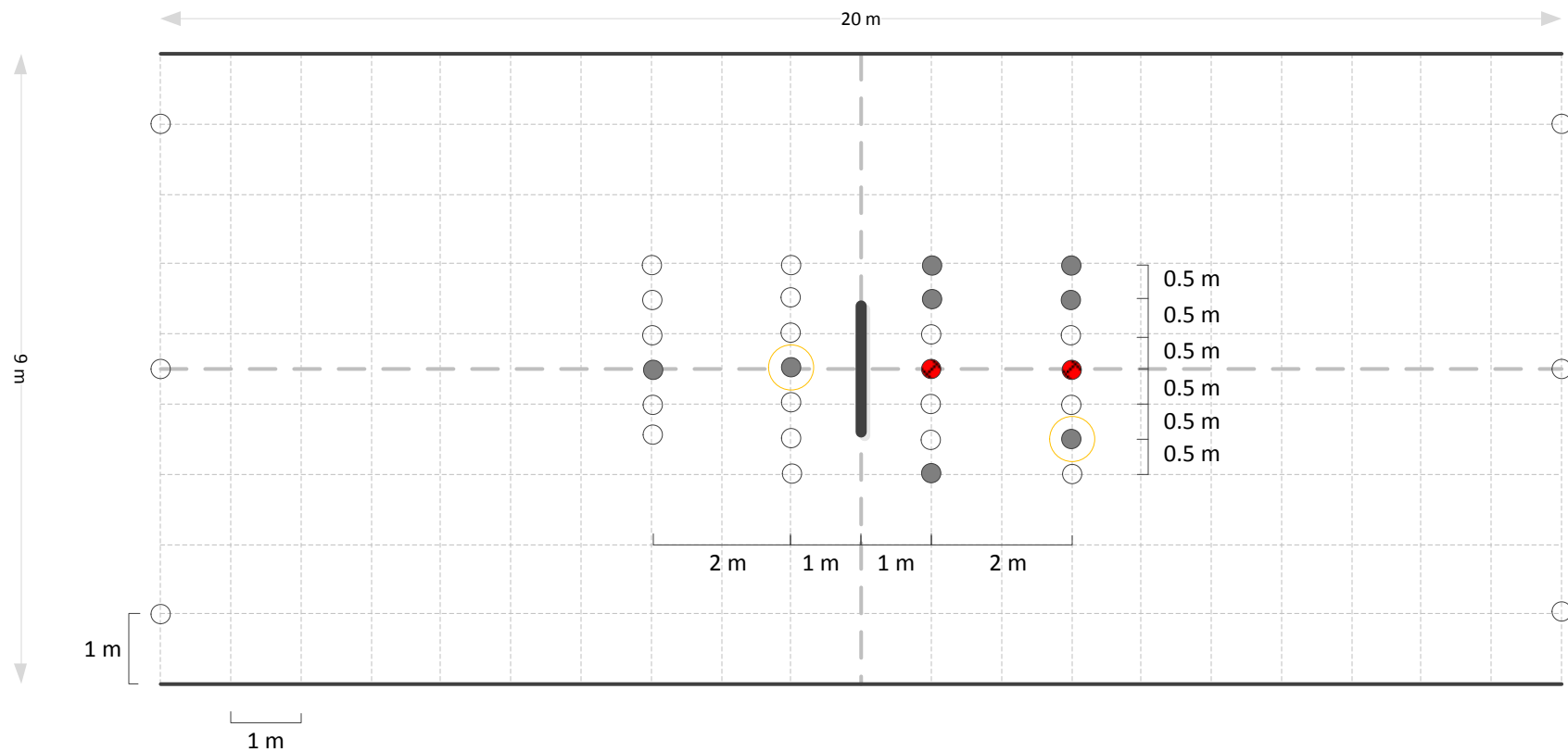
-  ADV point measurement
-  ADV depth profile (refer to specification for details)
-  Propeller meter measurement
-  Turbine Fence

NOTE: (1) Wave probes to be placed at all locations where velocity measurements are made
 (2) Or denotes the origin
 (3) All fences are 1.8 m long

Test 1: Close grid no turbine

PerAWAT

Date: 24/12/2011



Key

- ADV point measurement
- ⊗ ADV depth profile (refer to specification for details)
- Propeller meter measurement
- ▬ Turbine fence

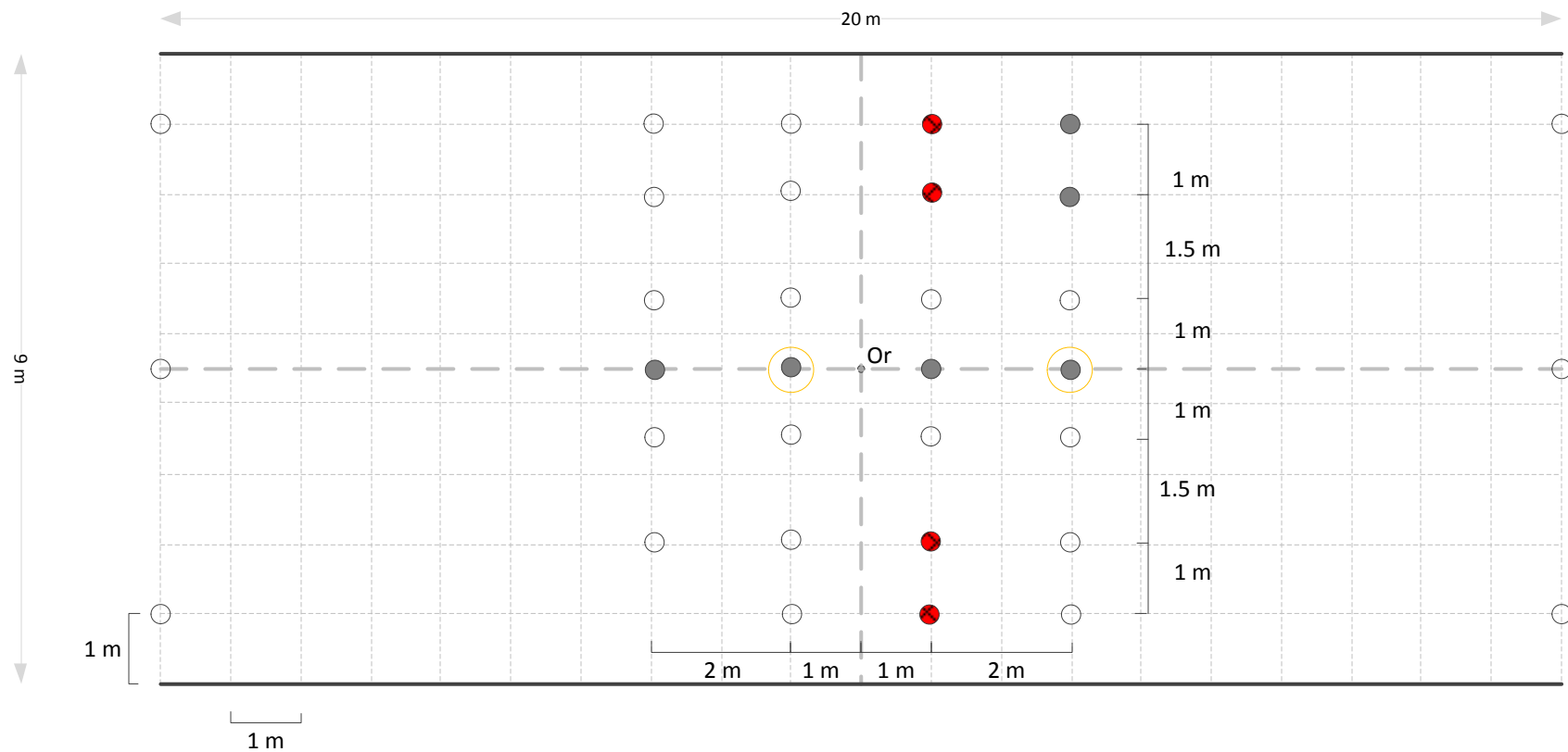
NOTE: (1) Wave probes to be placed at all locations where velocity measurements are made
 (2) Or denotes the origin
 (3) All fences are 1.8 m long: Fence centre at (0,0)


○ This could be changed to propeller meter if not enough ADVs

Test 2: Close grid with turbine





PerAWAT

Date: 24/12/2011



 This could be changed to propeller meter if not enough ADVs

Key

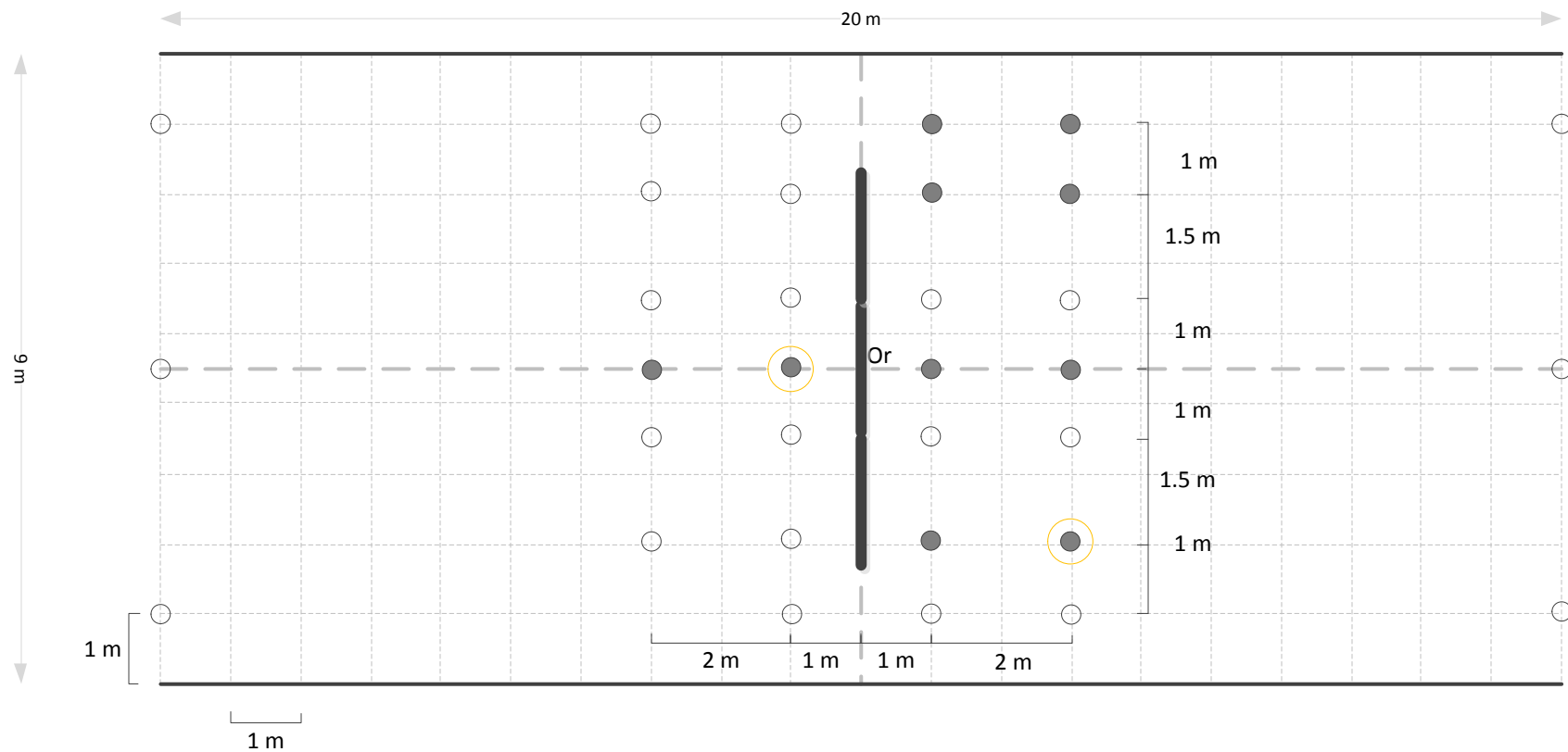
-  ADV point measurement
-  ADV depth profile (refer to specification for details)
-  Propeller meter measurement
-  Turbine Fence


NOTE: (1) Wave probes to be placed at all locations where velocity measurements are made
 (2) Or denotes the origin
 (3) All fences are 1.8 m long

Test 3: Wider grid no turbines





PerAWAT

Date: 24/12/2011



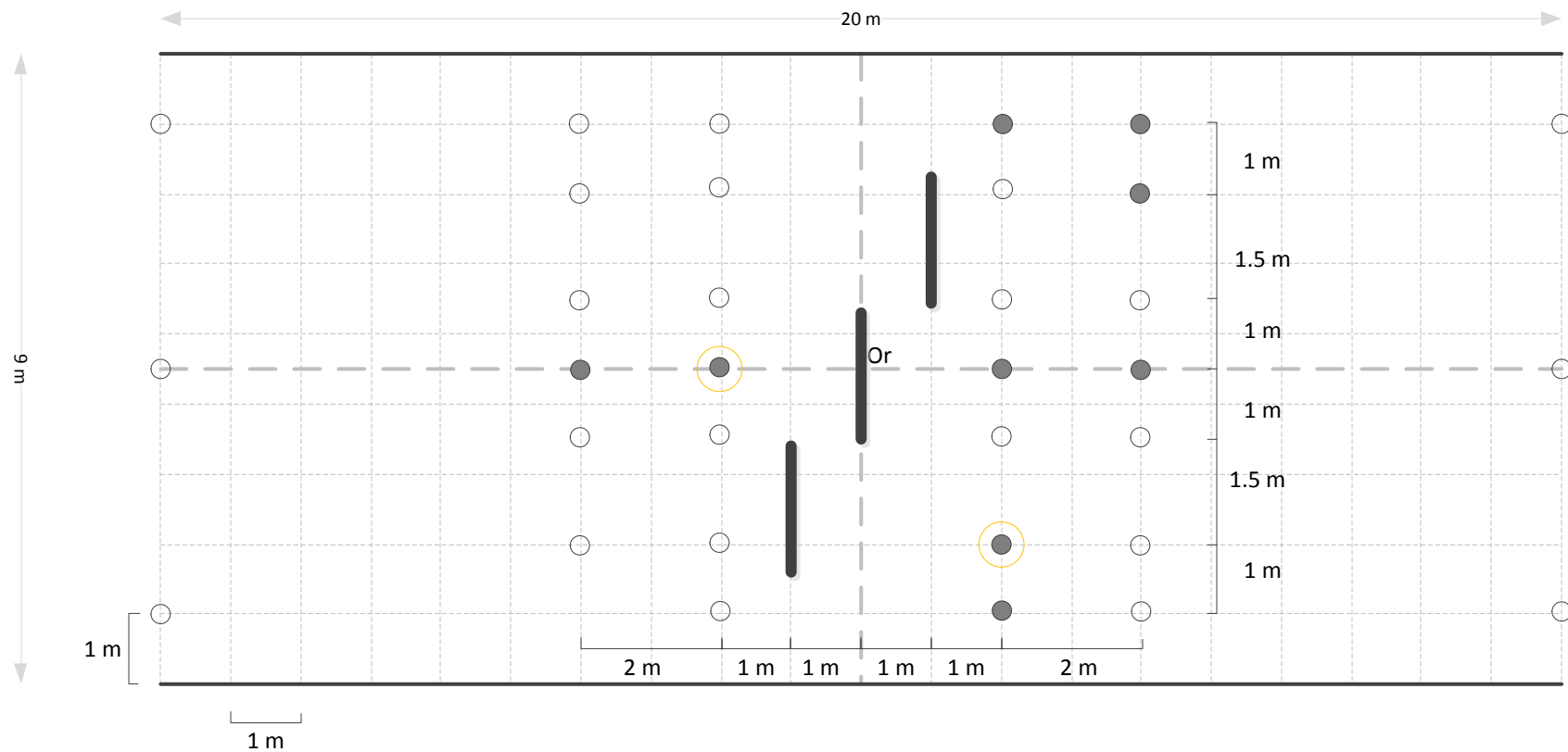
 This could be changed to propeller meter if not enough ADVs


Key

-  ADV point measurement
-  ADV depth profile (refer to specification for details)
-  Propeller meter measurement
-  Turbine Fence





NOTE: (1) Wave probes to be placed at all locations where velocity measurements are made
 (2) Or denotes the origin
 (3) All fences are 1.8 m long: Fence centres at (0,0), (0,1.8), (0,-1.8)

Test 4: Wider grid all together	
PerAWAT	Date: 24/12/2011



 This could be changed to propeller meter if not enough ADVs

Key

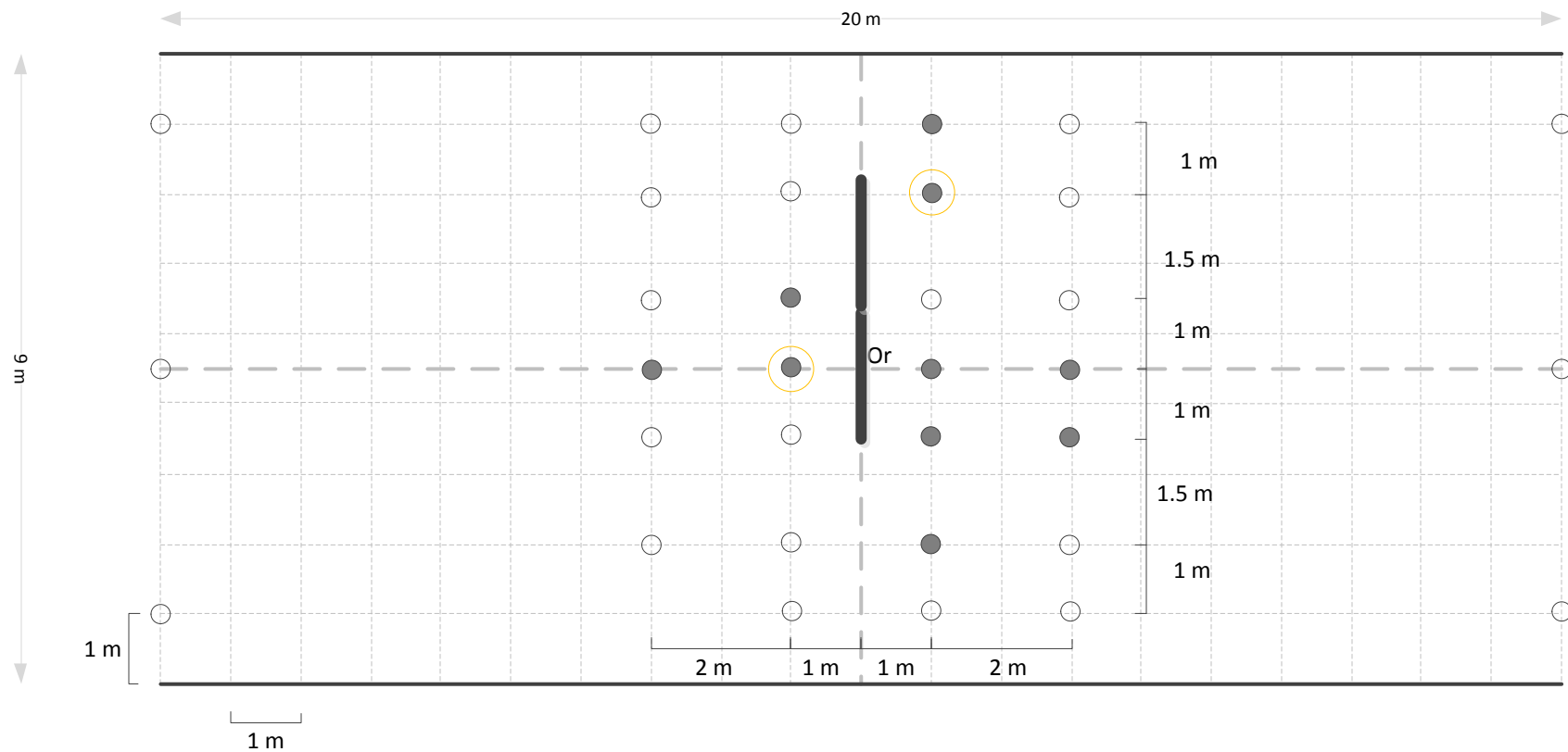
-  ADV point measurement
-  ADV depth profile (refer to specification for details)
-  Propeller meter measurement
-  Turbine Fence


NOTE: (1) Wave probes to be placed at all locations where velocity measurements are made
 (2) Or denotes the origin
 (3) All fences are 1.8 m long: Fence centres at (0,0), (1,1.8), (-1,-1.8)

Test 5: Staggard





PerAWAT

Date: 24/12/2011



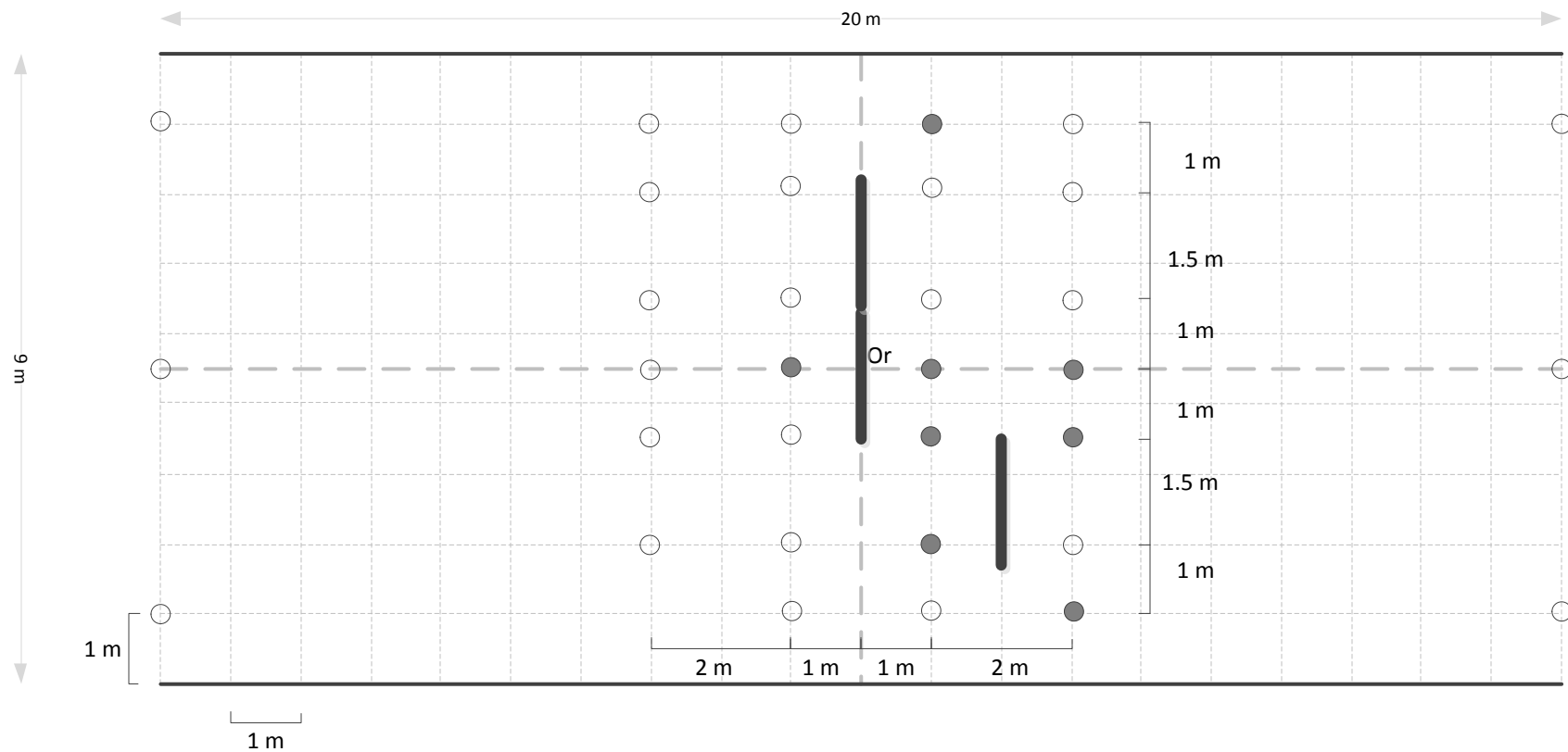
 This could be changed to propeller meter if not enough ADVs

Key

-  ADV point measurement
-  ADV depth profile (refer to specification for more details)
-  Propeller meter measurement
-  Turbine Fence

NOTE: (1) Wave probes to be placed at all locations where velocity measurements are made
 (2) Or denotes the origin
 (3) All fences are 1.8 m long: Fence centres at (0,0), (0,1.8)

Test 6: Wide grid asymmetric	
PerAWAT	Date: 24/12/2011



○ This could be changed to propeller meter if not enough ADVs

Key

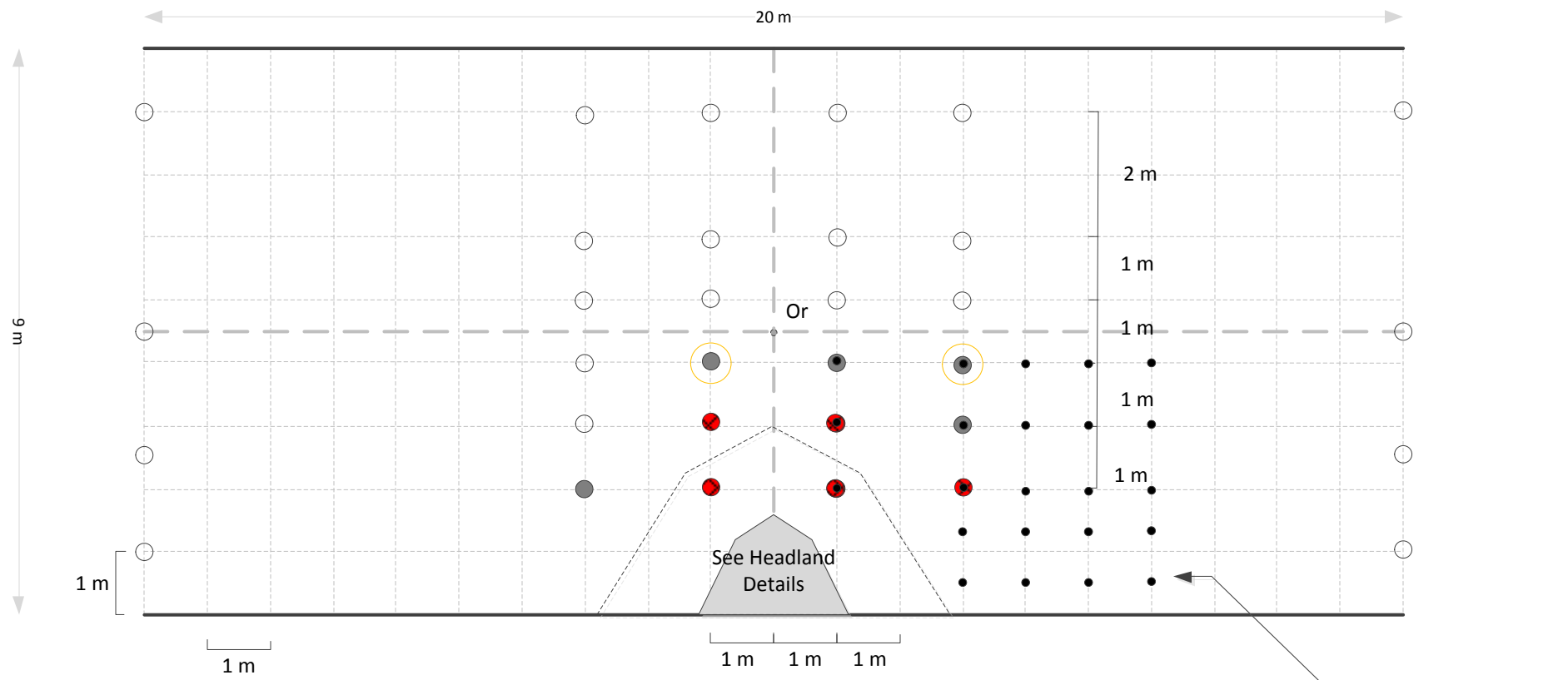
- ADV point measurement
- ⊗ ADV depth profile (refer to specification for more details)
- Propeller meter measurement
- Turbine Fence

NOTE: (1) Wave probes to be placed at all locations where velocity measurements are made
 (2) Or denotes the origin
 (3) All fences are 1.8 m long: Fence centres at (0,0), (0,1.8), (2,-1.8)

Test 7: Wider grid 2 asymmetric

PerAWAT

Date: 24/12/2011



○ This could be changed to propeller meter if not enough ADVs

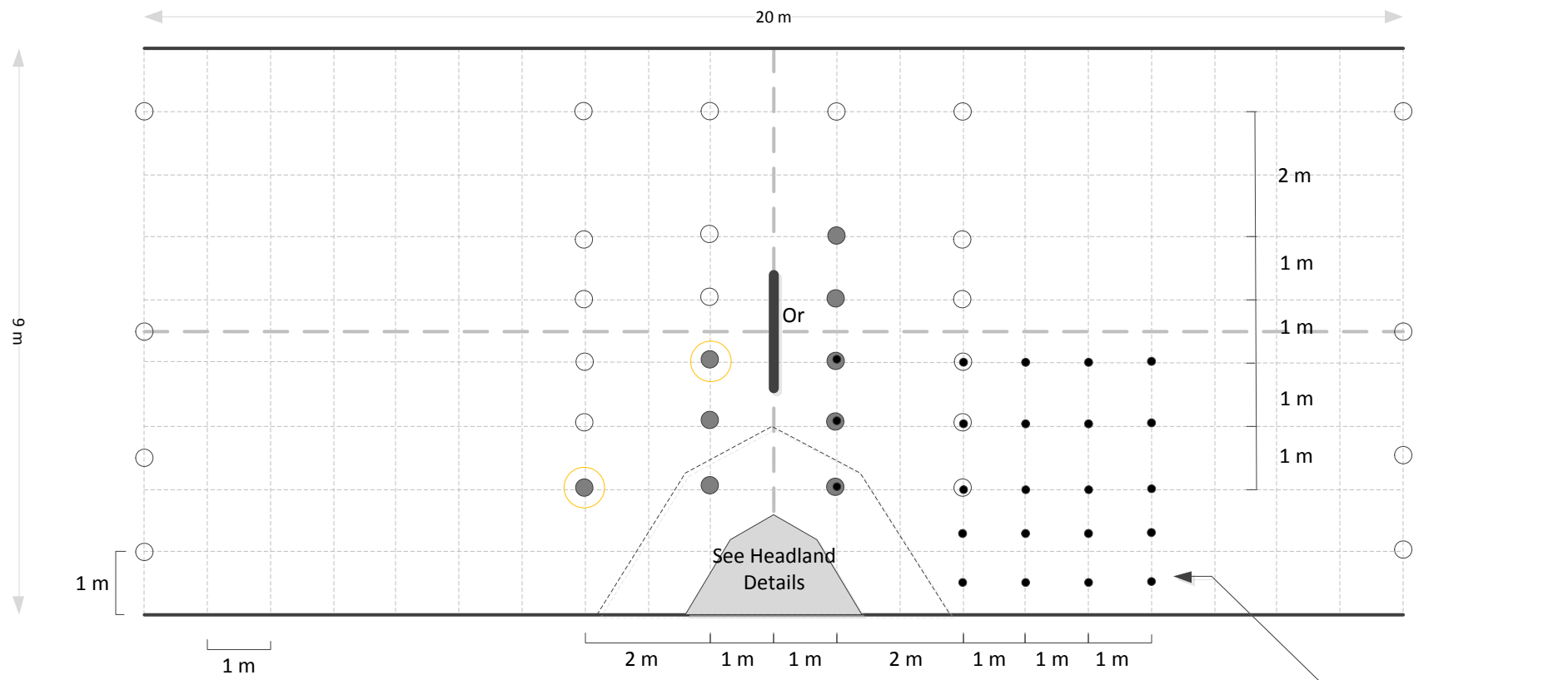
Points in Second Measurement

Key

- ADV point measurement
- ⊗ ADV depth profile (refer to specification for more details)
- Propeller meter measurement
- ▬ Turbine Fence

NOTE: (1) Wave probes to be placed at all locations where velocity measurements are made
 (2) Or denotes the origin
 (3) All fences are 1.8 m long

Test 8: Base Case 1	
PerAWAT	Date: 24/12/2011

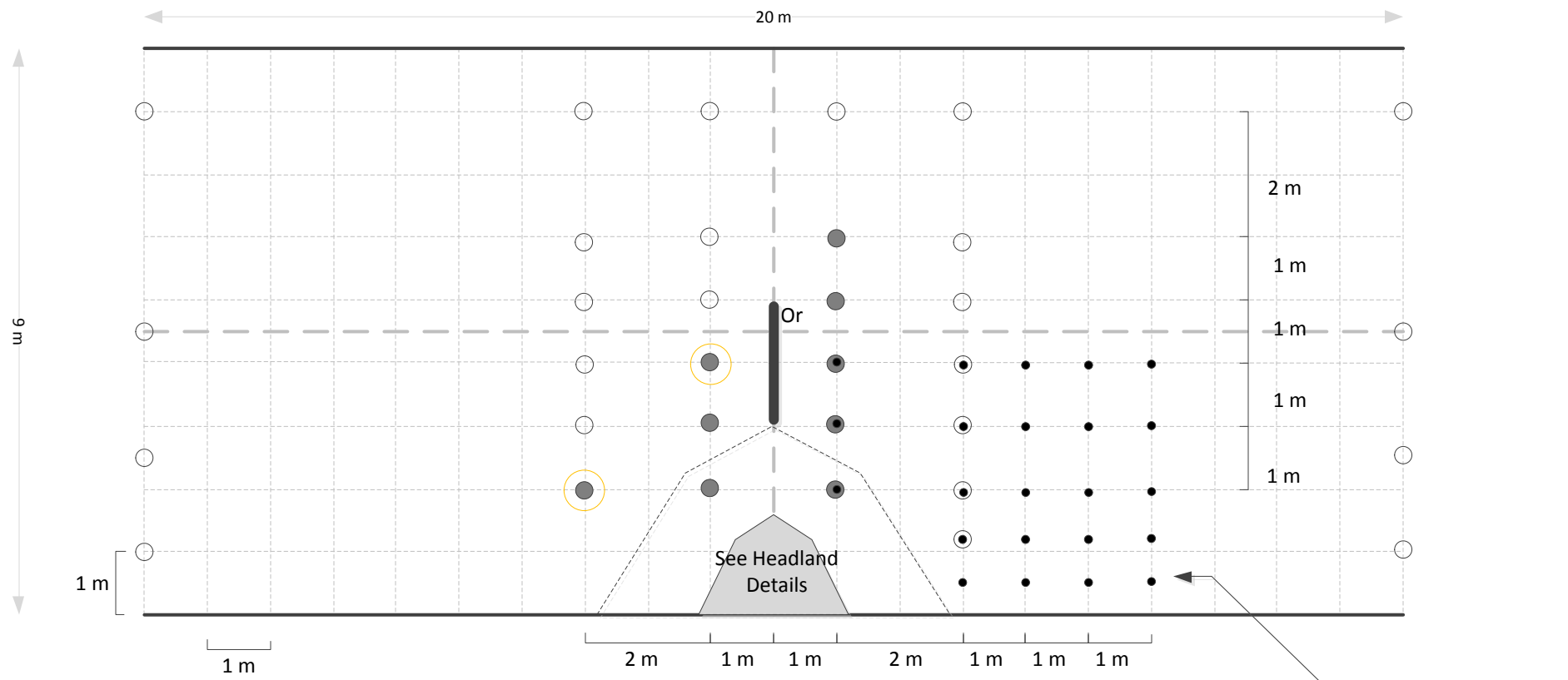


Key

- ADV point measurement
- ⊗ ADV depth profile (refer to specification for more details)
- Propeller meter measurement
- ▬ Turbine Fence

NOTE: (1) Wave probes to be placed at all locations where velocity measurements are made
 (2) Or denotes the origin
 (3) All fences are 1.8 m long: Fence centres at (0,0)

Test 9: Turb 1	
PerAWAT	Date: 24/12/2011



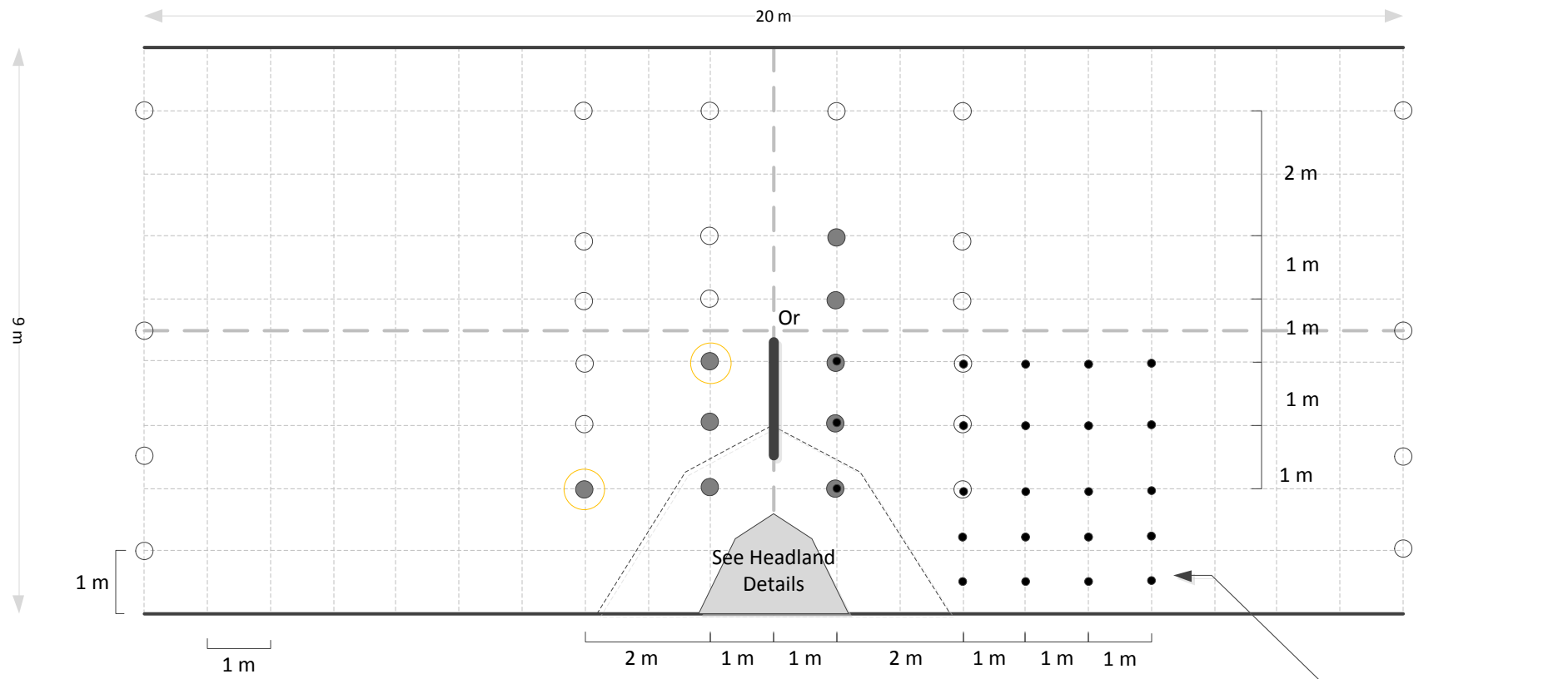
○ This could be changed to propeller meter if not enough ADVs

Points in Second Measurement

- Key**
- ADV point measurement
 - ⊗ ADV depth profile (refer to specification for more details)
 - Propeller meter measurement
 - ▬ Turbine Fence

NOTE: (1) Wave probes to be placed at all locations where velocity measurements are made
 (2) Or denotes the origin
 (3) All fences are 1.8 m long: Fence centres at (0,-0.5)

Test 10: Turb 2	
PerAWAT	Date: 24/12/2011



○ This could be changed to propeller meter if not enough ADVs

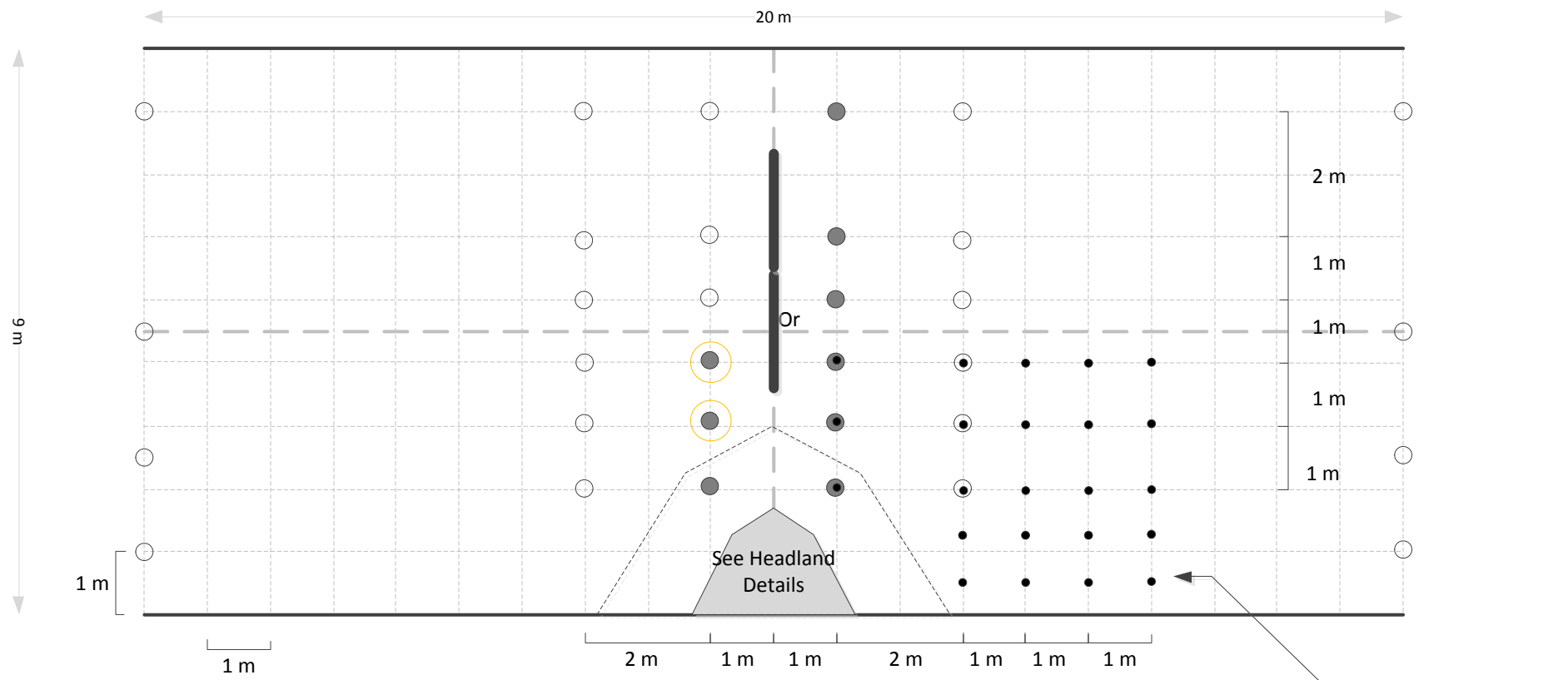
Points in Second Measurement

Key

- ADV point measurement
- ⊗ ADV depth profile (refer to specification for more details)
- Propeller meter measurement
- ▬ Turbine Fence

NOTE: (1) Wave probes to be placed at all locations where velocity measurements are made
 (2) Or denotes the origin
 (3) All fences are 1.8 m long: Fence centres at (0,-1.0)

Test 11: Turb 3	
PerAWAT	Date: 24/12/2011



○ This could be changed to propeller meter if not enough ADVs

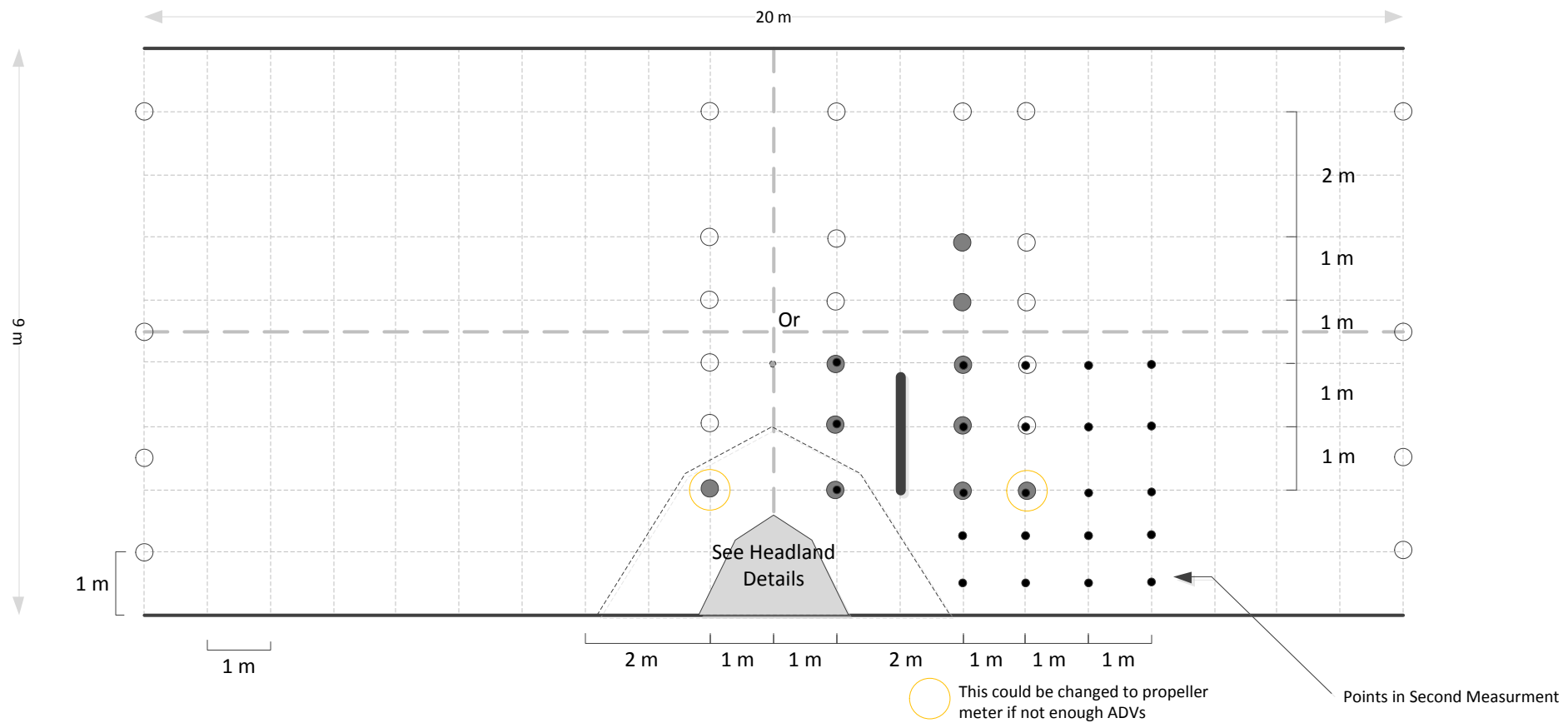
Points in Second Measurement

Key

- ADV point measurement
- ⊗ ADV depth profile (refer to specification for more details)
- Propeller meter measurement
- ▬ Turbine Fence

NOTE: (1) Wave probes to be placed at all locations where velocity measurements are made
 (2) Or denotes the origin
 (3) All fences are 1.8 m long: Fence centres at (0,0), (0,1.8)

Test 12: Turb 4	
PerAWAT	Date: 24/12/2011

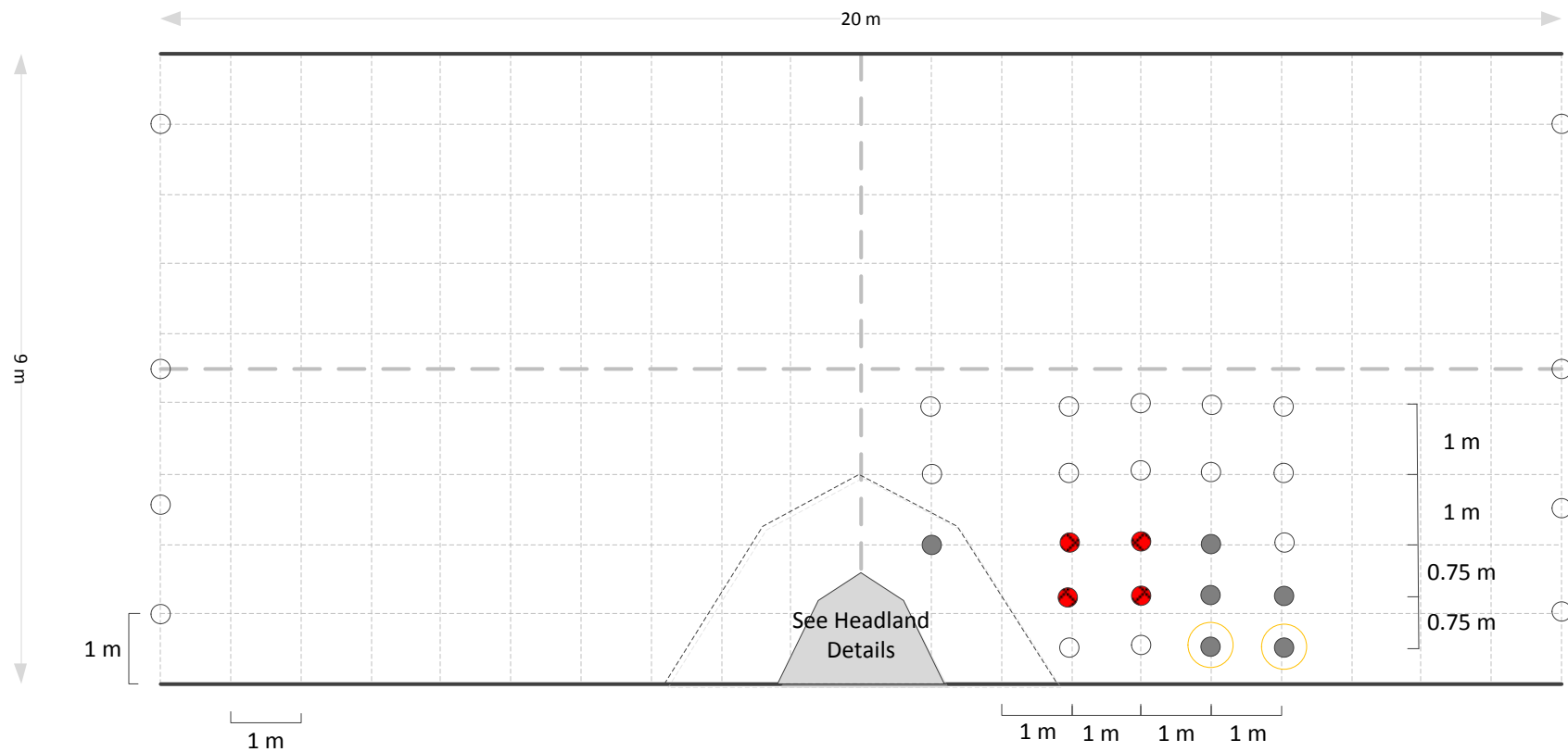


Key

- ADV point measurement
- ⊗ ADV depth profile (refer to specification for more details)
- Propeller meter measurement
- ▬ Turbine Fence

NOTE: (1) Wave probes to be placed at all locations where velocity measurements are made
 (2) Or denotes the origin
 (3) All fences are 1.8 m long: Fence centres at (2,-1.0)

Test 13: Turb 5	
PerAWAT	Date: 24/12/2011



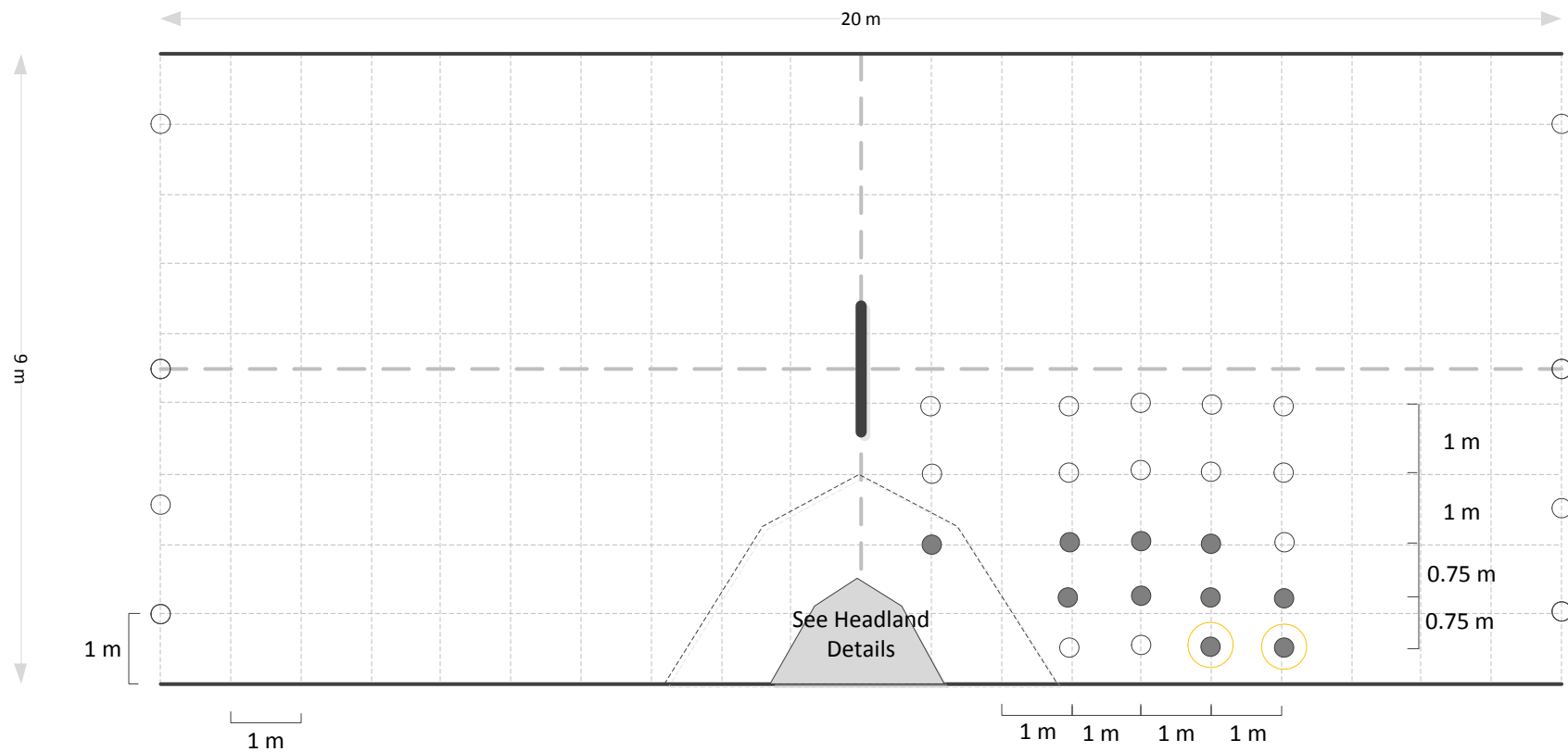
○ This could be changed to propeller meter if not enough ADVs

Key

- ADV point measurement
- ⊗ ADV depth profile (refer to specification for more details)
- Propeller meter measurement
- ▬ Turbine Fence

NOTE: (1) Wave probes to be placed at all locations where velocity measurements are made
 (2) Or denotes the origin
 (3) All fences are 1.8 m long

Test 14: Base Case 2	
PerAWAT	Date: 24/12/2011



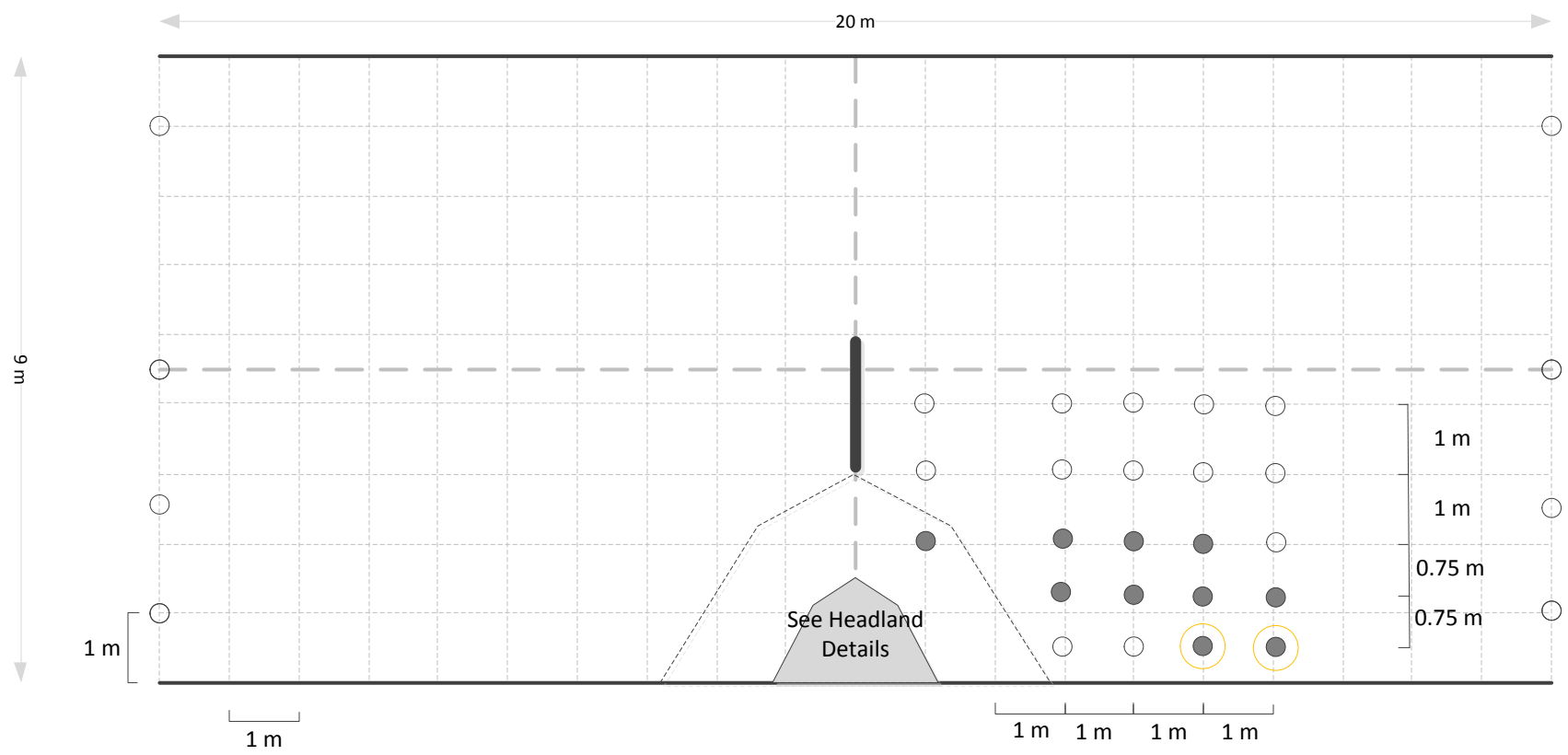
○ This could be changed to propeller meter if not enough ADVs

Key

- ADV point measurement
- ADV depth profile (refer to specification for more details)
- Propeller meter measurement
- Turbine Fence

NOTE: (1) Wave probes to be placed at all locations where velocity measurements are made
 (2) Or denotes the origin
 (3) All fences are 1.8 m long: Fence centres at (0,0)

Test15: Turb 1, wake meas.	
PerAWAT	Date: 24/12/2011

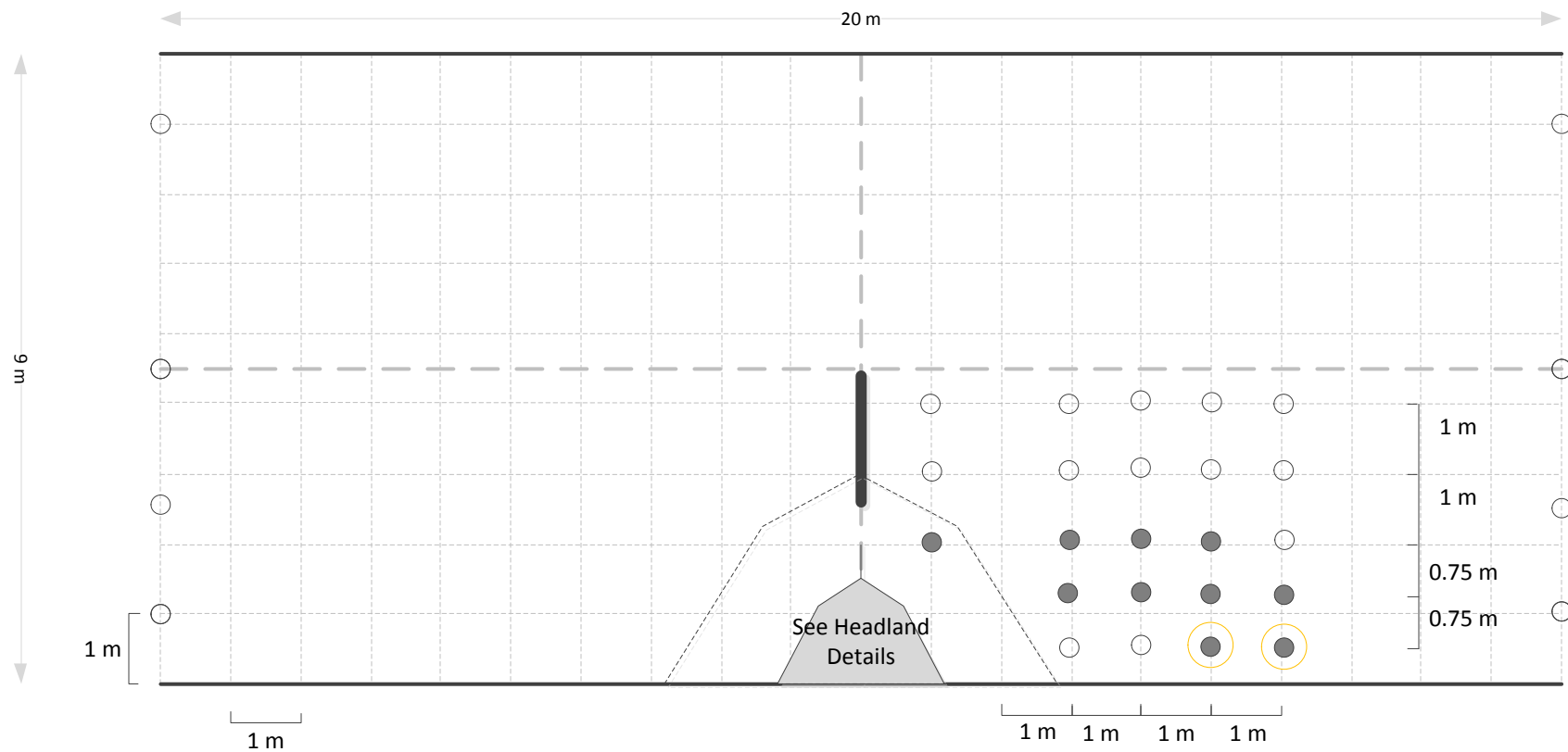


○ This could be changed to propeller meter if not enough ADVs

- Key
- ADV point measurement
 - ⊗ ADV depth profile (refer to specification for more details)
 - Propeller meter measurement
 - ▬ Turbine Fence

NOTE: (1) Wave probes to be placed at all locations where velocity measurements are made
 (2) Or denotes the origin
 (3) All fences are 1.8 m long: Fence centres at (0,-0.5)

Test16: Turb 2, wake meas.	
PerAWAT	Date: 24/12/2011



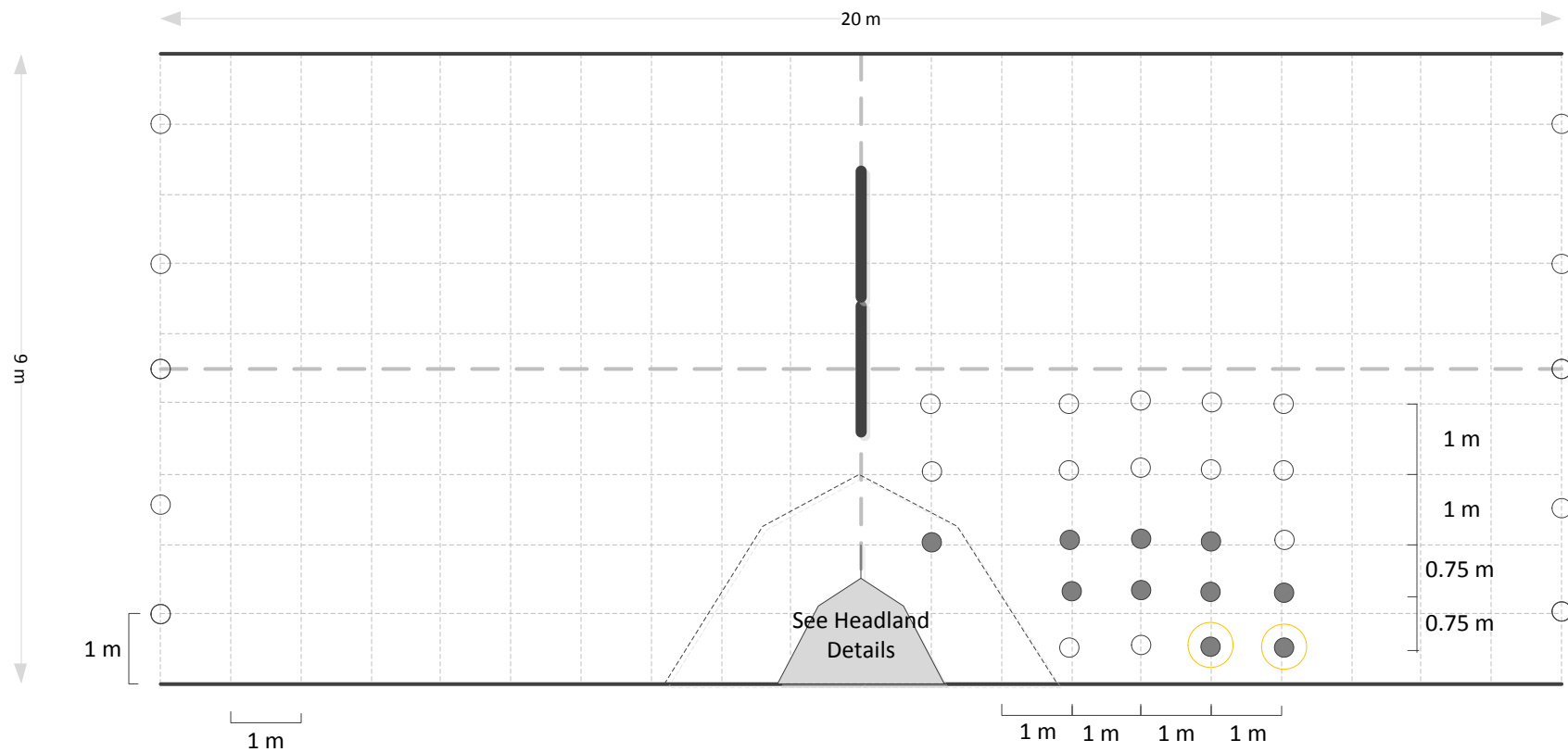
○ This could be changed to propeller meter if not enough ADVs

Key

- ADV point measurement
- ⊗ ADV depth profile (refer to specification for more details)
- Propeller meter measurement
- ▬ Turbine Fence

NOTE: (1) Wave probes to be placed at all locations where velocity measurements are made
 (2) Or denotes the origin
 (3) All fences are 1.8 m long: Fence centres at (0,-1.0)

Test17: Turb 3, wake meas.	
PerAWAT	Date: 24/12/2011



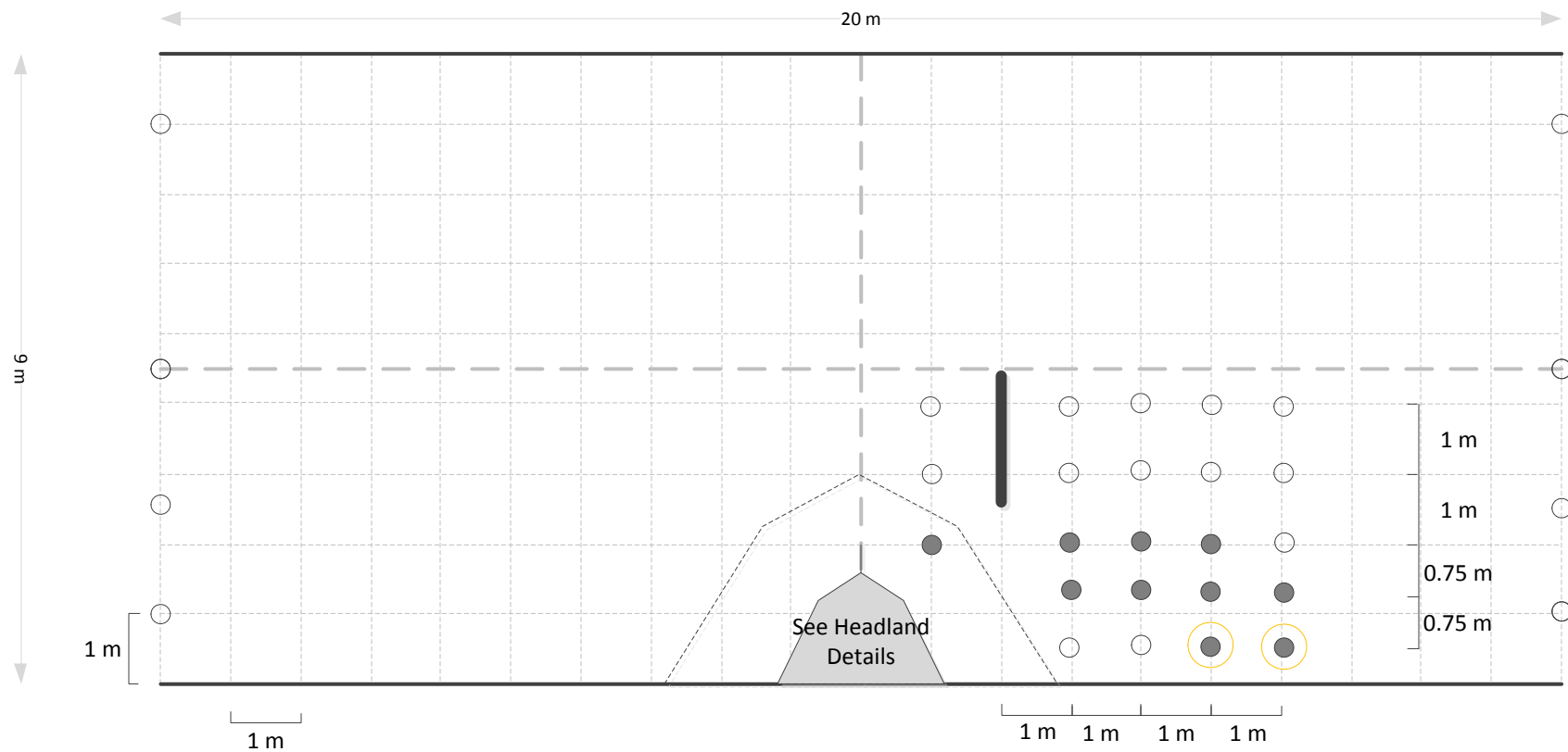
○ This could be changed to propeller meter if not enough ADVs

Key

- ADV point measurement
- ⊗ ADV depth profile (refer to specification for more details)
- Propeller meter measurement
- ▬ Turbine Fence

NOTE: (1) Wave probes to be placed at all locations where velocity measurements are made
 (2) Or denotes the origin
 (3) All fences are 1.8 m long: Fence centres at (0,0), (0,1.8)

Test18: Turb 4, wake meas.	
PerAWAT	Date: 24/12/2011



○ This could be changed to propeller meter if not enough ADVs

Key

- ADV point measurement
- ⊗ ADV depth profile (refer to specification for more details)
- Propeller meter measurement
- ▬ Turbine Fence

NOTE: (1) Wave probes to be placed at all locations where velocity measurements are made
 (2) Or denotes the origin
 (3) All fences are 1.8 m long: Fence centres at (2,-1.0)

Test19: Turb 5, wake meas.	
PerAWAT	Date: 24/12/2011